AD-A092 518 AIR FORCE INST OF TECH WRIGHT-PATTERSON AFB OH F/G 4/2
LATITUDINAL AND VERTICAL RELATIONSHIP BETWEEN TROPOSPHERIC OZON--ETC(U)
JUN 80 F X ROUTHIER
UNCLASSIFIED AFIT-CI-80-18T NL

1 OF 3
AD A
092518

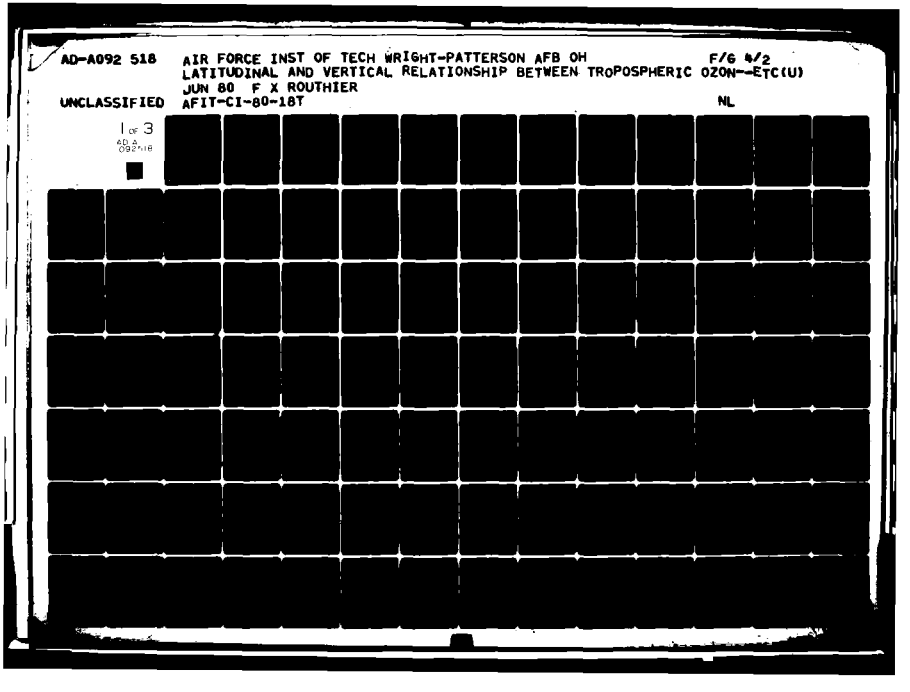

AD A092518

LEVEL II 1

UNCLASS
SECURITY CLASSIFICATION OF THIS PAGE *(When Data Entered)*

REPORT DOCUMENTATION PAGE	READ INSTRUCTIONS BEFORE COMPLETING FORM
1. REPORT NUMBER: 80-18T	2. GOVT ACCESSION NO.: AD92518 — 3. RECIPIENT'S CATALOG NUMBER:
4. TITLE *(and Subtitle)*: Latitudinal and Vertical Relationship Between Tropospheric Ozone and Water Vapor as Measured in Project Gametag,	5. TYPE OF REPORT & PERIOD COVERED: THESIS/DISSERTATION/
	6. PERFORMING ORG. REPORT NUMBER:
7. AUTHOR(s): Francis X. Routhier, Capt USAF	8. CONTRACT OR GRANT NUMBER(s):
9. PERFORMING ORGANIZATION NAME AND ADDRESS: AFIT STUDENT AT: Georgia Institute of Technology	10. PROGRAM ELEMENT, PROJECT, TASK AREA & WORK UNIT NUMBERS:
11. CONTROLLING OFFICE NAME AND ADDRESS: AFIT/NR, WPAFB OH 45433	12. REPORT DATE: June 1980
	13. NUMBER OF PAGES: 198
14. MONITORING AGENCY NAME & ADDRESS *(if different from Controlling Office)*	15. SECURITY CLASS. *(of this report)*: UNCLASS
	15a. DECLASSIFICATION DOWNGRADING SCHEDULE:

16. DISTRIBUTION STATEMENT *(of this Report)*

APPROVED FOR PUBLIC RELEASE; DISTRIBUTION UNLIMITED

DTIC ELECTE DEC 0 5 1980 S D E

17. DISTRIBUTION STATEMENT *(of the abstract entered in Block 20, if different from Report)*

18. SUPPLEMENTARY NOTES

APPROVED FOR PUBLIC RELEASE: IAW AFR 190-17

FREDRIC C. LYNCH, Major, USAF
Director of Public Affairs

Air Force Institute of Technology (ATC)
Wright-Patterson AFB, OH 45433

19. KEY WORDS *(Continue on reverse side if necessary and identify by block number)*

20. ABSTRACT *(Continue on reverse side if necessary and identify by block number)*

ATTACHED

80 11 24 145

DD FORM 1 JAN 73 1473 EDITION OF 1 NOV 65 IS OBSOLETE

UNCLASS
SECURITY CLASSIFICATION OF THIS PAGE (When Data Entered)

DDC FILE COPY

LATITUDINAL AND VERTICAL RELATIONSHIPS BETWEEN TROPOSPHERIC OZONE AND WATER VAPOR AS MEASURED IN PROJECT GAMETAG

A THESIS

Presented to

The Faculty of the Division of Graduate Studies

by

Francis X. Routhier

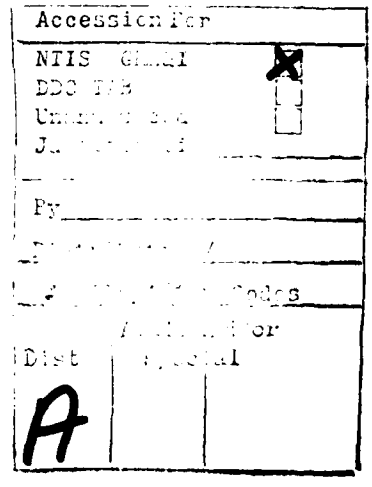

In Partial Fulfillment

of the Requirements for the Degree

Master of Science

in the School of Geophysical Sciences

Georgia Institute of Technology

June, 1980

ACKNOWLEDGEMENTS

I would like to express my thanks to Dr. Douglas D. Davis (D^4) for his admonishments and suggestions during the entire course of this research. I also thank Dr. Derek Cunnold and Dr. C. S. Kiang for their helpful comments concerning the preliminary stages of this manuscript.

Additionally, I would like to thank Mr. Matt Reynolds, Mr. Mike Rodgers, and Mr. Stu McKeen for allowing me to tap their computer expertise. The graphics assistance of Mr. Austin Maley and Ms. Leah Turner are greatly appreciated. And, to Ms. Annette Plunkett whose typing and administrative efforts have been so critical in this endeavor, "Thanks Annette."

I have always wondered why authors thank their families in this section of their manuscript; now I know. Marie, Michele, and David, thank you very much. Without you, this effort wouldn't have been worth it.

TABLE OF CONTENTS

Page

LIST OF TABLES

LIST OF ILLUSTRATIONS

Figure Page

Figure Page

LIST OF SYMBOLS

GAMETAG - Global Atmospheric Measurement Experiment of Trace Aerosols and Gases

hv - photon energy

ITCZ - Intertropical Convergence Zone

O('D) - electronically excited atomic oxygen

$O(^3P)$ - ground state atomic oxygen

M - third body reactant

SUMMARY

Reported in this thesis are the O_3 and dewpoint data recorded during the 1977 and 1978 GAMETAG field experiments. These data are primarily those recorded aboard an aircraft during horizontal flight legs at altitudes between 5-6.5 kilometers (free troposphere) and below one kilometer (boundary layer). The total latitude range covered was 70°N to 58°N and involved flight operations over Canada, Alaska, the eastern and central north Pacific, and the central and western south Pacific. The ozone data show: (1) extensive O_3 layering as a function of altitude, especially in the northern hemisphere; (2) systemmatically higher free tropospheric ozone levels in the northern versus southern hemisphere; (3) boundary layer ozone concentrations that were lower than the free tropospheric O_3 levels; and (4) in 1978, a boundary layer ozone minimum (1-3 ppbv) in the latitude range 13°S-2°N. The dewpoint data show: (1) very large variations in dewpoint within the free troposphere over small geographical distances; (2) very low dewpoint levels over the tropical and subtropical Pacific Ocean; and (3) the GAMETAG subtropical free tropospheric dewpoint data to be usually lower than the global subtropical dewpoint data found in the literature. A comparison of the GAMETAG ozone and dewpoint data shows a significant negative correlation

between O_3 and dewpoint; or if the comparison is made with dewpoint depression, a significant positive correlation. The strongest negative correlation between O_3 and dewpoint appears at those latitudes showing the highest ozone variability. This negative correlation when coupled with the presence of ozone layering implies that a major source of the ozone observed during the GAMETAG flights was that resulting from the downward sloping transport of ozone rich upper tropospheric or lower stratospheric air.

CHAPTER I

INTRODUCTION

A. General Background Information

Although present in the atmosphere at concentrations of a part per million or less, ozone is now recognized to be crucial atmospheric gas. In particular, ozone absorbs radiation in the wavelength range of 200 nm to 310 nm and thereby provides a UV radiation shield for life on the earth's surface. Molecules vital to life processes (proteins, DNA, etc.) exhibit a sharp rise in their absorption cross sections in the wavelength region near 300 nm (Baughner, 1978). Thus, critical states in the evolution of present life forms may be linked to the thickness of the stratospheric ozone shield. Equally important, an increase in the present levels of ultraviolet radiation reaching the earth's surface, due to a decrease in the stratospheric ozone shield, could have deleterious biological effects. Caldwell and Nachtwey (1975) estimate that a 5% decline in the total amount of atmospheric ozone could produce an additional 8,000 skin melanomas per 100 million caucasoid humans. Approximately 300 extra deaths could result annually.

In contrast to its recognized positive biological influence as an ultraviolet radiation shield in the strato-

$$O_3 + h\nu \xrightarrow{\lambda < 318\ nm} O_2 + O('D) \qquad (1)$$

followed by reaction (2)

$$O('D) + H_2O \longrightarrow 2OH \qquad (2)$$

produces hydroxyl radicals that are believed to play an important role in controlling the concentration levels of a large number of tropospheric species. Chemical processes of importance here include the oxidation of CO to CO_2, SO_2 to H_2SO_4, nitrogen oxide species to HNO_3 and all forms of hydrocarbons to CO and H_2O.

B. Global Tropospheric Ozone Budget

1. Introduction

Due to the critical atmospheric role of ozone, considerable effort has been made to understand the global ozone budget. Concerning the tropospheric budget, which is the principle focus of this thesis, there are two prevailing schools of thought: one emphasizes only transport, the other identifies both transport and chemistry as being important to the global ozone budget. Both schools of thought recognize the stratosphere as a significant ozone source. The transport position holds that ozone is transported across the tropopause, distributed throughout the troposphere and destroyed on contact with ocean or land surfaces (Reiter, 1961; Dütch, 1969; Danielsen, 1975; Wildbrandt, 1975; Fabian and Pruchniewicz, 1977; and Danielsen, 1980). The second

position taken is that, in addition to transport processes, tropospheric photochemistry can be a significant ozone source as well as a loss mechanism (Crutzen, 1974; Chameides and Walker, 1973; Fishman and Crutzen, 1978; Fishman, et al., 1980; Chameides and Davis, 1980). Details on each of these sources and sinks are discussed in the text that follows.

2. Stratospheric Source

The primary source of atmospheric ozone is the photolysis of upper atmospheric molecular oxygen. Chapman (1930) proposed a series of reactions involving odd oxygen species (O, O_3) in order to explain the presence of stratospheric ozone. The reaction scheme included the following processes

$$O_2 + h\nu \longrightarrow 2O \quad (3)$$

$$O_2 + O + M \longrightarrow O_3 + M \quad (4)$$

$$O_3 + h\nu \longrightarrow O + O_2$$

$$O + O_3 \longrightarrow 2O_2 \quad (6)$$

$$O + O + M \longrightarrow O_2 + M \quad (7)$$

These reactions were initially sufficient to describe equilibrium ozone photochemistry. Subsequent photokinetic studies led to reaction rate updates which resulted in calculated concentrations far in excess of those actually observed. Bates and Nicolet (1950) proposed that HO_x radicals (H, OH, HO_2) could result in the catalytic destruction of strato-

sphere, available data suggests that, in the troposphere, ozone can have toxic effects if present at excessive levels (Stokes and Seager, 1972; Hazucha, 1973; and Parent, 1978). Human health problems associated with increased ozone concentrations ($\sim$250 ppbv) include the aggrevation of various respiratory illnesses such as asthma, lung disease, heart disease and anemia. The results of controlled laboratory experiments indicate that at levels above 250 ppbv, ozone interferes with normal respiratory processes causing chest tightness, nausea, and laryngitis. A decrease in the athletic performance of healthy high school students was detected at 120 ppbv.

In addition to the just discussed biological significance of atmospheric ozone, studies of this trace gas have also shown it to be of major importance to improving man's understanding of the physical and chemical characteristics of the atmosphere (Newell, et al., 1969; Tiefenau, 1972; Chameides and Walker, 1973; Crutzen, 1973; Pruchniewicz, 1973; Chatfield and Harrison, 1976, 1977a, 1977b; Fabian and Pruchniewicz, 1977; Fishman and Crutzen, 1978; Fishman, et al., 1979; and Fishman, et al., 1980). It has been used as a tracer to study transport processes across the tropopause as well as transport mechanisms within the troposphere. Ozone is also recognized as one of the most significant species that controls tropospheric chemistry. The photolysis of ozone in process (1)

spheric ozone. Crutzen (1970) suggested that the presence of NO_x (NO, NO_2) in the stratosphere could also result in a catalytic ozone destruction mechanism. Stolarski and Cicerone (1974) proposed that chloride compounds in the stratosphere could either photolyze or react with radical species to release atomic chlorine which could again participate in catalytic chain mechanisms which destroy ozone. All of the above additional chemistry did not significantly modify the calculated production rate or alter the main ozone source location illustrated in Figure 1. They did, however, result in additional ozone losses at middle and upper stratospheric altitudes such that theory and observation are now in relatively close agreement (e.g., within the experimental uncertainties of each).

3. Stratospheric-Tropospheric Exchange Source

Many numerical models as well as observational studies have demonstrated that a cellular circulation exists in the stratosphere and troposphere (Hering, 1965; Dobson, 1974; London and Park, 1974; and Cunnold, et al., 1974). Figure 2 illustrates the stratospheric portion of that circulation during the equinox. The circulation transports air away from the equator and the pole towards the middle latitudes where it descends towards the tropospause. Some of this ozone rich air is transported back to the equator and the poles by smaller scale motions; some of it is transported across the tropopause into the troposphere.

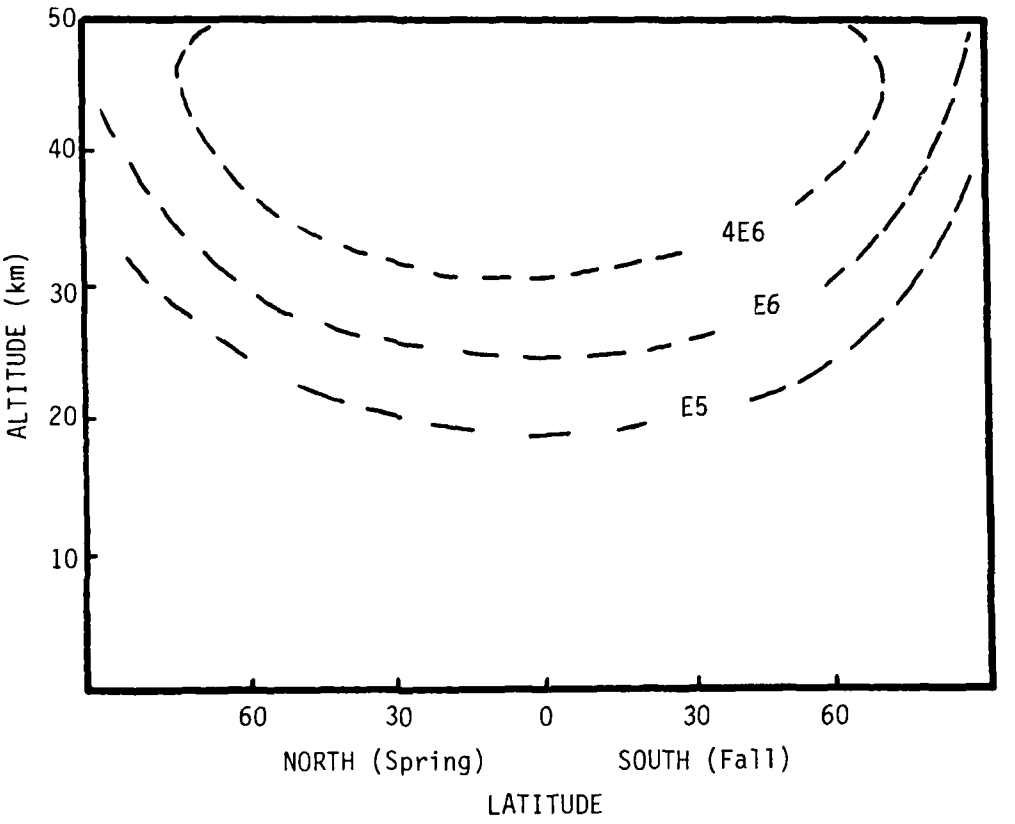

Figure 1. Primary Atmospheric Ozone Source Region (Johnston, 1974).

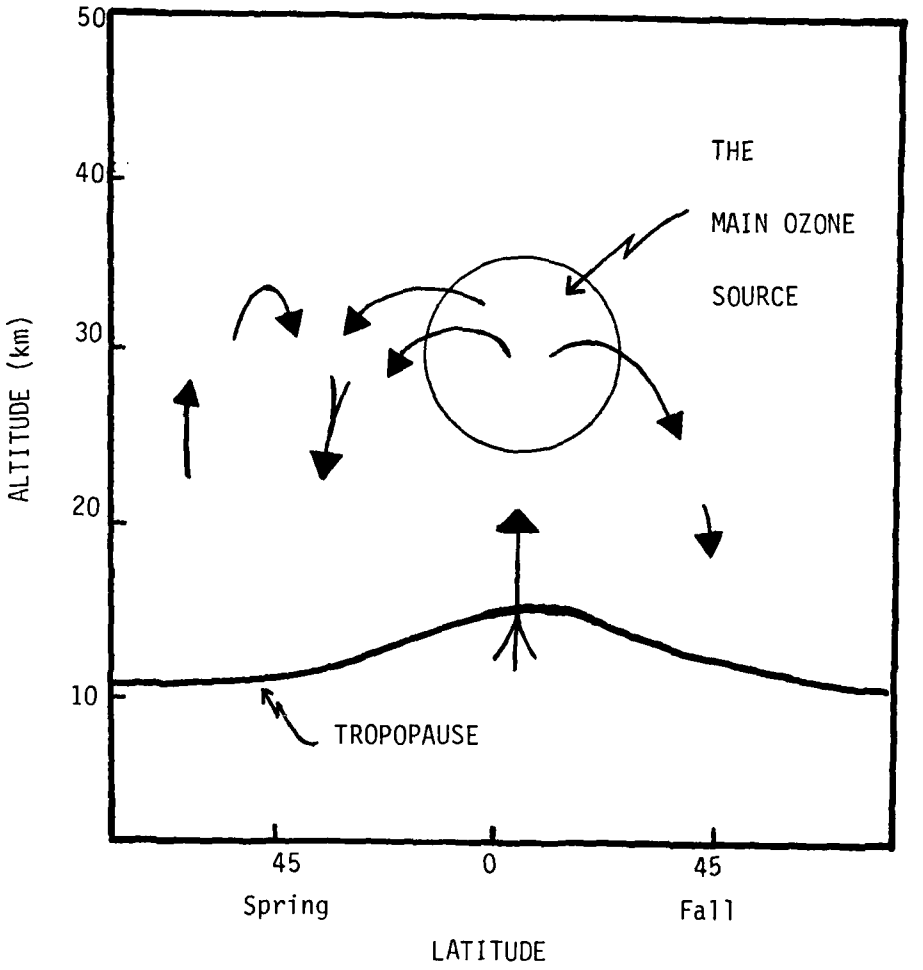

Figure 2. Simplified Mean Stratospheric Circulation. Adopted from Cunnold, et al., 1974.

Reiter (1978) contends that the two major stratospheric-tropospheric exchange processes are mean meridional flow which accounts for ∿59% of the mass transported across the tropopause and large scale eddies which account for ∿27%. [Reiter (1978) feels that small scale eddies are the only exchange processes which may be considered insignificant.] The mean circulation pattern, illustrated vertically in Figure 3 and horizontally at the surface in Figure 4, is believed to transport ozone rich stratospheric air across the tropopause and funnel it at high tropospheric altitudes to the extreme polar edge of the mean circulation Polar Cell and to the intersection of the Hadley and Ferrel Cells. From these regions, the ozone rich air is slowly transported in an anticyclonic and increasingly divergent flow towards the surface around the individual component high pressure cells which make up the polar and subtropical ridges. Danielsen (1980) estimates the time scale for this process to be on the order of three to nine months.

Danielsen (1977) contends that large scale eddies are the primary stratospheric-tropospheric exchange process. He estimates that eddies account for over 80% of the mass transported across the tropopause. One example of these large scale eddies which transports air from the stratosphere to the troposphere is the phenomenon of tropopause folding. Since the tropopause often becomes vertical near the center

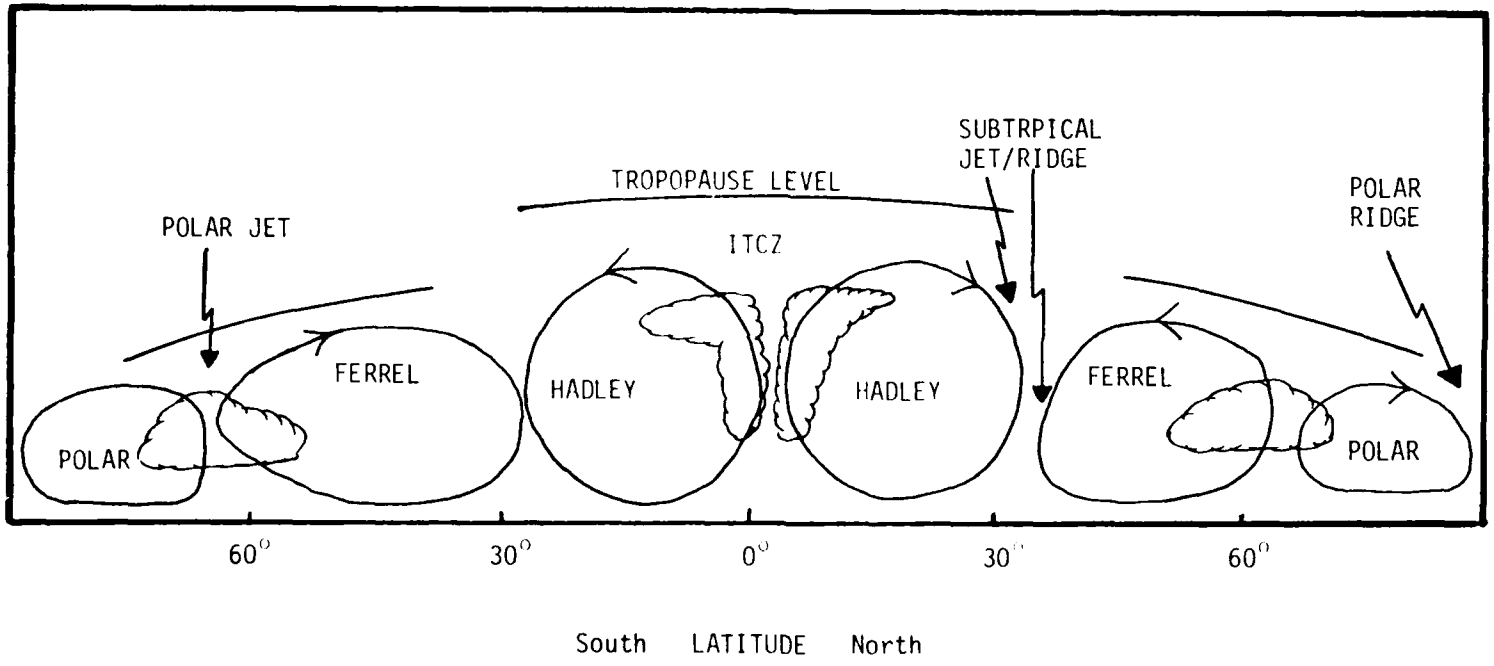

Figure 3. Simplified Mean Tropospheric Circulation (Vertical). Redrawn from Willet and Sanders, 1959.

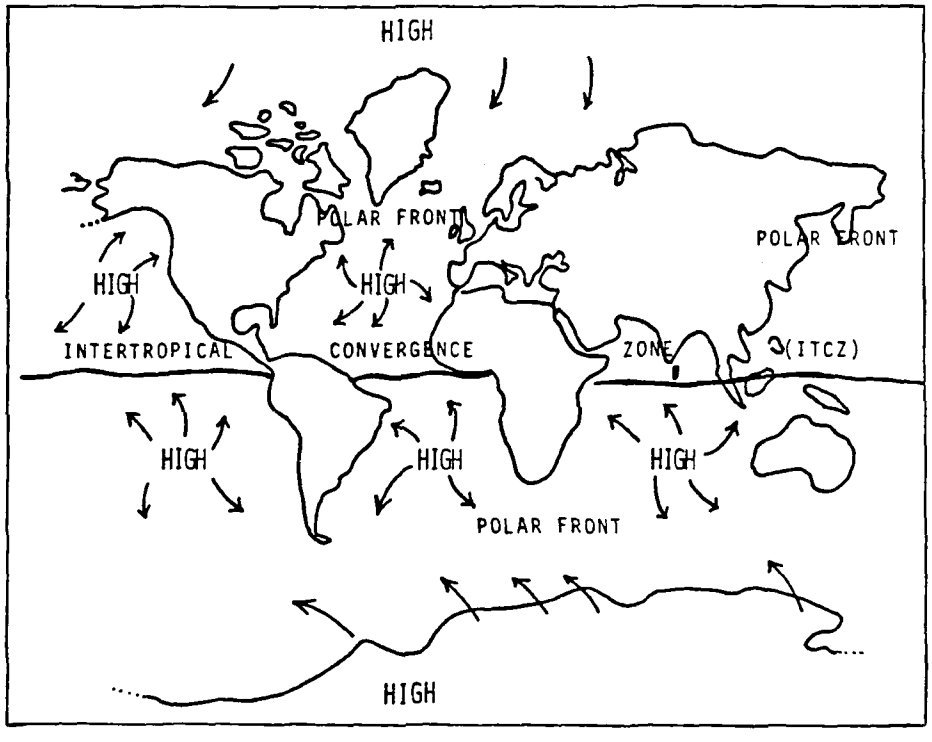

Figure 4. Mean Circulation Pattern (Horizontal) at the Surface. Redrawn from Willet and Sanders, 1959.

of the polar jet, the tropopause develops a trough shape or fold on the north side of the jet core (Figure 5). From this fold, stratospheric air parcels may be envisioned as following the wind component parallel to the isentropic surfaces. Danielsen (1980) contends that this enhanced mixing due to turbulent transport produces trajectories on the order of thousands of kilometers which may be transversed in several days.

4. Ozone Surface Destruction Loss

Ozone is known to be destroyed on contact with the earth's surface (Aldaz, 1969; Regener, 1974; Wilbrandt, 1975; and Garland and Penkett, 1976). These authors report the following (Table 1) ozone destruction rates for land and water surfaces. Since oceanic areas account for approximately 70% of the earth's surface, the above data indicate that, on the global scale, land surface may destroy four to eight times more ozone than ocean surface.

The land surface ozone loss rate has been reported for only a limited number of soil and vegetation types. The many different types of soil (i.e., mountain soils, tundra soils, gray-brown podzolic soils, etc.) and vegetation (i.e., needleleaf forest, sclerophyll forests, steppe and grassland, savanna, etc.) may have vastly different surface ozone loss rates which, when known, could significantly alter the average land O_3 destruction rate value that is used in present atmospheric models. The water surface ozone destruc-

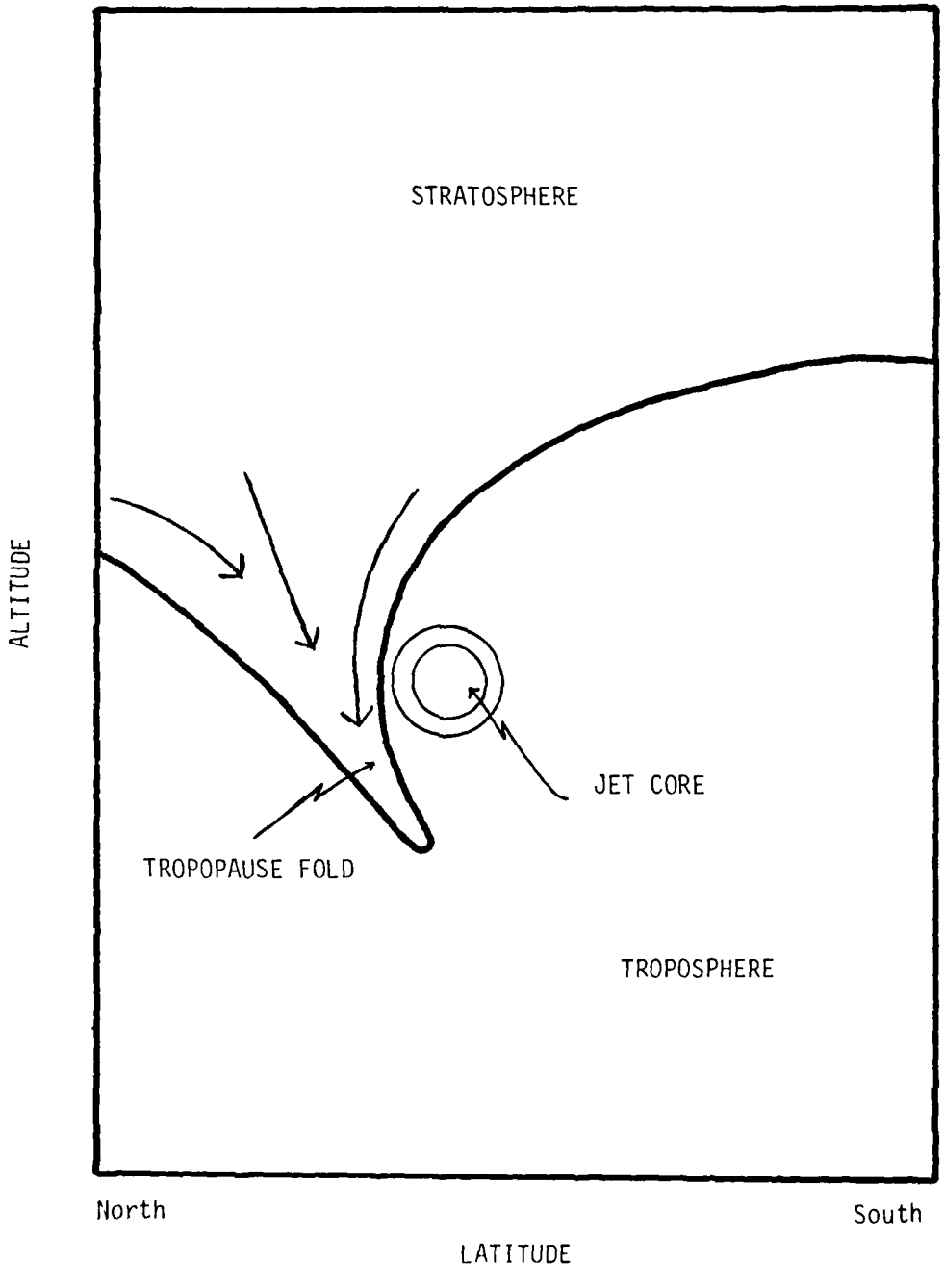

Figure 5. Simplified Tropopause Fold Geometry.

Table 1. Surface Ozone Destruction Rate.

Land	Sea	Ice	Reference
.6 cm/sec (Average)	.04 cm/sec	.20 cm/sec	Aldaz (1969)
-	.1 cm/sec	-	Regener (1974)
1.0 cm/sec (Average)	-	-	Wilbrandt (1975)
.47 cm/sec (Grass)	-	-	Garland and Penkett (1976)
.55 cm/sec (Grass	-	-	Garland and Penkett (1976)
1.6 cm/sec (Soil)	-	-	Garland and Penkett (1976)

tion rate was determined, under laboratory conditions, using two year old bottled ocean water samples and those removed from the Gulf Stream (Aldaz, 1969). Since ocean losses could be critically dependent on surface roughness and the composition of marine organic surface films, these measurements could be on the low side by a considerable amount. A second possible source of error in estimating the ocean versus land O_3 loss rate involves the recent calculations of Chameides and Davis (1980) which indicate that iodine atoms, derived from CH_3I or other iodine compounds released from marine waters, could act as a catalytic O_3 destruction mechanism (see test below). This atmospheric ozone loss mechanism which appears to be related to the ocean's surface could significantly influence the land to ocean O_3 destruction ratio.

5. Tropospheric Photochemical Ozone Formation

While the proponents of the tropospheric ozone transport position contend ozone to be inert in the troposphere, others have suggested possible tropospheric sources which may be quite large (Crutzen, 1974; Chameides and Walker, 1973, 1976; Crutzen and Fishman, 1978; Fishman, et al., 1979; Fishman, et al., 1980).

The formation of O_3 in the troposphere predominantly occurs by the oxidation of NO to NO_2, without using ozone, followed by the photodissociation of NO_2 to produce atomic oxygen and subsequently ozone. One possible reaction

sequence is as follows:

$$NO + HO_2 \rightarrow NO_2 + OH \quad (8)$$

$$NO_2 + h\nu \rightarrow NO + O(3P) \quad (9)$$

$$O(3P) + O_2 + M \rightarrow O_3 + M \quad (10)$$

$$\text{NET} \quad O_2 + HO_2 \rightarrow O_3 + OH$$

Important processes that produce HO_2 and therefore O_3 (in the presence of NO) are

$$OH + CO \rightarrow CO_2 + H \quad (11)$$

$$H + O_2 + M \rightarrow HO_2 + M \quad (12)$$

$$\text{NET} \quad OH + CO + O_2 \rightarrow HO_2 + CO_2$$

which, when combined with the NO oxidation sequence above results in a carbon monoxide oxidation cycle that produces ozone:

$$O_2 + HO_2 \rightarrow O_3 + OH \quad (8\text{-}10)$$

$$OH + CO + O_2 \rightarrow HO_2 + CO_2$$

$$\text{NET} \quad CO + 2O_2 \rightarrow CO_2 + O_3$$

A second O_3 formation process possibly involves the degradation of CH_4:

$$OH + CH_4 \rightarrow CH_3 + H_2O \quad (13)$$

$$CH_3 + O_2 + M \rightarrow CH_3O_2 \quad (14)$$

$$CH_3O_2 + NO \rightarrow CH_3O + NO_2 \quad (15)$$

$$NO_2 + h\nu \rightarrow NO + O(^3P) \quad (9)$$

$$O(^3P) + O_2 + M \rightarrow O_3 + M \quad (10)$$

$$CH_3O + O_2 \rightarrow CH_2O + HO_2 \quad (16)$$

$$HO_2 + NO \rightarrow OH + NO_2 \quad (17)$$

$$NO_2 + h\nu \rightarrow NO + O(^3P) \quad (9)$$

$$O(^3P) + O_2 + M \rightarrow O_3 + M \quad (10)$$

$$CH_2O + h\nu_2 \rightarrow CO + H_2 \quad (18)$$

$$CH_4 + 4O_2 + 2h\nu + h\nu_2 \rightarrow H_2O + CO + H_2 + 2O_3$$

6. Tropospheric Photochemical Ozone Loss

One of the major photochemical destruction mechanisms for ozone is that of the photodissociation of O_3 at wavelengths less than 318 nm followed by reaction with H_2O:

$$O_3 + h\nu \rightarrow O_2 + O('D) \quad (1)$$

$$O('D) + H_2O \rightarrow 2OH \quad (2)$$

$$\text{NET} \quad O_3 + H_2O + h\nu \rightarrow O_2 + 2OH$$

The O('D) from reactions (1-2) can also be deactivated to

ground state atomic oxygen and thereby produce no net O_3 loss.

$$O_3 + h\nu \rightarrow O_2 + O('D) \quad (1)$$

$$O('D) + M \rightarrow O(^3P) + M \quad (19)$$

$$O(^3P) + O_2 + M \rightarrow O_3 + M \quad (10)$$

No Change

Under tropospheric conditions, the latter reaction sequence defines the dominant cycling scheme for O_3, the efficiency of the O_3 destruction scheme being critically dependent on the absolute level of H_2O.

The oxidation of NO and NO_2 to NO_3 by O_3 has also been suggested as a possible photochemical ozone sink:

$$NO + O_3 \rightarrow NO_2 + O_2 \quad (20)$$

$$NO_2 + O_3 \rightarrow NO_3 + O_2 \quad (21)$$

$$NO_3 + h\nu \rightarrow NO + O_2 \quad (22)$$

$$\text{NET} \quad 2O_3 + h\nu \rightarrow 3O_2$$

The above cycle, however, must compete with the far more efficient reaction sequence:

$$NO + O_3 \rightarrow NO_2 + O_2 \quad (20)$$

$$NO_2 + h\nu \rightarrow NO + O(^3P) \quad (9)$$

$$O(^3P) + O_2 + M \rightarrow O_3 + M \qquad (10)$$

thus resulting in no net O_3 loss.

Another potential sink for ozone has been suggested by Chameides and Davis (1980). They contend that in the marine boundary layer, iodine atoms react with ozone to form IO. IO may then react with itself to form an ozone sink according to the coupled set of reactions (23-24):

$$2(I + O_3 \rightarrow IO + O_2) \qquad (23)$$

$$IO + IO \rightarrow 2I + O_2 \qquad (24)$$

$$2O_3 \rightarrow 3O_2$$

Alternatively, IO may react with NO (or CO) in which case there is no net destruction of O_3, i.e.,

$$I + O_3 \rightarrow IO + O_2 \qquad (25)$$

$$IO + NO \rightarrow I + NO_2 \qquad (26)$$

$$NO_2 + h\nu \rightarrow NO + O(^3P) \qquad (9)$$

$$O(^3P) + O_2 + M \rightarrow O_3 + M$$

A second reaction sequence which consumes IO without a net loss of O_3 involves the direct photolysis of IO:

$$I + O_3 \rightarrow IO + O_2 \qquad (23)$$

$$IO + h\nu \rightarrow I + O(^3P) \qquad (27)$$

$$O(^3P) + O_2 + M \rightarrow O_3 + M \qquad (10)$$

From the listing of the above cycles, it can be seen that one of the critical factors dictating the efficiency of the iodine-O_3 loss cycle is that of the absolute concentration level of atmospheric iodine in the form of IO.

It is to be noted here, that in the above discussion of photochemical O_3 sources and sinks, the author has not attempted to present a detailed model of tropospheric ozone chemistry. Only the major source and sink mechanisms, which are presently known, have been described. Their relative significance and therefore, the ambient concentration of ozone as controlled by them, are a function of a variety of variables including radiation intensity, temperature, and the absolute and relative concentrations of numerous chemical species.

C. Proposed Research Problem

The scientific community has been unable to answer the tropospheric ozone question because of the numerous problems in understanding both the chemical and dynamic mechanisms which operate in the atmosphere. The lack of reliable kinetic rate constants for many key reactions makes it difficult to specify trace gas concentrations as well as ozone photochemical production and loss within the troposphere. Similar difficulties remain in quantifying the transport of O_3 from the stratosphere to the troposphere. The number of surface types

for which ozone surface loss rates have been determined is sufficiently limited so as to bring the reliability of the proposed global ozone surface destruction value into question.

Progress can be expected on all of the above problems in the next ten years. For the present, however, it would appear that a further advancement in our state of knowledge of tropospheric O_3 may be achieved by expanding the global tropospheric ozone data base. This would prove to be particularly helpful if the ozone measurements were made simultaneously with other variables such as H_2O, CO, and NO_x. Water, like ozone, plays a significant role in both tropospheric dynamic and chemical processes. For example, besides being in the above mentioned important ozone sink sequence that generated hydroxyl radicals, water frequently changes phase in the troposphere thereby giving this constituent a pivotal role in the atmospheric energy budget.

Because stratospheric and upper tropospheric air has a lower dewpoint (higher dewpoint depression) and higher ozone levels than middle or lower tropospheric air, a negative correlation between these gases would reflect the large scale downward transport of O_3 rich stratospheric and upper tropospheric air. Since most of the present literature on tropospheric photochemical models indicate, at best, only a slight positive correlation between O_3 and H_2O, the presence of a negative correlation between the two gases over a wide latitude range would indicate that the downward transport of

O_3 represents a major middle tropospheric ozone source. It would not, however, give any significant indication of the photochemical sink strength.

Prior efforts to obtain tropospheric O_3 and H_2O data have primarily involved the use of ozonesonde and radiosonde platforms. While the H_2O data base was obtained from a predominately continental mid-latitude global network of upper-air stations, the ozone data was generated from a far more spatially limited set of sources, restricted to Europe, Africa, North America, and five isolated locations in the southern hemisphere At least three other free tropospheric ozone data bases have been made available for interpretative analysis. The most extensive of these has been the data collected by the North American Ozonesonde Network and reported by Hering and Borden (1964, 1965a,b, 1967). These have been analyzed by Pruchniewicz (1973), Chatfield and Harrison (1977b) and Fishman and Crutzen (1978). Another data base has resulted from the set of southern hemispheric ozonesonde stations, under the control of the Australian, Bolivian, New Zealand, and American governments. One set of O_3 data recorded on various aircraft platforms were reported by Tiefenau, et al. (1972). H_2O data have been collected almost entirely from radiosonde platforms and have been compiled by the United States government. The data have appeared in at least three major published summaries, Crutcher (1969), Oort and Rasmussen (1971), and Newell, et al. (1973).

In this thesis, I report O_3 and H_2O data that were collected from an aircraft platform during Project GAMETAG involving flight operations in 1977 and 1978. These data are primarily those simultaneously recorded during horizontal flight at two separate altitude ranges, 5 to 6.5 kilometers (free tropospheric) and below two kilometers (boundary layer). A limited report of vertical O_3 and H_2O data obtained during altitude changes is also included. The ozone and water vapor data will also be compared with the individual data bases presented in previous studies.

CHAPTER II

EXPERIMENTAL

A. Introduction

The GAMETAG program was designed to provide a limited but meaningful test of current chemical models and to expand the tropospheric data base of various atmospheric trace gases and aerosol species. Investigators, involved in Project GAMETAG, simultaneously measured at least 30 atmospheric chemical and meteorological variables. These variables included wind velocity, temperature, dewpoint, equivalent potential temperature, radiative flux, and the concentration of various gas and aerosol species (i.e., O_3, OH, HNO_3, CO, CO_2, $CH_3C\ell$, $CH_3CC\ell$, and SO_2).

B. Sampling Platform

The L-188C Electra, operated by the National Center for Atmospheric Research, was used as the GAMETAG sampling platform. (The Electra is an all-metal, low-wing, long-range, land-based, turbo-prop monoplane.) This aircraft, with its full complement of GAMETAG instrumentation, spare parts, and personnel, had a nominal operating ceiling of 6.4 kilometers and a maximum range of $\sim$3200 kilometers. When following the prescribed GAMETAG sampling scenario (discussed later in the text), the effective range of the Electra

was reduced to ∿2200 kilometers.

The instrumentation aboard the Electra consisted of instruments operated by both university and NCAR personnel. The aircraft meteorological sensors and on board NOVA 1200 computer system were maintained by NCAR flight technicians. This computer system stored navigational information, all meteorological data, and real time data from several instruments, that collected chemical information.

The location of each instrument on the Electra during GAMETAG has been shown in Figures 6 and 7. The dewpoint hygrometers were located on either side of the aircraft near the front end. The ozone sensors were just behind the right side dewpoint hygrometer. In order to reduce the contamination of one instrument by the exhaust of a second instrument, the exhaust from all real time sampling instruments (except for the OH analyzer) were dumped into a large diameter common exhaust line which exited near the aircraft tail. Additionally, the intake locations of all instruments, which analyzed atmospheric species that could have been influenced by engine exhaust gases, were positioned equal with, in front of, or above the engine propeller line. To minimize contamination of the instrument intakes while the aircraft was on the ground, all intake ports were capped off upon landing.

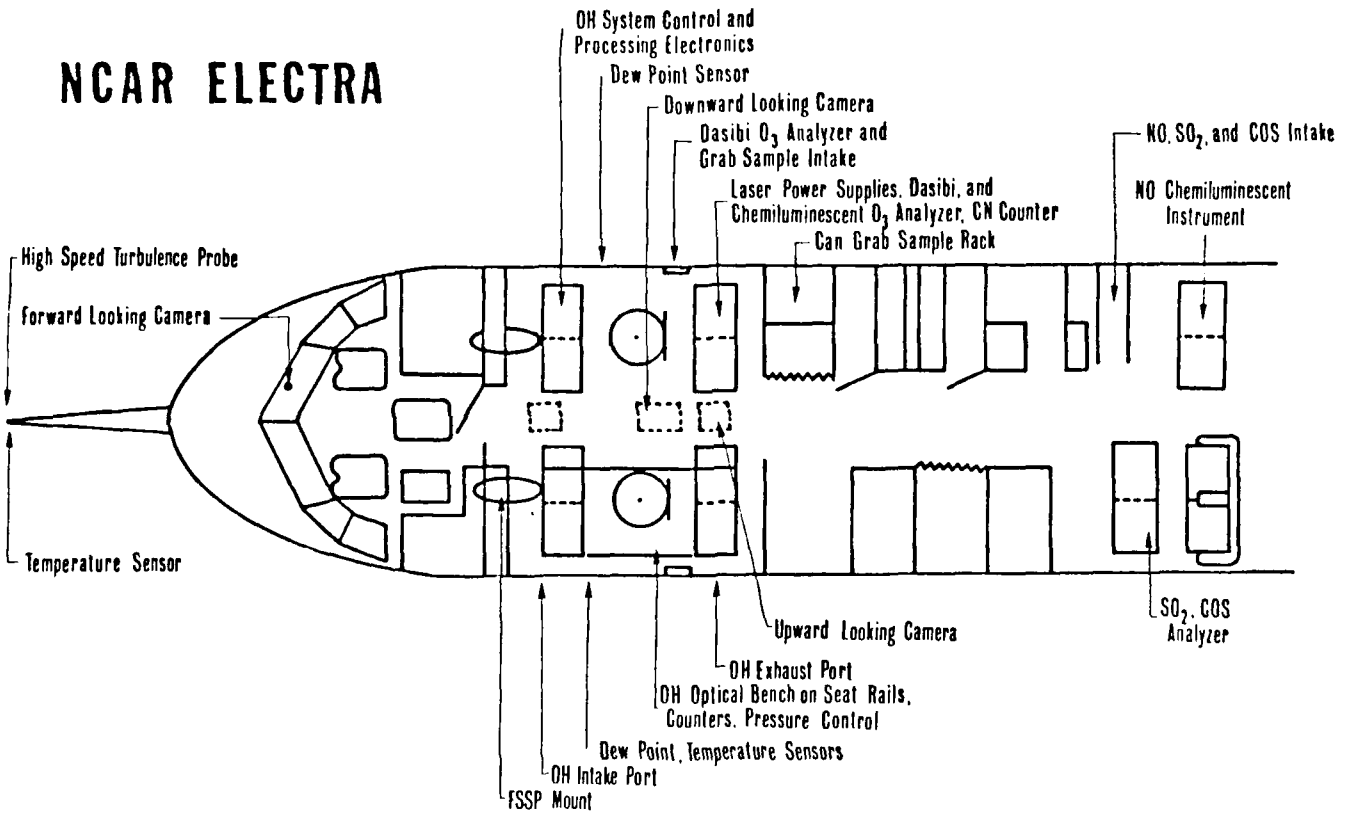

Figure 6. The Electra as Outfitted for Project GAMETAG (Front End).

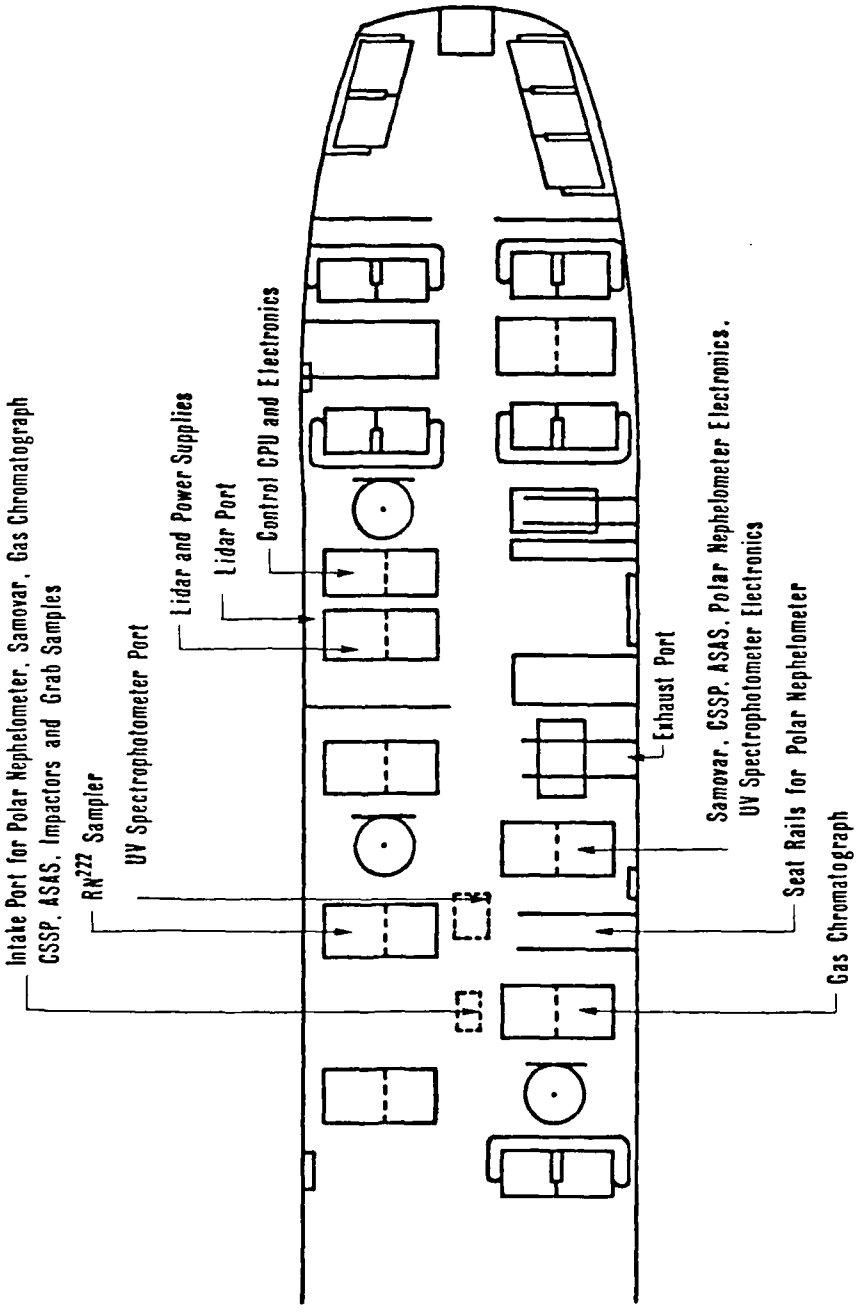

Figure 7. The Electra as Outfitted for Project GAMETAG (Back End).

C. Instrumentation

1. Temperature Sensor

The Rosemount Total Temperature System provided free air measurements. These consisted of the free air temperature compensated for the friction generated heat input. The instrument used a resistance element mounted in an external probe so as to minimize frictional effects. According to Reynolds (1979), appropriate corrections for dynamic heating were applied to the instrument readout; the recorded data represents the true air temperature.

2. Dewpoint Hygrometer

The EG and G Model 137-C3-S3 dewpoint/frost point hygrometer was used throughout the 1977-78 GAMETAG flights. These instruments (two) were owned and operated by NCAR. This model hygrometer consisted of four basic elements: (1) a mirror surface upon which water vapor was condensed; (2) a platinum resistance thermometer that defined the mirror surface temperature; (3) a thermoelectric cooler in contact with the mirror; and (4) an optical sensor that determined the degree of reflectivity of the mirror.

During aircraft operations, air was continuously directed into the hygrometer intake and passed over the mirror surface. While the mirror was dry, the optical sensor provided a continuous signal to the thermoelectric cooler in order to lower the mirror temperature. At the point where condensation appeared on the mirror, the thermoelectric

cooler current was decreased and, as a result, the mirror warmed thereby causing the water on the mirror surface to evaporate. The above cycle was quickly repeated; an equilibrium state was rapidly achieved and the thickness of the dew on the mirror remained constant. Under these conditions, the mirror temperature was the dewpoint temperature (frost point if below 0°C). This instrument model was reported by the manufacturer to have a measurement limit of 10% relative humidity.

Ruskin (1979), the original designer of the EG and G hygrometer has stated that the hygrometer should have had an active interface with an on-board operator if it were to achieve optimum performance (i.e., minimum dewpoint readings). Air Force standard operating procedures for this instrument have always included an active hygrometer-operator interface. As an Air Force flight meteorologist with 2500 flying hours experience, this author has found that, even with an active interface, the hygrometer frequently bottomed out at middle tropospheric altitudes ($\sim$6 kilometers). No interface between the hygrometer and an operator was maintained during GAMETAG flights.

During the GAMETAG free tropospheric flight sequences, it was frequently found that one or both of the aircraft hygrometers had bottomed out. As a result, only the dewpoint/frost point upper limit could be determined. The most commonly observed symptom of this bottoming out behavior was

a constant hygrometer output reading even though significant ambient temperature variations occurred during the same time interval. This behavior pattern has been illustrated in Figure 8. In this case, the "right side" hygrometer had bottomed out as indicated by its very stable readout. Both the "left side" hygrometer and the temperature sensor showed significant output variations during the same ∿18 minute period. Of the two hygrometer units on the aircraft, the "right side" instrument was always found to bottom out at warmer frost points. This instrument had a lower cooling capacity and therefore could not measure frost points as low as those measured by the "left side" hygrometer. Due to the very large dewpoint depressions encountered during the GAMETAG flights, it was found that both instruments were bottomed out during ∿1/3 to 1/2 of the free tropospheric flight sequences. As a result, almost 1/2 of the middle tropospheric data had to be labeled as upper limit frost point data only.

Frost point measurements (hygrometer outputs below 0°C) were converted into the more commonly used meteorological quantity dewpoint using the equation D.P. = .009109 + 1.1340 (F.P.) + .001038 $(F.P.)^2$ for the temperature range 0°C to -80°C (Hansen, 1980).

The EG and G hygrometers were calibrated by means of tower fly-buys and laboratory tests. Cross calibrations with the tower dewpoint hygrometer were usually limited to dewpoints over the range 0° to 20°C; the agreement was found to

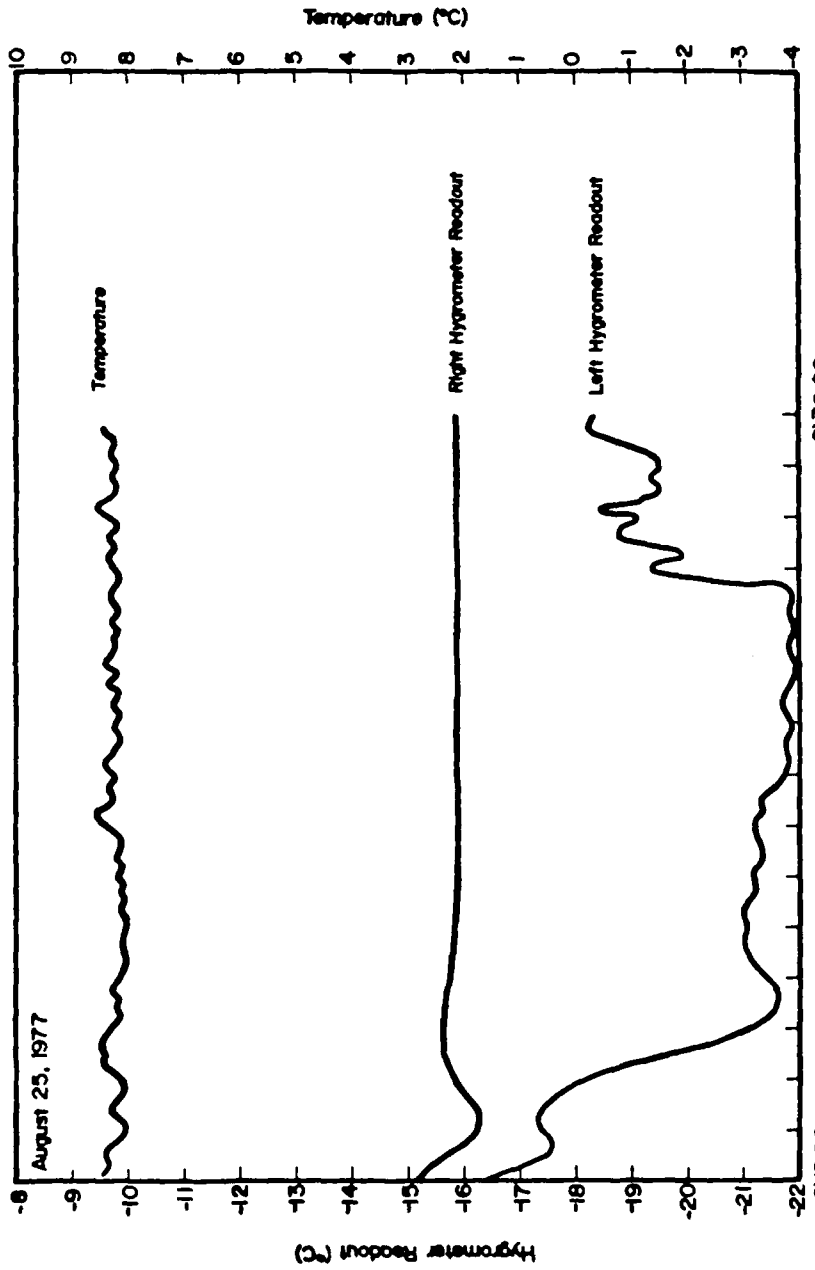

Figure 8. Performance Characteristics of Two Aircraft Hygrometers: One Functioning Properly, the Other Failing.

be ±.1°C. The hygrometer units' platinum resistance thermometers were checked in controlled laboratory temperature baths down to -20°C where the agreement was also found to be within a tenth of a degree.

3. Ozone Sensors

The system used for all Project GAMETAG ozone measurements consisted of four major elements: (1) an inlet system, (2) a pressure flow regulation system, (3) three ozone sensors (only two in 1977), and (4) a data recording system (see the schematic diagram in Figure 9).

Two Dasibi Model 1003AAS ultraviolet absorption instruments and one Columbia Scientific Industries (CSI) Model 2000 ethylene chemiluminescence ozone analyzer were used. The reason for having two different sensor types aboard the aircraft was to identify subtle yet important deviations in the normal operating behavior of each instrument type under various field sampling situations.

The elements of the Dasibi ozone system that were used during Project GAMETAG were (a) a continuous flow sampling manifold, (b) an ozone destruction filter, (c) a fixed path optical absorption cell, (d) an ultraviolet source mercury lamp, and (e) an ultraviolet photodetector with the necessary electronic components. During the sampling operations, air was passed directly through the Dasibi UV absorption cell and then through an ozone destruction filter before passing through the absorption cell. Throughout most of the GAMETAG

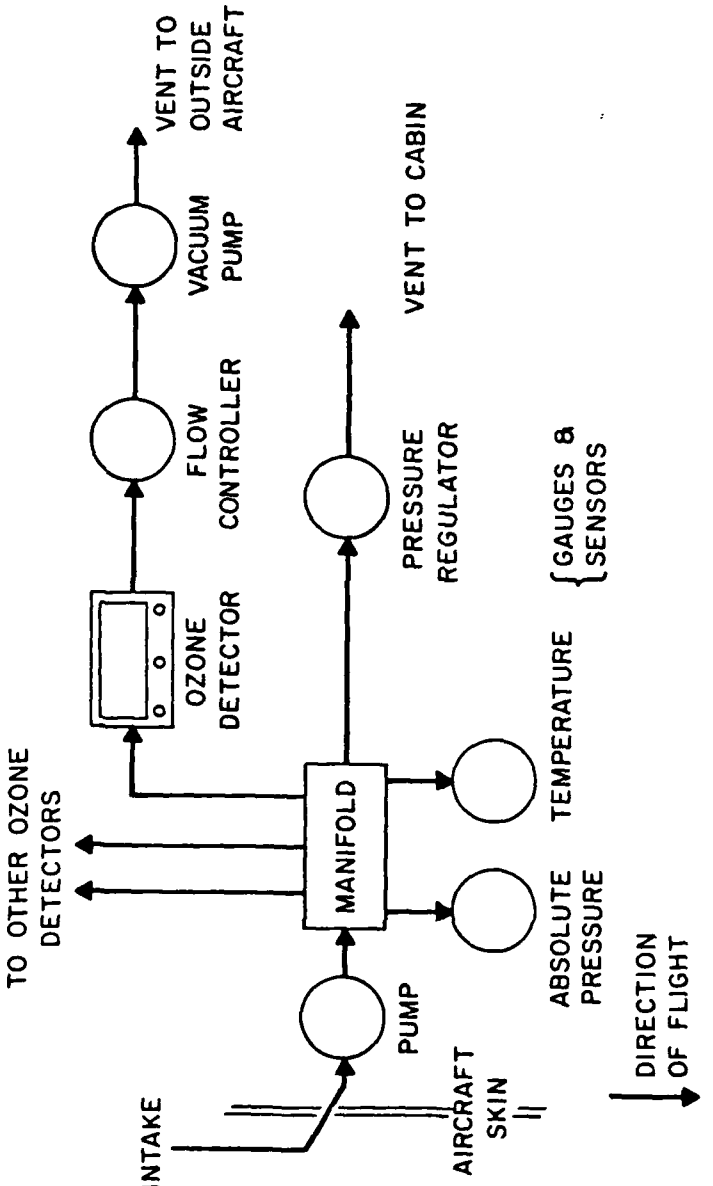

Figure 9. Ozone Sampling and Detection System Used During the 1977-1978 GAMETAG Field Operations.

flights, the Dasibi instruments were operated in a single 15 second cycle mode during which time the UV flux transmitted through the ambient sample was compared with the flux transmitted through the zero ozone sample. Digital electronics measured the small differences in the UV flux and converted it into a direct read-out of ambient ozone concentration. The Dasibi Model 1003AAS instrument was designed for a one second time resolution which required no re-zeroing; however; a systematic drift in the output signal was observed. The drift over a period of 10-15 seconds was not found to be acceptable by the GAMETAG investigators. The cycling time for alternating between ambient and zero ozone air was 15 seconds; this time specified the normal time resolution for the Dasibi analyzer.

The CSI ozone instrument consisted of four major elements: (1) a continuous flow sampling manifold, (2) a C_2H_4 flow system, (3) an ambient air and ethylene mixing and reaction chamber, and (4) a photon detector along with the associated electronics. In this instrument, excess ethylene was mixed with the ambient air to produce a chemical reaction whose products fluoresce. This chemiluminescence was monitored by a photomultipler tube equipped with a bandpass filtered. Unlike the Dasibi instruments, the CSI ozone analyzer was extremely sensitive to the ambient air flow rate. The $\sim$15 second time resoltuion for the CSI instrument was a function of the flow rates and gas mixing time.

The Dasibi was calibrated before and after each major GAMETAG flight operation. In 1977, before the field program began, these instruments were calibrated at the factory against a long path UV absorption cell. During the 1977 flight operation, the aircraft Dasibi was compared to the Dasibi instrument located at the NOAA field station at Pago Pago, American Samoa. After the 1977 flights and before the 1978 operations, one of the Dasibi instruments were calibrated against the Drexel University long path UV absorption cell. The second Dasibi was then calibrated against the one checked at Drexel. At the end of the 1978 flight program, one Dasibi was sent to the National Bureau of Standards for calibration against a long path UV cell. The results of this test are shown in Table 2. Particular care was taken to establish

Table 2. 1978 Dasibi O_3 Calibration Data.
(National Bureau of Standards)

(NBS) UV_{ppbv}	$Dasibi_{ppbv}$
14	15
23	20
31	33
33	31
39	38
42	44
57	51
202	192
325	313

Zero Offset 2.2 ppbv ±1.6

the Dasibi accuracy when sampling ozone free air.

Because the Dasibi was determined to have long term stability, it was used to calibrate the CSI instrument in the field. These calibration tests were carried out on the ground with all instruments stabilized. Ozone samples were generated by a MEC Model 1000 ozone generator and passed through the two different instrument types. When major differences were noted between the Dasibi and CSI instruments, adjustments were made to the CSI instrument in order to bring it into agreement with the Dasibi. During these ground calibration tests, the two different instrument types were found to be within 2 ppbv at ozone concentrations equal to 20 ppbv and within 4 ppbv at 103 ppbv ozone.

During Project GAMETAG, the ozone sampling system was mounted inside the Electra in a single rack next to the window insert plate containing the O_3 sample inlet tube. This tube was made from one half inch aluminum tubing with a teflon tube insert. The intake tube extended 30 centimeters beyond the fuselage exterior, beyond the boundary layer of the aircraft. The intake faced backwards in order to prevent rain or ice from entering the inlet tube. When sampled, air was drawn into the pressure regulation system and compressed to approximately 760 torr. Rech, et al. (1974) described a similar pressure regulation system that was designed for the same purpose. The GAMETAG system consisted of a diaphram pump, an intake manifold, a pressure relief valve, a tempera-

ture readout and three pressure transducers. The exhaust end of the system included a pump and two flow controllers across which a ∿460 torr differential pressure was maintained. This system exhausted into the central aircraft "garbage line" from which the sampled gases were expelled. The pressure regulation system flow controllers were required because the CSI instrument was sensitive to aircraft cabin pressure fluctuations. Altitude chamber tests showed the Dasibi instrument to be independent of simulated altitude changes; the CSI analyzer displayed response deviations in the pressure range 1000 millibars to 750 millibars. After the flow controllers were installed near the exhaust end of the pressure regulation system, the CSI unit was uninfluenced by changes in cabin pressure. In 1978, the ozone analyzer inlets were held at 1013 ±20 millibar; the individual instrument exhaust flow was controlled to within 1%.

The airborne agreement between the CSI and Dasibi instruments was usually found to be within ±8% during 1977 GAMETAG field operations and ±4% in 1978. The primary reasons for this improvement were the addition of the flow controllers to the pressure regulation system in 1978 and design changes in the Dasibi electrometer board.

The ozone values reported here are an arithmetic average of the readings from all operational aircraft ozone sensors. For ozone concentrations greater than 15 ppbv, the absolute accuracy of the 1977 ozone data is estimated to be

~10%; for the 1978 ozone data, it is 5%. For ozone levels less than 15 ppbv (1978 boundary layer ozone concentrations), the absolute error is considered to be much larger than quoted above. For ozone levels near 2 ppbv, calibration curves show that the error could be as large as 100%.

D. Project GAMETAG Flight Tracks

Because GAMETAG was an experiment to provide data about the remote troposphere, the overall flight track was laid out such that the maximum amount of time was in remote areas. During the summer of 1977, missions were flown over the northwest areas of North America; the Northeast, Central and South Central Pacific Ocean; and the Arctic region bordering Alaska. In 1978, the tracks covered a very similar pattern except the Southwest Pacific was investigated instead of the south-central area. Additionally, no Eastern Canada track was flown. Table 3 or Figures 10 and 11 provide a more graphic presentation of the flight paths.

The tracks were predominately flown at two altitudes: 5 to 6.5 kilometers in the free tropospheric and under two kilometers in the boundary layer. The boundary layer sequences were usually flown in the middle and at the end of each flight track. As a result, each flight included four vertical profiles (see Figure 12).

E. Data Processing

The inflight data was compiled and recorded by the

Table 3. Detailed Flight Track During the 1977 and 1978 GAMETAG Field Program.

1977 Flight Operation

Date	Initiation	Destination	Significant Turning Points
Aug. 7	Denver 39.6°N; 104.5°W	Portland 46.8°N; 122.7°W	
Aug. 8	Portland 46.8°N; 122.7°W	Anchorage 61.2°N; 150°W	50°N; 144.6°W
Aug. 9	Anchorage 61.2°N; 150°W	Anchorage 61.2°N; 150°W	64°N; 157.5°W 70.7°N; 159°W
Aug. 11	Anchorage 61.2°N; 150°W	Churchill 58.8°N; 94.2°W	Stop at Whitehorse 60.2°N; 134.8°W
Aug. 12	Churchill 58.8°N; 94.2°W	Denver 39.6°N; 104.5°W	
Aug. 22	Denver 39.6°N; 104.5°W	San Francisco 37.5°N; 122.1°W	33°N; 115°W
Aug. 23	San Francisco 37.5°N; 122.1°W	Hilo, Hawaii 20°N; 155°W	
Aug. 25	Hilo, Hawaii 20°N; 155°W	Johnston Island 16.8°N; 169.5°W	19.5°N; 169.5°W
Aug. 26	Johnston Island 16.8°N; 169.5°W	Pago Pago 14.3°N; 170.8°W	
Aug. 28	Pago Pago 14.3°N; 170.8°W	Pago Pago 14.3°N; 170.8°W	8°S; 171°W 8°S; 168°W

Table 3. Continued

Date	Initiation	Destination	Significant Turning Points
1977 Flight Operation			
Aug. 31	Pago Pago 14.3°N; 170.8°W	Pago Pago 14.3°N; 170.8°W	25.5°S; 170°W 25.5°S; 174°W
Sept. 1	Pago Pago 14.3°N; 170.8°W	Johnston Island 16.8°N; 169.5°W	
Sept. 2	Johnston Island 16.8°N; 169.5°W	Hilo, Hawaii 20°N; 155°W	13.0°N; 160.5°W
Sept. 5	Hilo, Hawaii 2o°N; 155°W	San Francisco 37.5°N; 122.1°W	
Sept. 6	San Francisco 37.5°N; 122.1°W	Denver 39.6°N; 104.5°W	33°N; 155°W
1978 Flight Operation			
Apr. 27	Denver 39.6°N; 104.5°W	San Francisco 37.5°N; 122.1°W	33°N; 115°W
Apr. 28	San Francisco 37.5°N; 122.1°W	Hilo, Hawaii 20°N; 155°W	
May 2	Hilo, Hawaii 20°N; 155°W	Johnston Island 16.8°N; 169.5°W	
May 3	Johnston Island 16.8°N; 169.5°W	Canton Island 2.5°S; 171.1°W	

Table 3. Continued.

1978 Flight Operation

Date	Initiation	Destination	Significant Turning Points
May 4	Canton Island 2.5°S; 171.1°W	Fiji Islands 17.7°S; 177.4°E	
May 6	Fiji Islands 17.7°S; 177.4°E	Christchurch, N.Z. 43.8°S; 172.6°E	
May 10	Christchurch, N.Z. 43.8°S; 172.6°E	Christchurch, N.Z. 43.8°S; 172.6°E	58°S; 172.0°E
May 11	Christchurch, N.Z. 43.8°S; 172.6°E	Fiji Islands 17.7°S; 177.4°E	
May 12	Fiji Islands 17.7°S; 177.4°E	Canton Island 2.5°S; 171.1°W	
May 13	Canton Island 2.5°S; 171.1°W	Johnston Island 16.8°N; 169.5°W	
May 14	Johnston Island 16.8°N; 169.5°W	Hilo, Hawaii 20°N; 155°W	
May 17	Hilo, Hawaii 20°N; 155°W	San Francisco 37.5°N; 122.1°W	
May 18	San Francisco 37.5°N; 122.1°W	Denver 39.6°N; 104.5°W	33°N; 155°W
May 27	Denver 39.6°N; 104.5°W	Great Falls 47.0°N; 113.0°W	

Table 3. Continued.

1978 Flight Operation

Date	Initiation	Destination	Significant Turning Points
May 28	Great Falls 47.0°N; 113.0°W	Whitehorse 60.2°N; 134.8°W	
May 30	Whitehorse 60.2°N; 134.8°W	Whitehorse 60.2°N; 134.8°W	62.9°N; 144.5°W 70.0°N; 132.5°W
May 31	Whitehorse 60.2°N; 134.8°W	Great Falls 47.0°N; 113.0°W	
June 1	Great Falls 74.0°N; 133.0°W	Denver 39.6°N; 104.5°W	

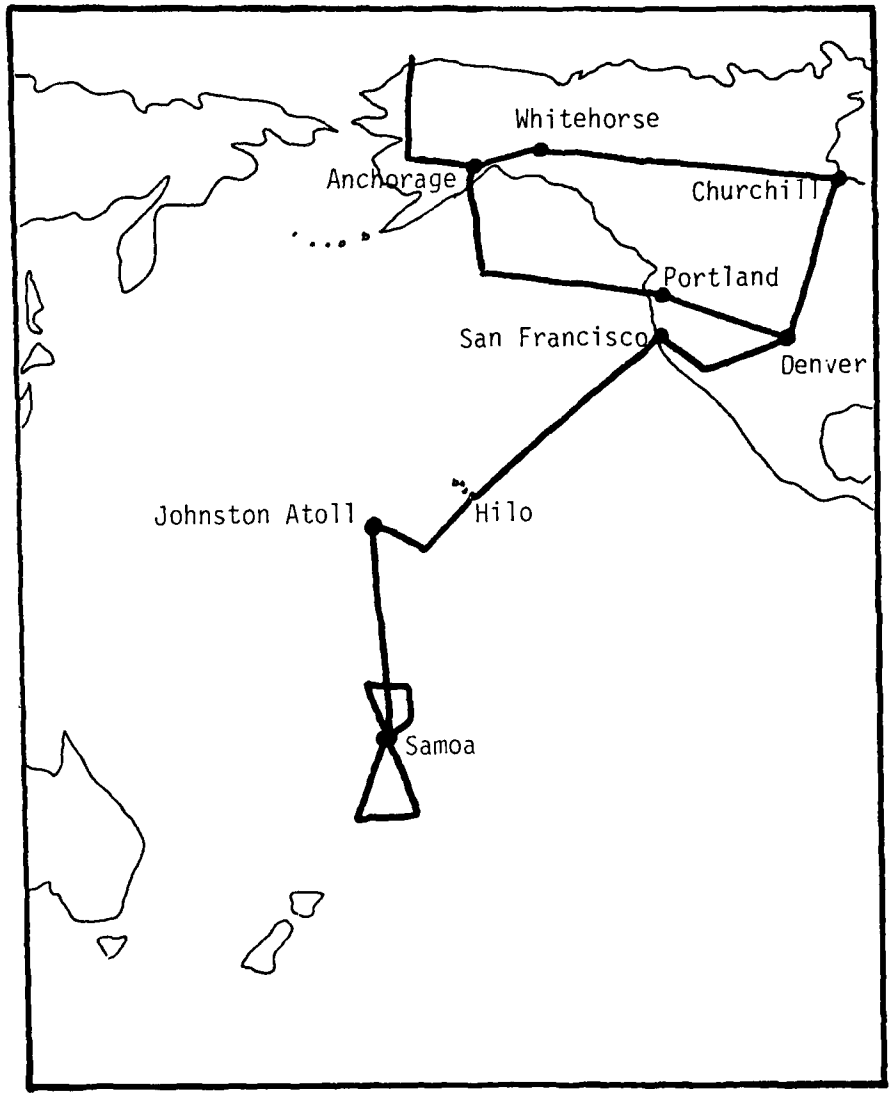

Figure 10. 1977 GAMETAG Field Operations.

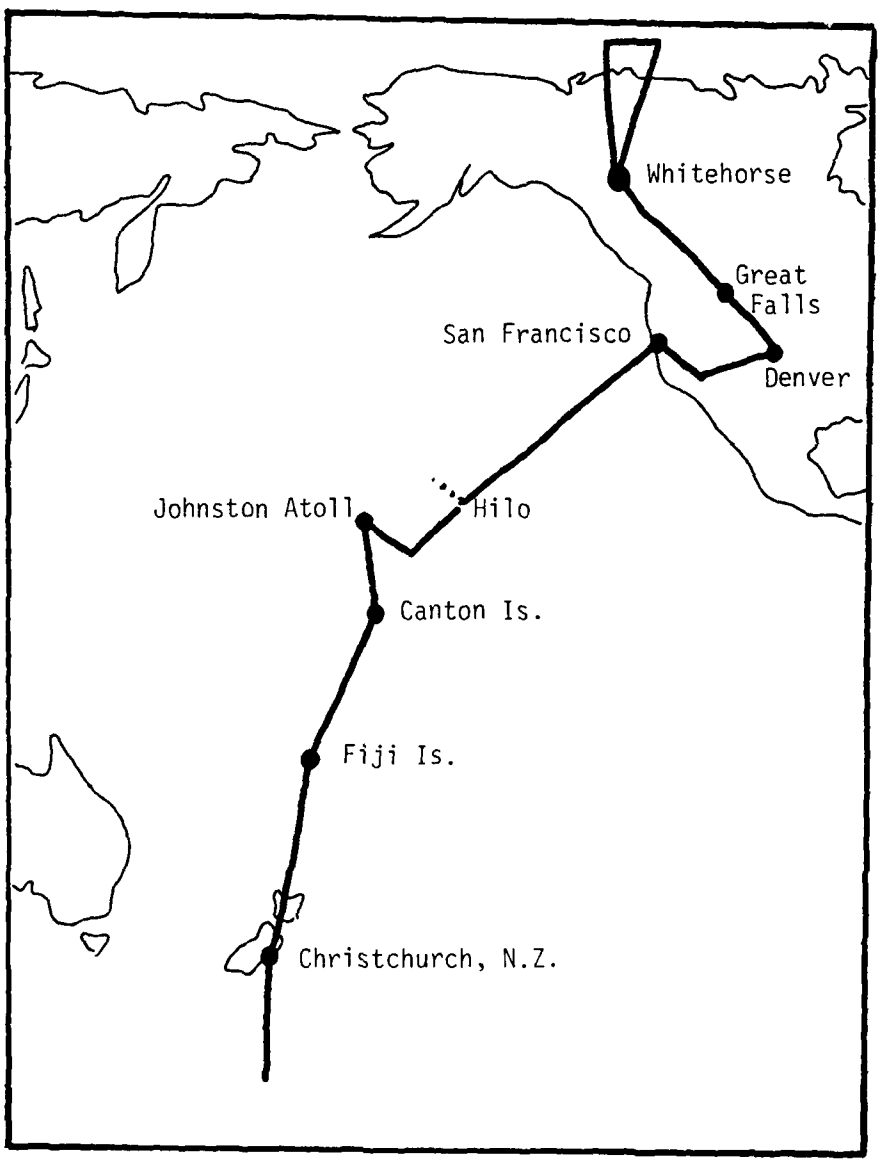

Figure 11. 1978 GAMETAG Field Operations.

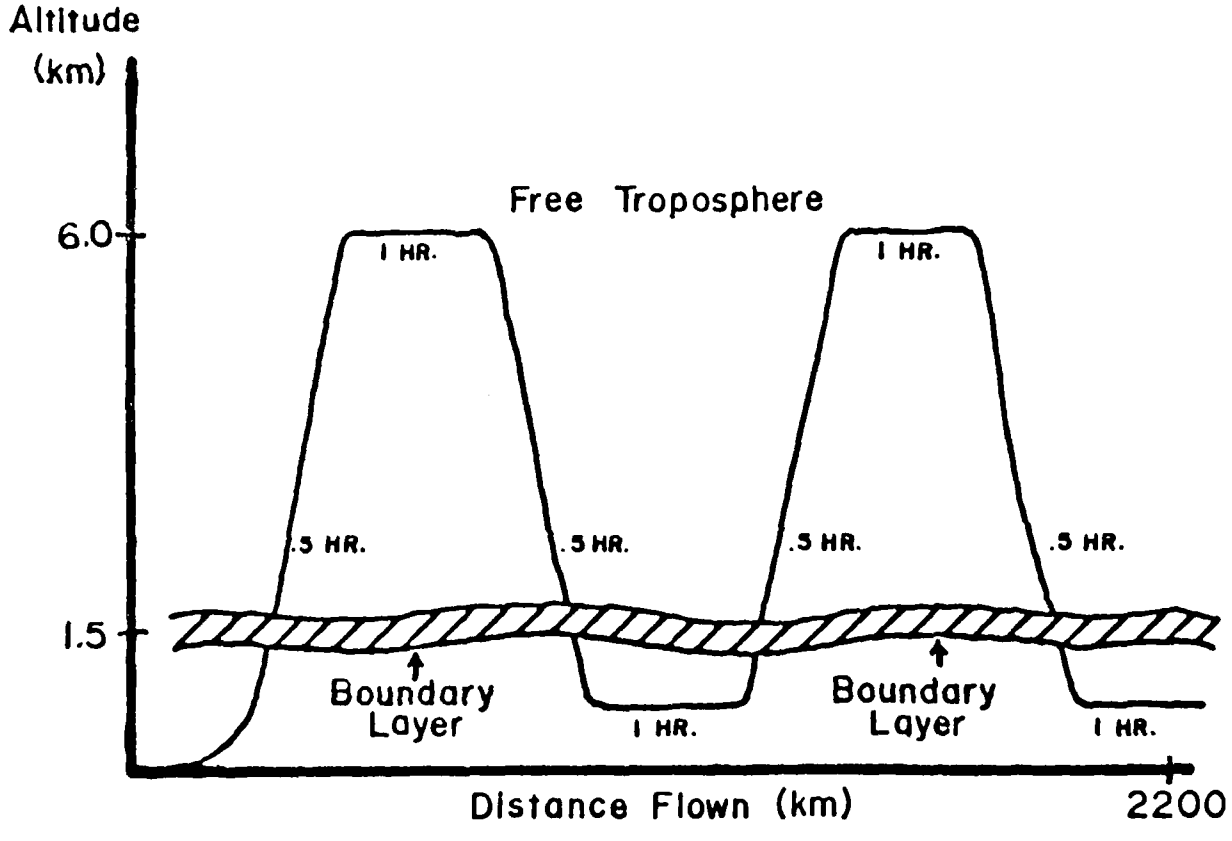

Figure 12. Typical GAMETAG Flight Profile.

Electra Data Management System. The EDMS is a dual mini-computer system.

The preliminary meteorological data, which was used for this investigation, was tabulated on the aircraft real time printer output. This information was generated directly by the aircraft systems with corrections applied to temperature and static pressure readouts. The time resolution of this tabulation was five hertz averaged to one hertz and printed every seven seconds. The second level of data was that reduced by the NCAR computer system from the magnetic tapes produced by the Electra acquisition system. This stage of the data base included corrections for frost point to dew-point conversion. The third set was an assembleage of data on magnetic tape at a rate of one each per second. Certain parameters were eliminated or encoded to provide an increased concentration of frequently used data. Dewpoint depression and ozone sensor output signals replaced dewpoint and equivalent potential temperature. Additional processing of this data base will be accomplished in the future.

The initial format for the ozone data was an NCAR computer facility by-product plot of ozone versus time. For each instrument, two chronological plots were provided: a raw data readout and a one minute filtered graph. A chart of the average ozone was developed. The next ozone stage was a time based ozone tabulation on magnetic tape. For 1977, the ozone data was compiled on tapes separate from

those mentioned above; for 1978, the ozone data was incorporated into the meteorological tapes.

CHAPTER III

RESULTS

A. Introduction

Reported here are the ozone, dewpoint, and temperature data collected during the 1977 and 1978 Project GAMETAG field operation. All horizontal flight data collected in the middle free troposphere (5 to 6.5 kilometers) are included. Six high resolution ozone, dewpoint, and temperature profiles recorded during vertical ascents and descents are also presented. Finally, a low resolution analysis of the entire vertical ascent and descent ozone and dewpoint data is reported.

Both the free tropospheric and boundary layer ozone and dewpoint data are presented here as a function of latitude (i.e., Figures 14-43). In each of these plots, the average ozone or dewpoint value for a latitudinal band of two degrees or less is represented by a horizontal bar. If a given flight segment did not transverse a full 2° of latitude, only that geographic latitude range in which data was actually recorded is represented. Each vertical bar through the horizontal average value represents the full range of ozone concentrations or dewpoints which are incorporated into that average. The rectangular boxes indicate the maximum

and minimum ozone and dewpoint values within which 50% of all data was recorded. The numeral above each vertical bar has been used to indicate the flight data on which the data was recorded, whereas the number below each vertical bar is a coded value designed to indicate the total amount of time during which data was collected in that latitudinal band. The code employed is summarized as follows:

a) 1 = 10-20 minutes

b) 2 = 20-40 minutes

c) 3 = 40-80 minutes

d) 4 = >80 minutes

All of the above information has been presented in graphic form in Figure 13.

For the dewpoint data only a dot above the vertical bar specifies the average temperature in that given latitude band while the downward pointing arrows below the horizontal and vertical bars indicate measurements where the hygrometer had bottomed out 50% of the time or more. In this case, the plotted dewpoint is the highest possible average value for that latitude band; the lower limit is not known. If the hygrometer had bottomed out 100% of the time, only the average value and two downward pointing arrows are shown. The dewpoint data are also presented in the form of a dewpoint depression plot in separate figures. Only the average dewpoint depression for each latitude band, or part thereof, is shown. For measurements where the hygrometer was partially bottomed

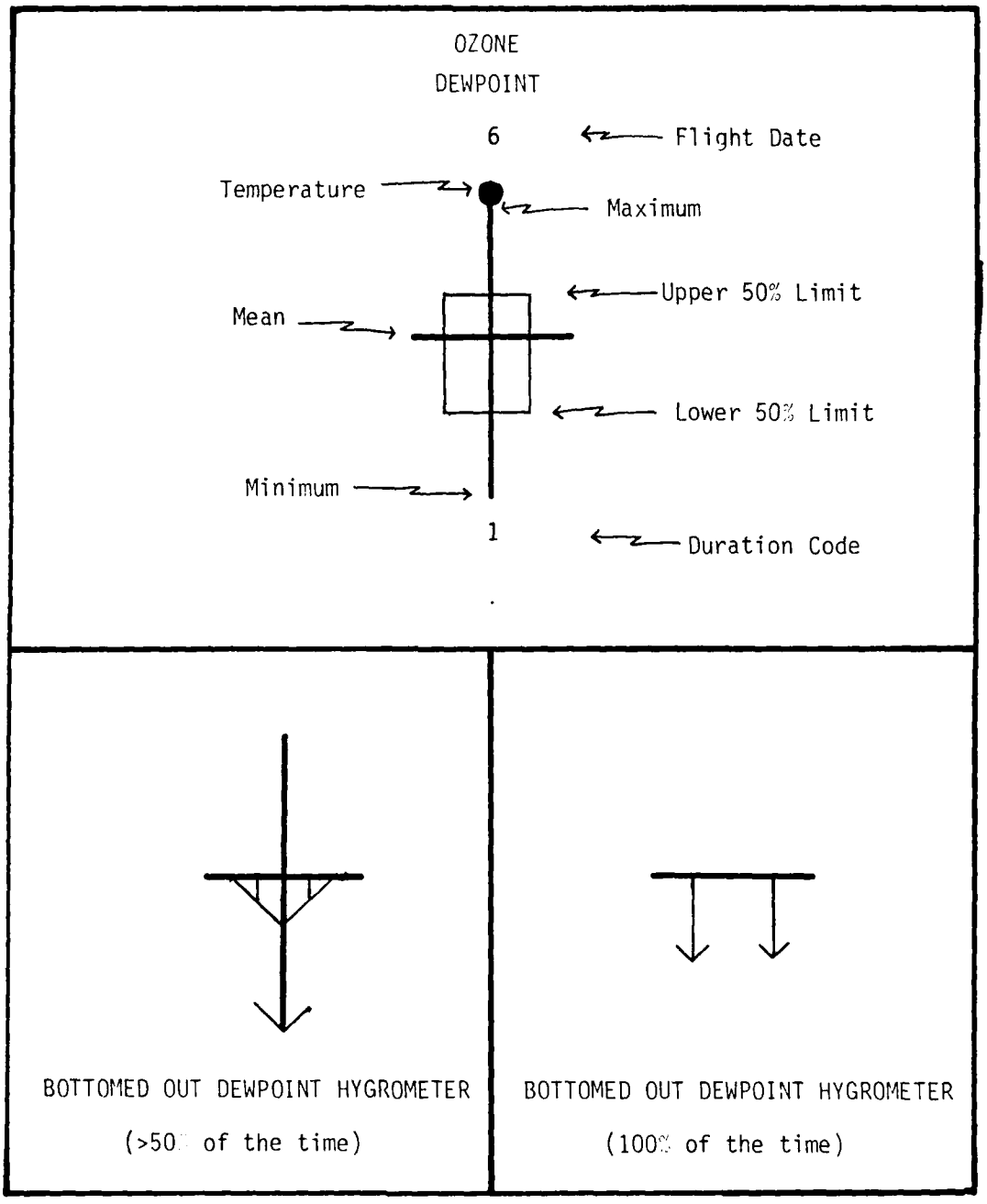

Figure 13. Explanation of Graph Symbolism for Figures 14-43.

out, upward pointing arrows have been placed above the horizontal bar in order to indicate that the plotted dewpoint depression is the lowest possible value. Dewpoint depressions associated with totally bottomed out hygrometer conditions have been omitted.

The high resolution analysis of the vertical ozone, dewpoint and temperature data has been shown as a function of altitude. For the low resolution analysis of the ozone and dewpoint vertical data, the 1977 and 1978 GAMETAG vertical ascents and descents were segregated first by year then by ten degree latitude bands. Each ascent and descent was then divided into three altitude blocks (>4500 m, 4500-3000 m, and 3000-1500 m). For each ascent or descent altitude block, the average ozone and dewpoint value was calculated. All the O_3 and dewpoint average values for the same altitude block within a given latitude band were then averaged and are presented here as a function of latitude.

B. Horizontal Ozone and Dewpoint Data (1977)

Table 4 contains a tabulated summary of the 1977 GAMETAG free tropospheric and boundary layer ozone and dewpoint data. This table shows the average values for each two degree latitude band.

1. Free Tropospheric Ozone and Dewpoint Data (1977)

a. Ozone Data. Shown in Figure 14 through 17 are the free tropospheric ozone data collected during the 1977 GAMETAG

Table 4. 1977 GAMETAG Data Summary.

Latitude	Free Troposphere		Boundary Layer	
Block	O_3 (1)	DP (1)	O_3	DP
26°S	61	≤-39	32	+11
24°S	59	≤-38	-	-
22°S	56	≤-36	-	-
20°S	18	-15	-	-
18°S	18	-15	-	-
16°S	-	-	-	-
14°S	29	-14.5	21	+21.5
12°S	30	-15	-	-
10°S	32	-12	-	-
8°S	29	-13	20	+13.5
6°S	28	≤-18	-	-
4°S	29	-32	-	-
2°S	25	-28.5	21	+20
0	28	-23	20	+21
2°N	28	-27	21	+21
4°N	29	-16	-	-
6°N	34	-12	-	-
8°N	36	≤-20	-	-
10°N	41	-20	-	-
12°N	33	-21.5	20	+20
14°N	36	-28.5	-	-
16°N	45	-34	29	+19
18°N	42	≤-29	29	+19
20°N	39	-27	30	+16.5
22°N	58	-28	-	-
24°N	62	-33	-	-
26°N	54	≤-37.5	-	-
28°N	67	≤-33	-	-
30°N	63	≤-31	-	-

Table 4. Continued.

Latitude	Free Troposphere		Boundary Layer	
Block	O_3 (1)	DP (1)	O_3	DP
32°N	65	≤-28.5	49	+13
34°N	71	≤-32	-	-
36°N	49	≤-31.5	-	-
38°N	70	-32.5	-	-
40°N	47	-	67	-6
42°N	54	-28.5	63	-9
44°N	47	-	33	4
46°N	38	-20.5	32	2
48°N	40	-17.5	-	-
50°N	43	-21	-	-
52°N	55	-	-	-
54°N	56	-	-	-
56°N	52	≤-22.5	27	6
58°N	60	≤-21.5	24	2
60°N	133	-	28	3
62°N	49	-	28	-3
64°N	44	-14.5	-	-
66°N	30	-13	-	-
68°N	35	-15	31	7

(1) The units of O_3 and dewpoint are P.P.B.V. and degrees Celsius, respectively.

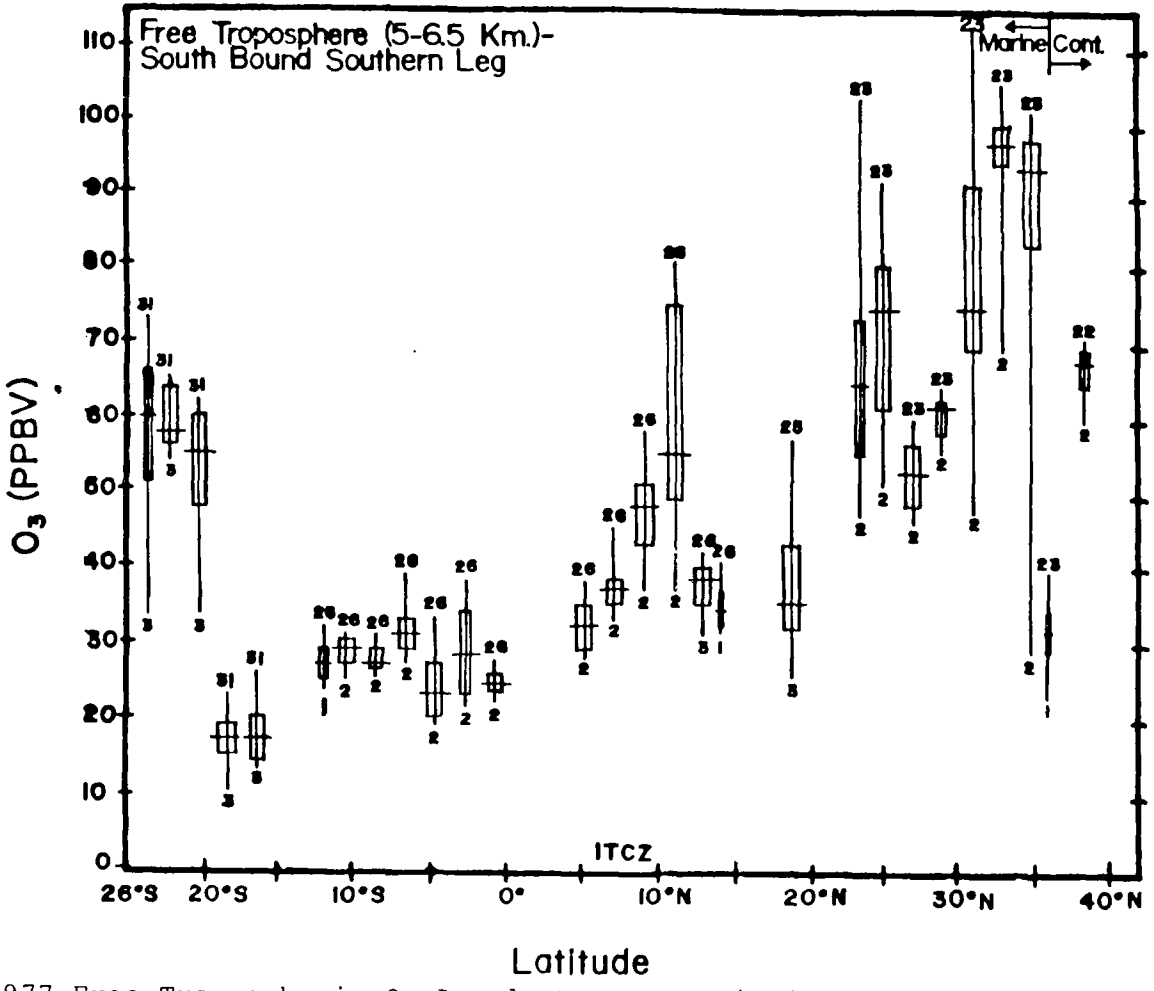

Figure 14. 1977 Free Tropospheric O_3 Levels Versus Latitude. Measurements are for flight tracks southbound from continental U.S.A. (August 22-31, 1977).

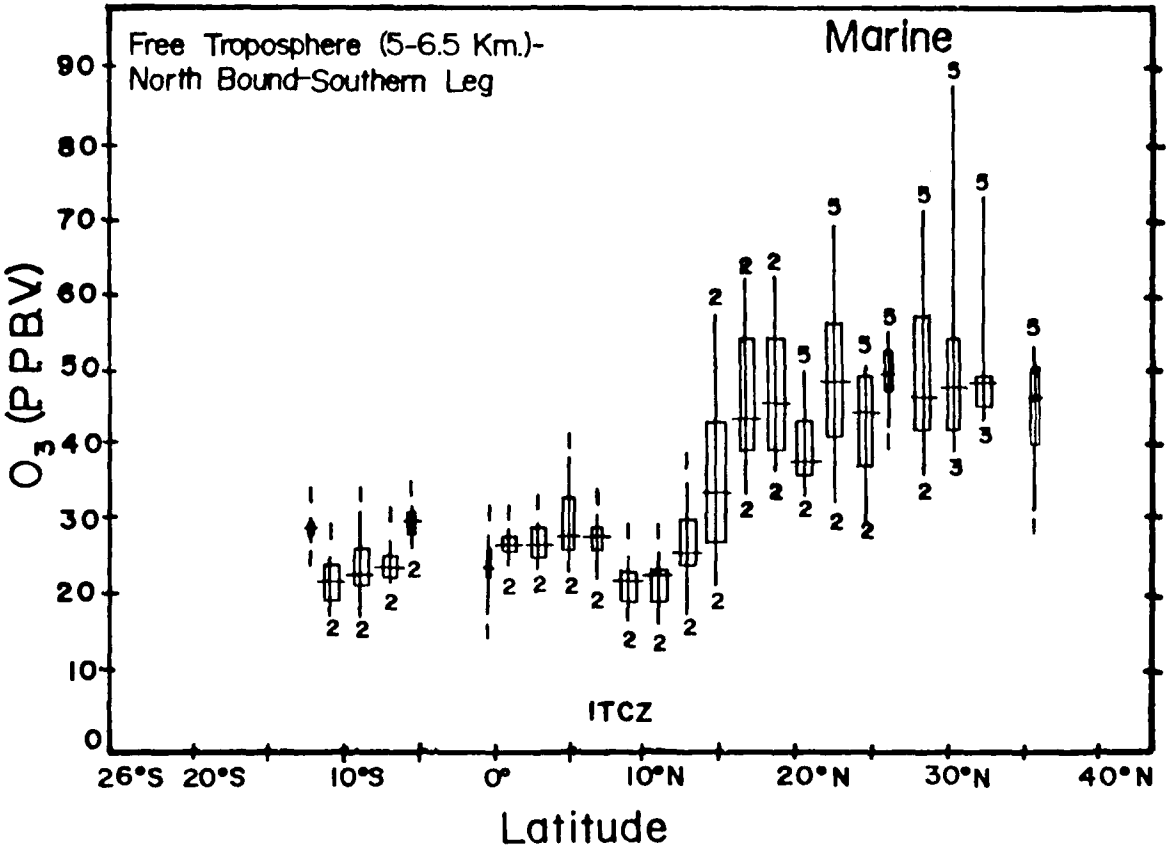

Figure 15. 1977 Free Tropospheric O_3 Levels Versus Latitude. Measurements are for flight tracks northbound from Pago Pago, American Samoa. (Sept. 15, 1977).

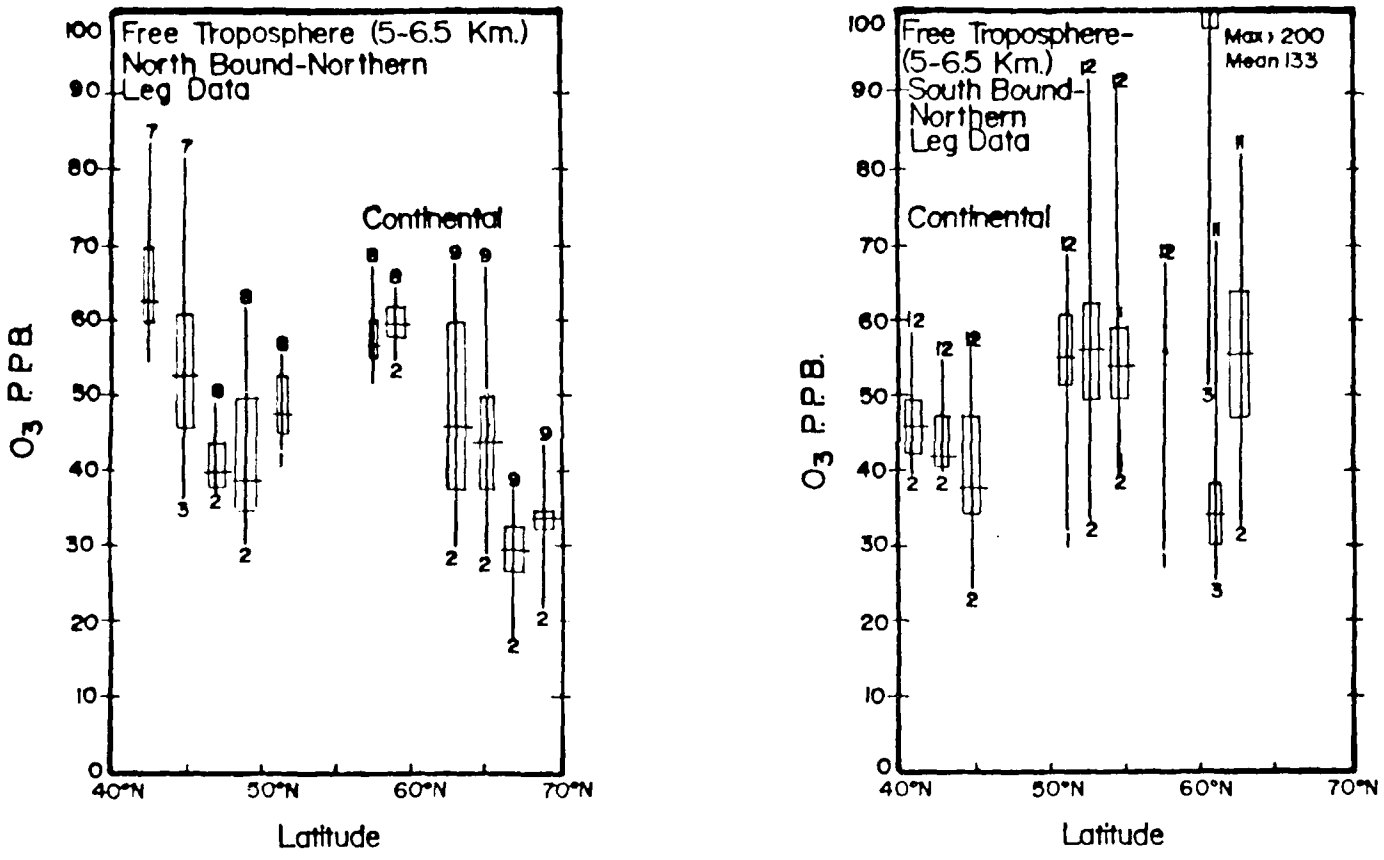

Figure 16. 1977 Free Tropospheric O_3 Levels Versus Latitude. Measurements are for flight tracks northbound from continental U.S.A. and southbound from Anchorage, Alaska. (Aug. 7-12, 1977)

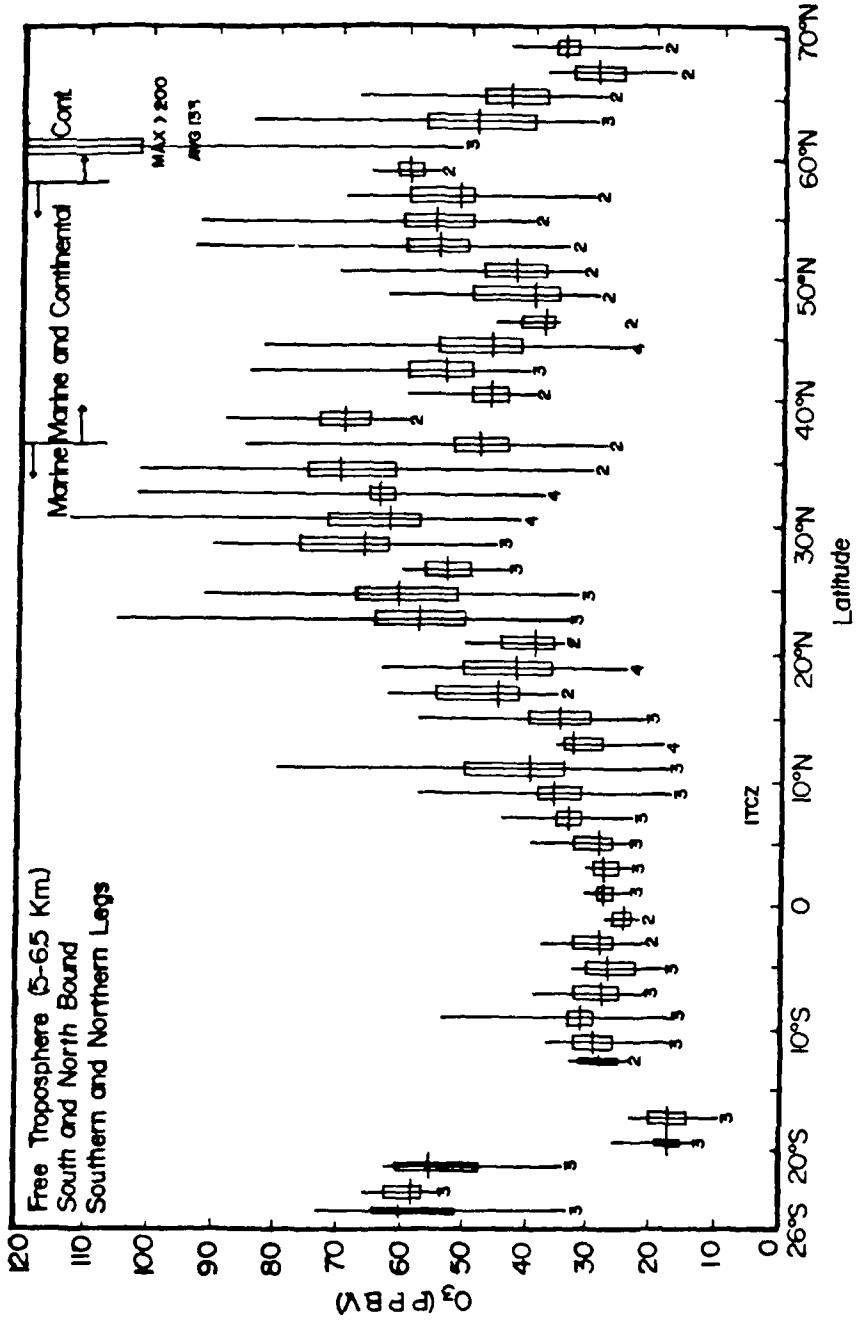

Figure 17. Summary Plot of all 1977 Free Tropospheric O_3 Data Versus Latitude. (Aug. 7-Sept. 6, 1977).

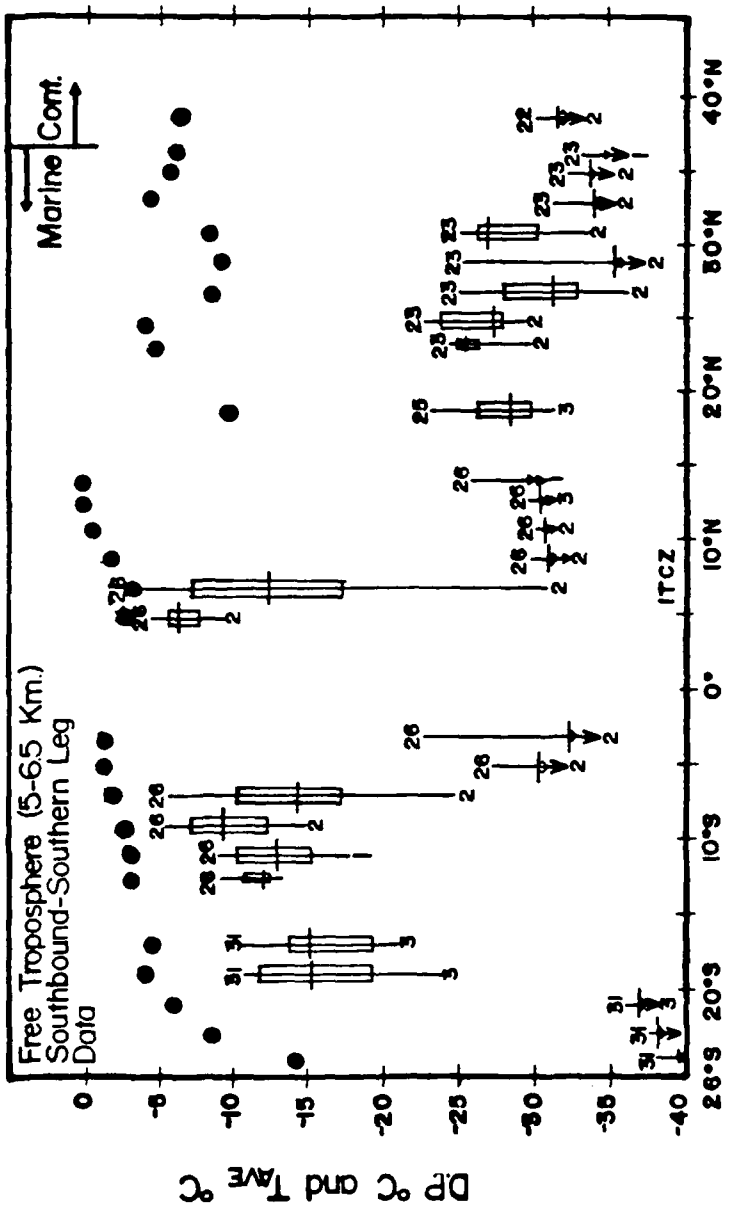

Figure 18. 1977 Free Tropospheric Dewpoint and Temperature Data Versus Latitude. Measurements are for flight tracks southbound from continental U.S.A. and round-robin flights from Samoa (Aug. 22-31, 1977).

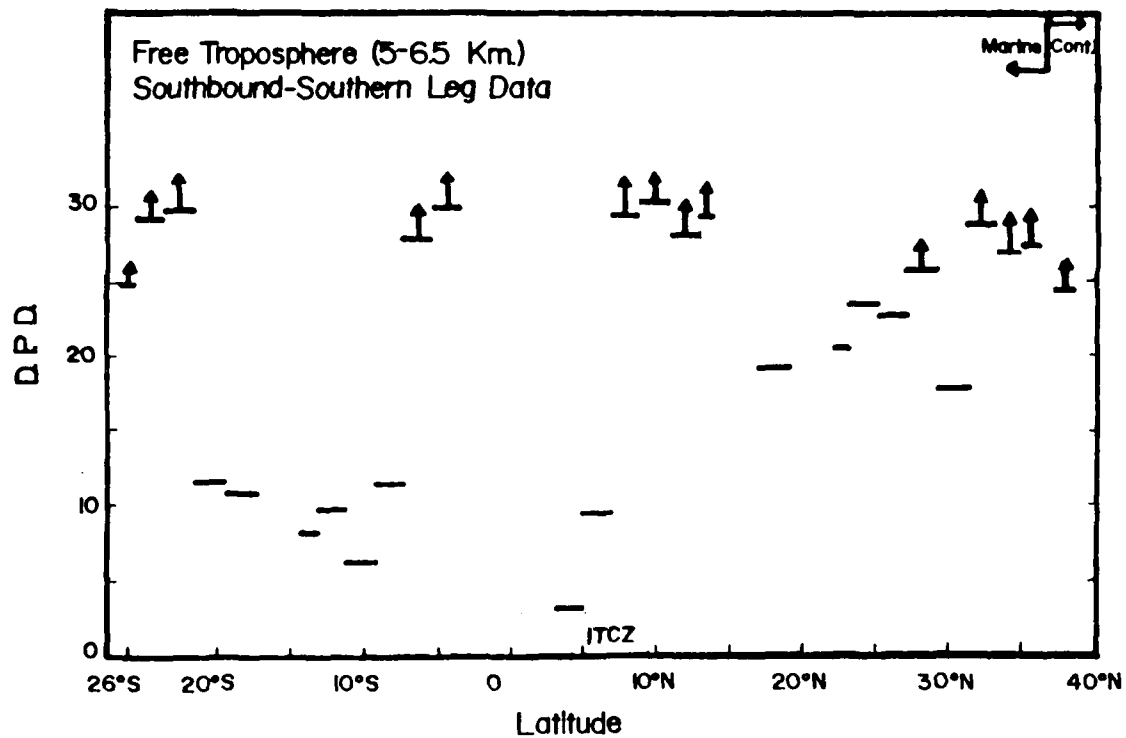

Figure 19. 1977 Free Tropospheric Dewpoint Depression Data Versus Latitude. Measurements are for flight tracks southbound from the continental U.S.A. and round-robin flights from Samoa (Aug. 22-31, 1977).

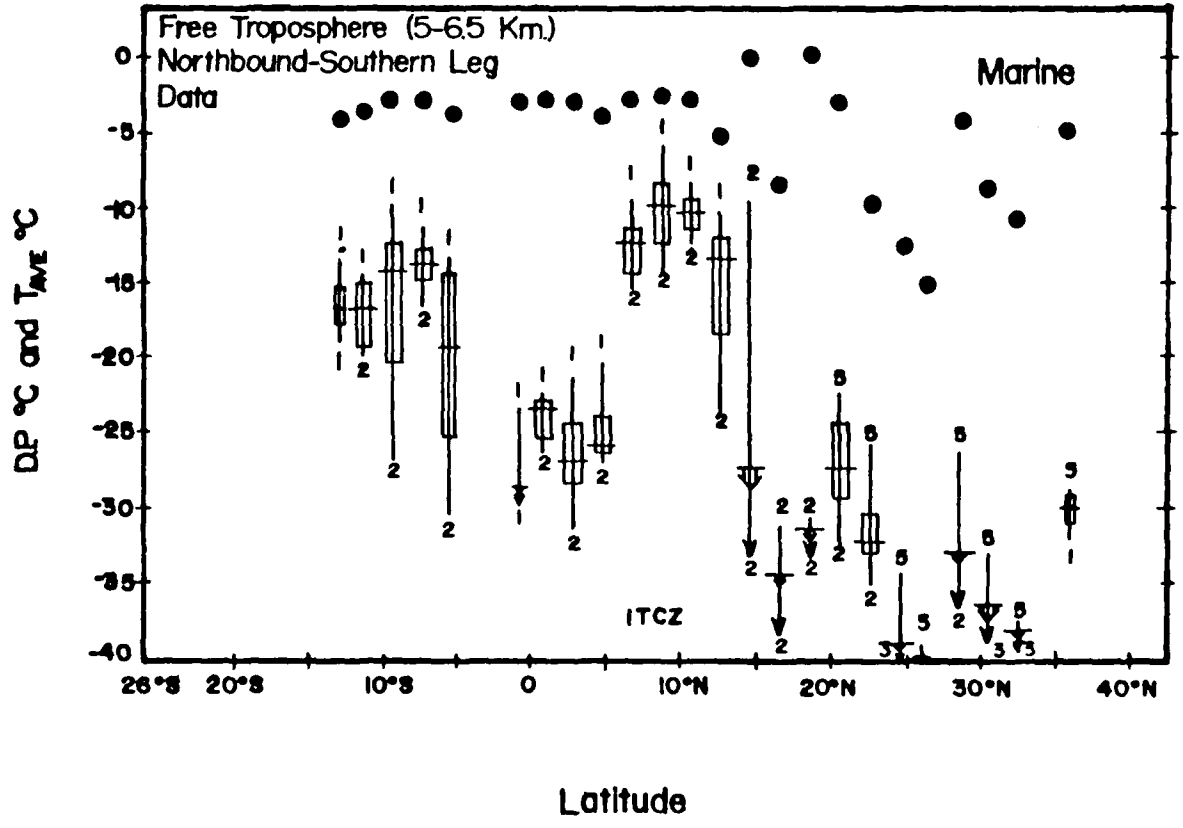

Figure 20. 1977 Free Tropospheric Dewpoint and Temperature Data Versus Latitude. Measurements are for flight tracks northbound from Samoa (Sept. 1-5, 1977).

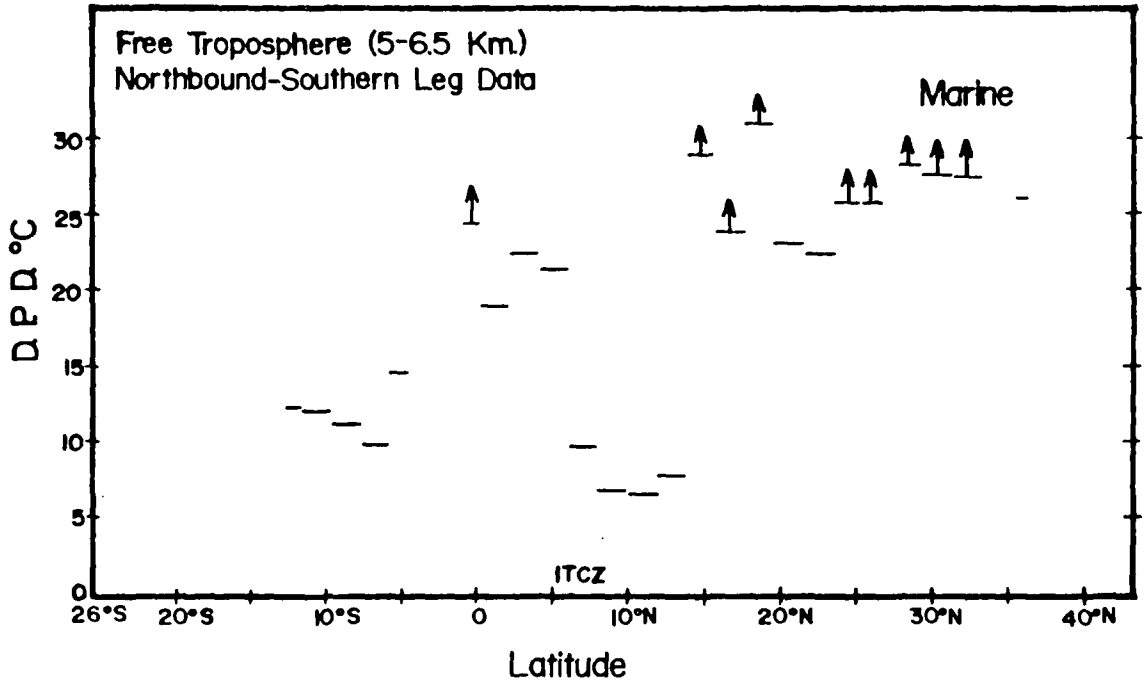

Figure 21. 1977 Free Tropospheric Dewpoint Depression Data Versus Latitude. Measurements are for flight tracks northbound from Samoa (Sept. 1-6, 1977).

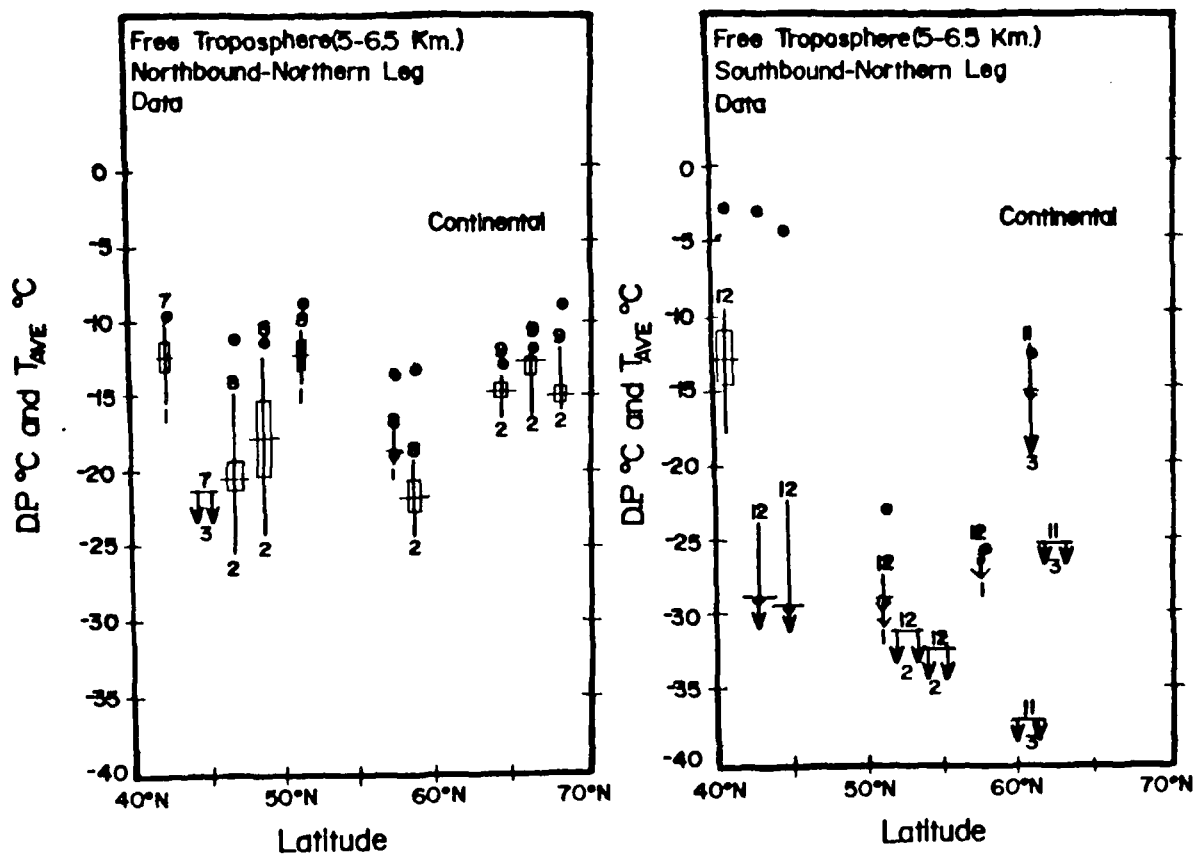

Figure 22. 1977 Free Tropospheric Dewpoint and Temperature Data Versus Latitude. Measurements are for flight tracks northbound from the continental U.S.A. and southbound from Anchorage, Alaska (Aug. 7-12, 1977).

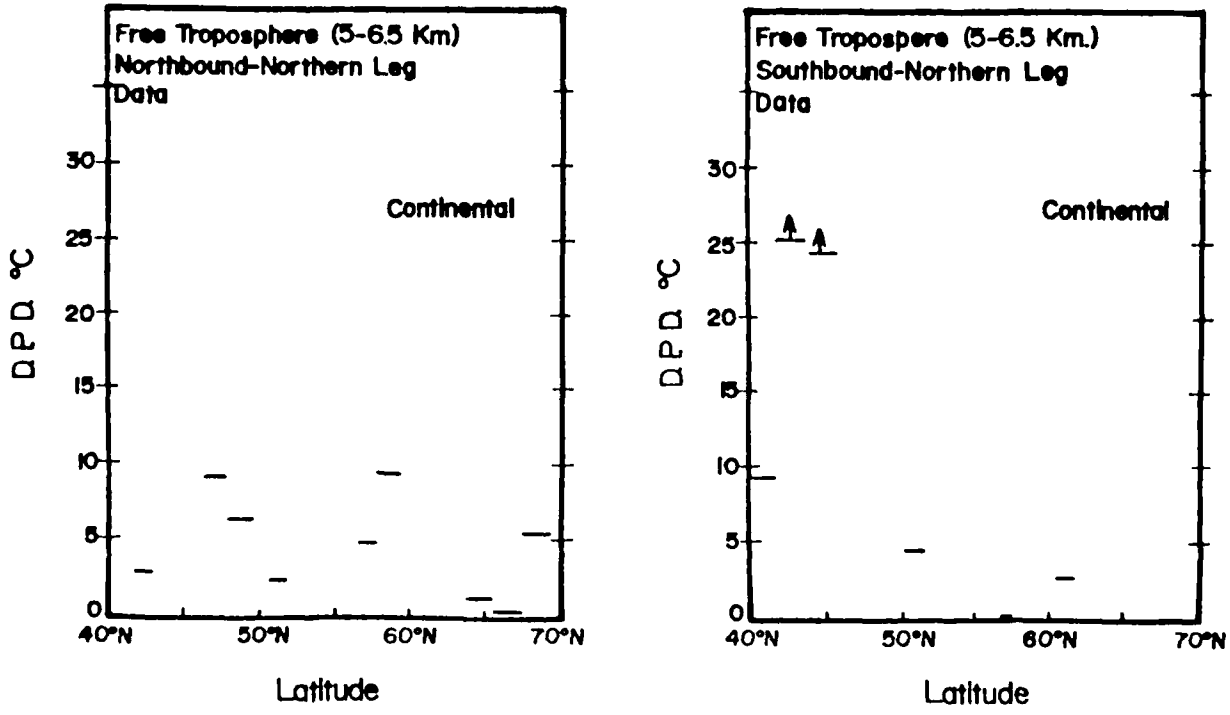

Figure 23. 1977 Free Tropospheric Dewpoint Depression Data Versus Latitude. Measurements are for flight tracks northbound from the continental U.S.A and southbound from Anchorage, Alaska (Aug. 7-12, 1977).

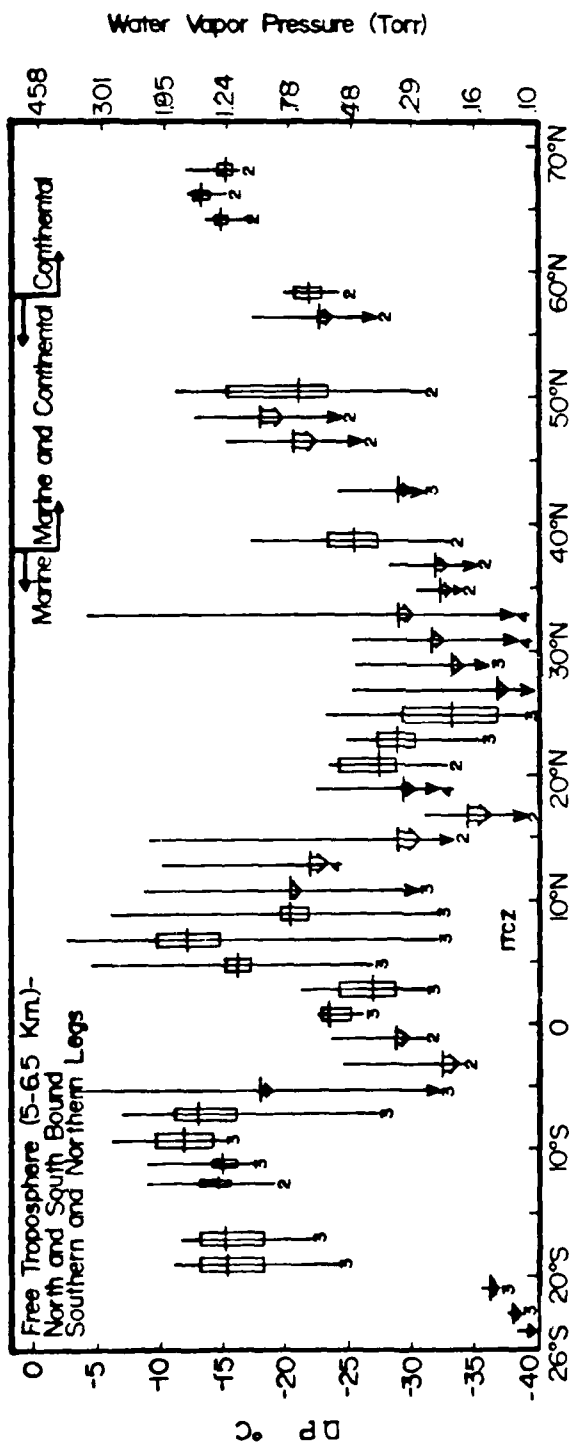

Figure 24. Summary of all 1977 Free Tropospheric Dewpoint Data Versus Latitude. Temperature and calendar dates are not indicated here (Aug. 7-Sept. 6, 1977).

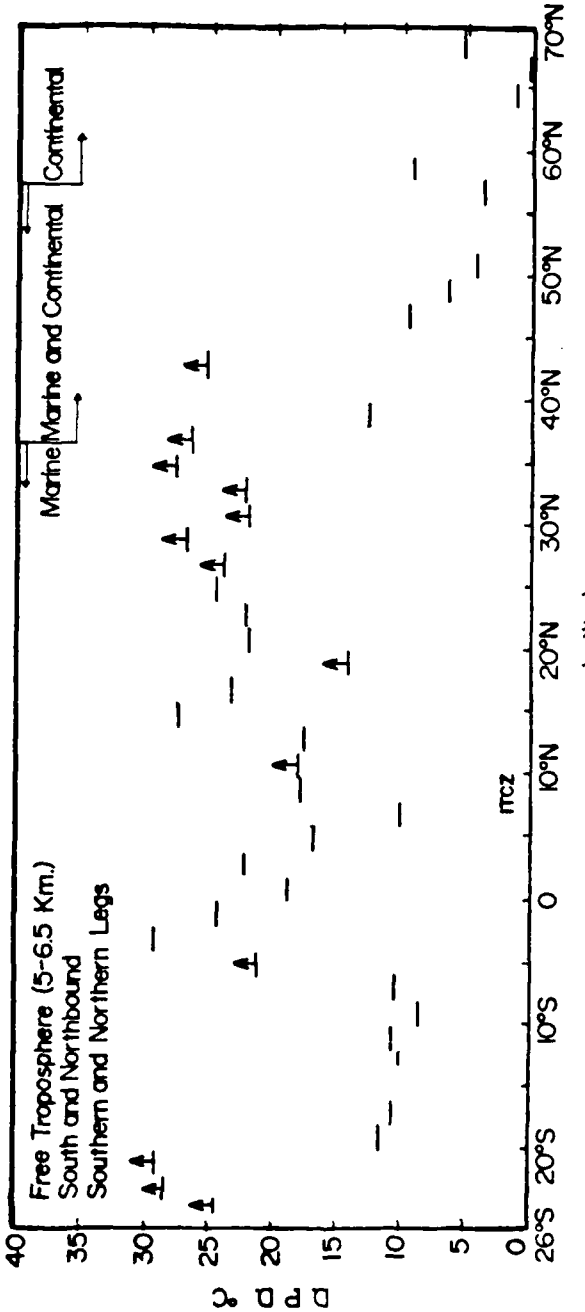

Figure 25. Summary of all 1977 Free Tropospheric Dewpoint Depression Data Versus Latitude (Aug. 7-Sept. 6, 1977).

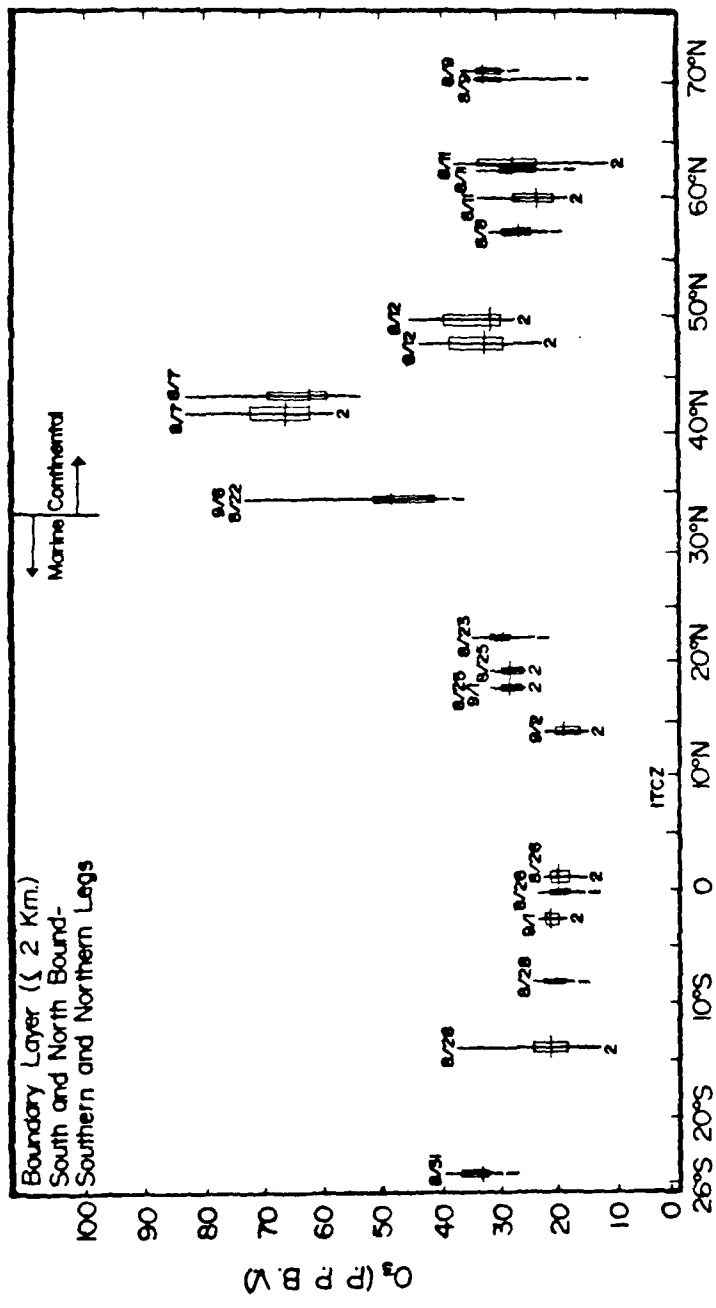

Figure 26. Summary of 1977 Boundary Layer O_3 Levels Versus Latitude (Aug. 7-Sept. 6, 1977).

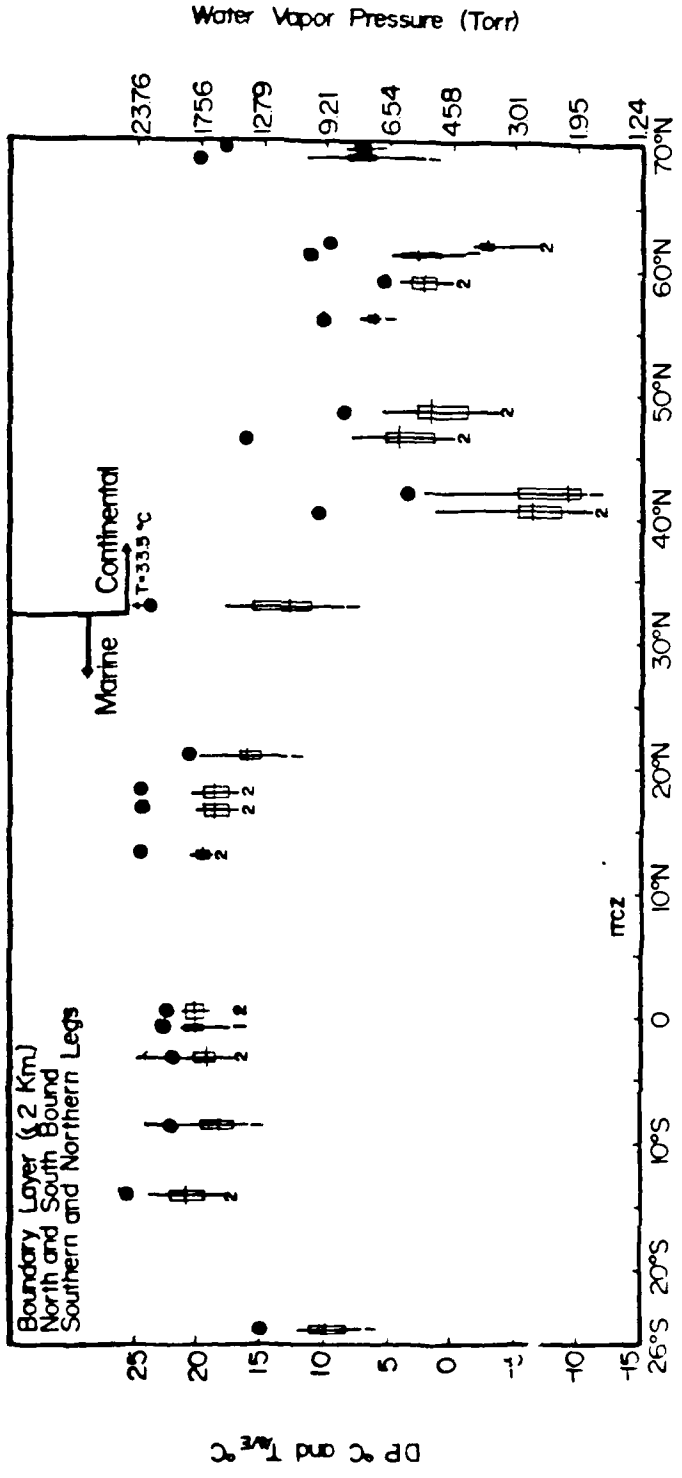

Figure 27. Summary of 1977 Boundary Layer Dewpoint and Temperature Versus Latitude. Calendar dates are not indicated (Aug. 7-Sept. 6, 1977).

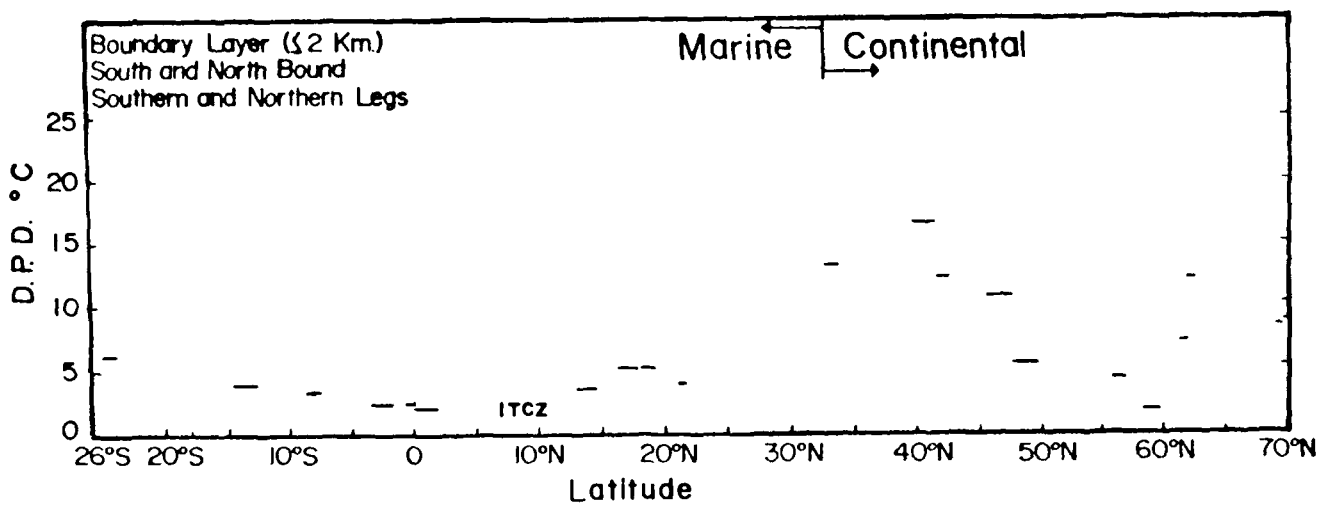

Figure 28. Summary of 1977 Boundary Layer Dewpoint Data Versus Latitude. Calendar dates are not indicated (Aug. 7-Sept. 6, 1977).

field experiment. Figures 14 and 15 display the ozone data collected from the south and northbound flights over the Pacific Ocean; whereas Figure 16 shows data collected during flights north of Denver, Colorado. Figure 17 is a summary of all 1977 free tropospheric ozone data.

Figures 14 through 17 show that the ozone concentration is more variable in the subtropical, middle, and high latitudes than in the equatorial region (15°S to 12°N). The northern hemispheric subtropical ozone concentration, observed during the period of August 22 to 26, display a greater variability and higher concentrations (115 ppbv-23 ppbv) than those values observed on the return trip (September 1-5) (87 ppbv-31 ppbv). Southern hemispheric subtropical O_3 concentrations (~55 ppbv) measured on August 31 are approximately equal to the northern hemispheric subtropical average values found on the southbound southern leg and 8-10 ppbv higher than those collected on the northbound southern leg flights through this region. From Figure 17, ozone maxima can be seen near 25°S, 35°N, and 60°N (measured during the southbound northern leg). Besides the tropical ozone minima, low ozone concentrations are also evident near 45°N and 66°N (measured during the northbound northern leg). Average ozone values north of 15°N and south of 20°S are approximately 1.8 times higher than those in the equatorial region (20°S-15°N). The single highest ozone concentration (~200 ppbv) was recorded over northern Canada on August 11.

b. Dewpoint and Dewpoint Depression Data. Figures 18 through 25 show free tropospheric dewpoint and dewpoint depression data collected during 1977 GAMETAG flights from August 7 to September 6. Dewpoint and dewpoint depression data, collected at the same time, are displayed consecutively. The first four figures, presented here, show data recorded over the Pacific Ocean; the following two plots involve data collected north of Denver; and finally, the last two figures are summary plots of all data from 1977.

The 1977 free tropospheric dewpoint data have a pronounced peak ranging from 7°S to 7°N, measured during both north and southbound flights, and individual maximums found during the northbound northern leg at 48°N and at 65°N. Low dewpoints are also evident at 26°S (August 31) 0° (southern leg both directions), 18°N (northbound southern leg), 26°N (northbound southern leg), and 56°N (southbound northern leg). The major variability in dewpoint can be seen to occur in the tropics and subtropics; the tropical dewpoint variability is the larger of the two and can be seen during both north and southbound flights. Almost one quarter of this entire data base has been identified as upper limit dewpoint data.

The 1977 free tropospheric dewpoint depression data have peaks near 22°S (August 31), 2°S (north and southbound southern leg), 25°N (southbound southern leg), 30°N (both directions southern leg), and 56°N (southbound northern leg)

and minimum values in the region between 20°S and 5°S, and at ∿5°N, 50°N, and 65°N. The minimum values were consistently found during flights in both directions over the given latitudinal positions.

2. Boundary Layer Ozone and Dewpoint Data (1977)

a. Ozone Data. The 1977 boundary layer ozone data are shown in Figure 26. Minimum ozone values are indicated near the equator with an almost symmetrical increase at both northern and southern latitudes. Higher O_3 concentrations (50-75 ppbv) between 35°N and 42°N can be seen for data collected during low level flight tracks over the western regions of the United States. These are the only 1977 boundary layer O_3 concentrations that approach free tropospheric levels. These high ozone levels appear to reflect a significant anthropogenic input.

b. Dewpoint and Dewpoint Depression Data. All the 1977 boundary layer dewpoint and dewpoint depression data are presented in Figures 27 and 28. These figures show high dewpoint between 15°S and 18°N.

C. Horizontal Ozone and Dewpoint Data (1978)

Table 5 contains a tabulated summary of the 1978 Project GAMETAG free tropospheric and boundary layer ozone and dewpoint data. This table shows the average values for each two degree latitude band.

Table 5. 1978 GAMETAG Data Summary.

Latitude	Free Troposphere		Boundary Layer	
Block	O_3 (1)	DP (1)	O_3	DP
60°S	-	-	-	-
58°S	38	-33	-	-
56°S	44	≤-37	-	-
54°S	39	≤-36	-	-
52°S	39	≤-36	-	-
50°S	38	≤-34.5	-	-
48°S	34	≤-38	32	+5
46°S	35	≤-38	35	-2
44°S	-	-	-	-
42°S	38	≤-36.5	-	-
40°S	37	≤-36	-	-
38°S	33	≤-38	-	-
36°S	31	≤-40	-	-
34°S	-	-	33	+11
32°S	-	-	32	+11
30°S	37	≤-31.5	34	+12.5
28°S	38	≤-31.5	31	+17.5
26°S	38	≤-20	-	-
24°S	31	≤-22	-	-
22°S	30	≤-22	-	-
20°S	39	≤-23	-	-
18°S	30	≤-18	27	+16
16°S	-	-	18	+22.5
14°S	27	≤-29.5	11	+21.5
12°S	27	≤-24	2	+22.5
10°S	26	≤-23	-	-
8°S	25	≤-23	-	-
6°S	26	≤-23	4	+22.5
4°S	-	-	4	+23.5

Table 5. Continued.

Latitude	Free Troposphere		Boundary Layer	
Block	O_3 (1)	DP (1)	O_3	DP
2°S	-	-	3	+22
0	22	-19	3	+22
2°N	23	-17.5	-	-
4°N	23	-19	-	-
6°N	25	-17	-	-
8°N	25	-15.5	18	+21.5
10°N	28	-16.5	-	-
12°N	43	-22	-	-
14°N	60	$\leq$-27.5	20	+20
16°N	61	-30	22	+20
18°N	60	$\leq$-27	27	+20
20°N	42	$\leq$-37	-	-
22°N	41	$\leq$-34	-	-
24°N	48	-29.5	-	-
26°N	46	$\leq$-28	-	-
28°N	54	$\leq$-25	-	-
30°N	51	$\leq$-32	-	-
32°N	48	$\leq$-34.5	75	0
34°N	47	$\leq$-34	-	-
36°N	64	-34.5	-	-
38°N	61	$\leq$-38	-	-
40°N	90	-37	-	-
42°N	59	-33	-	-
44°N	49	$\leq$-36.5	-	-
46°N	40	-36	36	-4.5
48°N	43	-27.5	-	-
50°N	37	-28.5	-	-
52°N	44	$\leq$-33.5	47	-3.5
54°N	-	-	44	-1.5

Table 5. Continued.

Latitude	Free Troposphere		Boundary Layer	
Block	O_3 (1)	DP (1)	O_3	DP
56°N	44	-35	40	-3.5
58°N	31	-31	-	-
60°N	37	-34	40	-6.5
62°N	42	-30.5	38	-7
64°N	47	-33	37	-7
66°N	-	-	33	-3
68°N	-	-	35	-7

(1) The units of O_3 and dewpoint are ppbv and degrees Celsius, respectively.

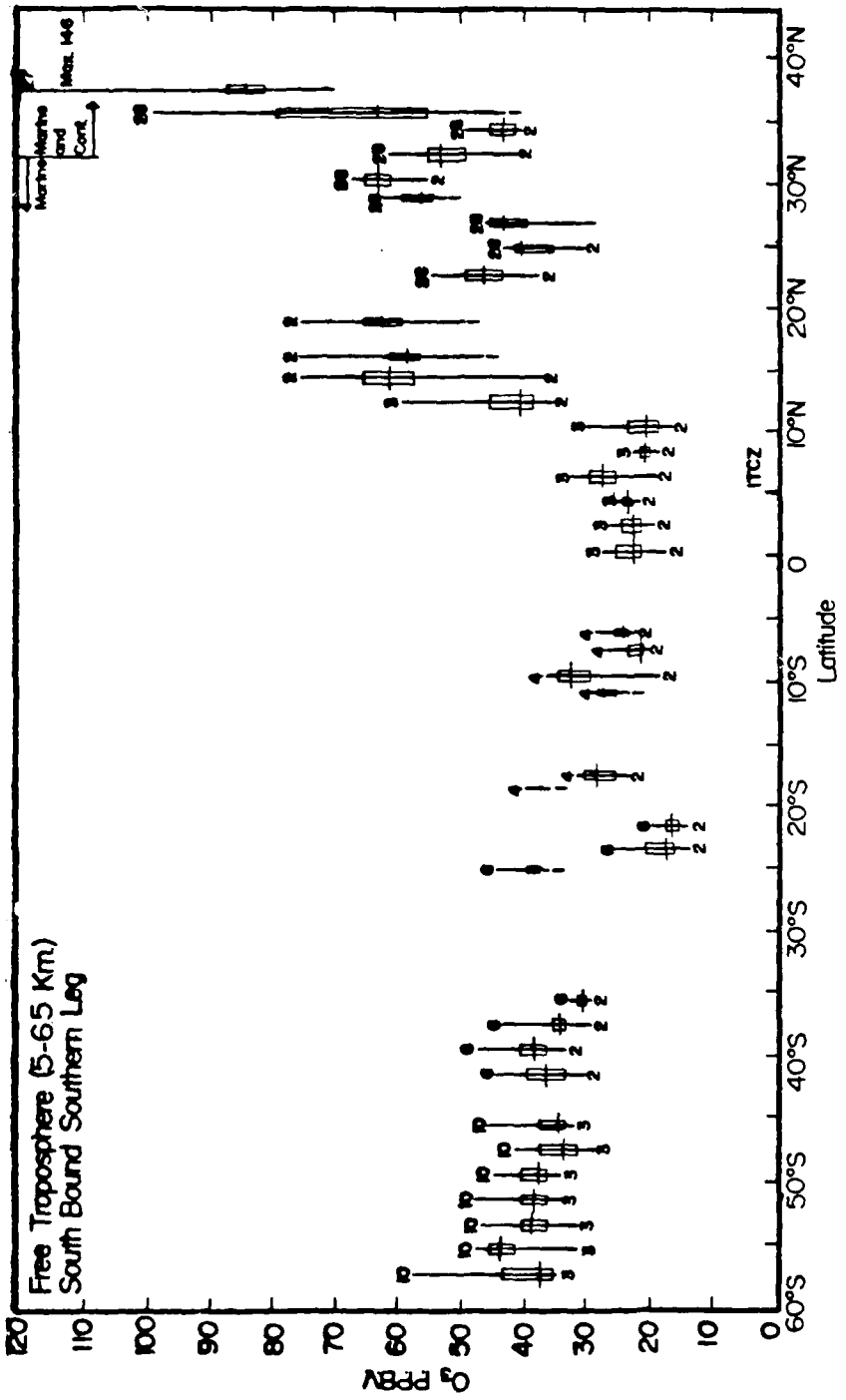

Figure 29. 1978 Free Tropospheric O_3 Levels Versus Latitude. Measurements are for flight tracks southbound from continental U.S.A. (Apr. 27-May 10, 1978).

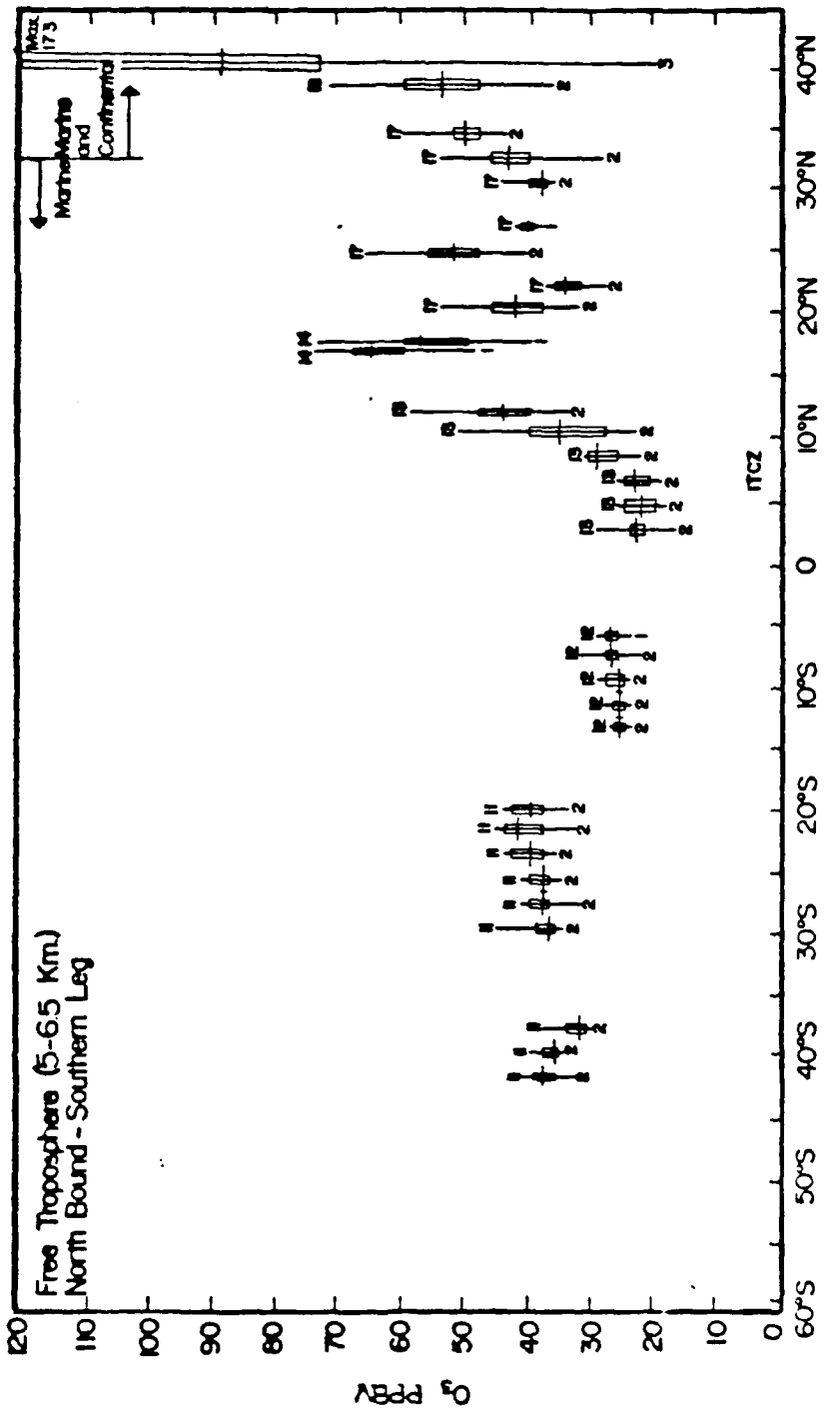

Figure 30. 1978 Free Tropospheric O_3 Levels Versus Latitude. Measurements are for flight tracks northbound from Christchurch, New Zealand (May 11-18, 1978).

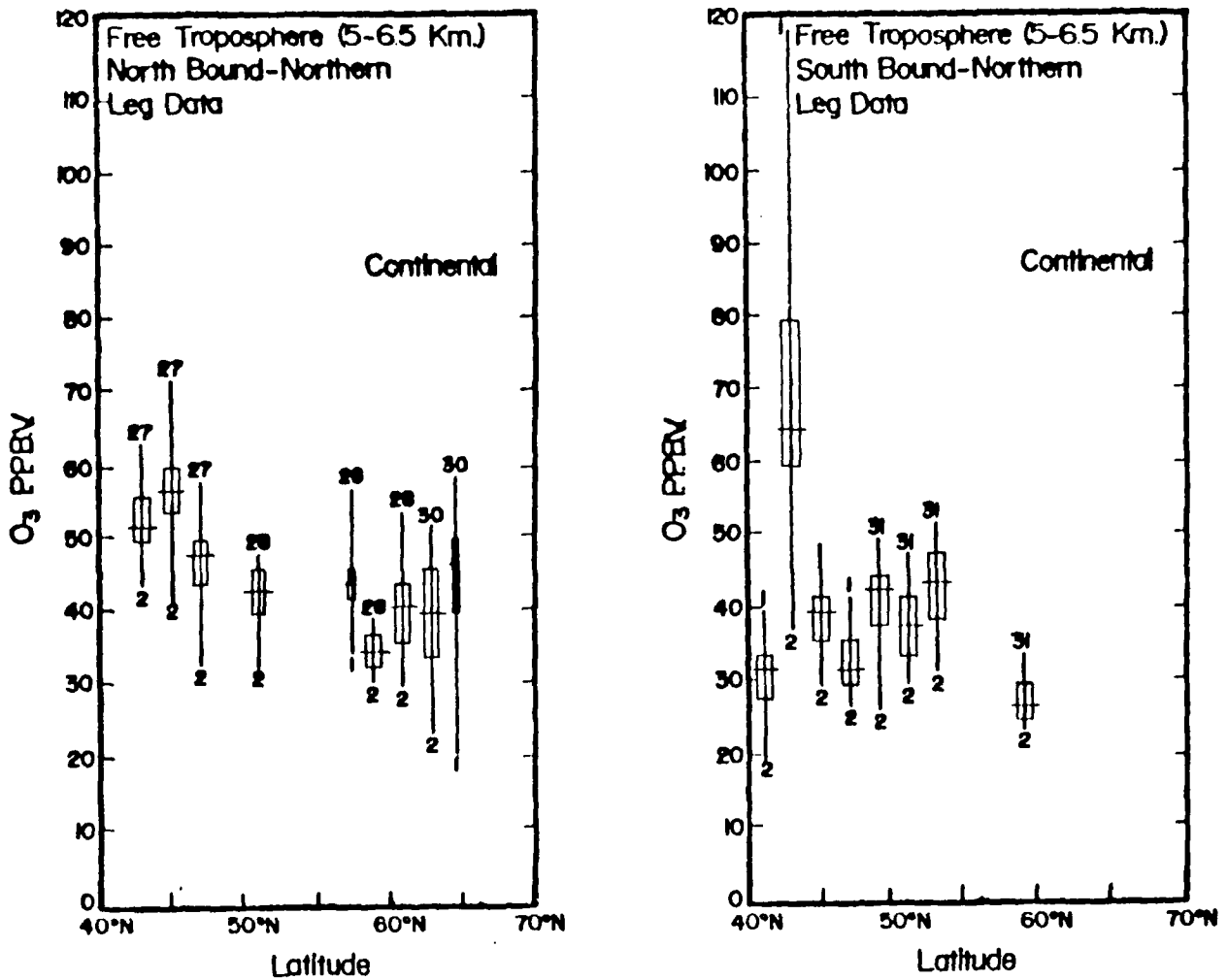

Figure 31. 1978 Free Tropospheric O_3 Levels Versus Latitude. Measurements are for flight tracks northbound from continental U.S.A. and southbound from Whitehorse, Canada (May 27-June 1, 1978).

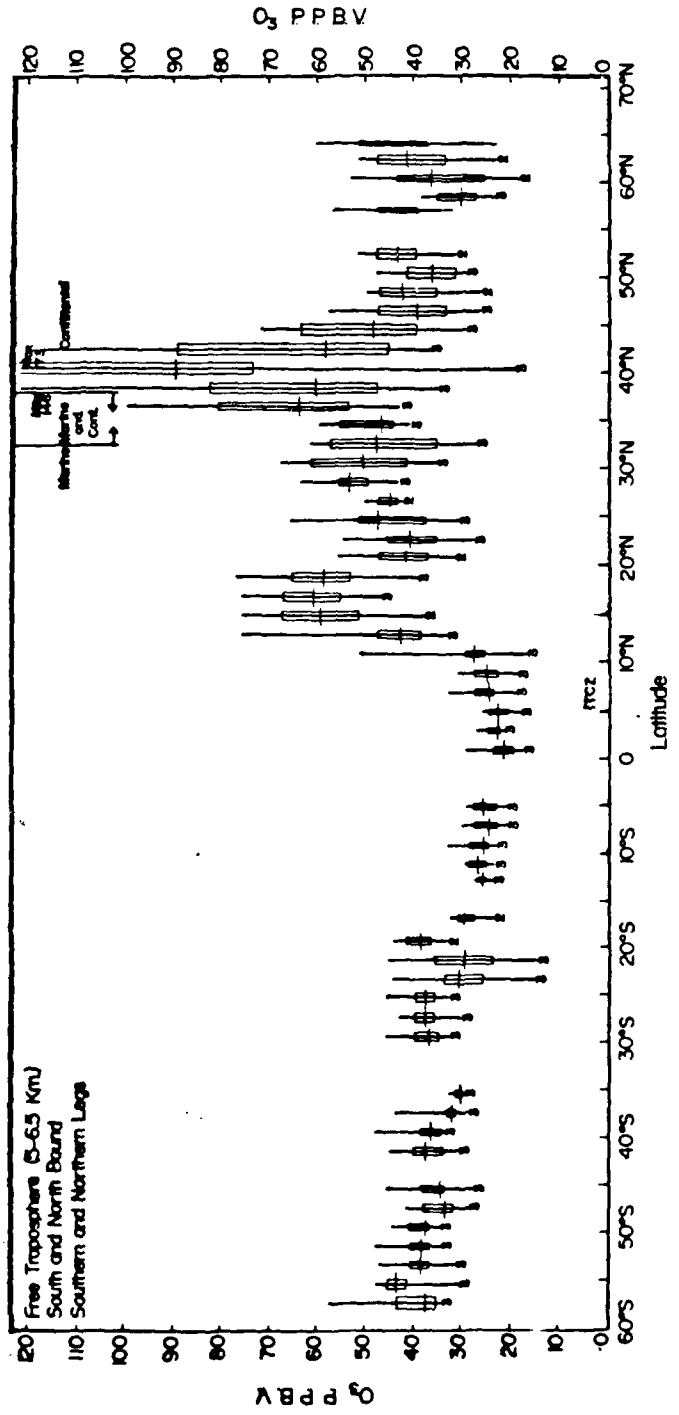

Figure 32. Summary Plot of all 1978 Free Tropospheric O_3 Data Versus Latitude (Apr 27-June 1, 1978).

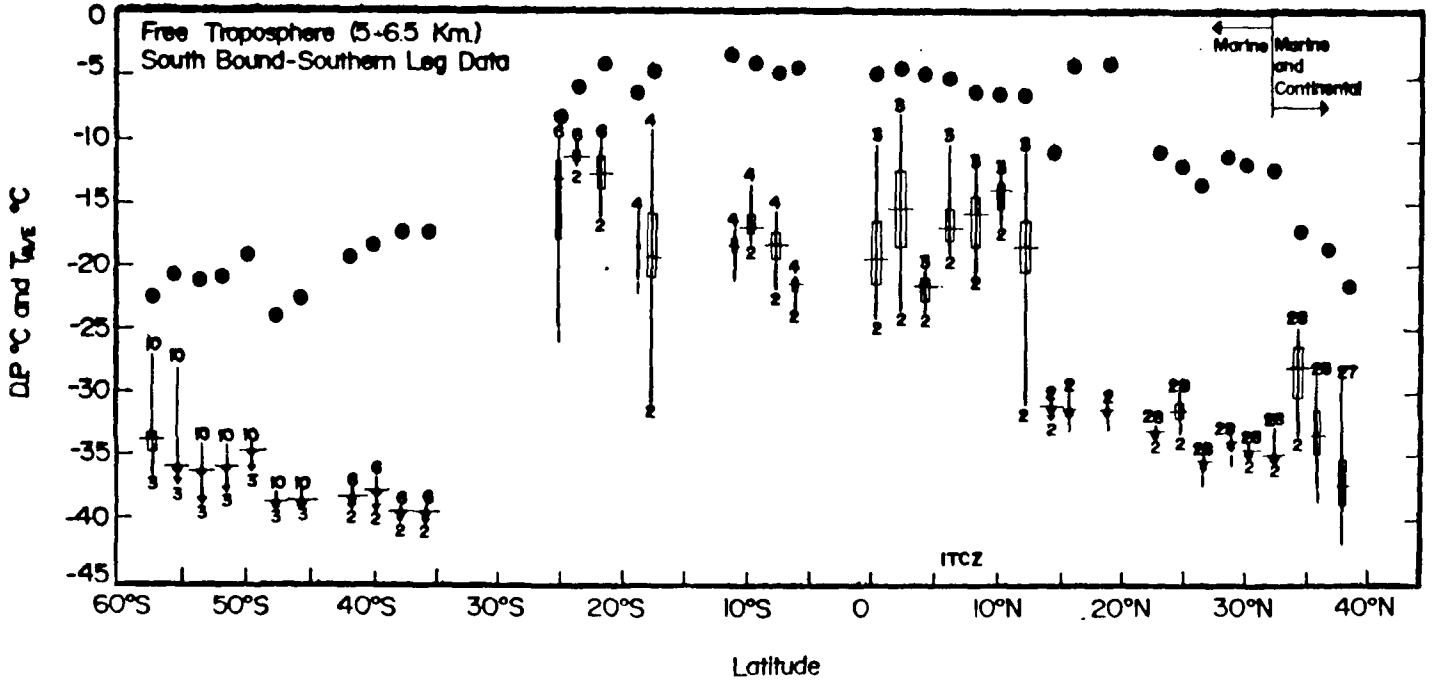

Figure 33. 1978 Free Tropospheric Dewpoint and Temperature Data Versus Latitude. Measurements are for flight tracks southbound from the continental U.S.A. and Christchurch, New Zealand (Apr. 27-May 10, 1978).

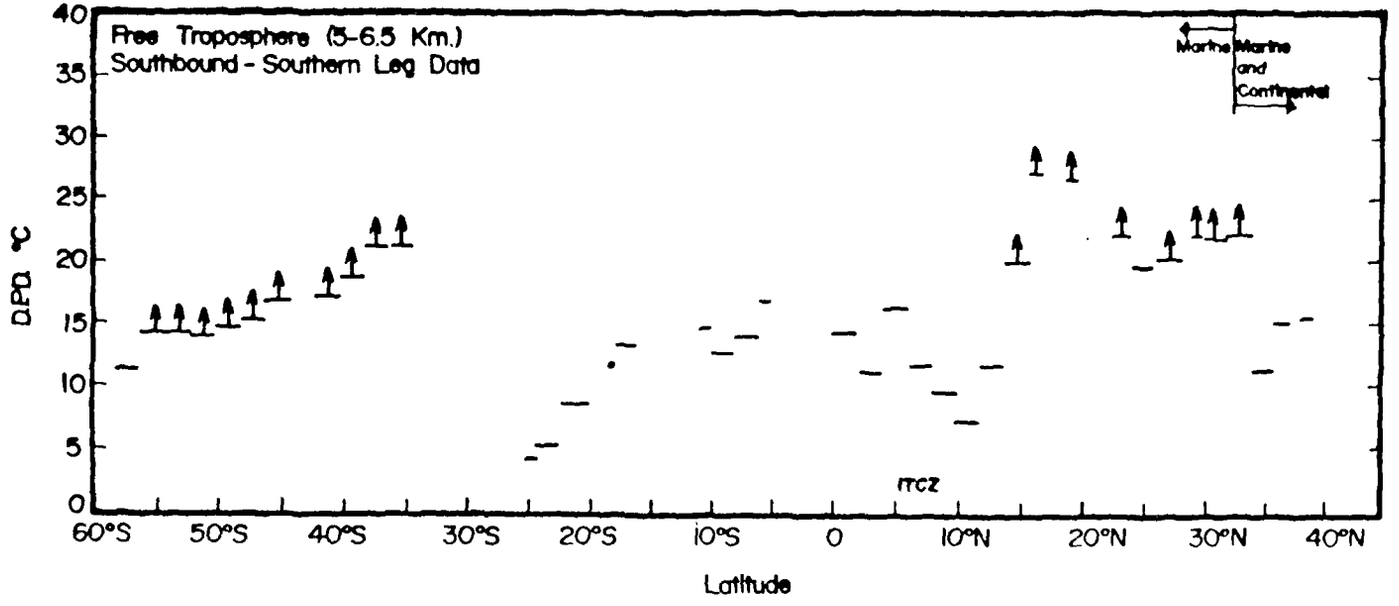

Figure 34. 1978 Free Tropospheric Dewpoint Depression Data Versus Latitude. Measurements are from flight tracks southbound from the continental U.S.A. and Christchurch, New Zealand (Apr. 27-May 10, 1978).

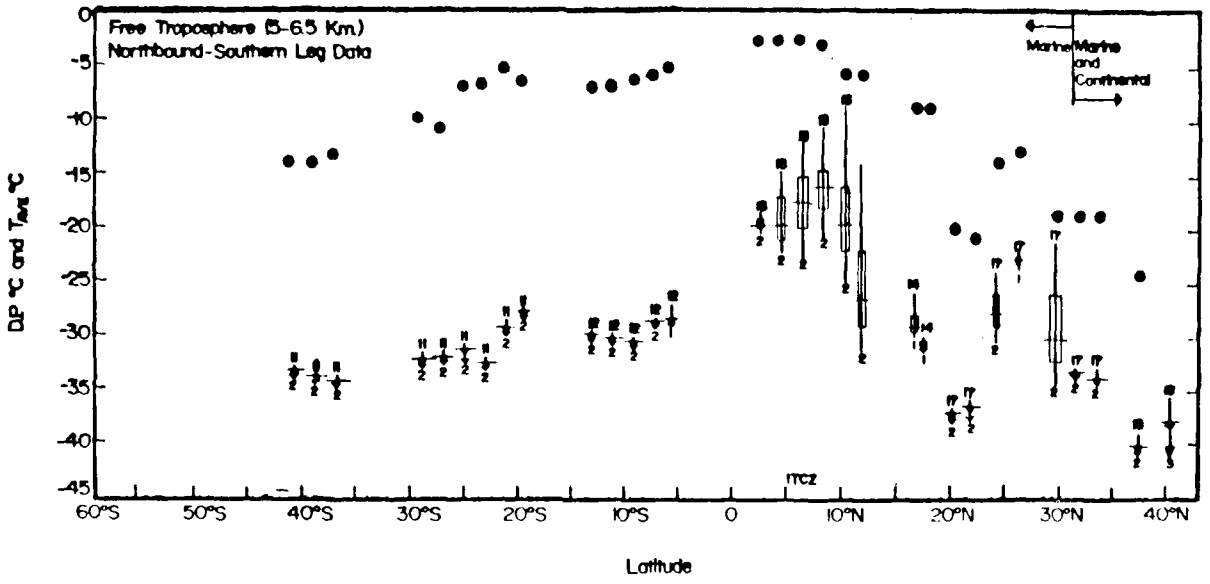

Figure 35. 1978 Free Tropospheric Dewpoint and Temperature Data Versus Latitude. Measurements are for flight tracks northbound from New Zealand (May 11-18, 1978).

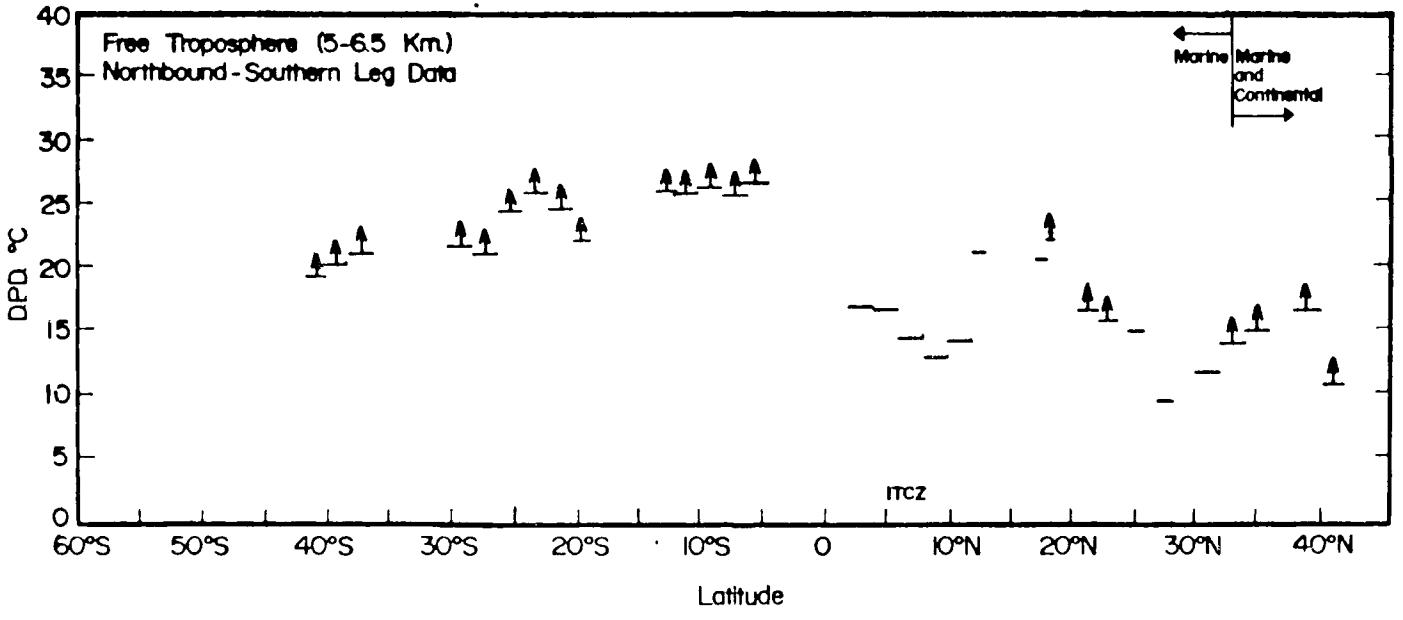

Figure 36. 1978 Free Tropospheric Dewpoint Depression Data Versus Latitude. Measurements are for flight tracks northbound from New Zealand (May 11-18, 1978).

AD-A092 518 AIR FORCE INST OF TECH WRIGHT-PATTERSON AFB OH F/G 4/2
LATITUDINAL AND VERTICAL RELATIONSHIP BETWEEN TROPOSPHERIC OZON--ETC(U)
JUN 80 F X ROUTHIER
UNCLASSIFIED AFIT-CI-80-18T NL

2 OF 3
AD A 092518

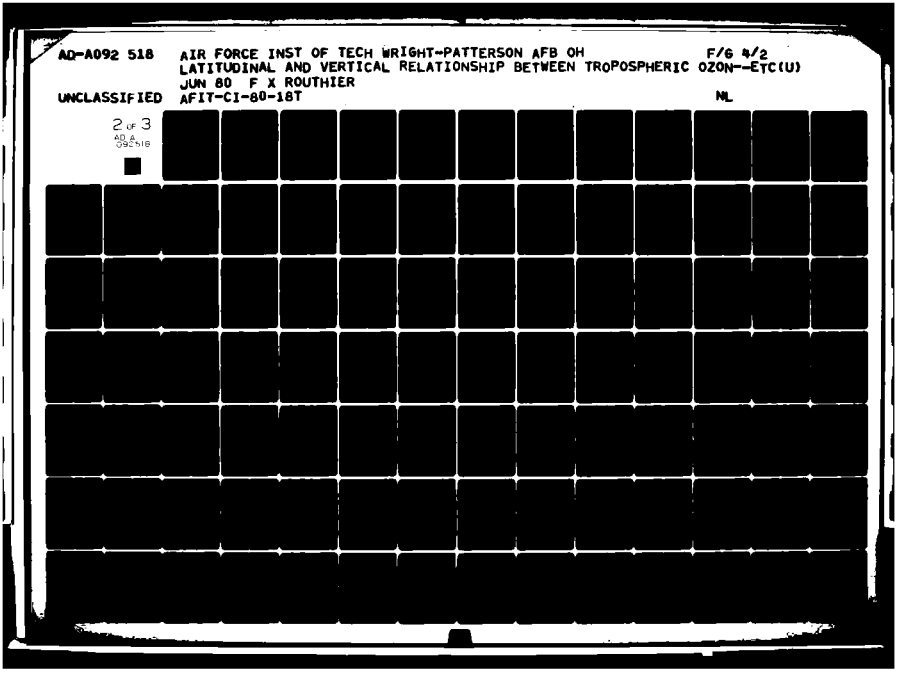

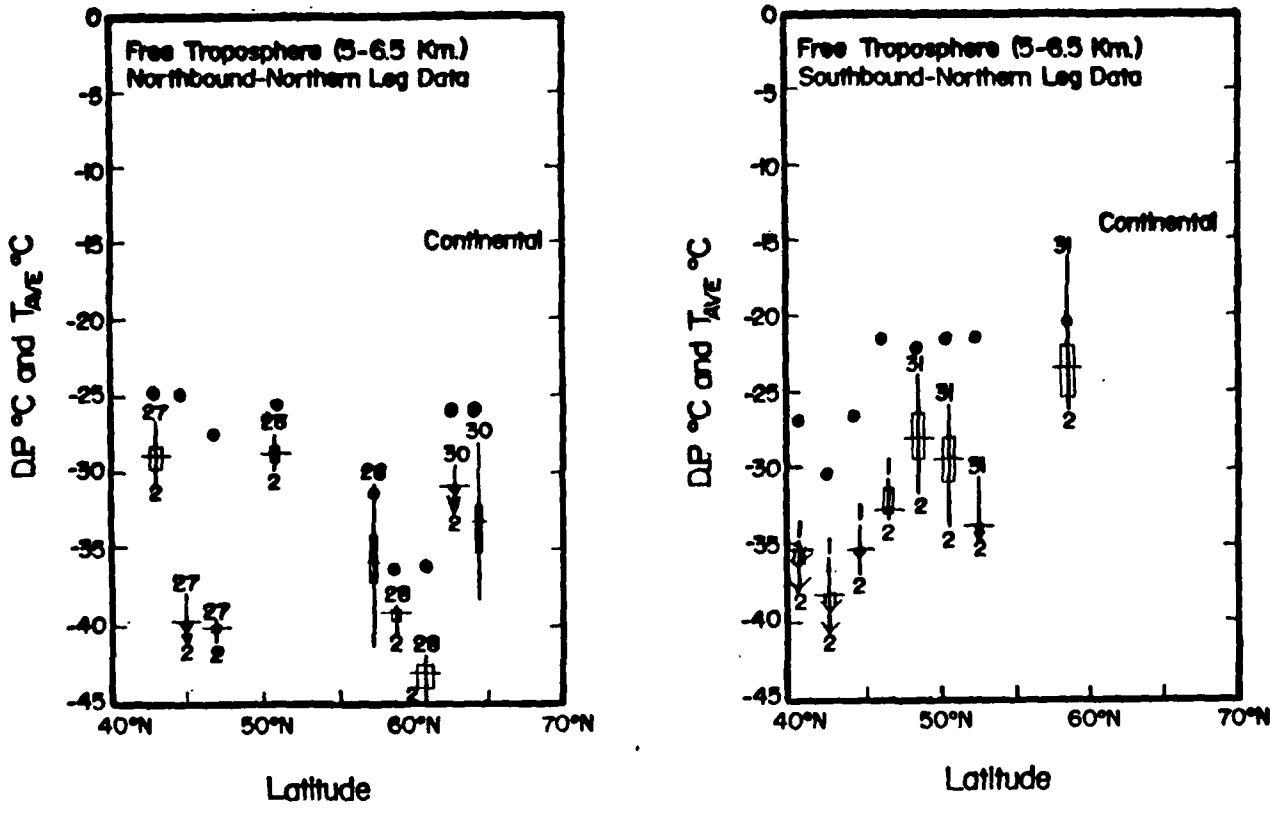

Figure 37. 1978 Free Tropospheric Dewpoint and Temperature Data Versus Latitude. Measurements are for flight tracks northbound from the continental U.S.A. and southbound from Whitehorse, Canada (May 27-June 1, 1978).

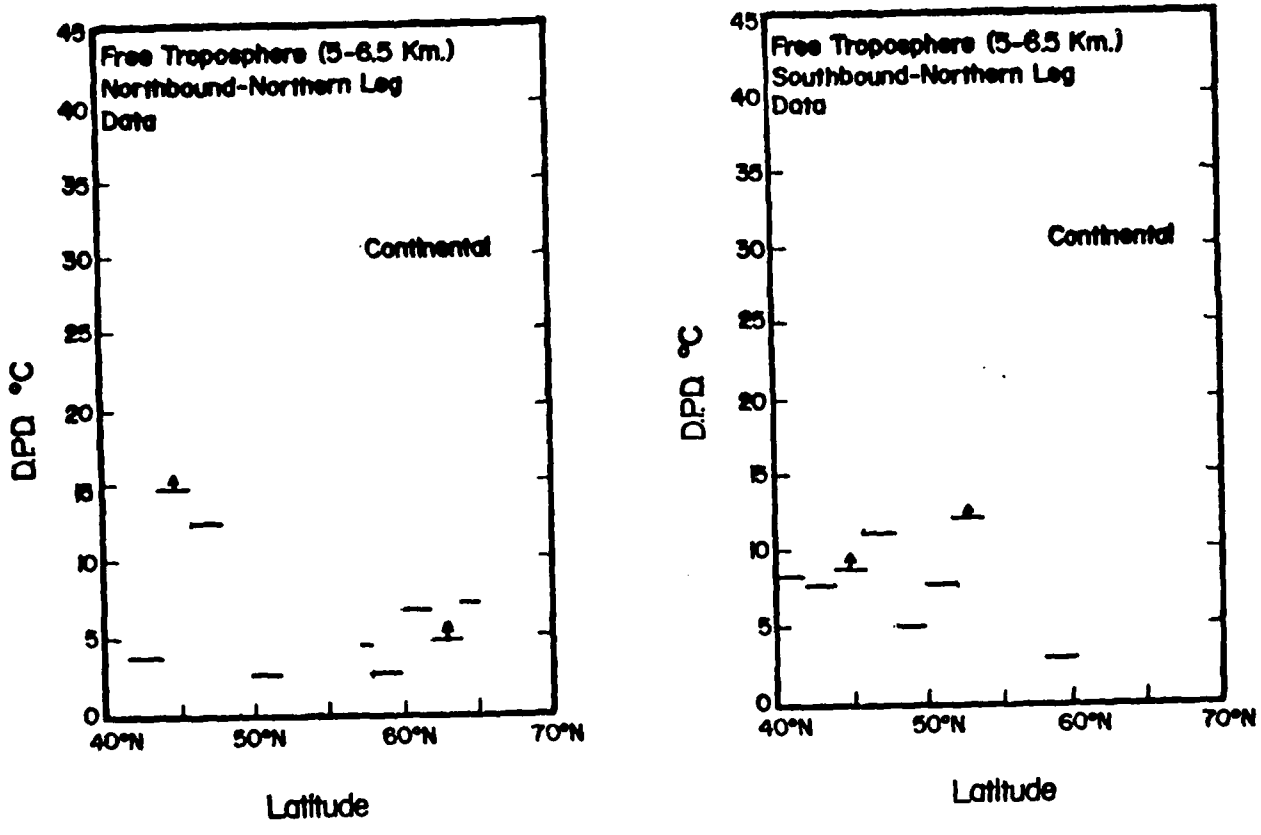

Figure 38. 1978 Free Tropospheric Dewpoint Depression Versus Latitude. Measurements are for flight tracks northbound from the continental U.S.A. and southbound from Whitehorse, Canada (May 27-June 1, 1978).

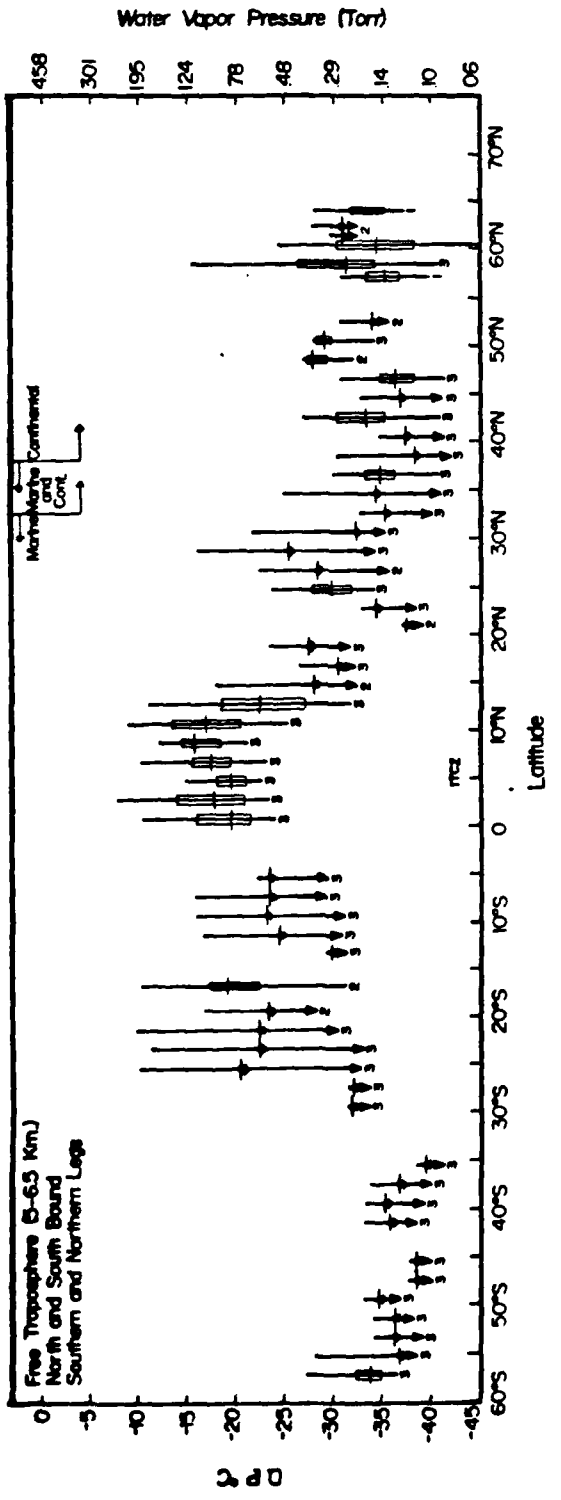

Figure 39. Summary of 1978 Free Tropospheric Dewpoint Versus Latitude. Temperature and calendar dates are not indicated (Apr. 27-June 1, 1978).

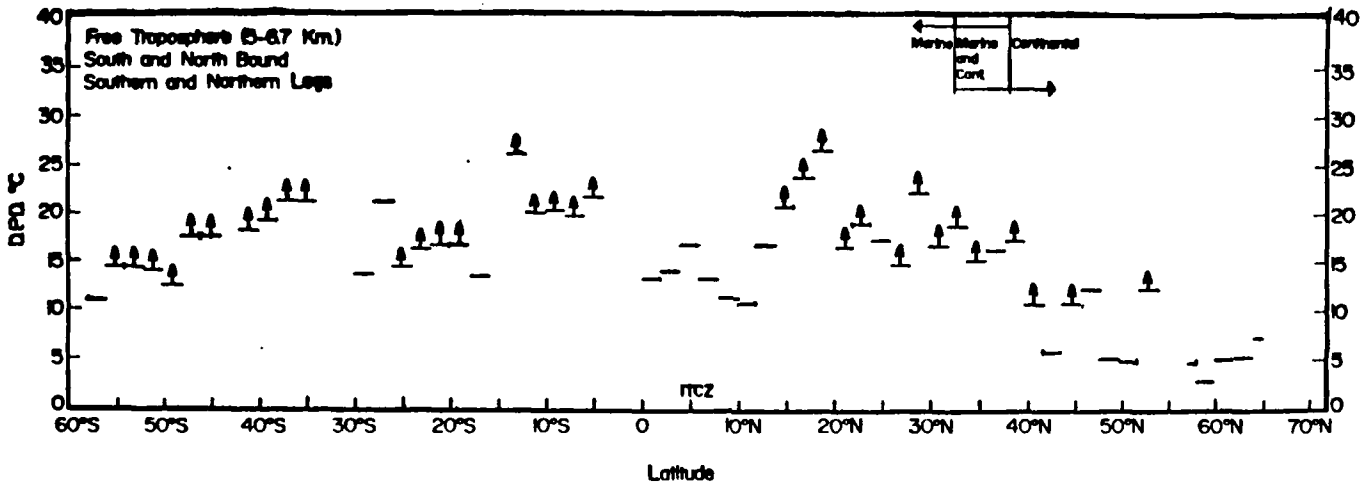

Figure 40. Summary of Free Tropospheric Dewpoint Depression Data Versus Latitude (Apr. 27-June 1, 1978).

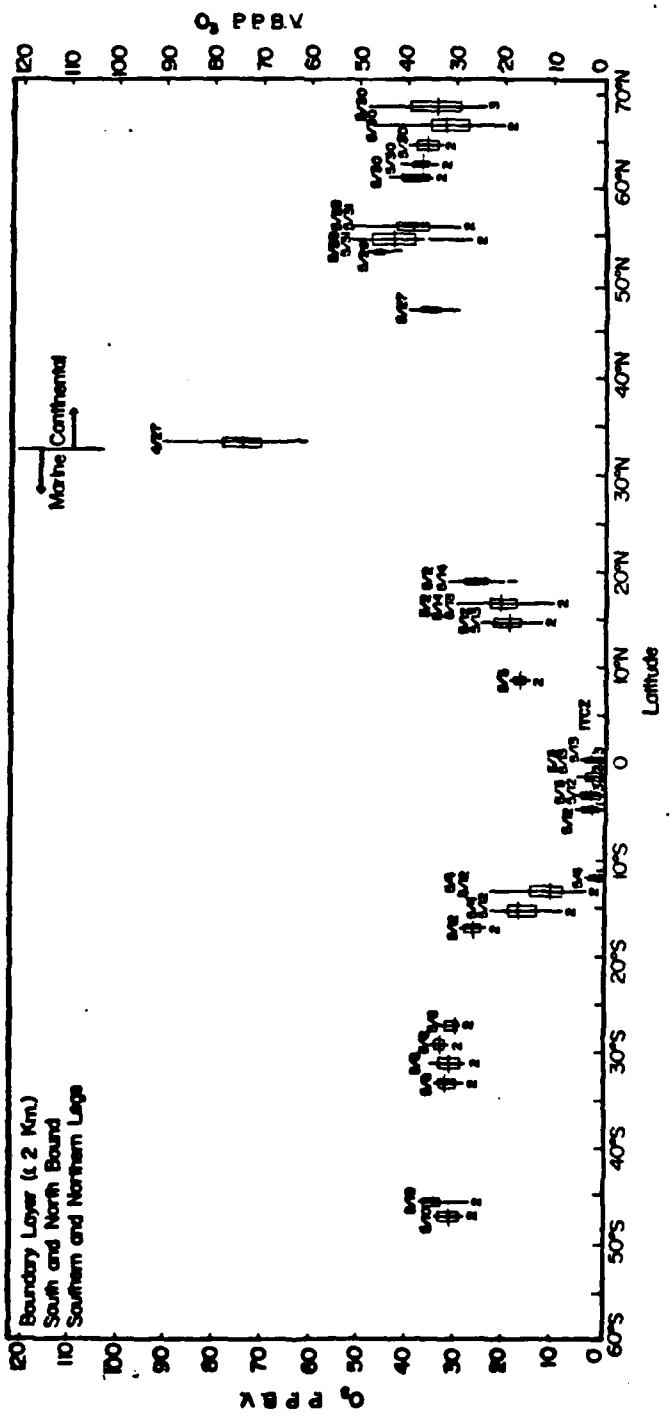

Figure 41. Summary of 1978 Boundary Layer O_3 Levels Versus Latitude (Apr. 27-June 1, 1978).

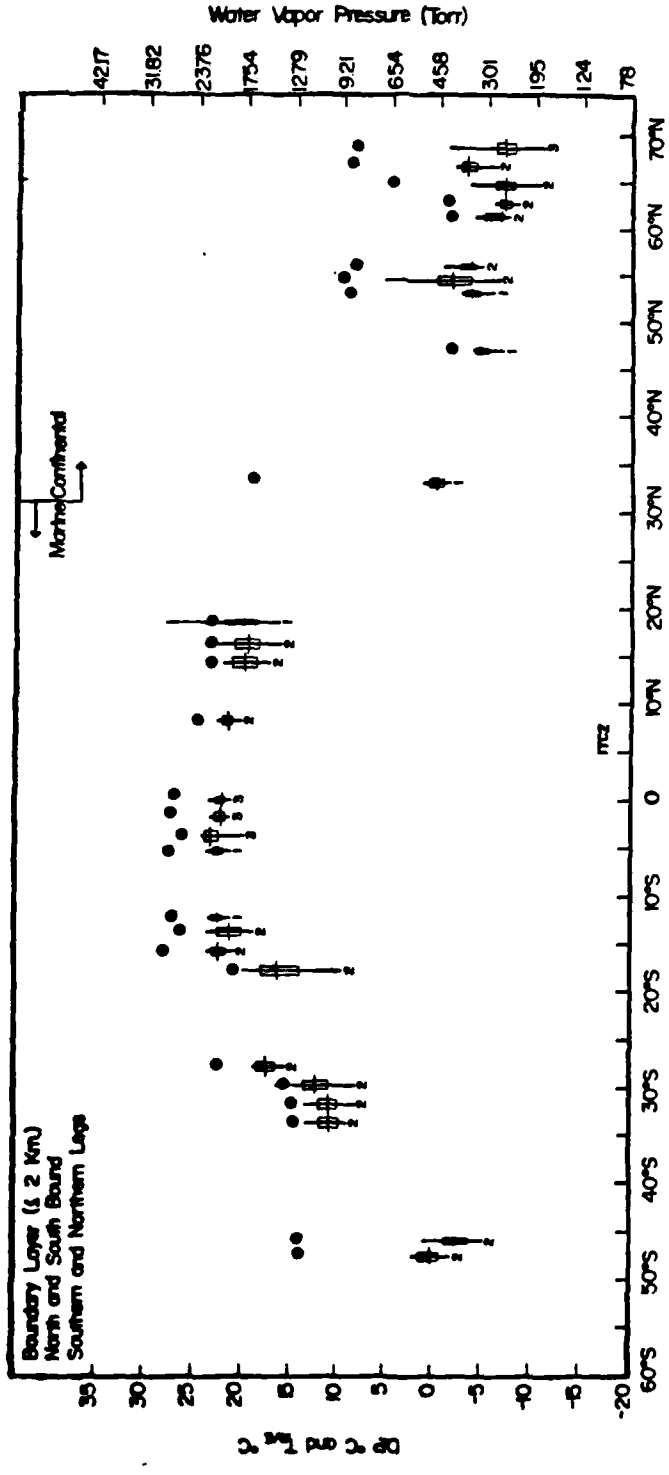

Figure 42. Summary of 1978 Boundary Layer Dewpoint and Temperature Versus Latitude Calendar dates are not indicates (Apr. 27-June 1, 1978).

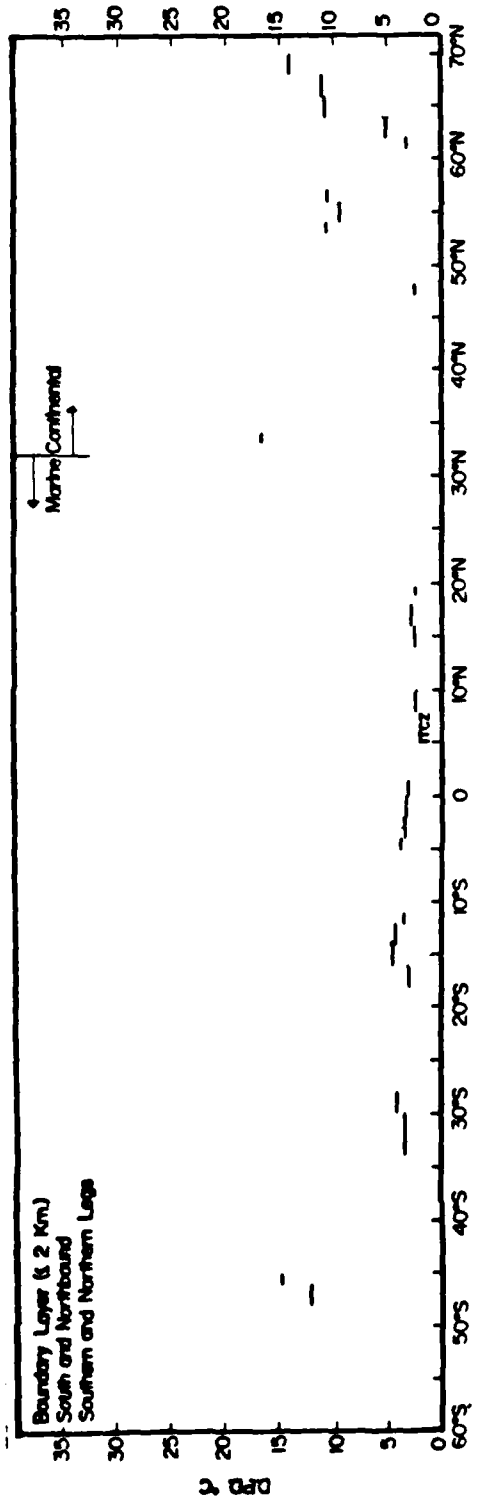

Figure 43. Summary of 1978 Boundary Layer Dewpoint Data Versus Latitude. Canendar dates are not indicated (Apr. 27-June 1, 1978).

1. Free Tropospheric Ozone and Dewpoint Data (1978)

a. Ozone Data. Figures 29 through 32 represent the free tropospheric ozone concentrations collected during the 1978 GAMETAG field experiment. Figures 18 and 19 show the data collected over the Pacific Ocean while Figure 20 shows the data collected on flights north of Denver. Figure 21 represents a summary of all 1978 free tropospheric ozone data.

In 1978, the ozone data collected north of the ITCA (∿5°N) show far more variability than the data at more southern latitudes. On the other hand, the northern hemispheric ozone data for the 1978 are less variable than those collected in 1977 for the same region. The major exception to the previous statement is the latitude region near 40°N. The average ozone value north of the ITCZ (∿10-12°N) is 1.4 times greater than the average value south of the ITCZ, while the ozone values north of 12°N are approximately 2.2 times higher than in the equatorial belt 12°N to 20°S. In 1978, ozone concentration peaks can be seen at 15°N and 40°N (both north and southbound southern leg); no southern hemispheric maximum is evident. In 1978, an ozone minimum at the tropical latitudes of 20°S-10°N can be seen in both Figures 29 and 30. Additionally, shallow minimums appear near 24°N (both north and southbound southern leg) and 55°N (northbound northern leg); no southern hemispheric minimum is evident. The single highest ozone concentration observed in

1978 (1973 ppbv) is seen to occur near 40°N (over Colorado). Particularly for the southern leg, the ozone data, collected over a two and one half week period, show consistently similar values for each latitude band. Between 45°S and 40°N, Figures 33 and 34 have very similar shapes.

b. Dewpoint and Dewpoint Depression Data. The 1978 free tropospheric dewpoint and dewpoint depression data collected during Project GAMETAG are displayed in Figures 33 through 40. As shown for 1977, dewpoint and dewpoint depression data relating to the same flights are displayed in sequential figures. The first four figures presented here show data collected over the Pacific Ocean; the next two represent data collected north of Denver; and the last two figures are summary plots for all 1978 data.

The dewpoint data recorded in 1978 have high values near the equator and low values poleward of 20° latitude. Almost half of the free tropospheric dewpoint data are beyond the EG&G hygrometer limits; the southern hemispheric data are almost entirely bottomed out. Dewpoint maximums can, however, be identified between 0° and 10°N (north and southbound southern leg) and at 50°N (north and southbound northern leg). Low dewpoint values can be see in the southern hemisphere and between 15°N and 30°N in Figures 33 and 35 which represent data collected one to three weeks apart.

The 1978 free tropospheric dewpoint depression data show low values near the equator and higher values near 17°N

and 40°N. Additionally, dewpoint depression minimum values can be seen near 25°N and 50°N (north and southbound southern and northern legs). As shown in the 1978 dewpoint data, the 1978 free tropospheric dewpoint depression data reflect lower limit measurements for about one half of the data.

2. Boundary Layer Ozone and Dewpoint Data (1978)

a. Ozone Data. The 1978 boundary layer ozone data are shown in Figure 41. Particularly low ozone levels (1-3 ppbv) are evident between 13°S and 2°N. (As noted earlier, the accuracy of these measurements is probably not better than 2 ppbv, therefore, the true O_3 concentration could be as low as 0 or as high as 5 ppbv.) The highest boundary layer ozone concentration in 1978 occurred over the United States (33°N) and exceeded the free tropospheric values at that latitude.

b. 1978 Boundary Layer Dewpoint Dewpoint Data and Dewpoint Data. Figures 42 and 43 show all the 1978 boundary layer dewpoint and dewpoint depression data. The data show higher dewpoints and lower dewpoint depressions between 18°S and 18°N than in the subtropical, middle, or high latitude regions. An anomaly in the dewpoint depression data can be seen near 33°N where the value is extremely high. This data value was measured over the Imperial Valley (California). The dewpoint value is particularly low at this latitude also.

D. Vertical Ozone, Dewpoint, and Temperature Data

1. Vertical Data Microscale Analysis

Representative vertical profiles of ozone, dewpoint, and temperature data collected during Project GAMETAG are presented in Figures 44 through 49. Of the six profiles selected, three are from the 1977 GAMETAG data base and three are from the 1978. Four of the six data profiles selected also show evidence of ozone layering. These profiles that do not display ozone layering were collected near 14°N and 10°S while the other data profiles that contained layering were obtained in the subtropical, middle, or high latitudes.

Figure 44 represents data collected near 68°N 159°W on August 9, 1977. This data show an average positive upward vertical gradient for O_3 and a negative one for dewpoint. This figure shows a significant layer of ozone rich dry air near 3600 meters altitude. There are four other less significant ozone rich layers of air near 5200 meters, 5000 meters, 4500 meters, and 2000 meters altitude.

Figure 45 represents data collected on August 25, 1977 near 19°N 155°W. This figure also shows an average positive upward vertical gradient for O_3 and a negative one for dewpoint. A layer of ozone rich dry air is evident near 4600 meters. Another high ozone, low dewpoint layer can be seen near 3000 meters altitude. Layers of low ozone, high dewpoint air can be identified near 5200 meters and 3600 meters altitude.

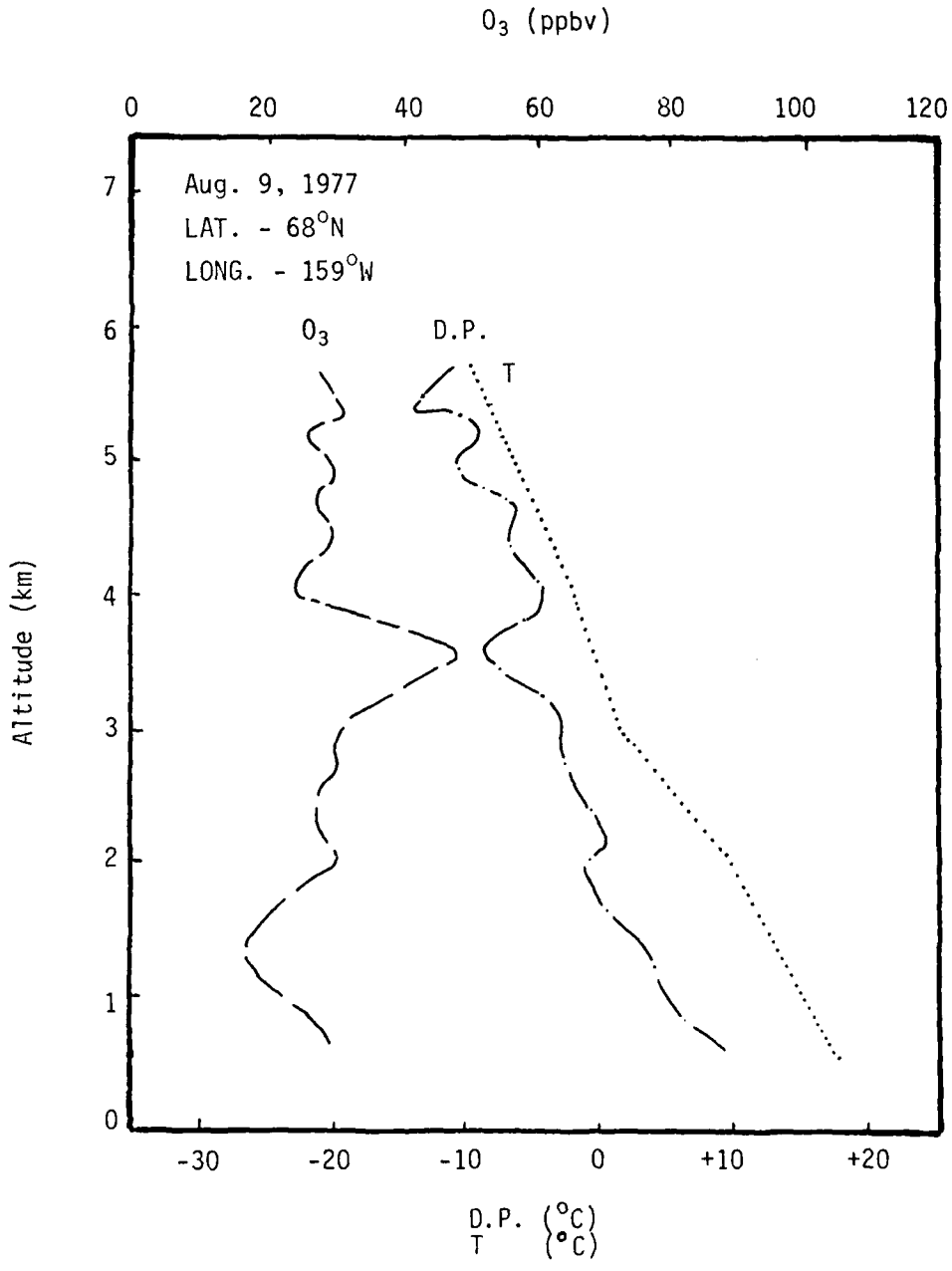

Figure 44. Representative Vertical Profile of Ozone, Dewpoint, and Temperature as Measured by Project GAMETAG.

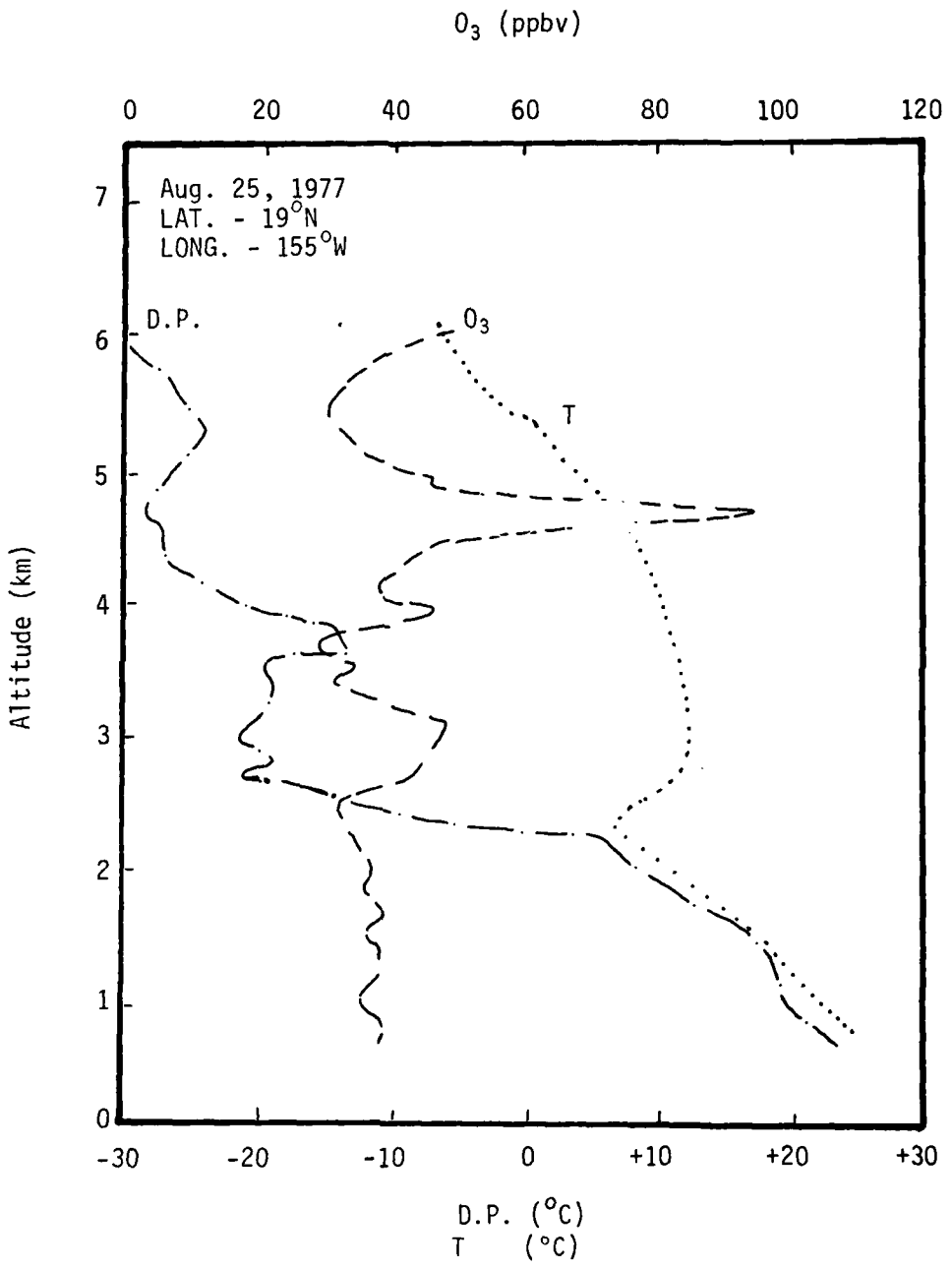

Figure 45. Representative Vertical Profile of Ozone, Dewpoint, and Temperature as Measured by Project GAMETAG.

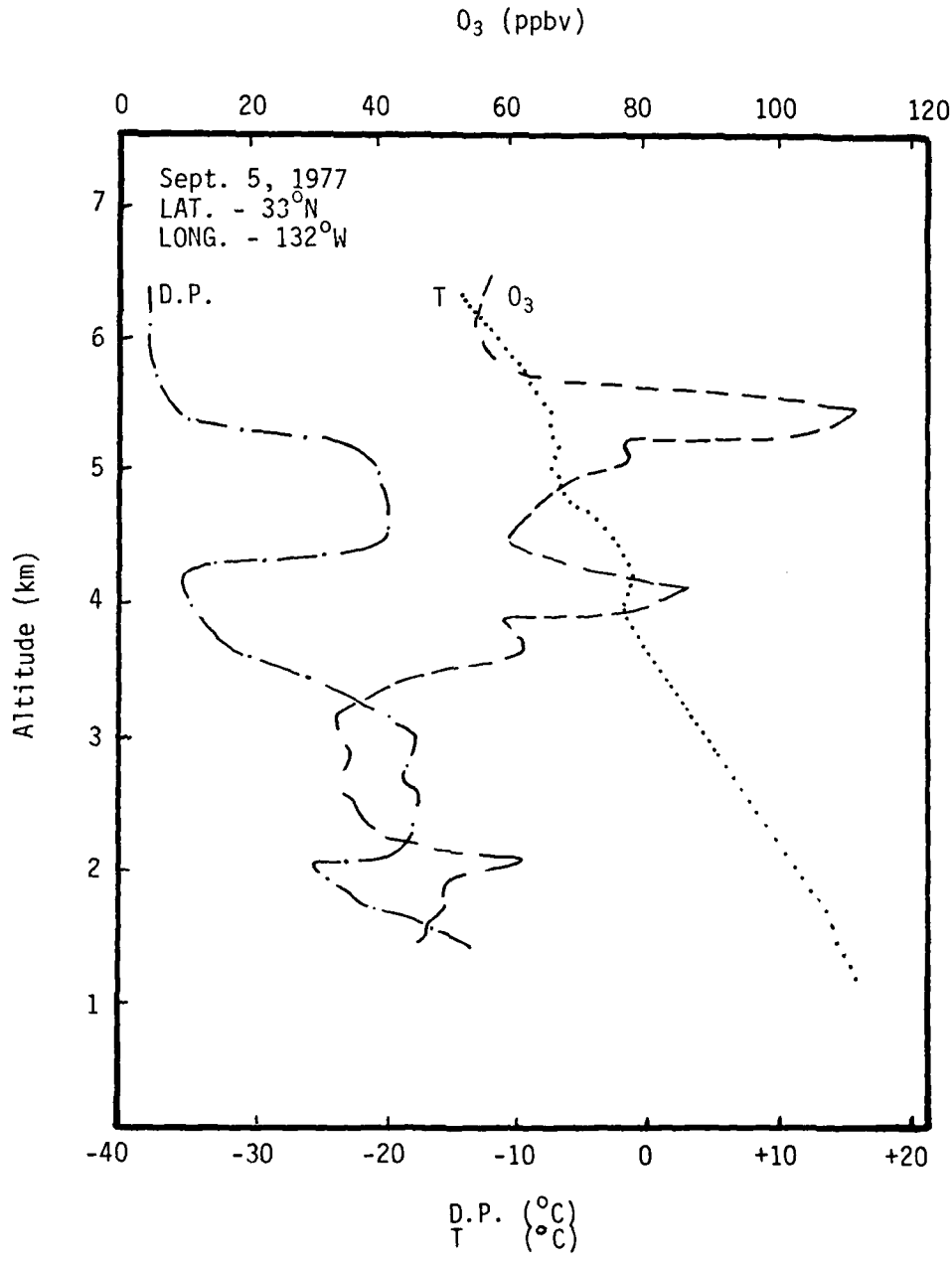

Figure 46. Representative Vertical Profile of Ozone, Dewpoint, and Temperature as Measured by Project GAMETAG.

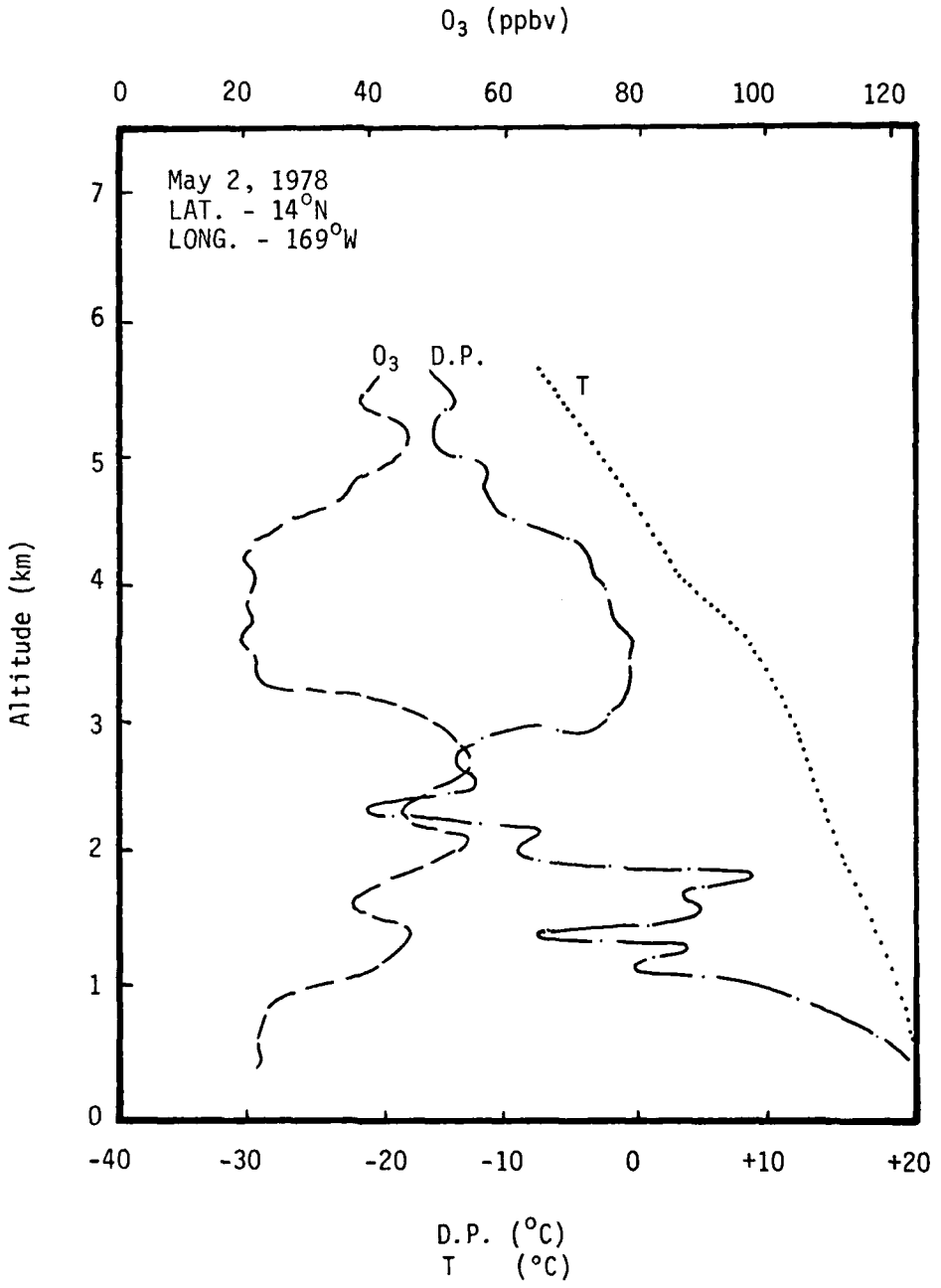

Figure 47. Representative Vertical Profile of Ozone, Dewpoint and Temperature as Measured by Project GAMETAG.

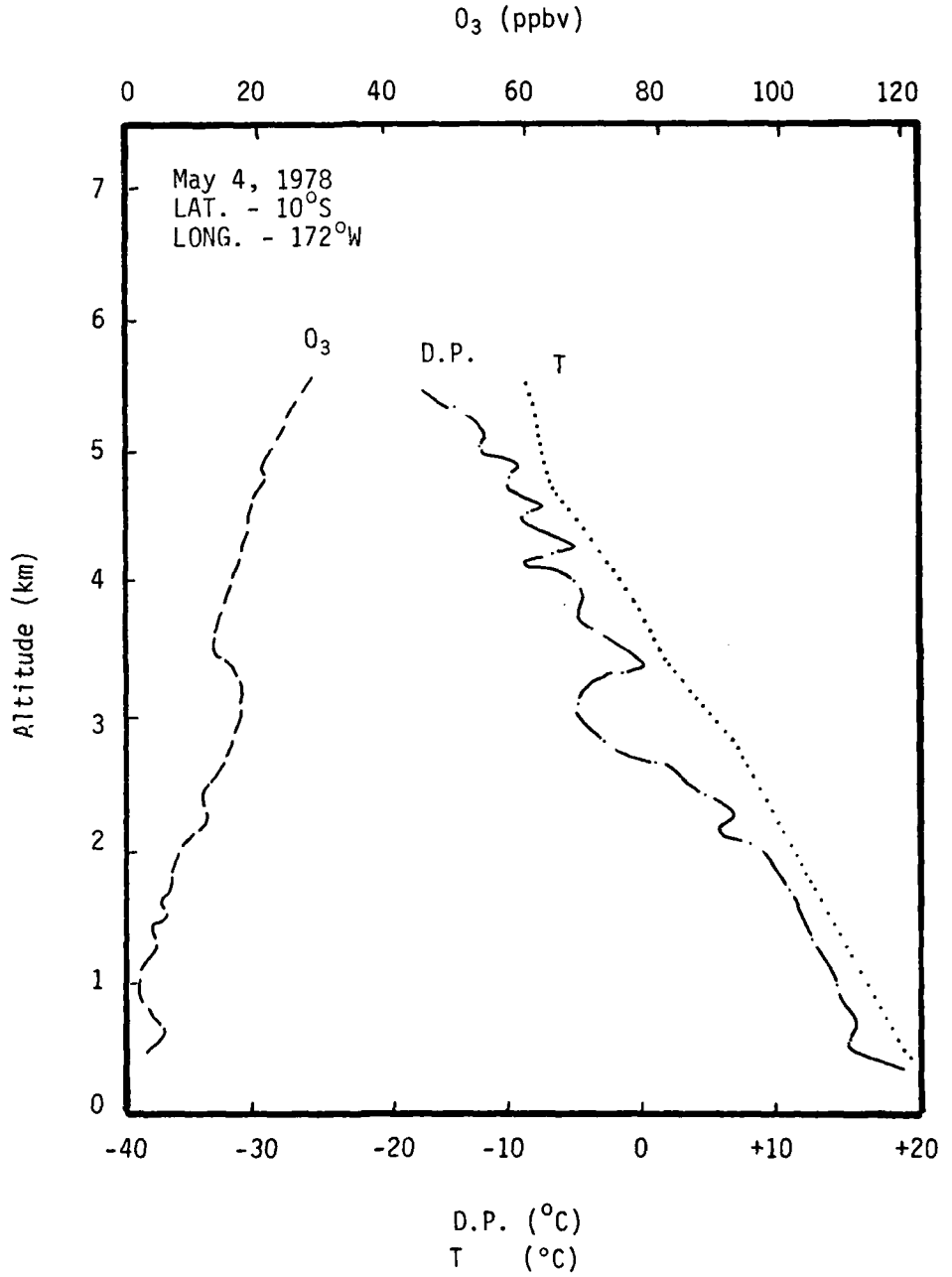

Figure 48. Representative Vertical Profile of Ozone, Dewpoint, and Temperature as Measured by Project GAMETAG.

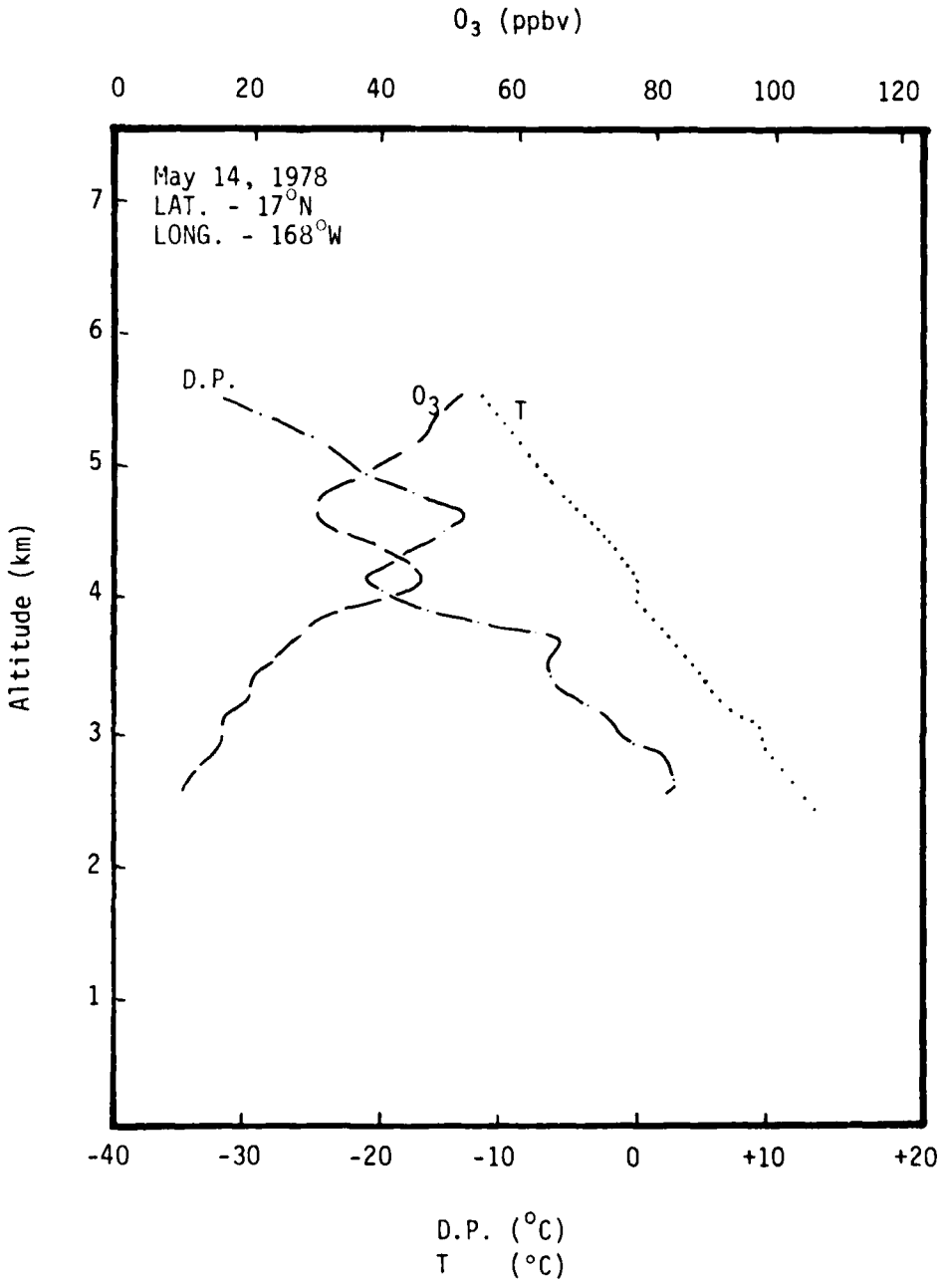

Figure 49. Representative Vertical Profile of Ozone, Dew-point, and Temperature as Measured by Project GAMETAG.

Figure 46 shows data collected on September 5, 1977 near 33°N and 132°W. This figure shows the same average upward vertical gradients for O_3 and dewpoint as the previous figures. During the descent, the dewpoint hygrometer was bottomed out above 5400 meters; this dewpoint data is upper limit data only. Layers of high ozone, low dewpoint air are still evident near 5400 meters, 4100 meters, and 2000 meters altitude.

Figure 47 represents data collected on May 2, 1978 near 14°N 169°W. This data show an average upward vertical gradient for O_3 of $\sim$+0 and for dewpoint of $\sim$-2.5°C/km. The most notable feature of this profile is a low ozone high dewpoint layer between 5000 meters and 2900 meters altitude. There are three layers of high ozone near 2700 meters, 2000 meters, and 1200 meters altitude. Low dewpoint can be seen near 2700 meters, 1900 meters, and 1200 meters altitude. The ozone and dewpoint data between 3000 and 1000 meters altitude appears to indicate that a layer of ozone rich dry air may have experienced enough mixing with low ozone air so as to partially destroy its original characteristics.

Figure 48 is a plot of data collected on May 4, 1978 near 10°S to 172°W. This data show a strong positive upward vertical gradient for O_3 and a strong negative one for dewpoint. Except for the one possible ozone layer near 3000 meters, this profile is devoid of layering. This ozone and dewpoint data was collected above the extremely low

boundary layer ozone concentrations of 2-4 ppbv in the tropics (latitudes 13°S-3°N).

Figure 49 shows data collected on May 14, 1978 near 17°N 168°W. The data during this descent was terminated at 2500 meters altitude. This figure shows an average upward vertical gradient for O_3 of ∿12 ppbv/km and for dewpoint ∿-12°C/km. A layer of ozone rich dry air can be seen near 4000 meters altitude.

2. Vertical Data Low Resolution Analysis

Figures 50 through 61 represent ozone and dewpoint vertical data that have been processed on a low resolution scale as a function of latitude for three altitude blocks: >4500 meters, 4500-3000 meters, and 3000-1500 meters. The 1977 ozone data, presented in Figures 50, 51, and 52 in descending altitude order, show minimum ozone levels between 10°N and 10°S. The maximum ozone values can be seen near 20°S-30°S and 40°N-50°N. There appears to be no systematic vertical ozone gradient in this free tropospheric data. The 1977 dewpoint data, presented in Figures 53, 54, and 55 in descending altitude order, show minimum dewpoint levels between 20°S and 30°S and maximum values between the equator and 10°N for the two highest altitude blocks. The highest altitude block (>4500 meters) data indicate an additional minimum dewpoint level between 30°N and 40°N that is missing from the lower two 1977 dewpoint data altitude block figures. The lowest altitude block (3000 meters-1500 meters) dewpoint

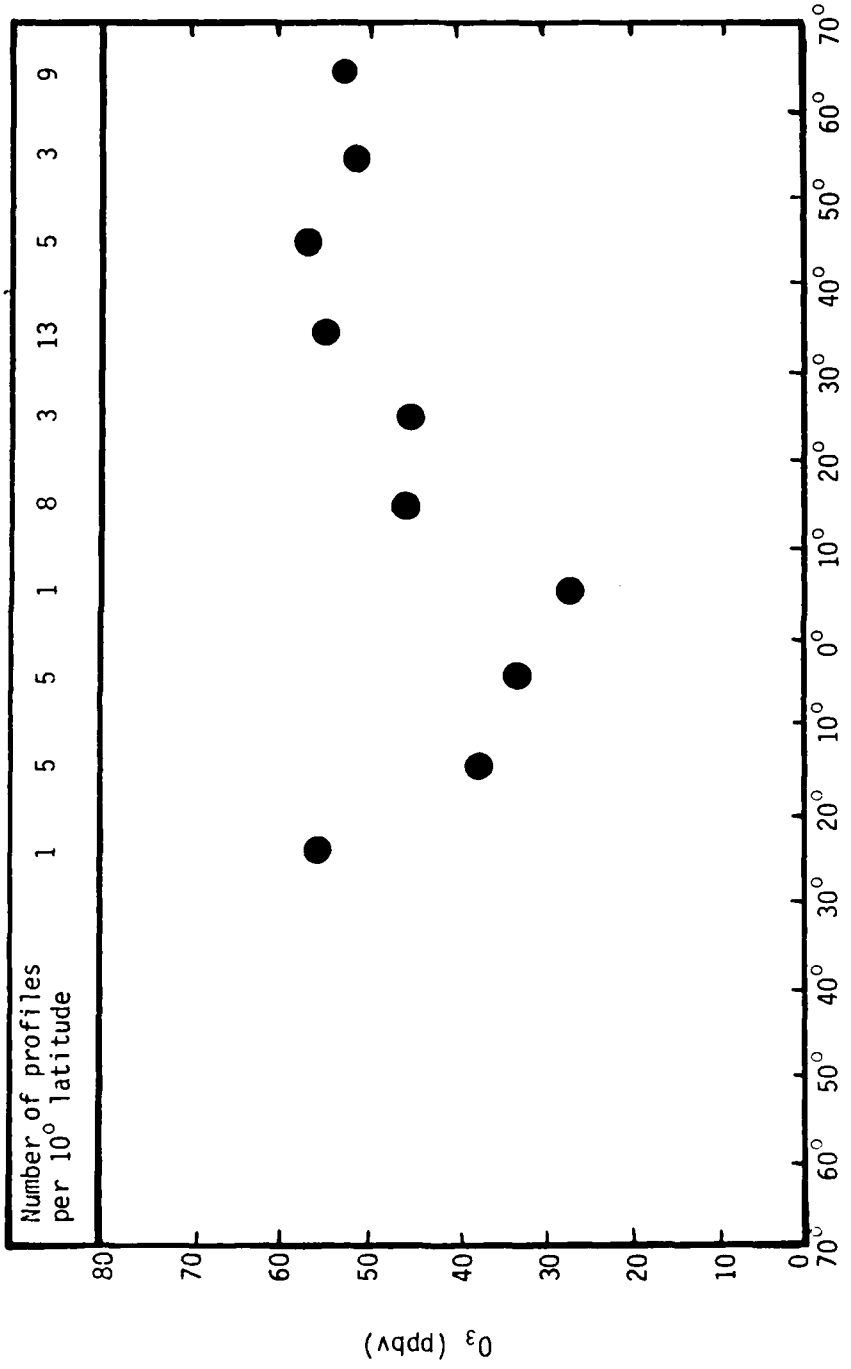

Figure 50. 1977 GAMETAG Low Resolution Vertical Ozone Data Versus Latitude for the Altitude Block: >4500 meters.

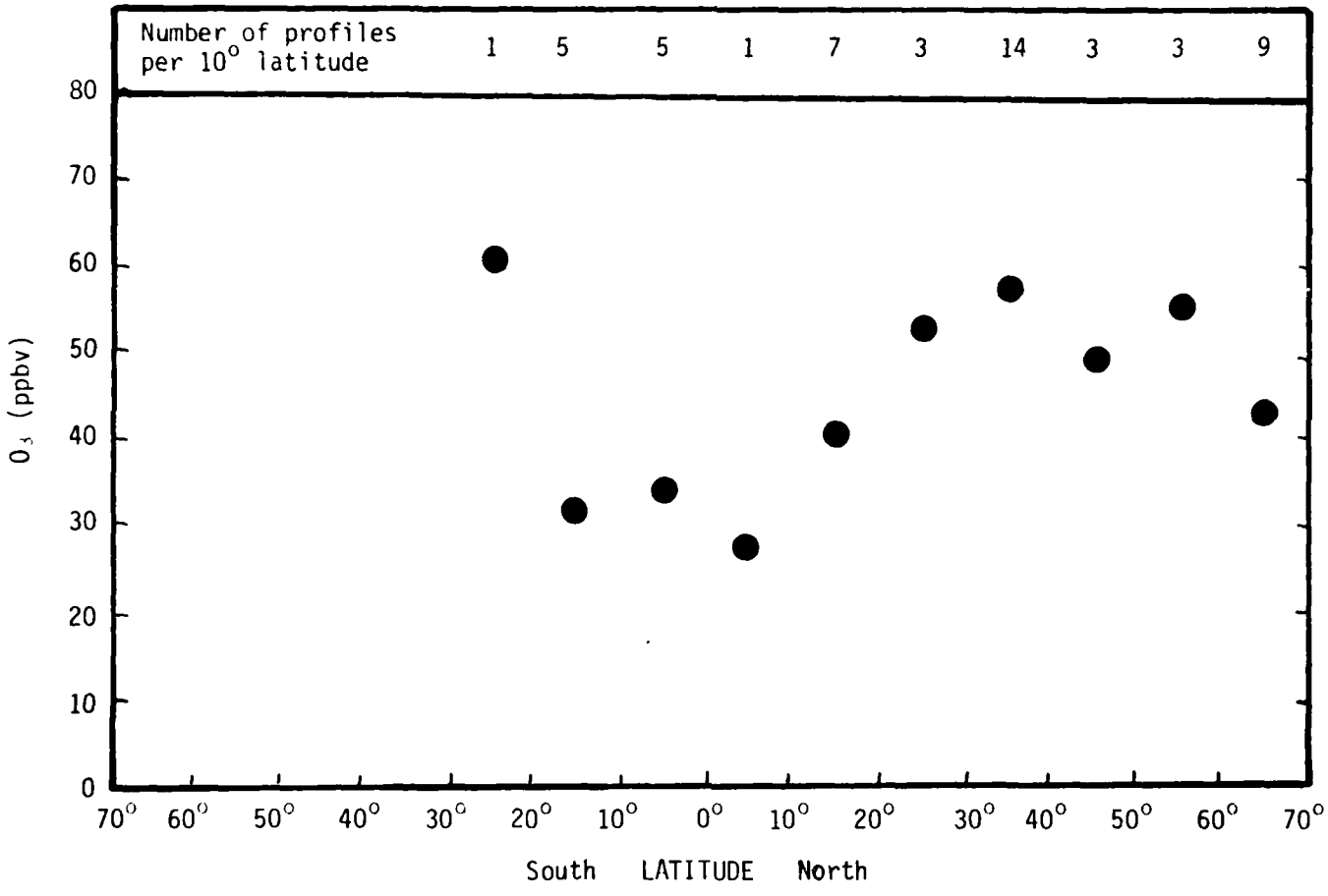

Figure 51. 1977 GAMETAG Low Resolution Vertical Ozone Data Versus Latitude for the Altitude Block: 4500-3000 meters.

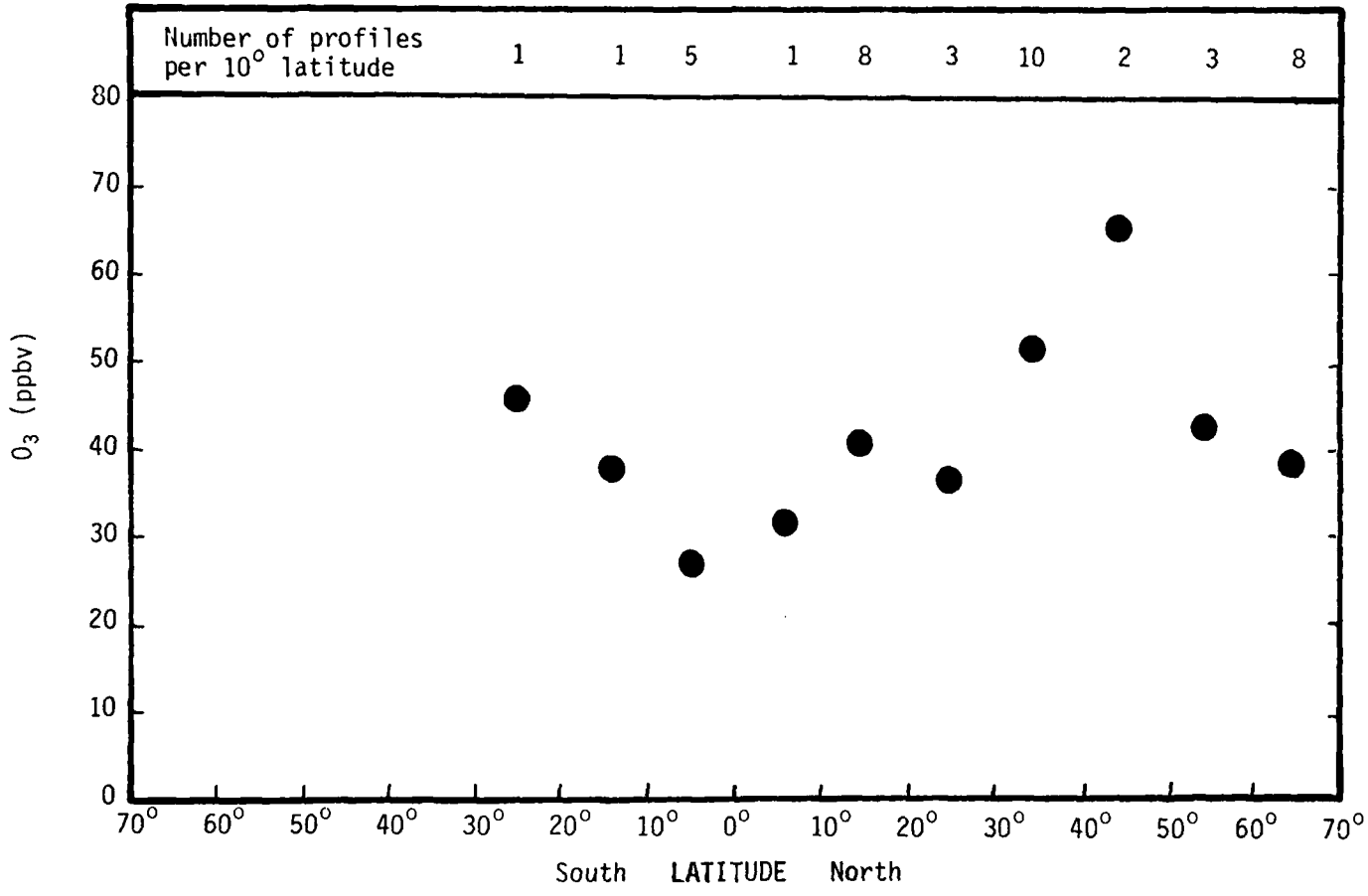

Figure 52. 1977 GAMETAG Low Resolution Vertical Ozone Data Versus Latitude for the Altitude Block: 3000-1500 meters.

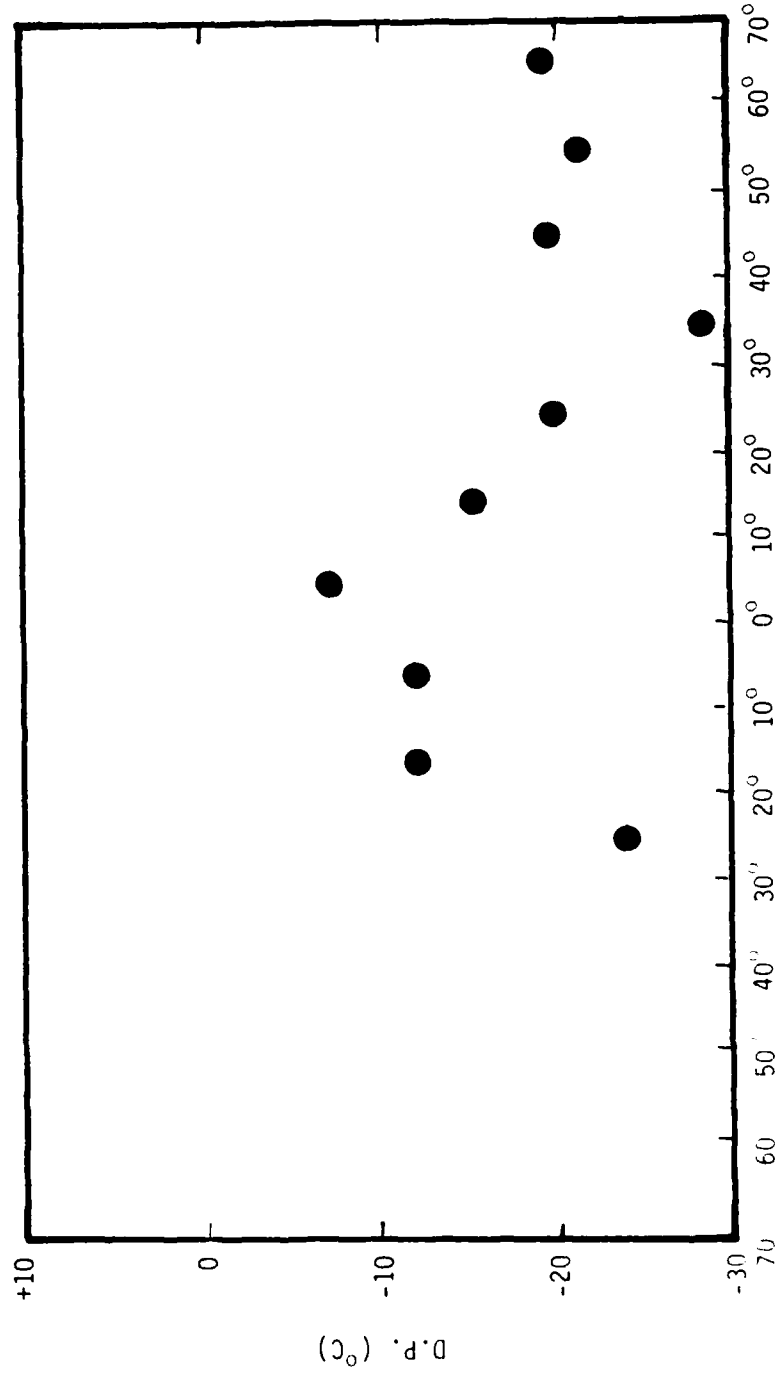

Figure 53. 1977 GAMETAG Low Resolution Vertical Dewpoint Data Versus Latitude for the Altitude Block: >4500 meters.

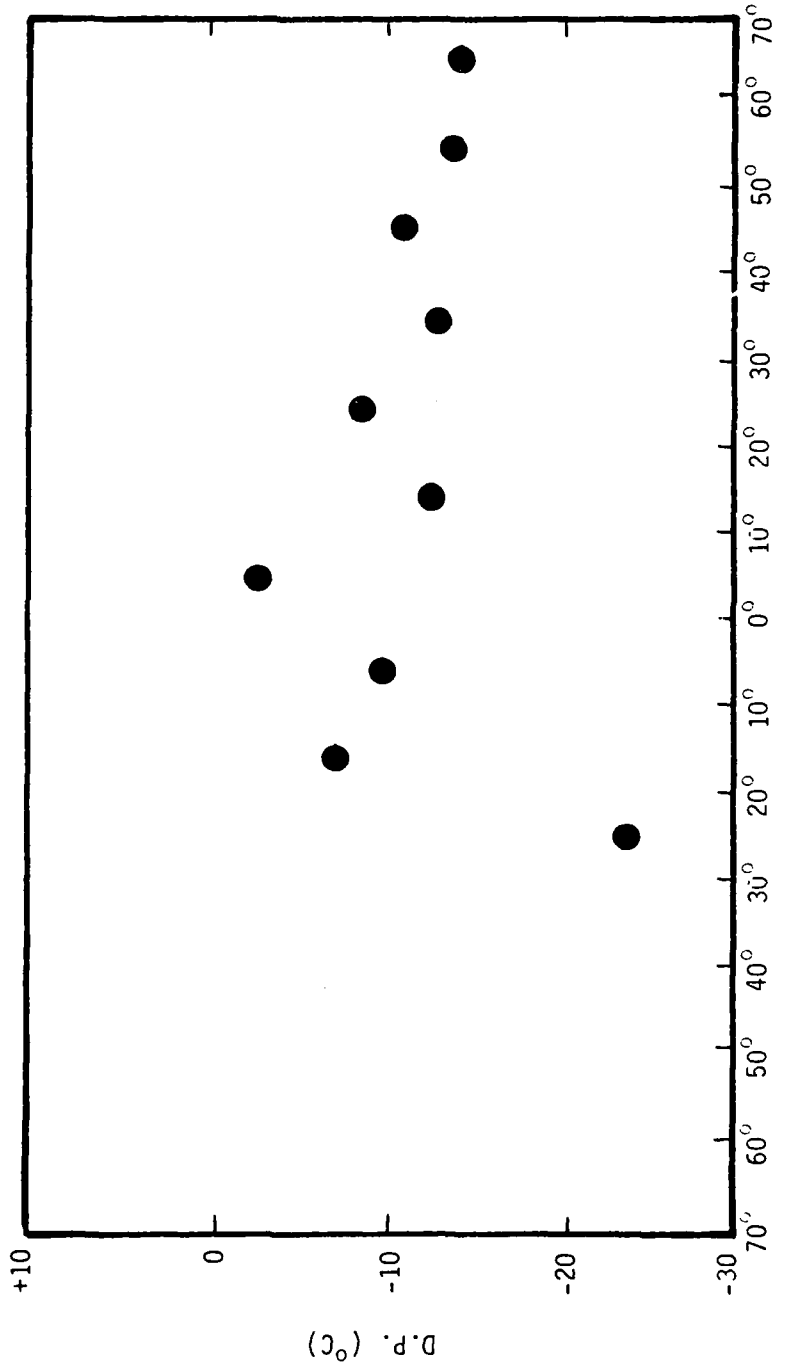

Figure 54. 1977 GAMETAG Low Resolution Vertical Dewpoint Data Versus Latitude for the Altitude Block: 4500-3000 meters.

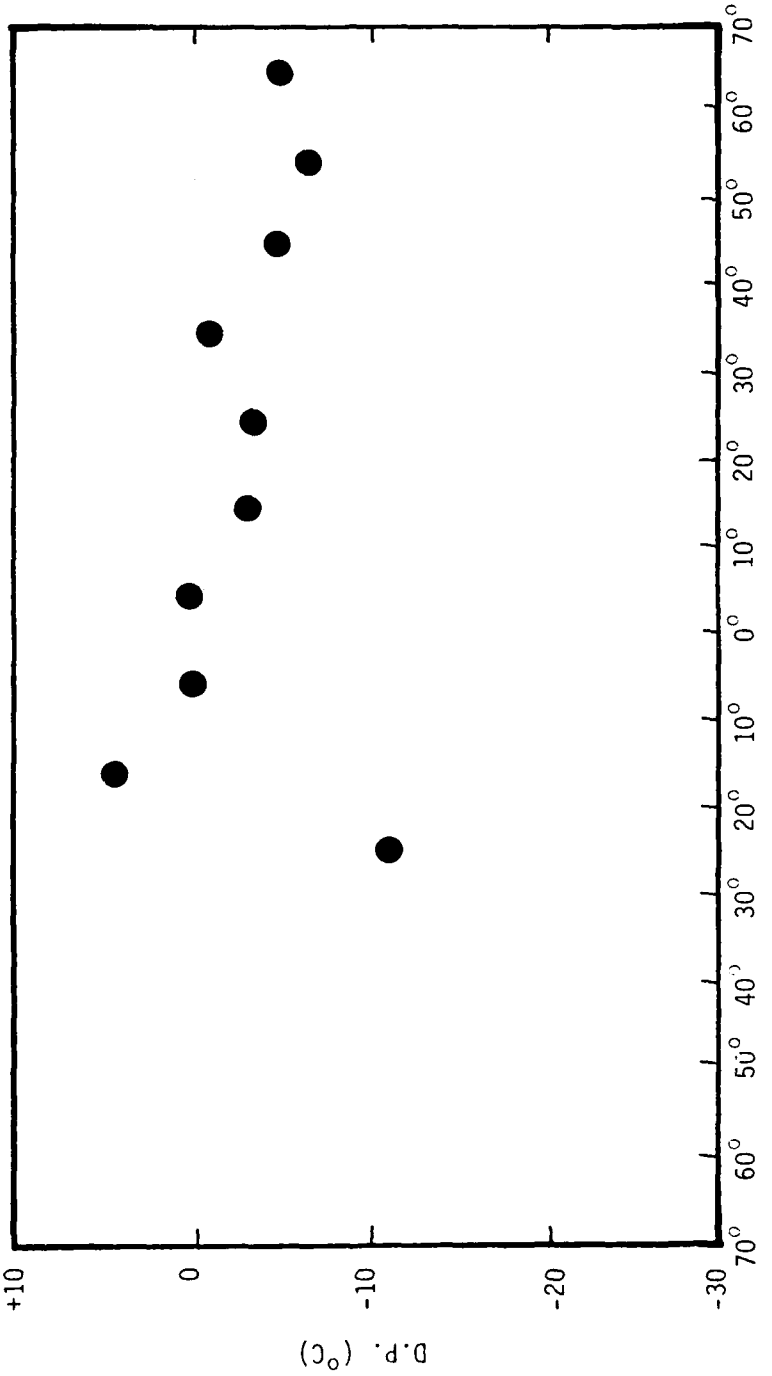

Figure 55. 1977 GAMETAG Low Resolution Vertical Dewpoint Data Versus Latitude for the Altitude Block: 3000-1500 meters.

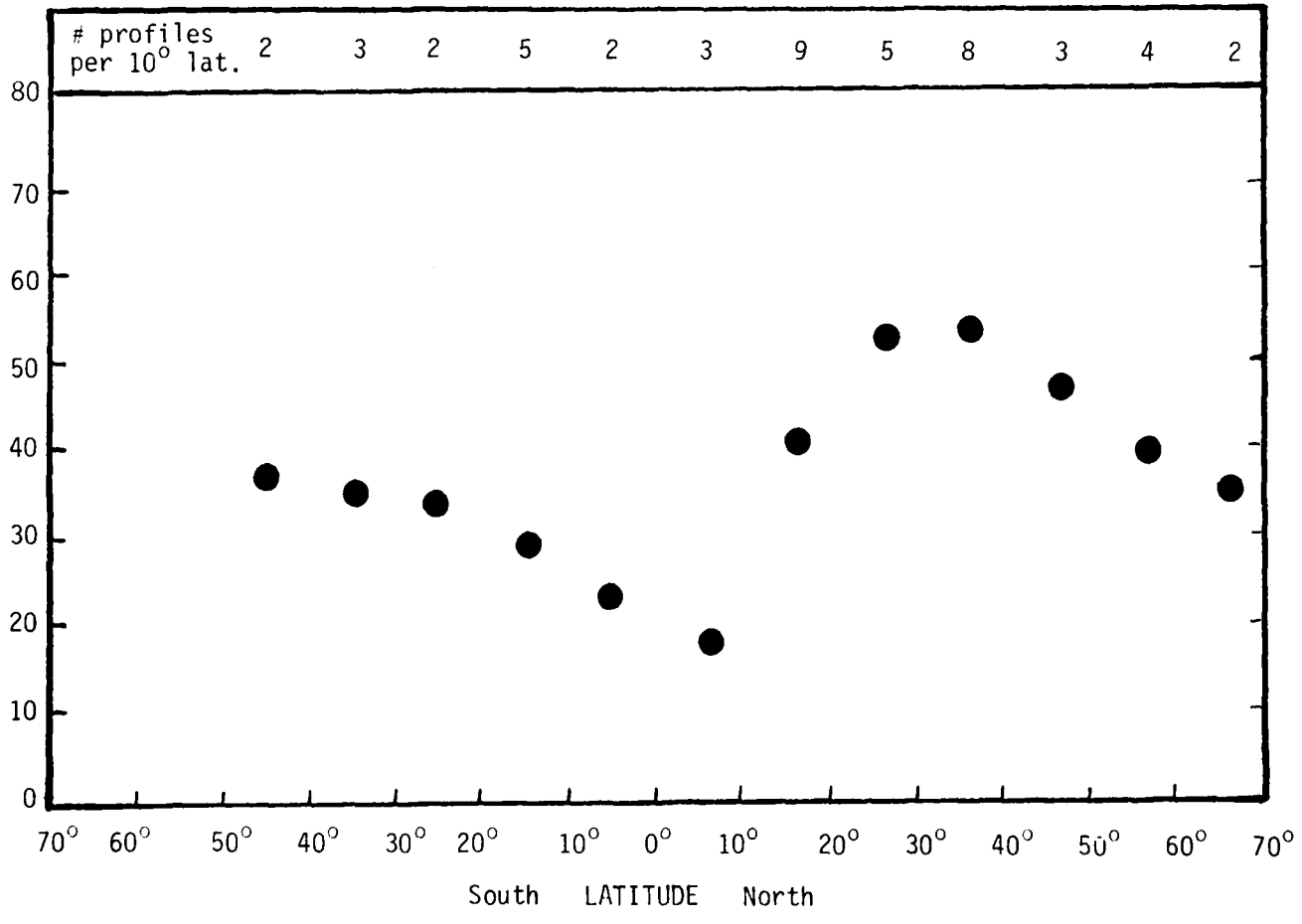

Figure 56. 1978 GAMETAG Low Resolution Vertical Ozone Data Versus Latitude for the Altitude Block: >4500 meters.

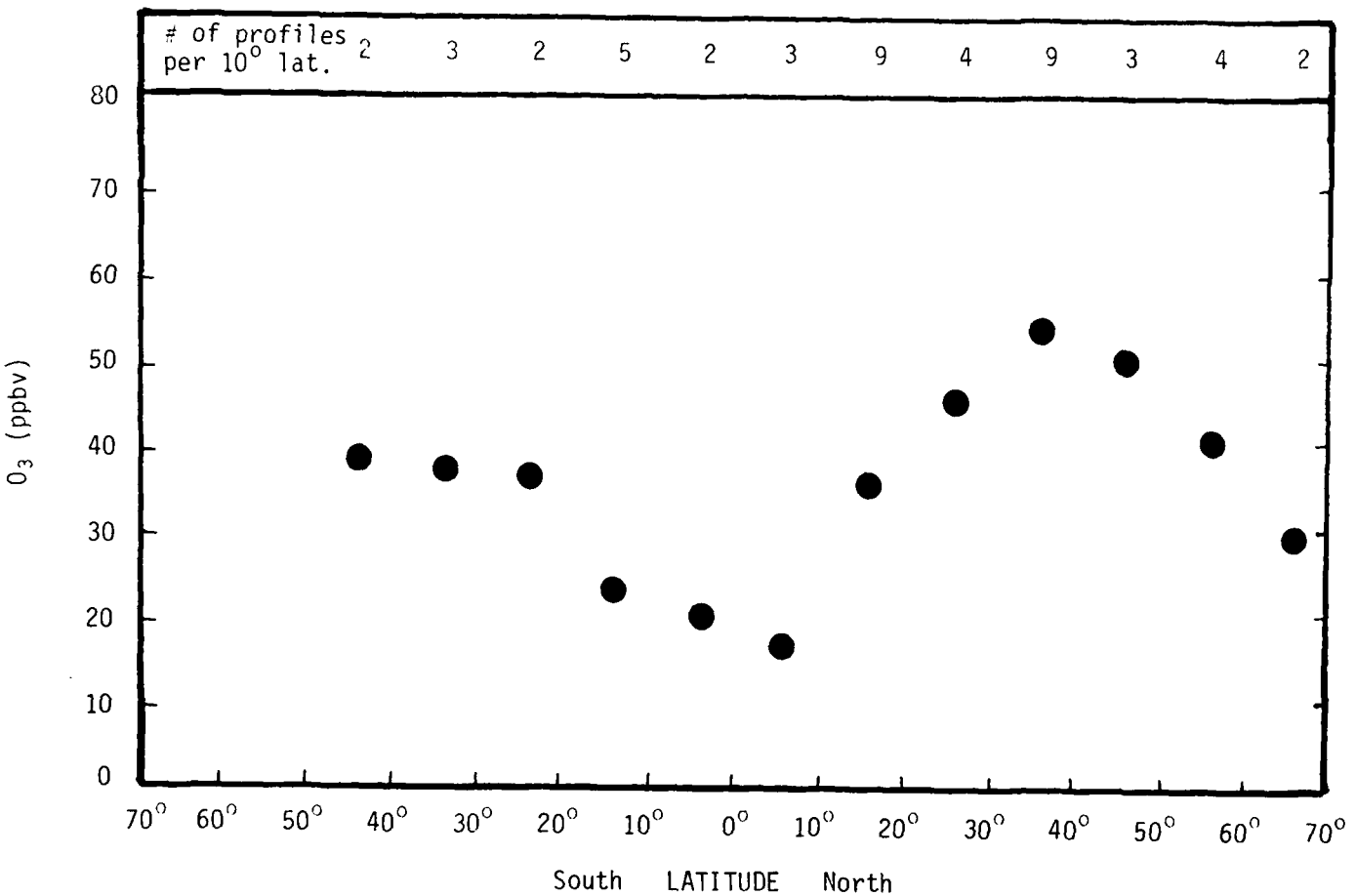

Figure 57. 1978 GAMETAG Low Resolution Vertical Ozone Data Versus Latitude for the Altitude Block: 4500-3000 meters.

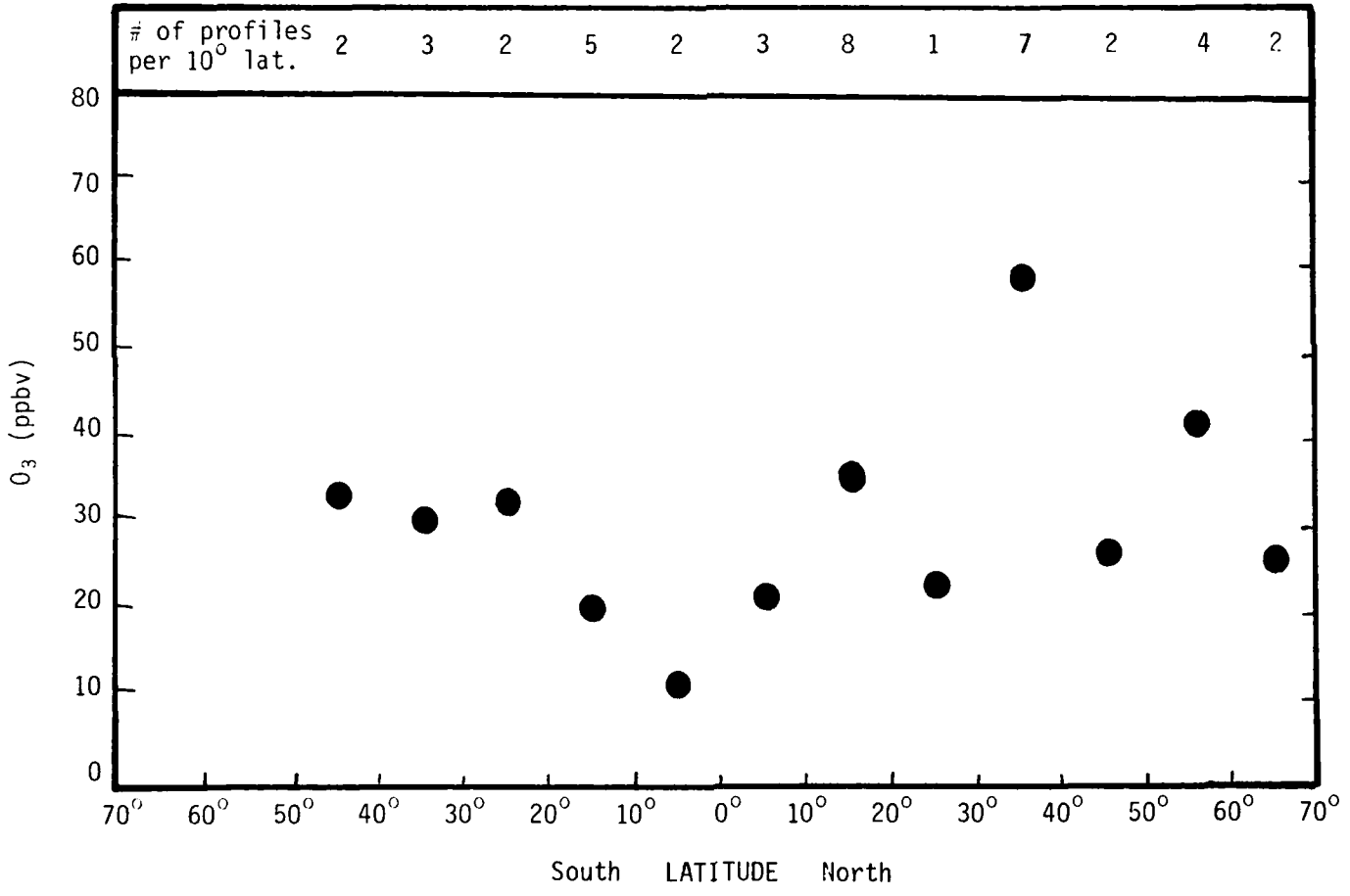

Figure 58. 1978 GAMETAG Low Resolution Vertical Ozone Data Versus Latitude for the Altitude Block: 3000-1500 meters.

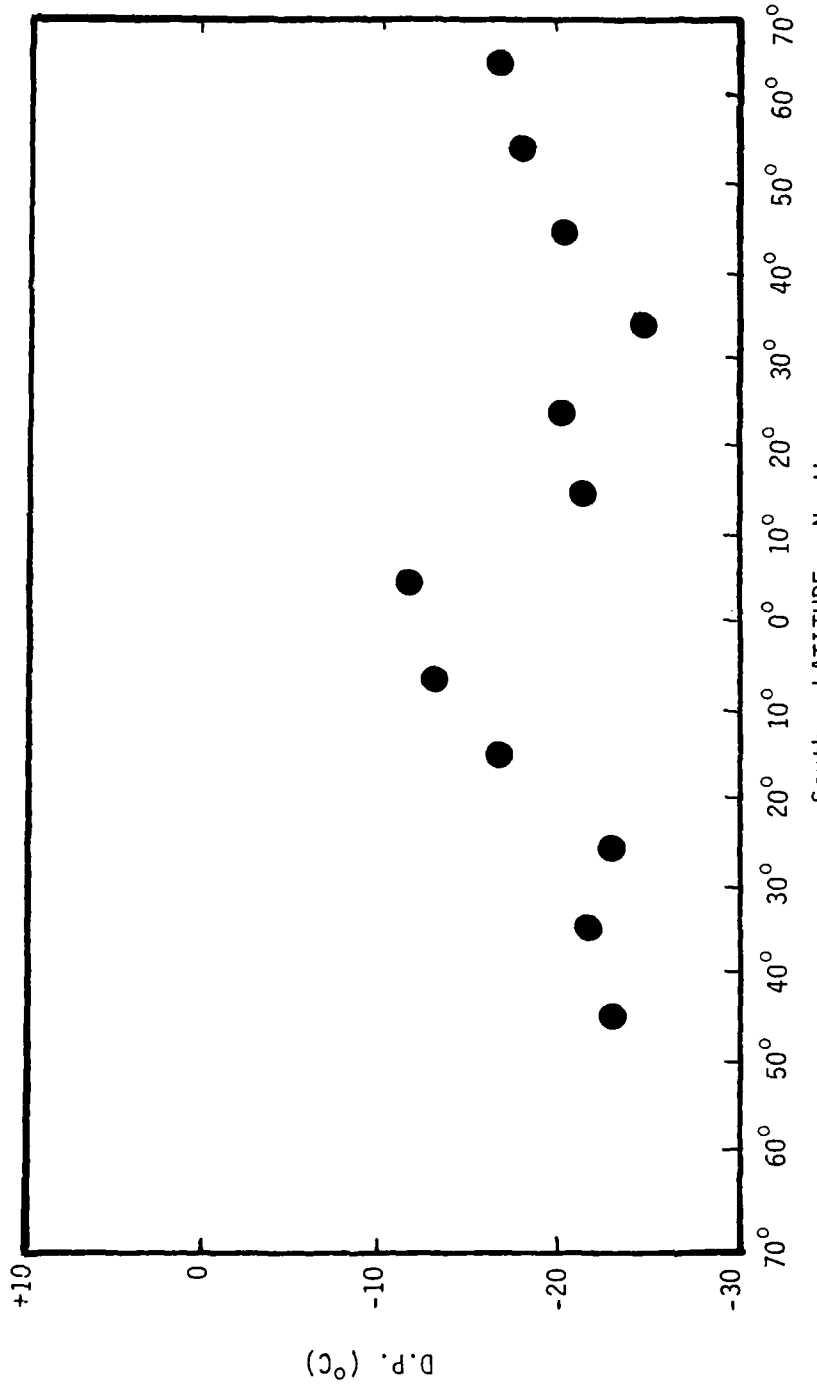

Figure 59. 1978 GAMETAG Low Resolution Vertical Dewpoint Data Versus Latitude for the Altitude Block: >4500 meters.

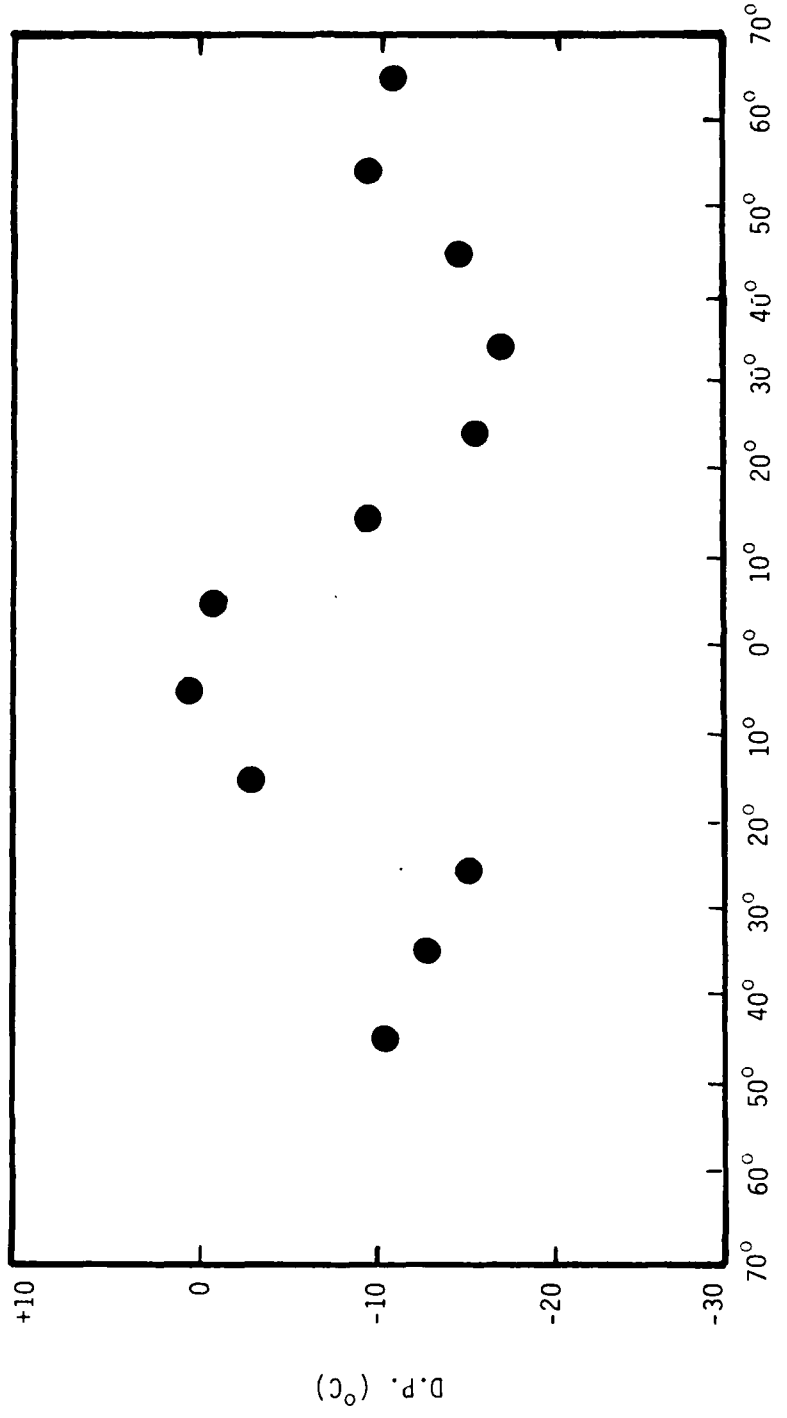

Figure 60. 1978 GAMETAG Low Resolution Vertical Dewpoint Data Versus Latitude for the Altitude Block: 4500-3000 meters.

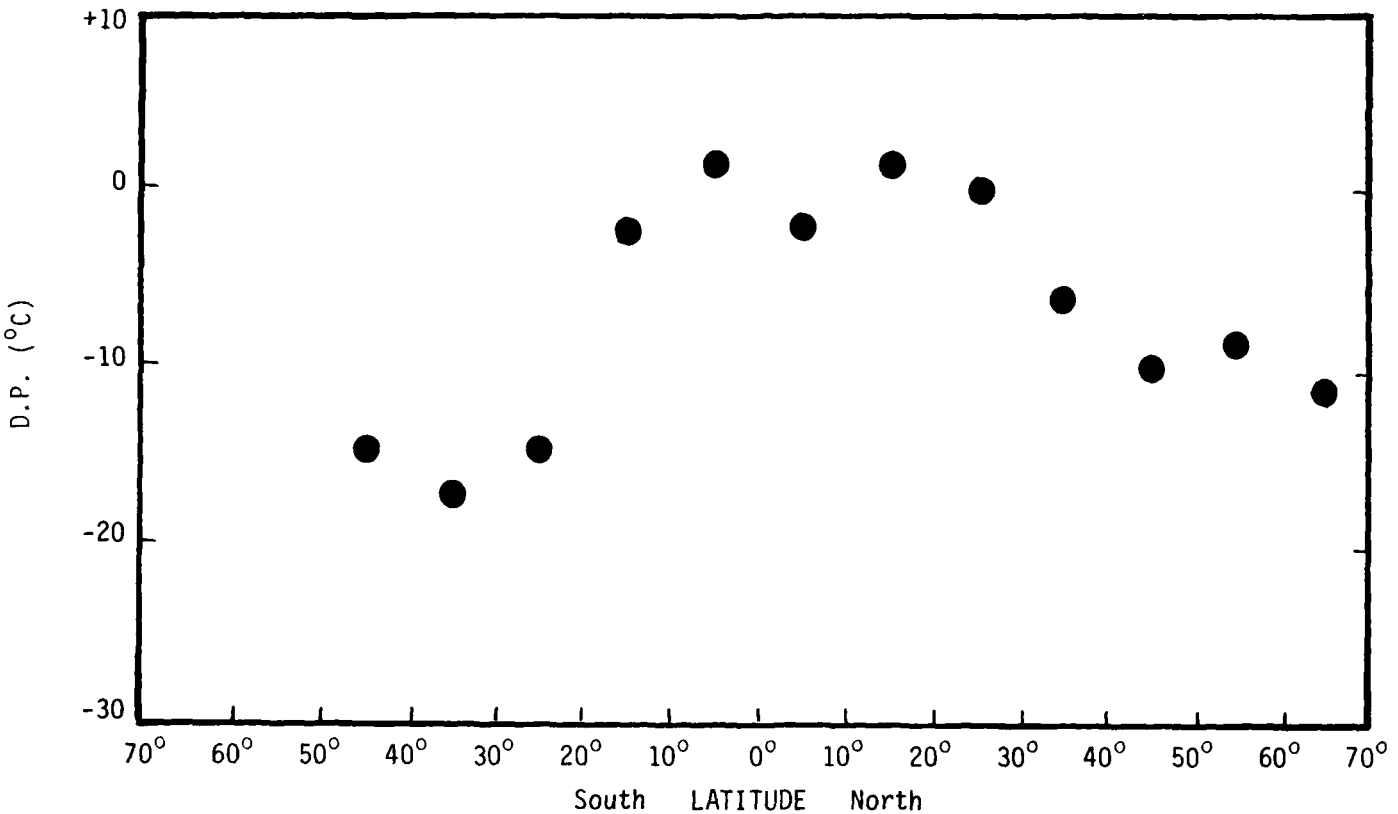

Figure 61. 1978 GAMETAG Low Resolution Vertical Dewpoint Data Versus Latitude for the Altitude Block: 3000-1500 meters.

data show a maximum dewpoint level at 10°S-20°S; this maximum is not apparent in the higher altitude block dewpoint data. The 1977 low resolution vertical dewpoint data show a systematic increase in dewpoint with decreasing altitude for every 10° latitude band. The 1978 low resolution vertical ozone data, shown in Figures 56, 57, and 58, indicate a minimum between 10°N and 10°S. Maximum ozone levels can be identified between 30°N and 40°N. While there is no systematic vertical trend in the 1978 low resolution vertical ozone data, the data plots for the upper two altitude blocks are extremely similar and indicate ozone levels for each latitude band almost equal in magnitude. The lower altitude block ozone data plot indicates slightly lower ozone concentrations and far more data variability than the upper two altitude block ozone plots. The 1978 dewpoint data, illustrated in Figures 59, 60, and 61, show peak dewpoint values between 10°N and 10°S while minimum values can be seen between 20°S-40°S and 30°N-50°N. A trend toward increasing dewpoint values with decreasing altitude can be identified in the 1978 low resolution vertical dewpoint data.

E. Intercomparison of the GAMETAG 1977 and 1978 Ozone Data

The 1978 GAMETAG ozone data are more extensive than the 1977 data in that the later year's data base extends 32° of latitude further into the southern hemisphere.

1. Free Tropospheric Ozone

Both the 1977 and 1978 GAMETAG free tropospheric ozone data show minimum ozone concentrations in the equatorial region and higher ozone levels in the northern hemispheric subtropical, middle, and high latitudes. In the southern hemisphere, the limited 1977 subtropical data (20°-26°S) are higher than the 1978 subtropical ozone data in that latitude band. Obvious discontinuities in the Project GAMETAG ozone data appear near 12°N and 18°N in 1978 and near 20°S and 60°N in 1977. These discontinuities appear to indicate the presence of ozone layering that was horizontally intersected by the GAMETAG sampling aircraft. The ozone gradients between the equatorial region average value and the average value for those regions north (12°N-70°N) and south (20°S-58°S) are indicated in Table 6.

Table 7 provides a comparison of the 1977 and 1978 GAMETAG ozone maximum and minimum values and their latitude positions.

The ozone maximums in the northern hemispheric subtropics, the ozone minimum values in the equatorial region, as well as the ozone minimum values near 46°N in 1977 and 50°N in 1978 appear to be consistent and may, in fact, be permanent features in the latitudinal distribution of ozone. The other ozone data peaks and valleys appear to be more transitory since they do not appear in both year's ozone.

Table 6. Comparison of GAMETAG Free Tropospheric Ozone Latitudinal Gradients

Latitudinal Relationship	Average Gradient 1977	1978
Equatorial Region[1] Northbound (12°N-70°N)	1.8	2.2
Equatorial Region[1] Southbound (20°S-26°/58°S)	1.8	1.6

[1]The equatorial region in this case is defined as 20°S to 12°N.

Table 7. Comparison of GAMETAG Free Tropospheric Ozone Data Extreme Values.

1977		1978	
	O_3 Maximum		
Geographical Location	Ave. O_3 Concentration	Geographical Location	Ave. O_3 Concentration
26°S	60 ppbv	15°N	63 ppbv
36°N	70 ppbv	40°N	90 ppbv
60°N	133 ppbv	-	-
	O_3 Minumum		
19°S	18 ppbv	14°S-10°N	24 ppbv
8°S-5°N	26 ppbv	22°N	40 ppbv
46°N	38 ppbv	50°N	38 ppbv
60°N	30 ppbv	-	-

data.

2. Boundary Layer Ozone

Both the 1977 and 1978 GAMETAG boundary layer ozone data show minimum equatorial ozone levels with higher concentrations north and south. For both years, peak values appear near 33°N and, in 1977, an ozone maximum is evident near 42°N. Excluding these isolated peak values, the 1977 boundary layer ozone data show far less variability (20 ppbv-30 ppbv) than the 1978 data (2 ppbv-46 ppbv). In 1978 strong ozone gradients can be seen on either side of the equatorial region 12°S-3°N. The 1978 ozone minimum near the equator is an order of magnitude lower than the 1977 minimum.

The boundary layer ozone peak values near 33°N were measured during flight sampling operations over the United States. These consistent peaks appear to reflect a single ozone source that was operating during two time intervals nine months apart. Although natural processes cannot be excluded, there appears to be an indication that an anthropogenic pollution source was responsible for these high ozone levels. The 1977 peak near 42°N does not seem to be a consistent feature; however, the same geographic location was not overflown in 1978, therefore, the 1977 higher ozone levels near 42°N may have existed in 1978, but were not observed by GAMETAG.

Except for the peak boundary layer ozone levels mentioned above, the free tropospheric values were consistently

higher. This is corroborated by the positive vertical ozone gradient observed during GAMETAG ascents and descents. Throughout most of the GAMETAG flight operations, the free tropospheric ozone levels were two to ten times higher than the boundary layer data.

F. Intercomparison of the GAMETAG 1977 and 1978 Dewpoint Data

The 1978 GAMETAG dewpoint data are more extensive than the 1977 GAMETAG dewpoint data for the reasons given above.

1. Free Tropospheric Dewpoint

The 1977 fr e tropospheric dewpoint data are approximately one fourth bottomed out hygrometer data. In 1978, almost one half of the dewpoint data are upper limit only values. In particular, the data collected in the southern hemisphere, in 1978 are almost completely bottomed out data. Although upper limit data do not provide the actual dewpoint, they do imply dry air conditions.

Unsurprisingly, both the 1977 and 1978 GAMETAG free tropospheric dewpoint data show maximum dewpoint values in the tropics (20°S-20°N) and generally lower values toward the subtropics. The 1977 dewpoint data appear to be increasing far more rapidly between 30°N and 60°N than the 1978 data over the same latitude region. A comparison between the 1977 and 1978 GAMETAG dewpoint data extreme values is given in Table 8.

Dewpoint minima and surrounding maxima values appear

in both the 1977 and 1978 data in the tropics. Additionally, dewpoint data peaks near 50°N as well as data minimums near 30°N and 56°N are evident in both year's data. The anomolous dewpoint minimum values that persist near the equator may be a reflection of the equatorial Pacific dry belt which extends from South America westward to 160°E (Trewartha, 1968).

2. Boundary Layer Dewpoint

High dewpoint values between 20°S and 20°N are apparent in both the 1977 and 1978 boundary layer dewpoint data. For each year, the dewpoint values near the equator at ~25°C. The values decrease in the northern hemisphere at approximately the same rate each year and in the southern hemisphere at approximately the same rate. There is exceptionally dry air near 42°N in 1977 and near 33°N in 1978. These data reflect the interior continental regions where the sampling occurred.

Table 8. Comparison of GAMETAG Free Tropospheric Dewpoint Data Extreme Values.

1977		1978	
	Dewpoint Maximum		
Geographical Location	Ave. D.P. Level	Geographical Location	Ave. D.P. Level
20°S-8°S	∿-15°C	23°S-17°S	∿-18°C
4° -8°N	∿-12°C	0°-10°N	-15.5°C
48°N	-17.5°C	28°N	-25°C
65°N	-13°C	50°N	-28°C
	Dewpoint Minimum		
26°S	<-39°C	36°S	<-40°C
3°S	-32°C	8°S	-23°C
36°N	<-37.5°C	20°N	<-37°C
56°N	<-22.5°C	40°N	<-38°C
-	-	56°N	-35°C

CHAPTER IV

DISCUSSION

A. Introduction

The GAMETAG data were collected during two separate one month long field experiments, conducted nine months apart. Additionally, while these data were collected over a wide range of latitudes (70°N-58°S), the GAMETAG flight operations covered a very limited longitude range, especially south of 40°N. During both year's flight operations in the Pacific, southbound and northbound flights often covered the same geographic routes. At least one very important reason for this longitudinal restriction over the Pacific Ocean was logistic in nature; a compromise had to be achieved between the Electra's restricted operational range (only 2200 kilometers during GAMETAG mission profile flights as described in Chapter II) and the very long distances between remote Pacific island airfields that were capable of providing adequate ground support for the aircraft and personnel. For all the above reasons, it must be emphasized that the GAMETAG data base is statistically weak. Thus, the GAMETAG data should not be interpreted as representative of an annual average. Whether or not the latitudinal profiles can be extrapolated to other global areas and other times has not yet been

determined.

The primary thrust of this discussion and thesis will be to show that the simultaneously measured GAMETAG ozone and dewpoint data are negatively correlated, particularly in flight regions of significant ozone variability. Indications of a negative correlation between these two atmospheric variables suggest that the transport of stratospheric and upper tropospheric ozone into and within the middle and lower troposphere was the most probable mechanism which influenced the ozone levels over those regions sampled by GAMETAG operation.

B. Intercomparison of GAMETAG Ozone Data with Other Ozone Data Sets

1. Free Tropospheric Ozone Data

a. Introduction. At least three other major free tropospheric ozone data bases have been collected and analyzed. These include ozone measurements from the North American ozonesonde network (Hering and Borden, 1964, 1965a,b, 1967) and from five stations in the southern hemisphere (Aspendale, Australia; Christchurch, New Zealand; Antarctica, Canton Island; and La Paz, Bolivia). The southern hemispheric data have been reported in the bimonthly series, "Ozone Data of the World," published by the Canadian Department of Transportation (Solomon, 1980). Additionally, ozone data were recorded aboard commercial airliners by investigators associated with the German project, Troposphärisches Ozon

(TROZ). These flights provided logistic support to the TROZ surface stations which measured O_3 concentrations along a line from Tromso, Norway to Hermanus, South Africa (Fabian and Pruchniewicz, 1977). These aircraft data were primarily collected near ten kilometers altitude. An additional source of ozone data ia that compiled by Fishman, et al. (1980) aboard aircraft flights from Germany to southern South America via Iceland, Greenland, and North America.

Concurrent with the GAMETAG operations, the National Aeronautics and Space Administration's Global Atmospheric Sampling Program (GASP) used specially equipped commercial Boeing 747 airliners to collect trace gas concentrations. Flight levels varied between 6 kilometers and 13.5 kilometers. The sampling missions between North America and Australia used special performance Boeing 747 SP aircraft that maintained the exceptionally high 13.5 kilometer altitude throughout most of the flight. Although several instances of tropospheric GASP data have been identified, most of the data from this project may be more representative of the stratosphere than the troposphere (Gauntner, et al., 1978).

The geographical sampling corridors of the first five data sets as well as Project GAMETAG's sampling tracks are illustrated in Figure 62. The plus or minus ten degree corridor placed about the GAMETAG Pacific Ocean tracks depict the longitudinal width of the sampling region. This subjective decision was based on the atmospheric lifetime of O_3

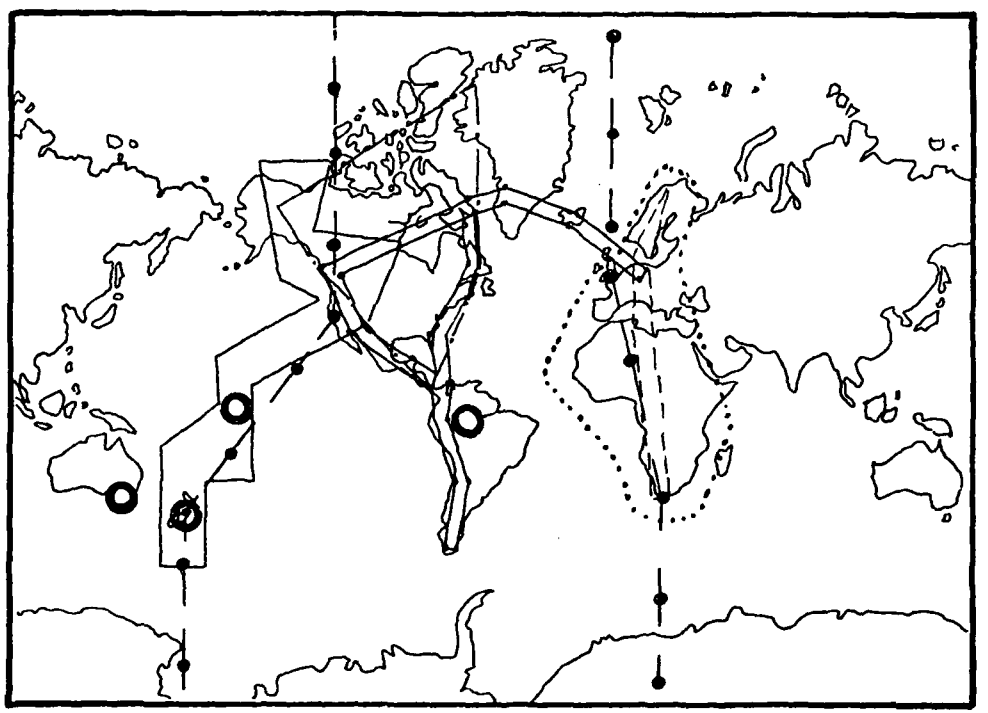

Figure 62. Global O_3 Sampling Locations: ——— GAMETAG Sampling Corridor; —·— North American Ozonesonde Network; ···· Project TROZ Aircraft Sampling Corridor; ---- Project TROZ Ground Base O_3 Sampling Stations; ◎ Southern Hemisphere Ozonesonde Stations; —●— Fishman, et al. (1980) Aircraft Sampling Corridor; -●- - GASP.

and the efficiency of zonal transport. The ozonesonde stations in the southern hemisphere are indicated by the use of concentric rings.

Several analyses of the above data have appeared in literature (Tiefenau, et al., 1973; Pruchniewicz, 1973; Chatfield and Harrison, 1977a,b,; Fabian and Pruchniewicz, 1977; and Fishman and Crutzen, 1978; Fishman, et al., 1980). Tiefenau, et al. (1972) reported an upper tropospheric ozone distribution based on data collected during approximately 25 commercial airline flights during the time period September, 1970-November, 1971. All the measurements were carried out with the same Brewer type electrochemical cell instrument. Although they reported data for each flight in absolute mixing ratio units, a subsequent analysis by Fabian and Pruchniewicz (1977) presented the same information in relative units (Figure 63). This was done in an attempt to eliminate possible systematic errors. The data presented and analyzed by Purchniewicz (1973) were obtained by the North American ozonesonde network between the years 1963-1965. Ozone profiles from the Antarctic were also included. During this time period, Regener type chemiluminescent sondes were used. Regener (1969) estimated a 15% error with this instrument. This analysis, illustrated in Figure 64 is a meridional profile of the annual mean tropopsheric concentration. Chatfield and Harrison (1977b) presented an analysis of data collected by the North American Ozonesonde Network for the

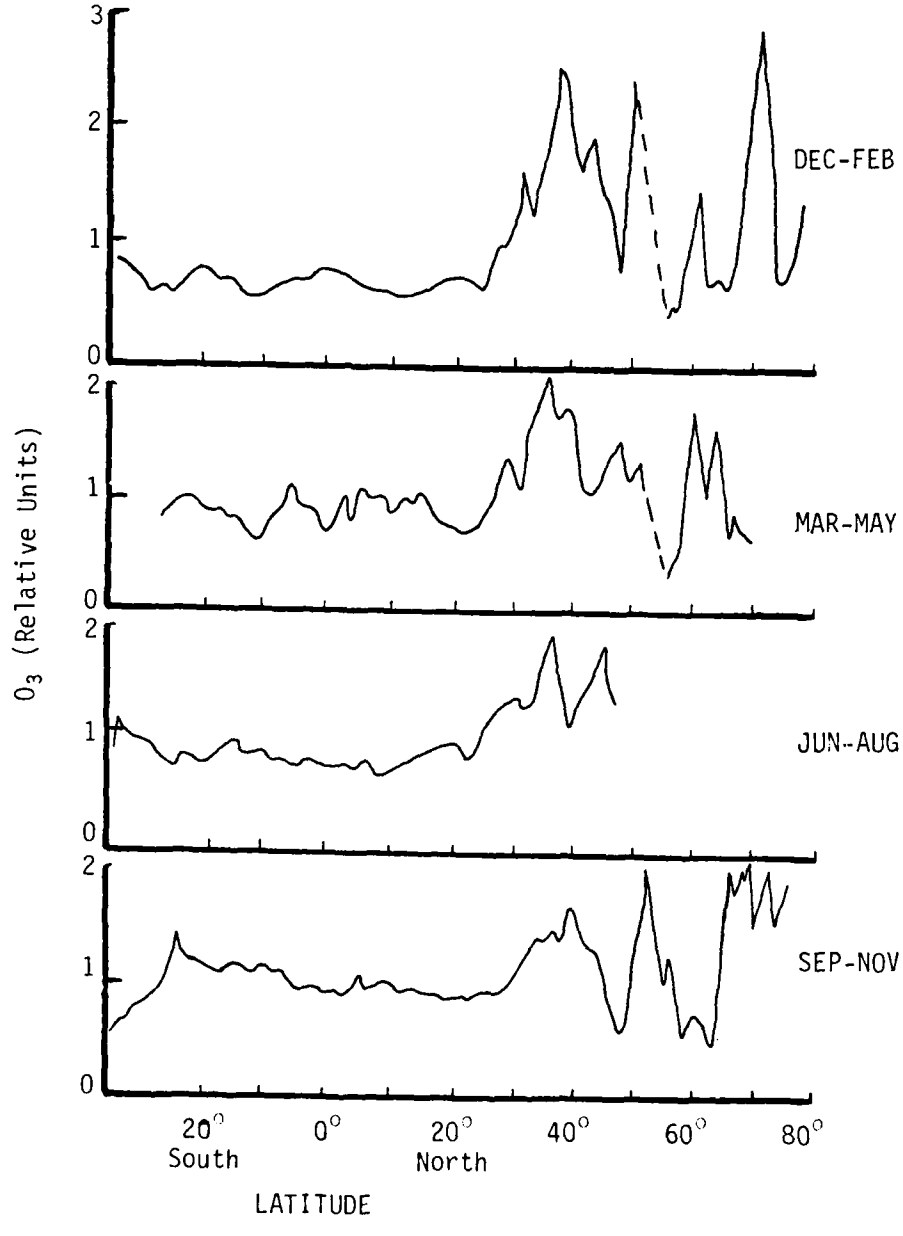

Figure 63. Free Tropospheric O_3 Measurements from Project TROZ. Redrawn from Fabian and Pruchniewicz, 1977.

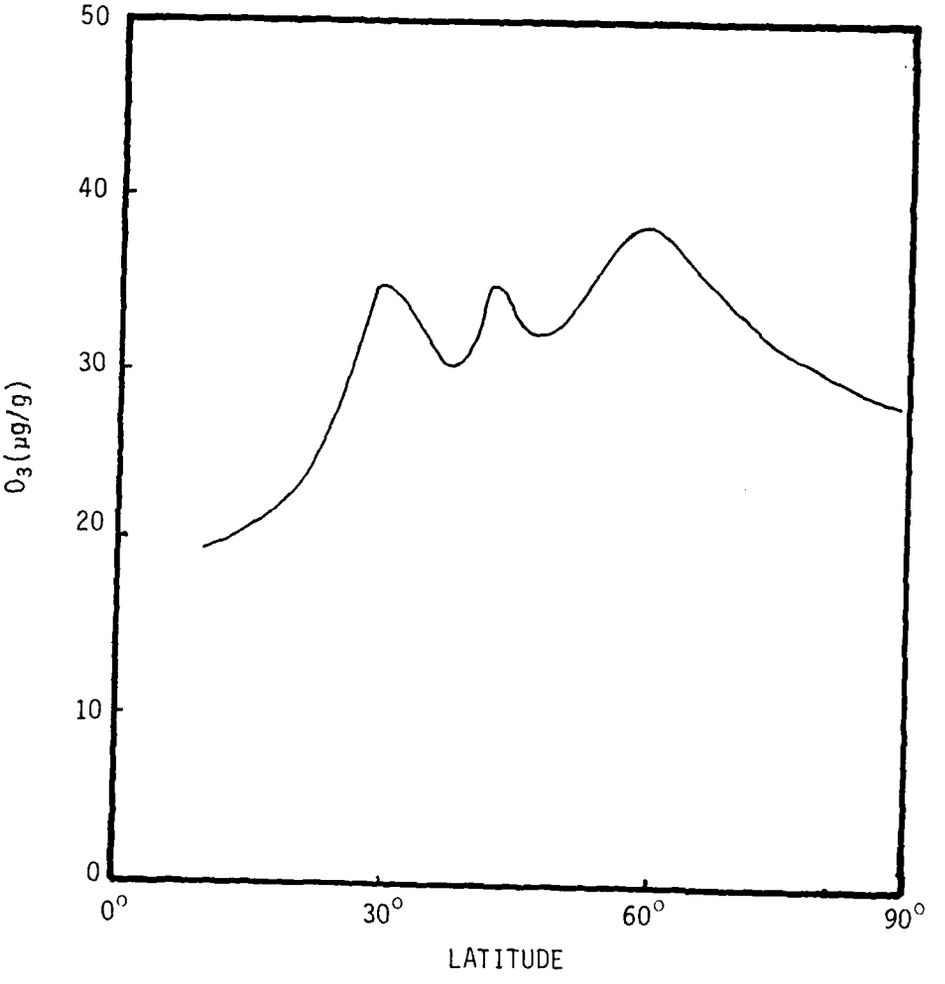

Figure 64. North American Ozonesonde Network Measurements Analyzed by Pruchniewicz, 1973.

years 1966 to 1969. Brewer-mast type electrochemical sondes were used during this period. The resulting analysis showed ozone as a function of latitude, altitude, and time of year. From their data analysis, four latitudinal distributions of ozone have been extracted: an annual average, an average for April and May, one for August and September, and finally an average representative of April, May, August, and September. These five kilometer altitude profiles have been illustrated in Figure 65. Fishman and Crutzen (1978) have been the only authors to project ozone distribution profiles based only on ozonesonde data into the southern hemisphere. The northern hemispheric profiles were based on both chemiluminescent and electrochemical sondes. By contrast, the La Paz, Boliva and Canton Island data were based on 1965 chemiluminescent ozonesonde ascents. The other three southern hemispheric stations used electrochemical sonde ascents from 1965. The Fishman and Crutzen (1978) analysis illustrates ozone as a vertical and latitudinal function. Figure 66 is a reproduction of their analysis. Using this information in tabular form, four latitudinal profiles, similar to that derived from Chatfield and Harrison, were developed and are provided in Figure 67. Both the GASP data and that presented by Fishman, et al. (1980) were collected using electrochemical type ozone sensors. However, while the Fishman, et al. (1980) field experiment was completed using only one aircraft, the GASP data has been collected using multiple B-747 aircraft.

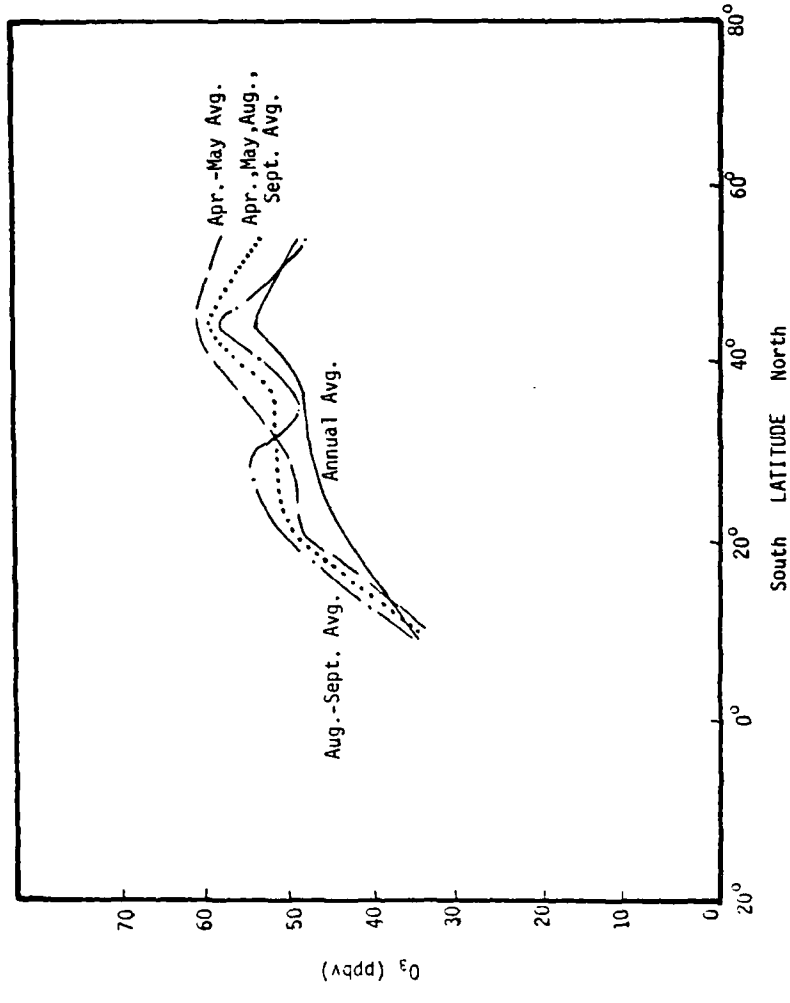

Figure 65. North American Ozonesonde Network Measurements Analyzed by Chatfield and Harrison, 1977b.

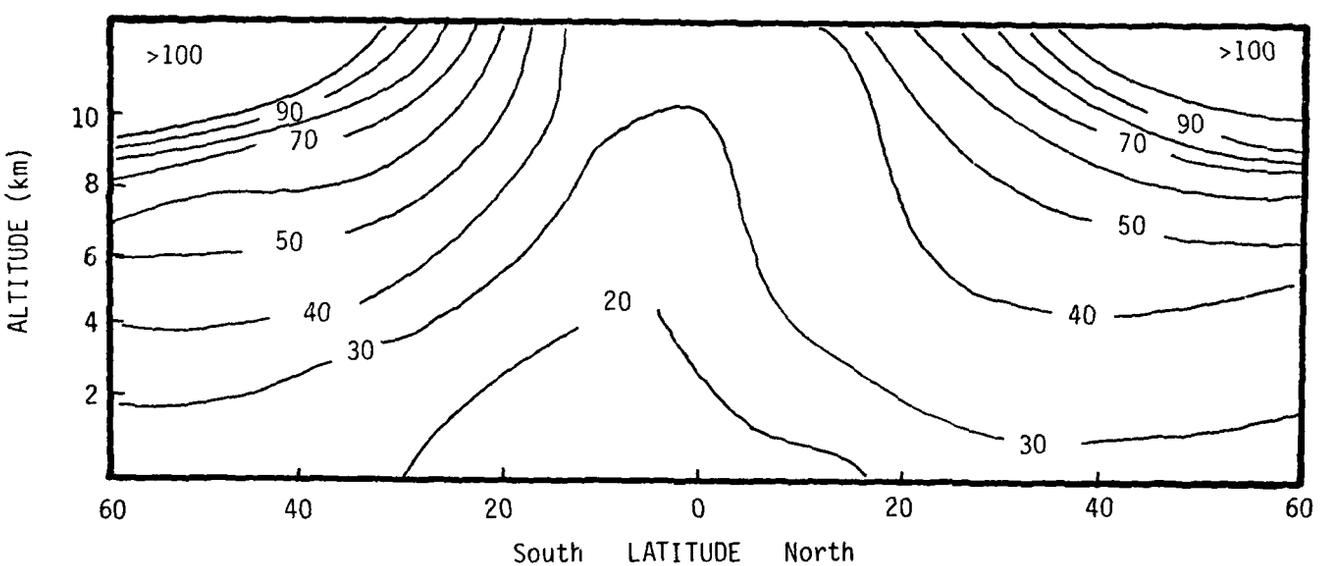

Figure 66. Global Ozonesonde Measurements as a Function of Latitude and Altitude. Redrawn from Fishman and Crutzen, 1978.

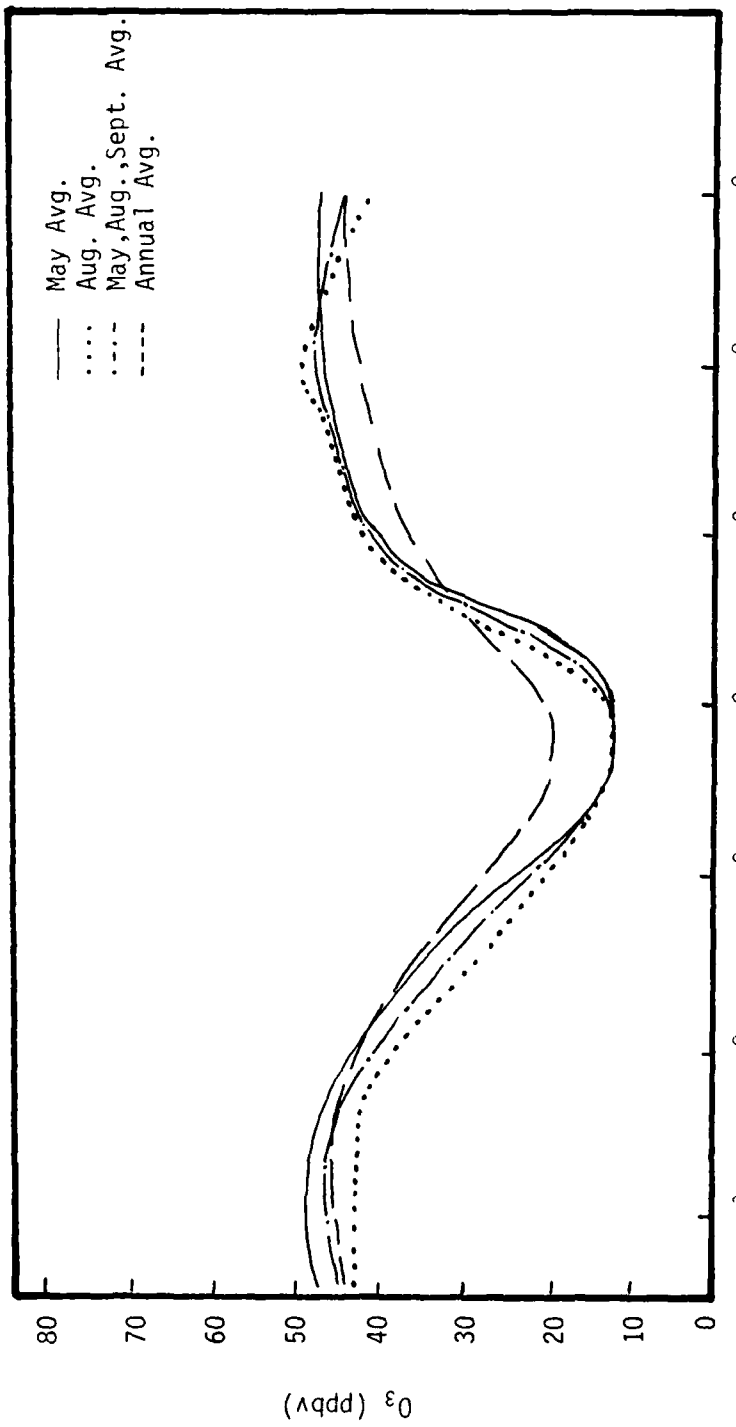

Figure 67. Global Ozonesonde Measurements Analyzed by Fishman and Crutzen, 1978.

b. Ozonesonde Data Sets. The electrochemical and chemiluminescent (different in design from the Project GAMETAG CSI ozone sensor) type ozonesondes have been compared by Chatfield and Harrison (1977b). These authors concluded that the chemiluminescent data showed such significant random and systematic errors that the O_3 data so derived needed to be shifted upward by a factor of 1.7 to make it compatible with the data derived from the newer electrochemical instrument. Fishman, et al. (1979) performed a similar test. They found electrochemical values to be 10-20% higher at altitudes below six kilometers and 5-10% lower between six and twelve kilometers. The ozone distributions developed by Pruchniewicz (1973) and Fishman and Crutzen (1978) utilized chemiluminescent data; the first author used only this type of information, while Fishman and Crutzen (1978) used a mix of the two instrument types. If Chatfield and Harrison (1977b) are correct, the entire profile of Pruchniewicz and that portion of Fishman and Crutzen's analysis just south of the equator may be a significant underestimation of the actual free tropospheric ozone concentration.

As shown in Figures 68 and 69, the Fishman-Crutzen (1978), Chatfield-Harrison (1977b), Pruchniewicz (1973), Fishman, et al. (1980), and GAMETAG data are similar. All data sets indicate minimum O_3 values near the equator and a general trend toward higher values in the middle latitudes. However, several distinct differences are evident.

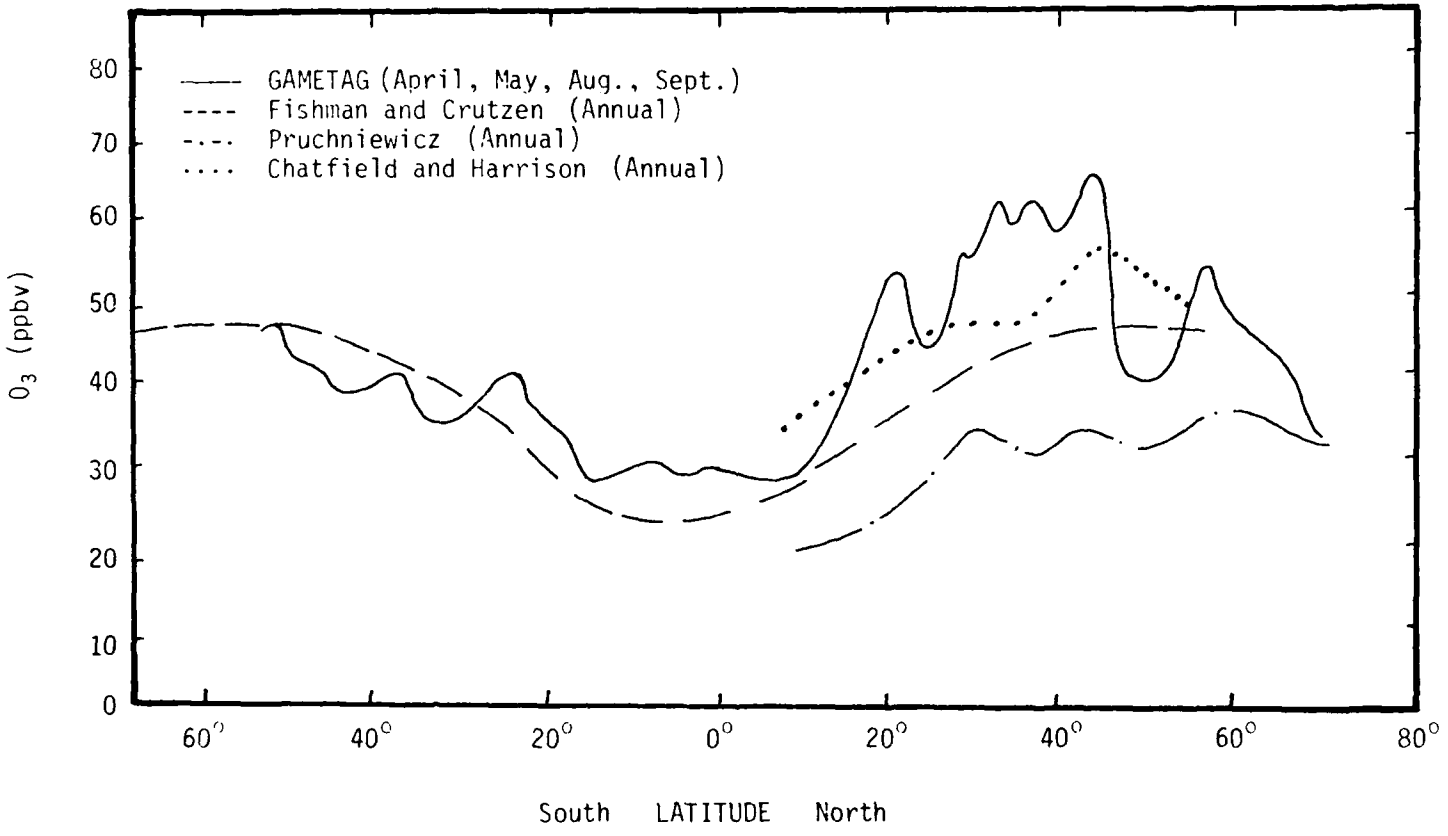

Figure 68. Comparison of the GAMETAG 1977/1978 Composite Free Tropospheric Ozone Data with Annual Average Ozonesonde Latitude Profiles.

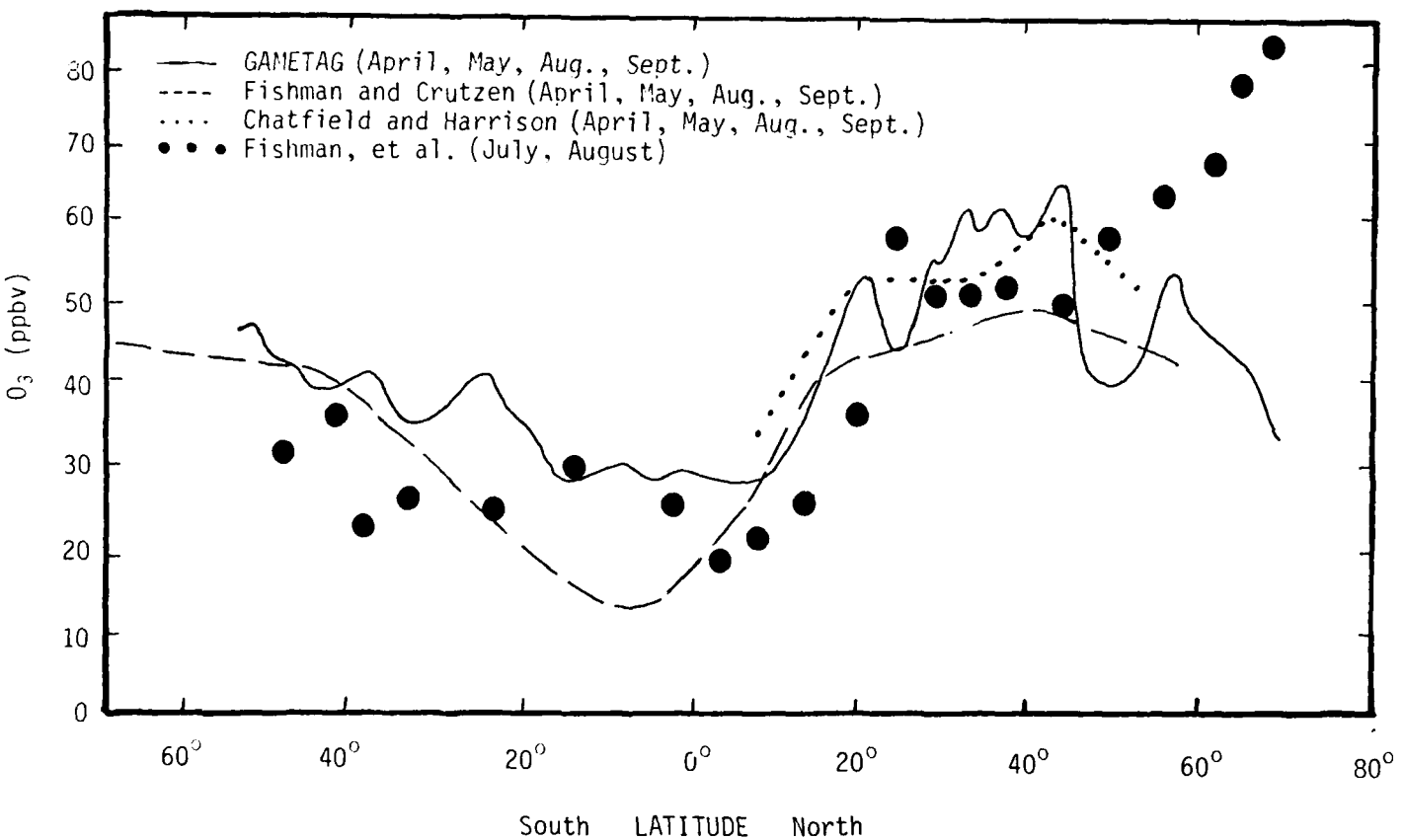

Figure 69. Comparison of the GAMETAG 1977/1978 Composite Free Tropospheric/Ozone Data with Other Free Tropospheric Ozone Profiles. Except for Fishman, et al. (1980) which is valid for the period Jul-Aug. 1974, all the profiles are valid for Apr-Sept.

Pruchniewicz's (1973) ozone data are considerably lower than the other annual averages. This profile is a mean tropospheric average rather than a five kilometer distribution. It also has a chemiluminescent sonde derived data base. Both Fishman and Crutzen (1978) analyses are five to ten ppbv lower than the corresponding profiles by Chatfield and Harrison (1977b). In the northern hemisphere, the Fishman and Crutzen (1978) ozone data is based on electrochemical and chemiluminescent ozonesonde derived data whereas the Chatfield and Harrison (1977b) data are derived from electrochemical ozonesonde measurements only. Those ozonesonde data profiles which correspond only to electrochemical derived data (all of Chatfield and Harrison, and Fishman and Crutzen south of 35°S) show close agreement to the GAMETAG free tropospheric distribution.

Pruchniewicz (1973) attributes the three peaks of his distribution to transport phenomena: tropopause gaps at 30° and 60°N and the Polar Jet at 42°N. Chatfield and Harrison (1977b) identify these gaps as the Subtropical and Arctic Fronts. For the analysis of their own data, Chatfield and Harrison (1977b) attribute the 40°N peak to the Polar Jet. They feel the maximum near 25°N relates to the Subtropical Ridge and to the southbound transport of ozone injected into the troposphere near 40°N. The proximity of the GAMETAG ozone data peaks to the Pruchniewicz (1973) and Chatfield and Harrison (1977b) ozone data peaks suggest that the same

mechanisms may be responsible for the three different distributions.

Fishman and Crutzen (1978) propose photochemistry as a significant factor influencing their ozone distribution. They contend that enhanced ozone concentrations in the northern hemisphere are the result of carbon monoxide, methane and NO_x chemistry. The concentrations of these ozone precursors should be highest over populated areas, therefore, the ozone levels should be higher in this region (30°-40°N) of the middle and low troposphere. GAMETAG had a similar finding: high ozone levels (50 ppbv) between 30° and 40°N, but these were observed in the remote regions of the Pacific, away from anthropogenic source regions. It should be expected from photochemical reasoning that this area would be a region of low ozone; it was not observed as such. High concentrations, in excess of 50 ppbv, were observed.

c. Aircraft Data Sources. The TROZ aircraft data, as analyzed by Fabian and Pruchniewicz (1977) have minimal ozone levels near the equatorial regions with higher values in the middle latitudes. Table 9 provides a comparison between the GAMETAG and TROZ data extreme values. Like the GAMETAG data, Project TROZ data indicates more variability and higher ozone concentrations in the northern hemisphere than the southern hemisphere. Both data sets in the southern hemisphere were obtained in regions away from high pressure cells. GAMETAG was flown between the anticyclones centered

Table 9. Comparison of the Latitudinal Positions of the GAMETAG and TROZ O_3 Data Extremes.

GAMETAG O_3 Max/Min	TROZ O_3 Max/Min
April/May	
14°S-10°N (Minimum)	--
40°N (Maximum)	25°-42°N (Maximum)
No Data Extreme Near 60°N	58°-65°N (Maximum)
August[1]	
26°S (Maximum)	31°S (Maximum)
8°S-5°N (Minimum)	8°-12°N (Minimum)
36°N (Maximum)	35°N, 44°N (Maximum)
60°N (Maximum)	No Data Near 60°N

[1]TROZ data for June-August.

over Australia and the Southeast Pacific. TROZ flew over Africa where no high pressure cell develops in the summer and only a weak one in the winter (Willet and Sanders, 1959). By contrast, in the northern hemisphere, both projects gathered data in regions under the influence of strong high pressure cells; the Northeast Pacific and North Atlantic (Bermuda) highs. In the winter, the development of the Icelandic low typifies the enhancement of cyclonic activity over Europe. Tiefenau, et al. (1972) relates the ozone peaks observed north of 40°N to this activity. No such cyclogenesis type feature develops over southern Africa (Willet and Sanders, 1959). The TROZ and GAMETAG aircraft data appear to have a similar reason for their interhemispheric ozone asymmetry.

Some examples of the GASP data were found in the literature (Holdeman, 1976; Holdeman and Falconer, 1976; Nastrom, 1977; Pratt and Falconer, 1979). Several instances of tropospheric data were explicitly identified in the mission profiles. These data, presented in Figure 70 on a relative scale, were collected on several flights: a) San Francisco to New York via Toyko, Hong Kong, Bangkok, Dehli, Karachi, Beruit, Instanbul, and Frankfurt; b) New York to London; c) San Francisco to Caracas.

A second set of GASP ozone data was recorded between October 28 and 31, 1977. Beginning in San Francisco, a Pan American World Airways B-747 SP flew a 54 hour circumpolar

flight back to San Francisco via London, Capetown and Auckland, New Zealand. These tropospheric ozone data were collected above eight kilometers altitude. These data, indicated in terms of absolute mixing ratios, are illustrated here in Figure 70.

The aircraft data that are shown in Figure 70 in terms of relative units indicate peak values near 55°N and 25°N. The two continuous lines in Figure 70 represent upper tropospheric concentrations measured less than two months after GAMETAG (1977) and, in the case of the Pacific leg, in close proximity to the GAMETAG sampling corridor. Like the GAMETAG measurements, these GASP ozone data show low ozone levels near the equator and peak values in the subtropical regions (Table 10). The authors presenting these data (Pratt and Falconer, 1979) noted a longitudinal gradient in the tropics but considered it to be climatologically insignificant since the difference is comparable with the "week to week" background concentrations at fixed tropical locations.

2. Boundary Layer Ozone Data

a. Introduction. In the boundary layer, there are several data sets which may be compared to the GAMETAG ozone data: Fabian and Pruchniewicz (1973, 1977) shown in Figure 71, Stallard, et al. (1975) and the low altitude ozone profiles from data reported by Chatfield and Harrison (1977b), and Fishman and Crutzen (1978). The data collected by Fabian and Pruchniewicz are related to the Project TROZ

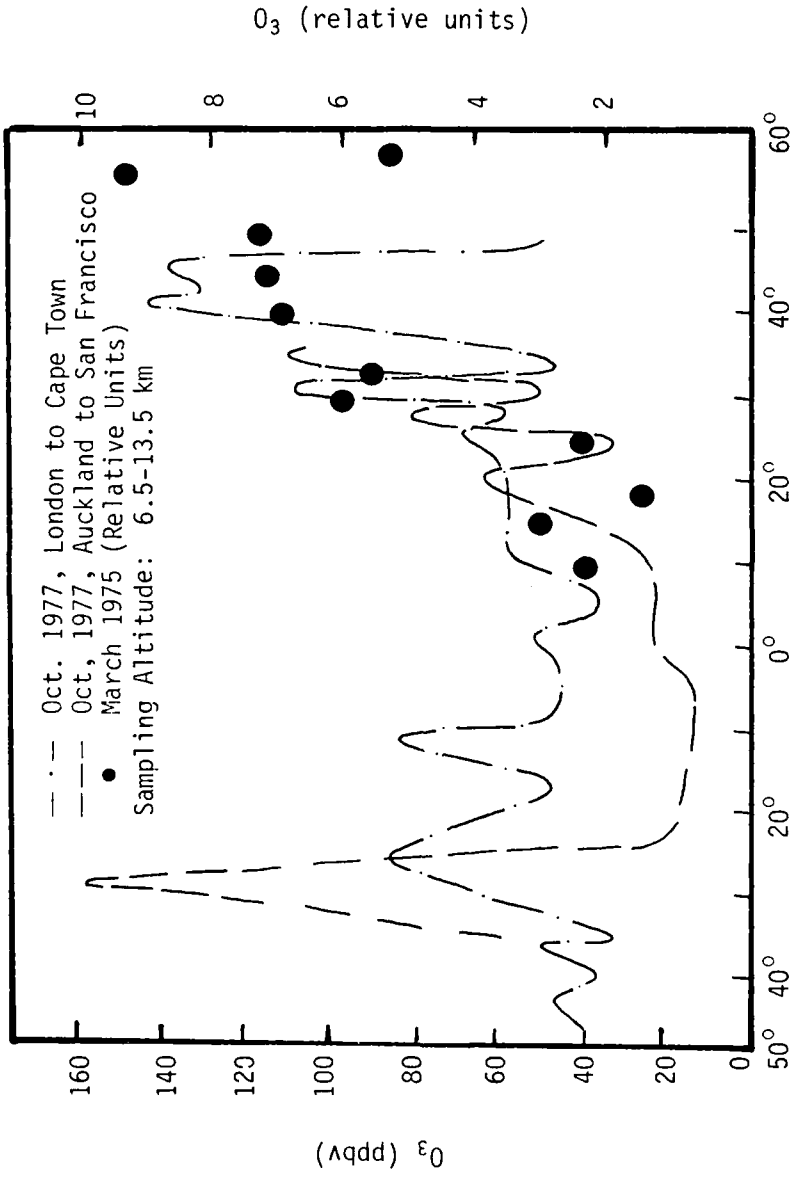

Figure 70. Selected GASP Free Tropospheric Ozone Measurements.

Table 10. GAMETAG and GASP Circumpolar Flight (Oct. 28-31, 1977) Ozone Data Comparison.

GAMETAG (1977) O_3 Data Extreme	GASP Pacific O_3 Data Extreme	GASP Atlantic O_3 Data Extreme
26°S (Peak)	29°S (Peak)	26°S (Peak)
8°S-6°N (Min)	20°S-10°N (Min)	4°N (Min)
36°N (Peak)	35°N (Peak)	38°N (Peak)
60°N (Peak)	-	-

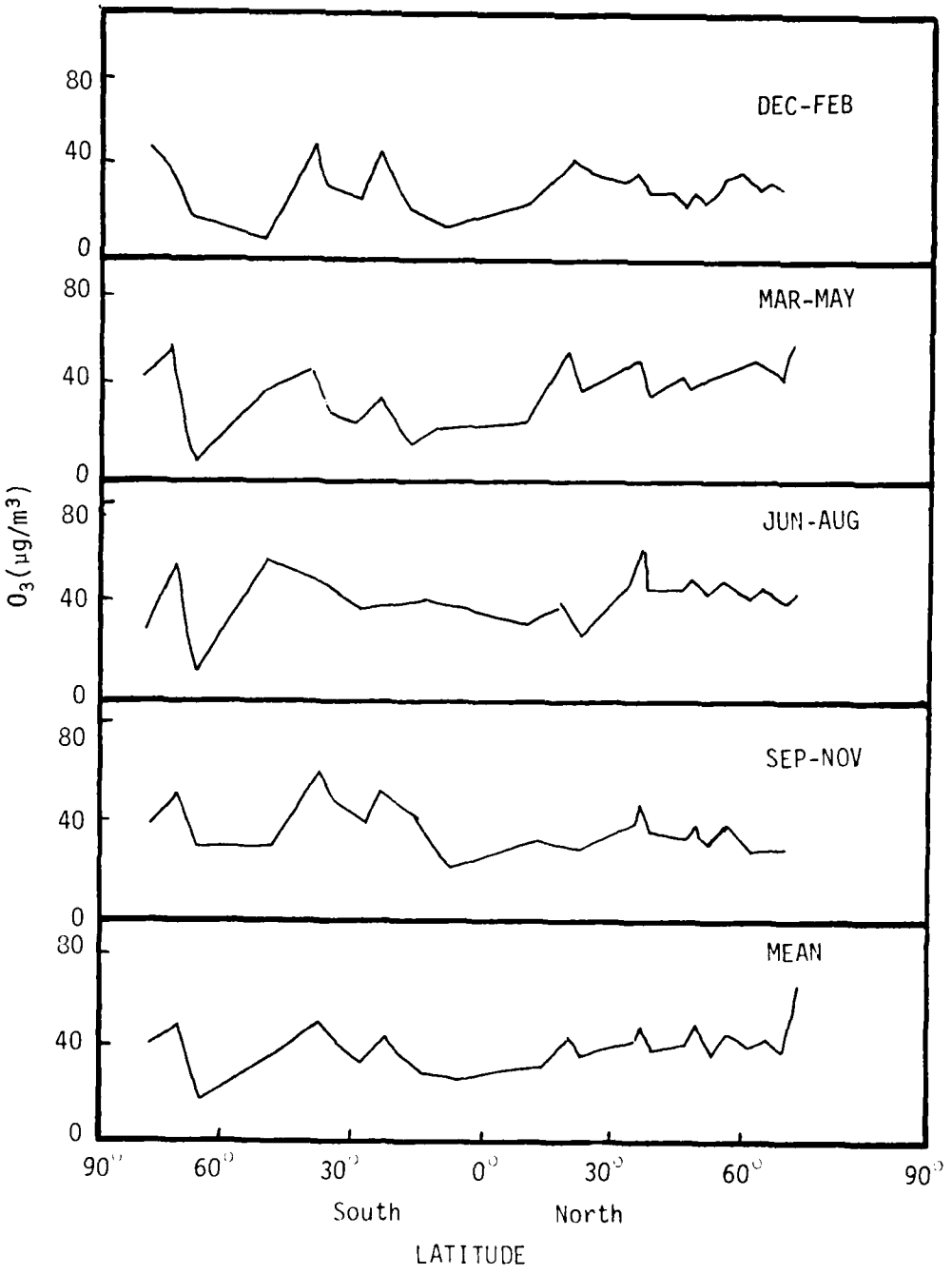

Figure 71. Surface Ozone Measurements from Project TROZ. Redrawn from Fabian and Pruchniewicz, 1977.

aircraft data reported earlier. Project TROZ established 16 surface ozone monitoring stations along a line between Norway and South Africa (see the inner Project TROZ corridor in Figure 62). Unlike TROZ, which collected its data over a three year period (1970-1973), Stallard, et al. (1975) gathered their information in one month, December 1973. They obtained their data while aboard a ship traveling between Dakar, Africa and Walvis Bay, South Africa. Both of these data sets were based on electrochemical determinations. The Fishman and Crutzen (1978) and Chatfield and Harrison (1977b) analyses were reexamined and new one kilometer profiles were determined. All five sets of boundary layer ozone data have been compared with the GAMETAG boundary layer ozone data in Figures 72 and 73.

With the exception of the Stallard, et al. (1975) data, the boundary layer ozone distributions show low concentrations near the equator and maximum values near 40° latitude. Fabian and Pruchniewicz (1973) feel that stratospheric-tropospheric interchange, surface destruction and mesoscale weather conditions contribute to their profile. They suggest that all their stations were located in pollution free areas. By contrast, Fishman and Crutzen (1978) suggest that the higher boundary layer ozone levels near 40°N could be due to increased anthropogenic emissions and subsequent O_3 photochemical production.

The ozone profile by Stallard, et al. (1975) is

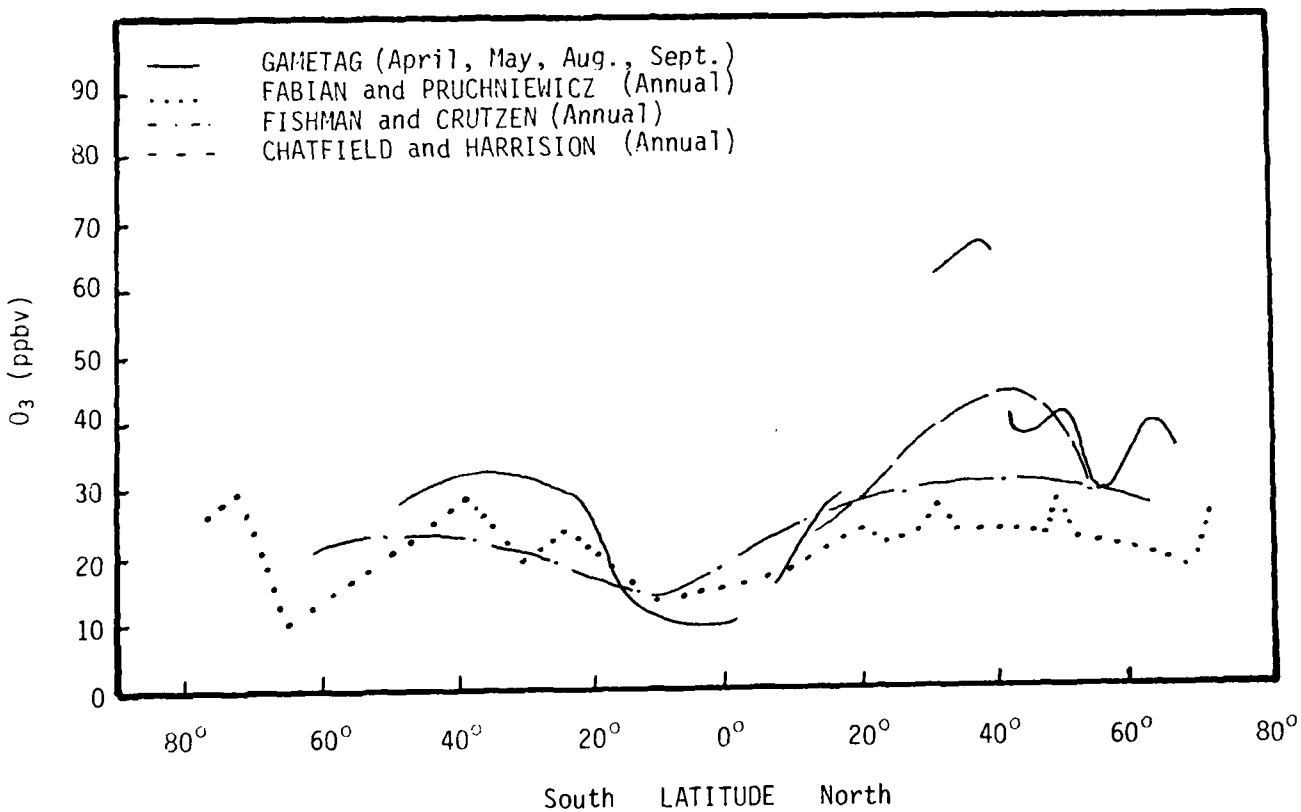

Figure 72. Comparison of GAMETAG 1977/1978 Composite Boundary Layer Ozone Data With Annual Average Boundary Layer Data.

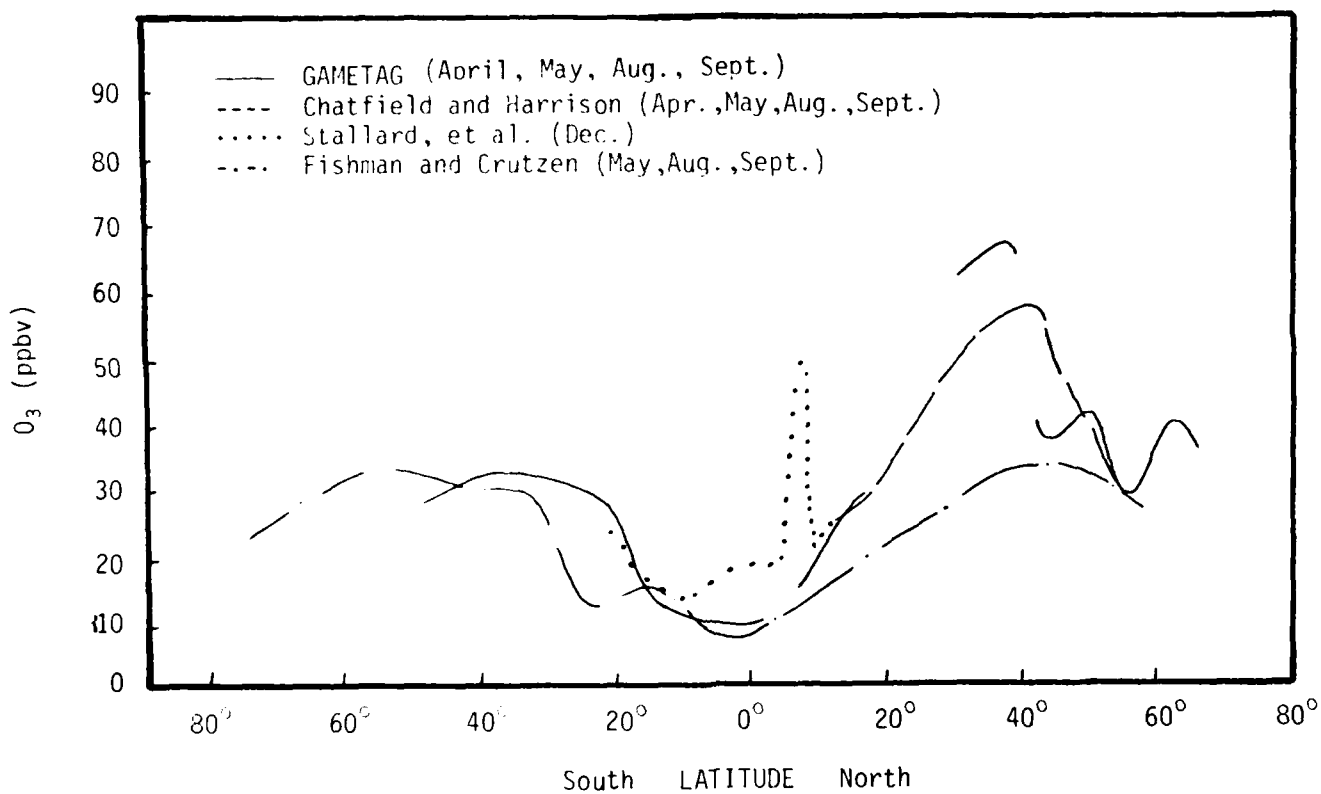

Figure 73. Comparison of GAMETAG 1977/1978 Composite Boundary Layer Ozone Data With Other Boundary Layer Ozone Data.

significantly different from the others in that it includes an ozone peak near 5°N. These data, taken during one pass through the ITCZ and the southern hemispheric subtropical ridge show high ozone in the ITCZ and lower values in the trade wind region. They attribute this ozone peak to mesoscale downdrafts from the stratosphere. According to Holton (1972), these downdrafts are necessary to maintain an adequate air mass balance in the tropical troposphere. If the mechanism, which causes these downdrafts, operates most of the time, this peak should form in other distributions, boundary layer and free tropospheric alike. GAMETAG ozone observations do not support this mesoscale downdraft hypothesis. Although GAMETAG boundary layer sampling was limited in the tropics, the four ITCZ passes (in two different years) observed free tropospheric levels equaling only 30-40 ppbv. For Stallard, et al. (1975) hypothesis to be true, high ozone levels (approaching 50 ppbv) would have to be transported down through the 5-6.5 kilometer level. Ozone concentrations near 50 ppbv were not observed by GAMETAG in the tropics. It is therefore difficult to accept the Stallard, et al. (1975) ozone maximum as a generalized case in the tropics.

C. Intercomparison of the GAMETAG Dewpoint Data with Other Dewpoint Data Sets

1. Introduction

There are at least three extensive data compilations of free tropospheric dewpoint. These compilations of the

global radiosonde network data base include the works of Crutcher (1969), Oort and Rasmussen (1971), and Newell, et al. (1972).

Cruther's (1969) analysis was presented in the form of a global dewpoint isopleth analysis for the months of January and July. The data used for this analysis were observed by the global radiosonde network during the period 1950 to 1963. Oort and Rasmussen (1971) used radiosonde data from 1958 to 1963. Their analysis was presented as monthly averages for every ten degrees of latitude from 10°S to 70°N. Newell, et al. (1972) were primarily concerned with the tropical and subtropical regions between 40°N and 40°S. They presented their data analysis in two forms: a global average for the months January, April, July, and October at every 5° latitude between 15°S and 75°N, and an isopleth analysis of dewpoint for the same four months between the latitudes 40°S and 40°N. All of these data bases are compared with the GAMETAG dewpoint values in Figures 74, 75, and 76.

2. Data Comparison

Figure 74 is a comparison among dewpoint data from GAMETAG (1977), Oort and Rasmussen (1973) (August-September global average), Newell, et al. (1972) (July and October global averages separately), Newell, et al. (1972) (this author's analysis of their July and October isopleths along the GAMETAG sampling corridor). Also indicated on this plot are the July and October average dewpoint values (July

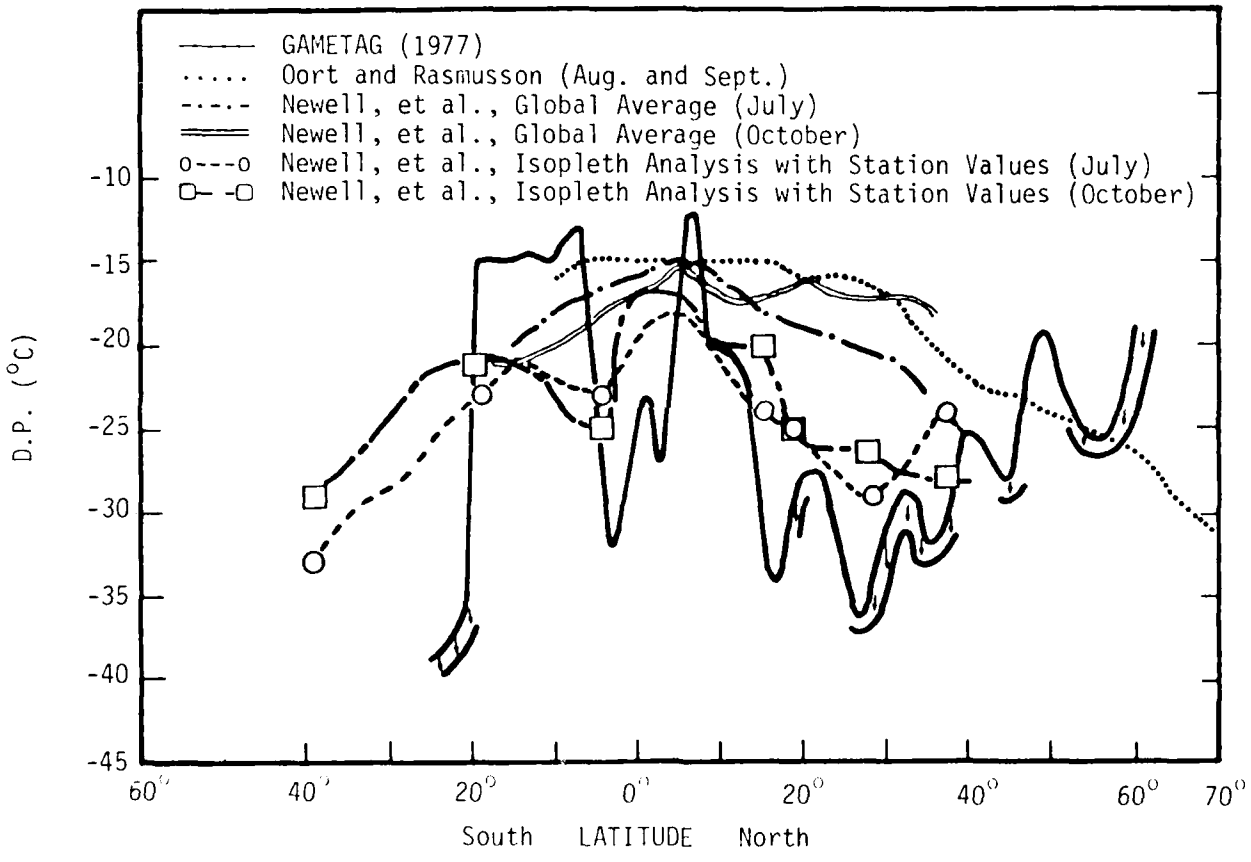

Figure 74. Free Tropospheric Dewpoint Data from GAMETAG (1977) and Other Sources.

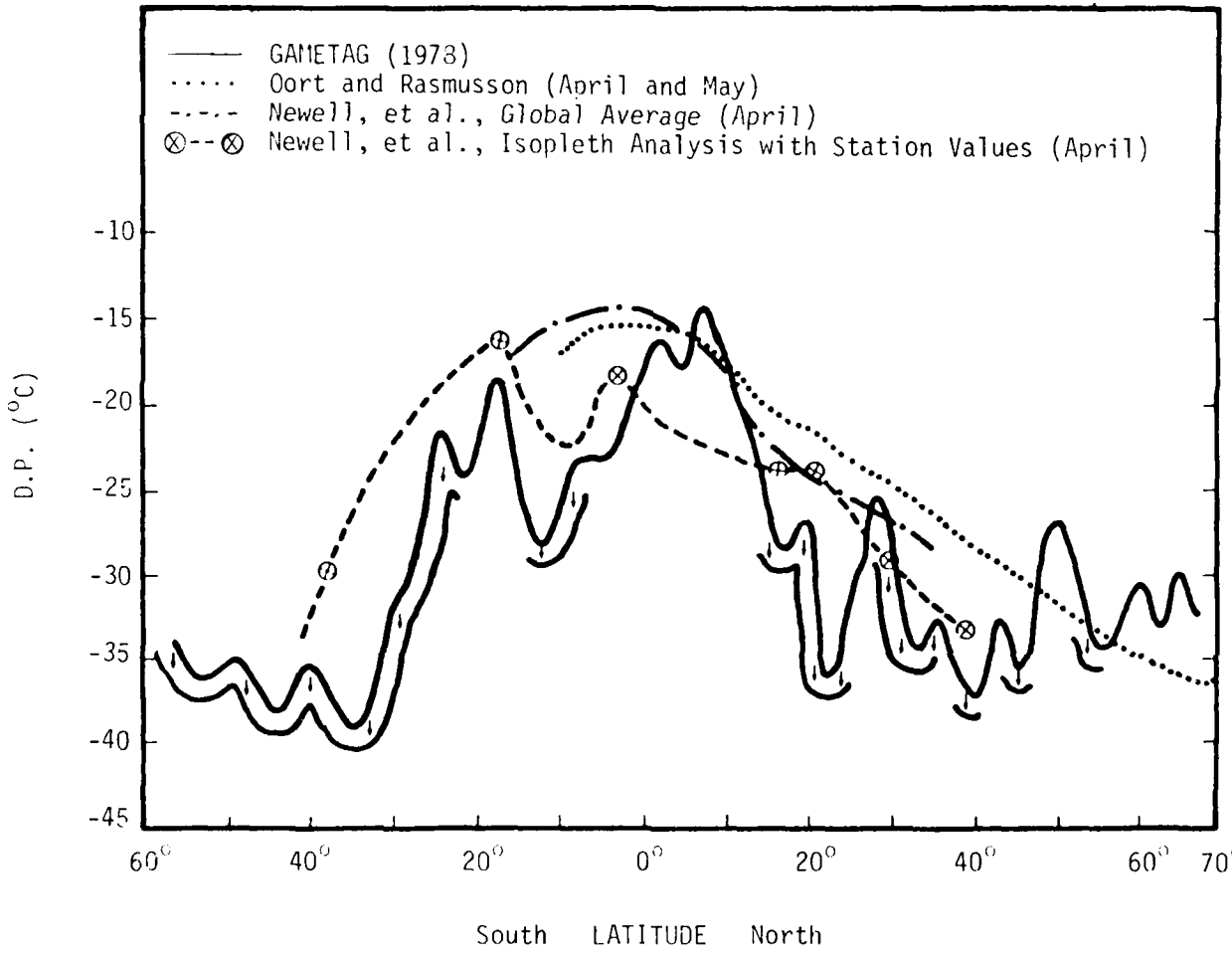

Figure 75. Free Tropospheric Dewpoint Data from GAMETAG (1978) and Other Sources.

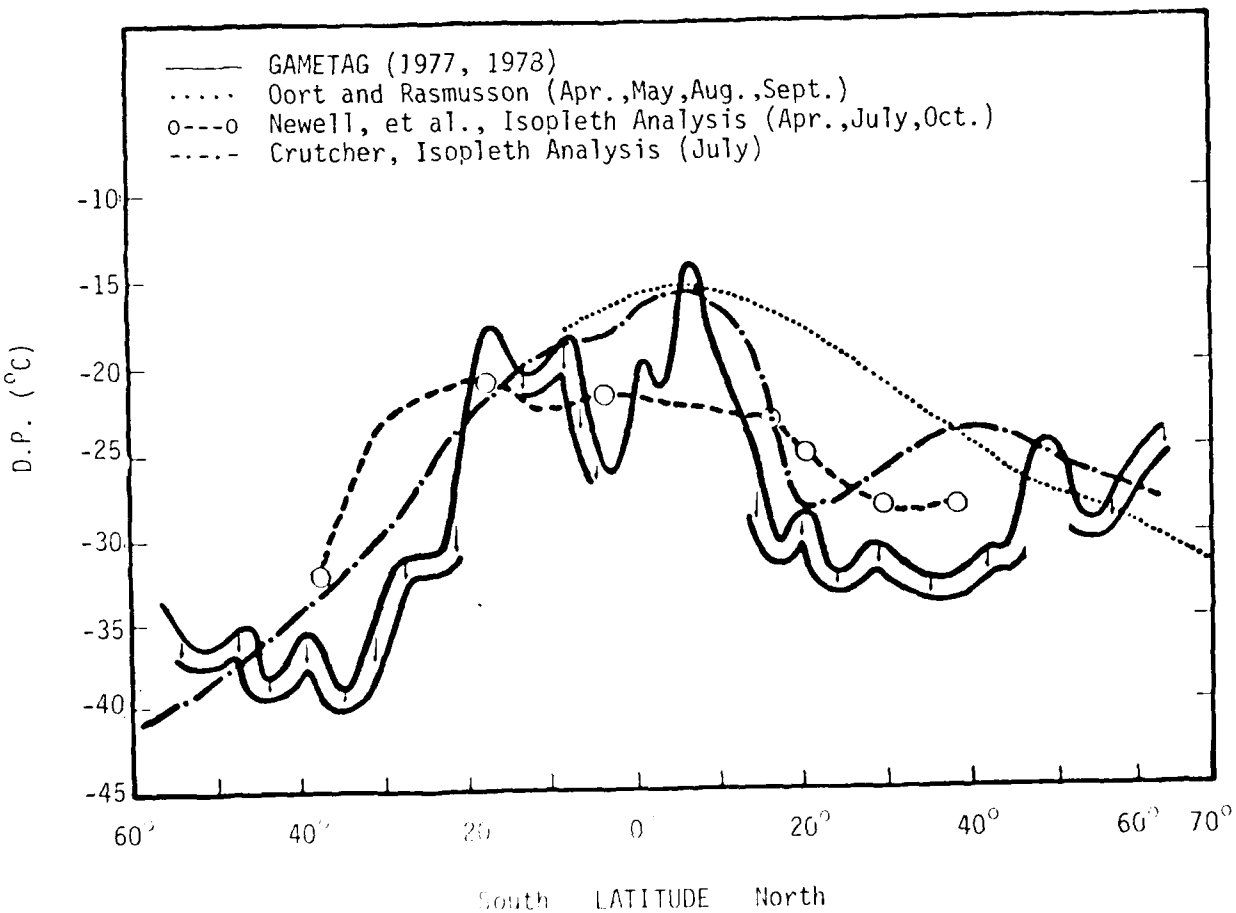

Figure 76. Free Tropospheric Dewpoint Data from GAMETAG (1977/1978) and Other Sources.

and October separately) for those radiosonde stations near the GAMETAG corridor in the Pacific. [This data was extracted from Newell, et al. (1972).] These stations represented by circles and squares respectively include Oakland, Hilo, Johnston Island, Canton Island, New Zealand and Weather Ship November near 30°N. Although all the profiles show similar values between 20°S and 15°N, the GAMETAG results show the lowest dewpoint levels in the subtropical regions. Those curves derived from the Newell, et al. (1972) analysis near the GAMETAG flight track are the closest to the aircraft data. The dryness of the troposphere in the region between 18°N and 40°N as compared to the global averages reflects the proximity of the aircraft and northern three radiosonde stations to the strong subsidence of the Northeast Pacific high pressure cell. The possible reasons for the high global averages will be discussed later in this chapter. Figure 75 is a similar comparison between GAMETAG (1978), Oort and Rasmussen (1971) (global average for April and May), and Newell, et al. (1972) (this author's analysis of their April isopleth plot). The dewpoint values for individual upper air stations along the GAMETAG flight tracks are identified as open circles. [As in Figure 74, these were extracted from the Newell, et al.'s (1972) isopleth analysis.] A similar relationship among the profiles is observed in this figure: highest dewpoints near the equator with decreasing values poleward. Figure 76 is a comparison between a composite of

the GAMETAG dewpoint data for both years and the data presented by the other authors. Included in this figure are the Oort and Rasmussen (1971) global averages for April, May, August, September; Newell, et al.'s (1972) global averages for April, July, and October; this author's analysis of Newell, et al.'s (1972) isopleth plot for April, July, and October (averaged) along the GAMETAG track; and this author's analysis of Crutcher's (1969) isopleth dewpoint plot for the month of July along the GAMETAG track. Again, the global averages are much higher than the profiles tailored near the Northeast Pacific. However, it must be noted that in this figure as in the two previous ones, the GAMETAG data agree with the other curves near the equator and middle latitudes, north and south.

3. Discussion

These differences in the dewpoint distributions may be explained, in part, by three factors: the variety of instrument types used, the difference in the data bases, and the natural and not completely understood dewpoint longitudinal gradient.

The humidity sensors contained in the various radiosonde intruments used throughout the global upper air network are generally less sophisticated than the EG and G hygrometer used in Project GAMETAG. In the former case, there are three major types of sensor operation employed: those which measure resistance as a function of humidity, those which measure a change in length of a sensor element as a

function of humidity, and those using wet bulb temperature variability as a function of humidity. The first of these types is the most widely used. The radiosonde instrument currently used by the United States, England, the Republic of China, and approximately thirty five other nations is manufactured by the VIZ Manufacturing Company of Philadelphia, PA. According to Freedman (1980), the humidity element is a carbon hygristor. In this system, a thin film of carbon is spread across a plastic plate. The resistance of this film, which is a function of both humidity and temperature, is measured, converted to an audio-visual signal and transmitted to the ground. Additionally, with the aid of temperature data from a ceramic rod thermistor, the humidity element signal may be deconvoluted into its temperature and humidity components. Although the sensor is specified as accurate to within ten percent relative humidity at temperatures above -40°C, American operators of this system often identify as bad any hygristor signal that can be traced to a relative humidity less than 20%. At 500 millibars, this relates to a dewpoint depression of approximately 20°C. The mode of operation for the second type element is based on the assumption that the length of a sensor element can be made to be primarily a function of humidity. Human hair and ox intestines (commonly known as gold-beater's skin) are the substances most frequently used. When hair is used, the fatty material is first removed by solvents such ethyl ether or

alcohol. The hair is then rolled and flattened to achieve better response rates, a higher coefficient of expansion, and more linearity. The problems associated with this instrument include sensor sensitivity to dust, variable (hair to hair) expansion coefficients, increases in response time with decreasing temperature and humidity, and reductions in reproducibility due to hysteresis. Widely used at one time, this type humidity element has been predominately replaced by the carbon hygristor. The third type element is a thermocouple psychrometer. Copper constantan thermocouples are used as both the dry and wet sensors. Cooling to the wet bulb temperature is accomplished by passing an air stream over a small water reservoir. The average cooling is about 70% of the wet bulb depression and provides a relative humidity reading to within 3% of a simultaneous precision measurement (Freedman, 1980). Like the human hair instrument, this element is rapidly becoming obsolete. By comparison, all the GAMETAG data were collected using a non-disposable hygrometer unit. Additionally, the GAMETAG data are the only set which have been singularly processed by computer from instrument output to dewpoint value. The radiosonde data, on the other hand, are the result of either computer or hand processing by thousands of different observers.

The radiosonde network is predominately restricted to mid-latitude northern hemispheric continental regions. There are 1.6 times more radiosonde stations between 30°N and 60°N

than in all other latitude spans combined; 21 times more stations between 20° and 60° (North and South) than in the tropics; six times more upper air observation sites north of the equatorial region than south of it; and lastly ten times more continental stations than oceanic ones (Oort and Rasmussen, 1971). This lack of hard data points in regions overflown by GAMETAG and the subsequent interpolation of dewpoint values into the Pacific Ocean areas by these other data sources may explain part of the difference in the aircraft and radiosonde dewpoint data.

The difference between Newell, et al.'s (1972) and Crutcher's (1969) versions of the Northeast Pacific dewpoint distribution as well as their differences from the GAMETAG data may be explained in terms of a longitudinal dewpoint gradient. Crutcher (1969) identifies a dry pocket near Hilo based only on that station's average 500 millibar dewpoint value; Newell, et al. (1972) places it far to the north, near the 35° to 40°N position of the North Pacific anticyclone's center. Both authors present a wide range of 500 mb continental dewpoint values: -35°C over Saudi Arabia to 0°C over Northern India. The definition of their gradient contours is far less over oceanic regions. This lack of an over water longitudinal gradient as compared to the dense continental variability may or may not be real. It certainly disagrees with the climatological positions of primary circulation systems and their associated meteorology (Willet

and Sanders, 1959). The difference in their analyses reflects the lack of oceanic radiosonde stations upon which Oort and Rasmussen (1971), Crutcher (1969), and Newell, et al. (1972) have based their semi-subjective analyses.

D. Comparison of GAMETAG Ozone and Dewpoint Data

1. Horizontal GAMETAG O_3 and Dewpoint Data

a. Introduction. According to Reiter (1961), Kroening and Ney (1962), and Danielsen (1968, 1980), the intrusion of stratospheric air into the troposphere is associated with the injection and subsequent layering of high ozone concentrations and low water vapor levels (low dewpoint, high dewpoint depression). On the other hand, since the earth's surface is an ozone sink (Aldaz, 1969) and a water vapor source (Sellers, 1965), air moving with a general upward vertical motion (ITCZ) may be expected to show low ozone concentrations, high dewpoint values, low dewpoint depressions, and little evidence of O_3 layering. A widespread negative correlation within many different sets of ozone and dewpoint data would indicate that dynamic mechanisms may play an important role in determining the global tropospheric ozone budget. The GAMETAG data set appears to be one such set that displays a negative correlation between ozone and dewpoint.

Figure 77 shows ozone and dewpoint levels for the GAMETAG flight on September 5, 1977 (Hilo, Hawaii to San

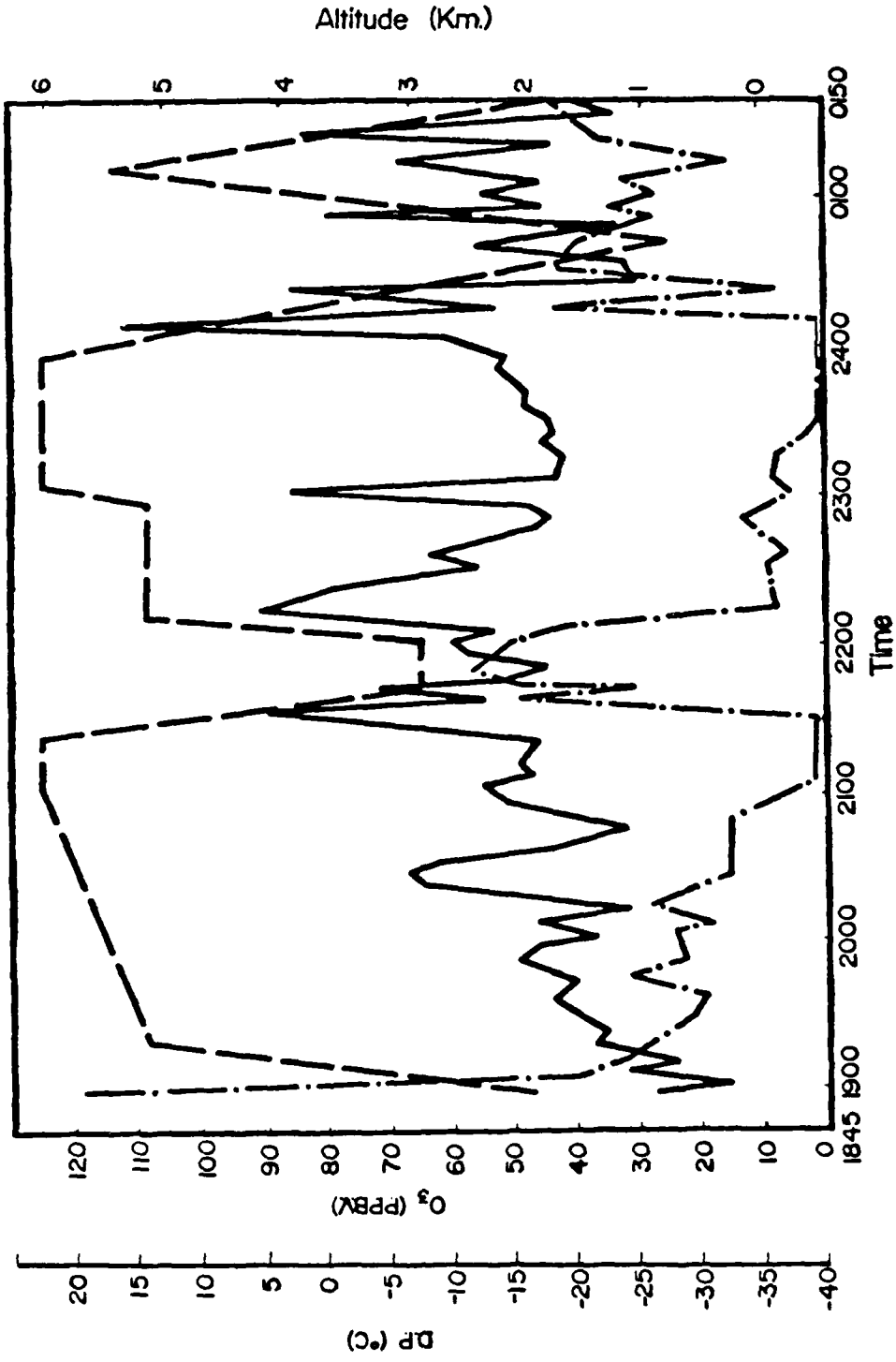

Figure 77. Real Time O_3 and Dewpoint Profiles Recorded During the 1977 Flight from Hilo, Hawaii to San Francisco, California.

Francisco). Although this flight through the northern hemispheric subtropical latitudes encountered far less ozone variability than the southbound flight through this same region (August 23, 1977), major ozone data peaks and valleys can qualitatively be seen to be negatively correlated with dewpoint. This negative correlation is not as clear cut in some periods of flight, primarily due to the hygrometer being bottomed out. Significant negative correlations can be seen during the period 2400 hours to 0150 hours when the hygrometer was completely operational; one exception is the boundary layer penetration at 0040 hours when ozone and dewpoint appear to be positively correlated.

b. Graphical Comparison of O_3 and Dewpoint as a Function of Latitude. One method employed here to compare the GAMETAG ozone and dewpoint data is to plot the average O_3 and dewpoint levels as a function of latitude for each major GAMETAG flight leg (Figures 67 through 85) and for Project GAMETAG as a whole (Figures 86 and 87). In these first eight figures, the averaging distance is 2° latitude. Where the dewpoint values were taken at the operational limit of the hygrometer, a downward pointing arrow has been attached to the horizontal dewpoint double line data bar. Dewpoint depressions have only been included for the latitude segments with reliable dewpoint data.

Figures 78, 79, and 80 cover the 1977 free tropospheric sampling program. High ozone values can be seen to be

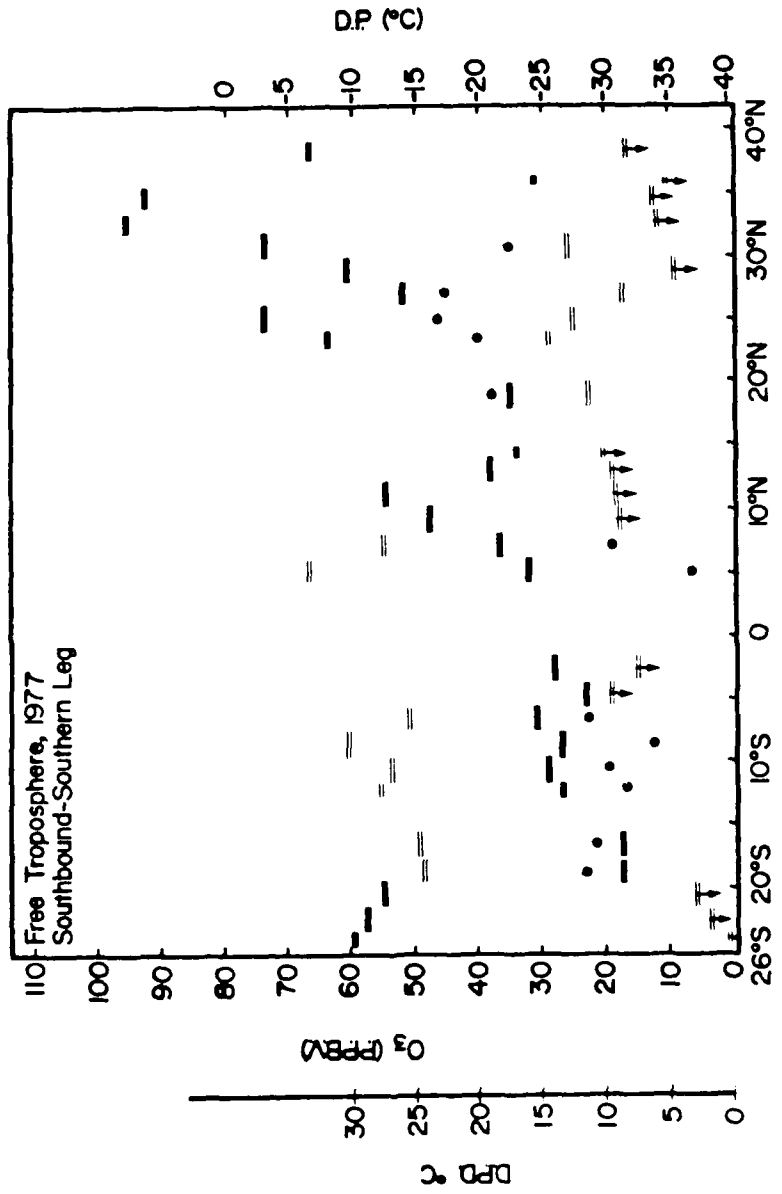

Figure 78. Comparison of 1977 Free Tropospheric O_3 and Dewpoint Values as a Function of Latitude. Measurements are for flight tracks southbound from the continental U.S.A. and round-robin flights from Samoa. Solid horizontal bars indicate O_3 levels; double line bars specify dewpoint values; solid circles indicate the dewpoint depression for those latitudinal segments for which absolute dewpoints were available.

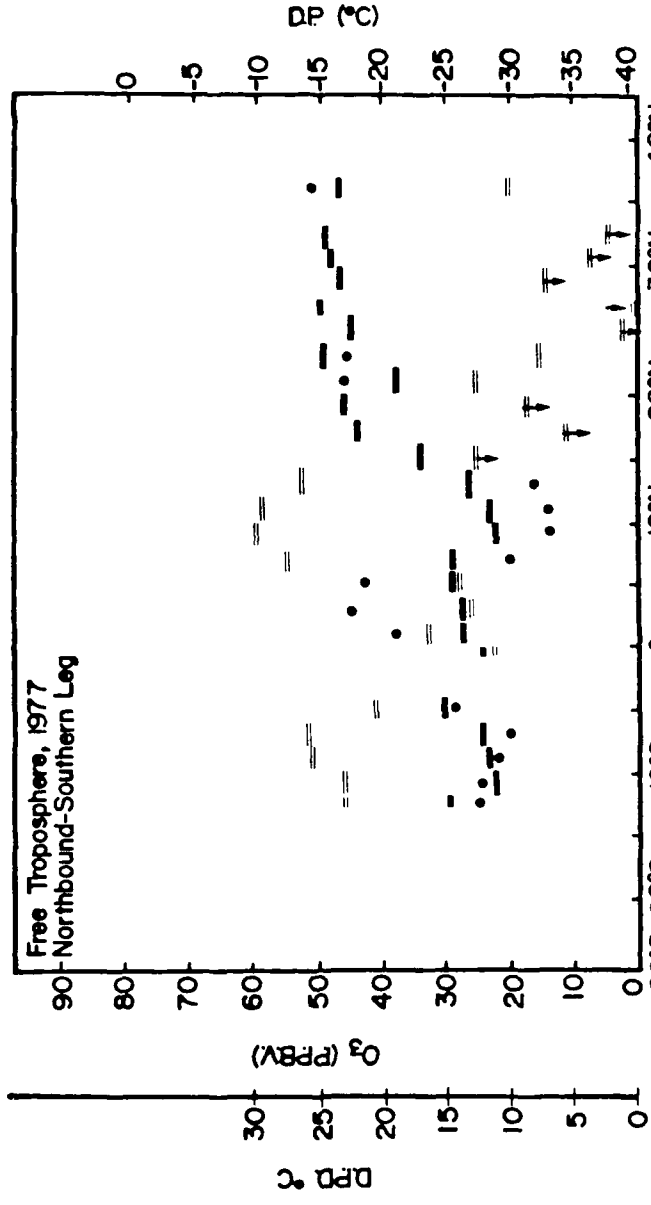

Figure 79. Comparison of 1977 Free Tropospheric O_3 and Dewpoint Values as a Function of Latitude. Measurements are for flights tracks northbound from Samoa. See Figure 78 for legend explanation.

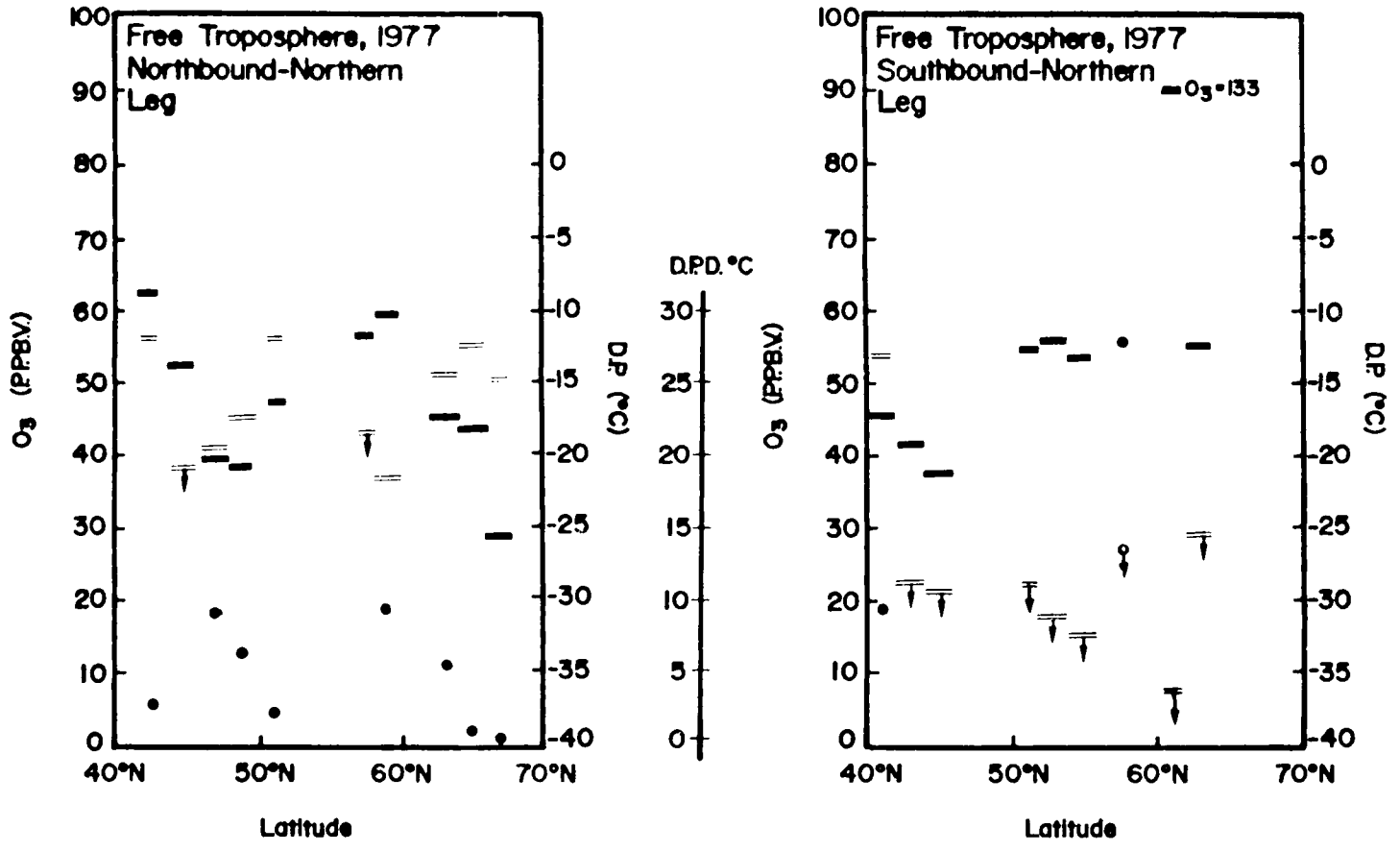

Figure 80. Comparison of 1977 Free Tropospheric O_3 and Dewpoint Values as a Function of Latitude. Measurements are for flight tracks northbound from the continental U.S.A. and southbound from Anchorage, Alaska. See Figure 78 for legend explanation.

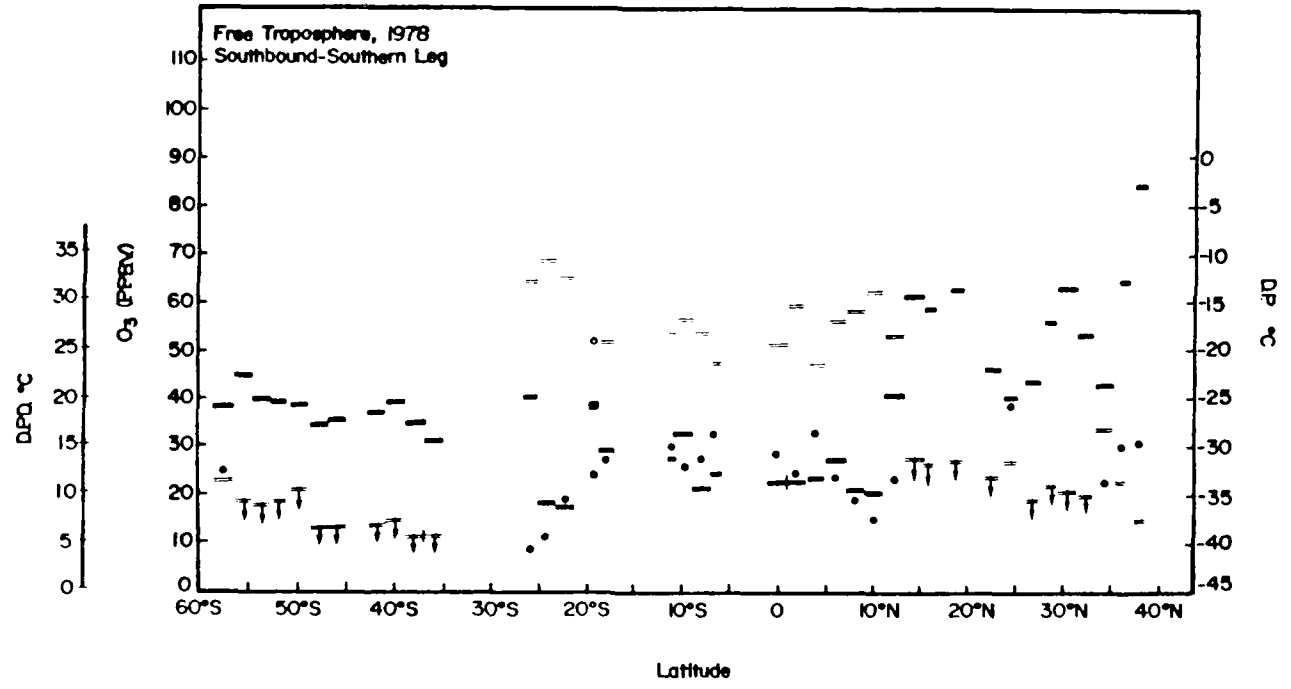

Figure 81. Comparison of 1978 Free Tropospheric O_3 and Dewpoint Values as a Function of Latitude. Measurements are for flight tracks southbound from the continental U.S.A. and Christchurch, New Zealand. See Figure 78 for legend explanation.

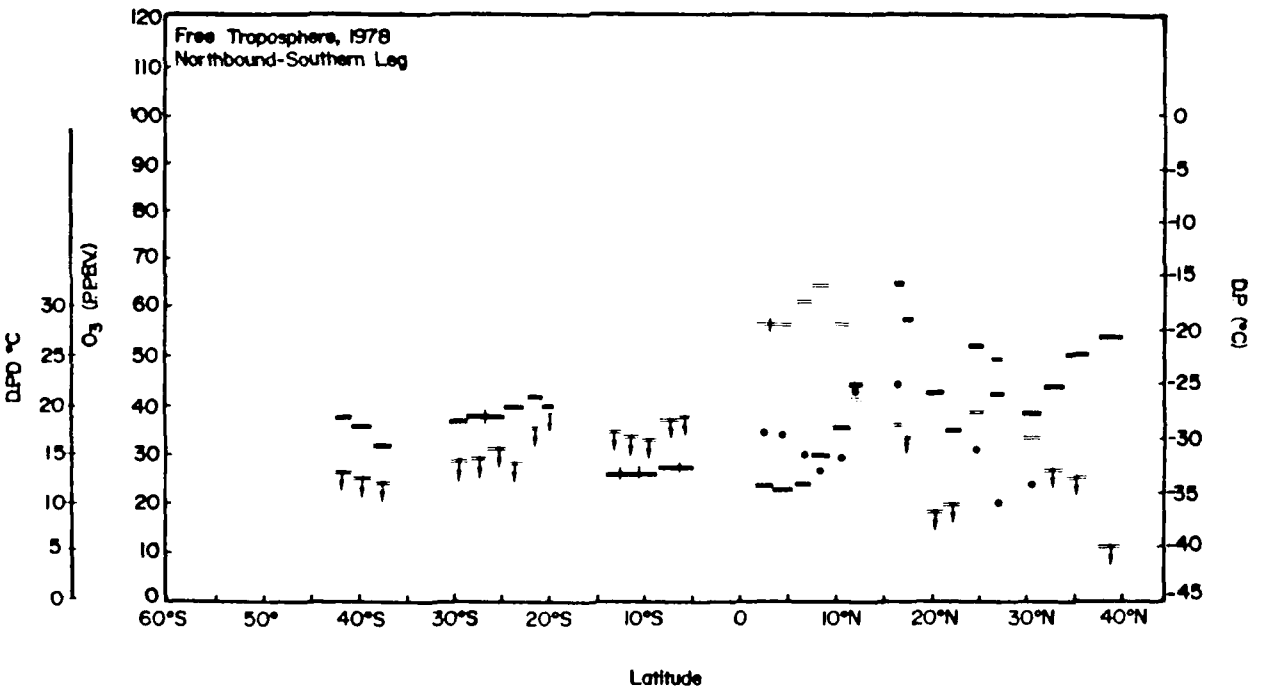

Figure 82. Comparison of 1978 Free Tropospheric O_3 and Dewpoint Values as a Function of Latitude. Measurements are for flight tracks northbound from Christchurch, New Zealand. See Figure 78 for legend explanation.

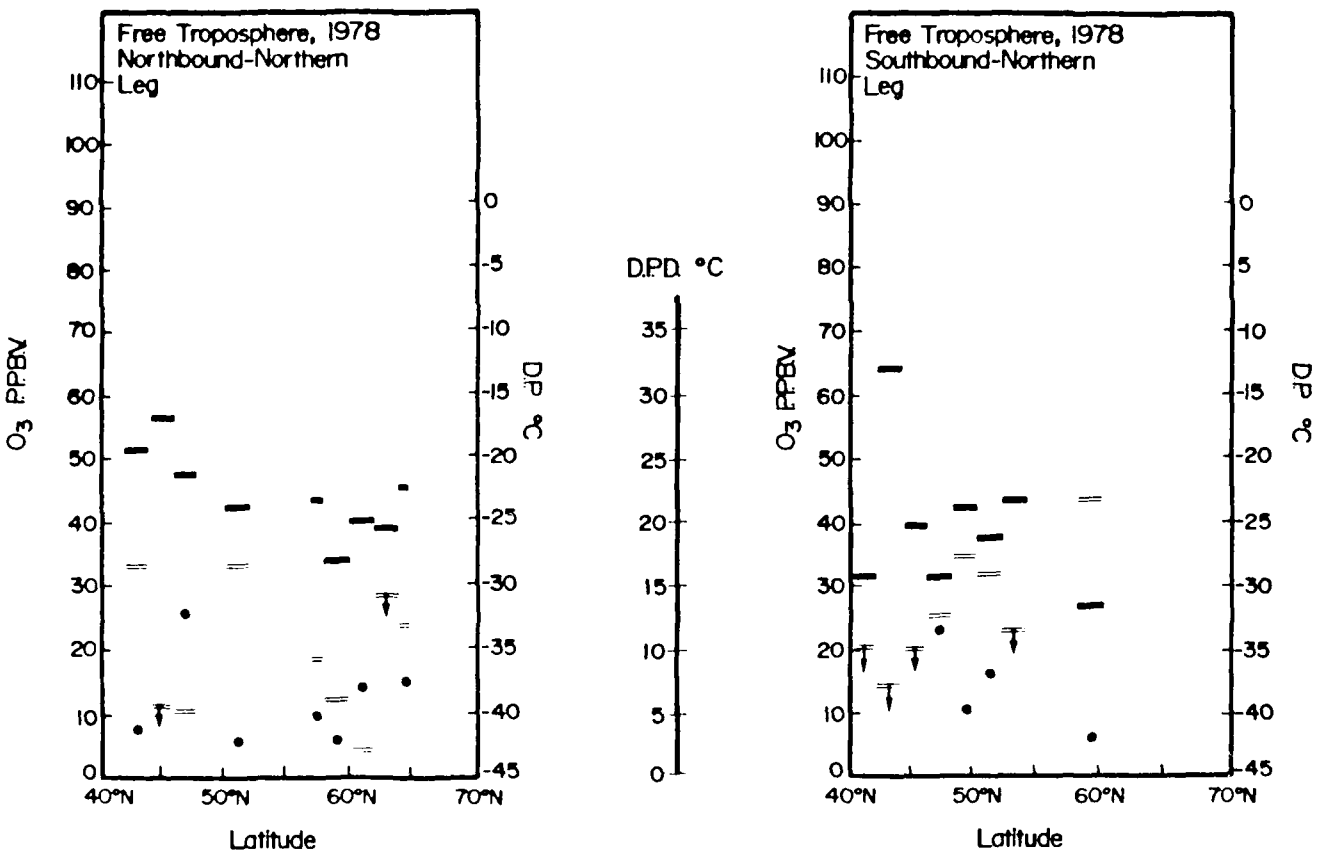

Figure 83. Comparison of 1978 Free Tropospheric and Dewpoint Latitudinal Distributions. Measurements are for tracks northbound from the continental U.S.A. and southbound from Whitehorse, Canada. See Figure 78 for legend explanation.

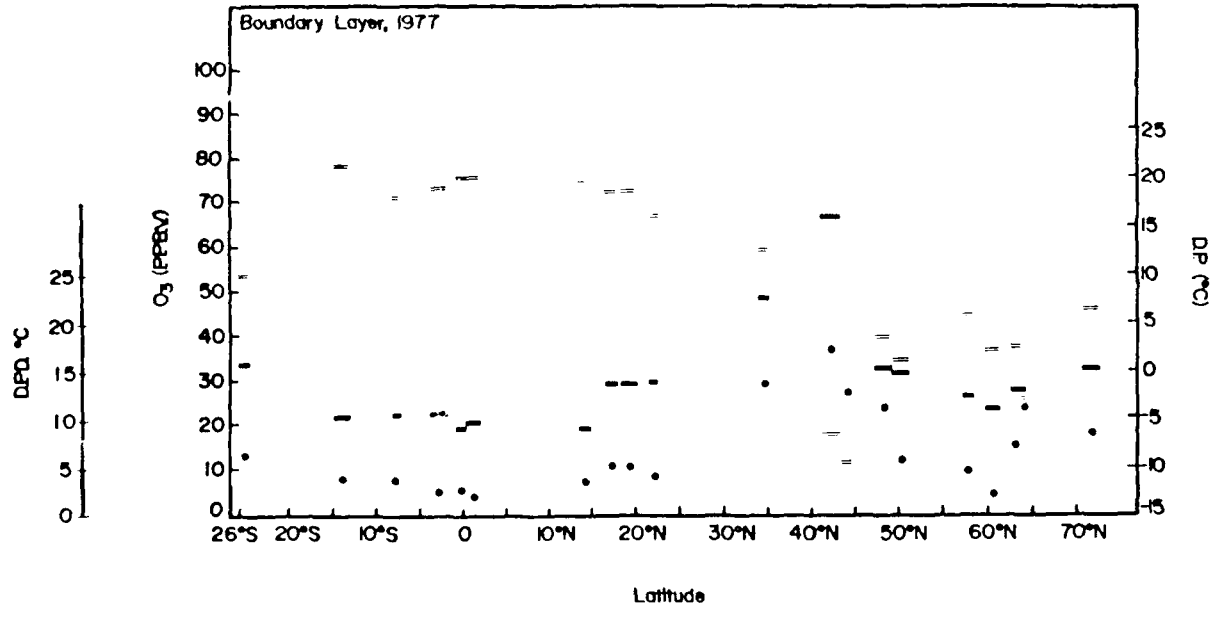

Figure 84. Comparison of 1977 Boundary Layer O_3 and Dewpoint Levels as a Function of Latitude. See Figure 78 for legend explanation.

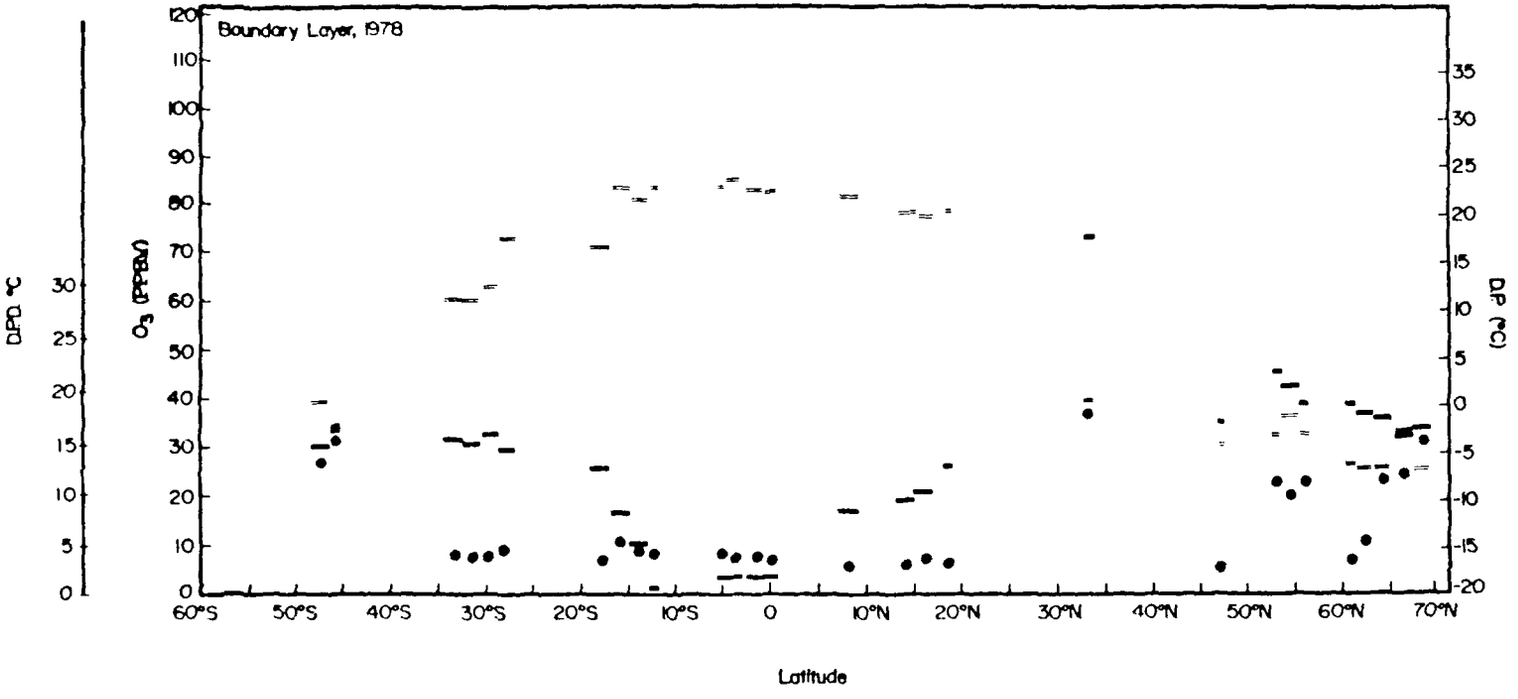

Figure 85. Comparison of 1978 Boundary Layer O_3 and Dewpoint Levels as a Function of Latitude. See Figure 78 for legend explanation.

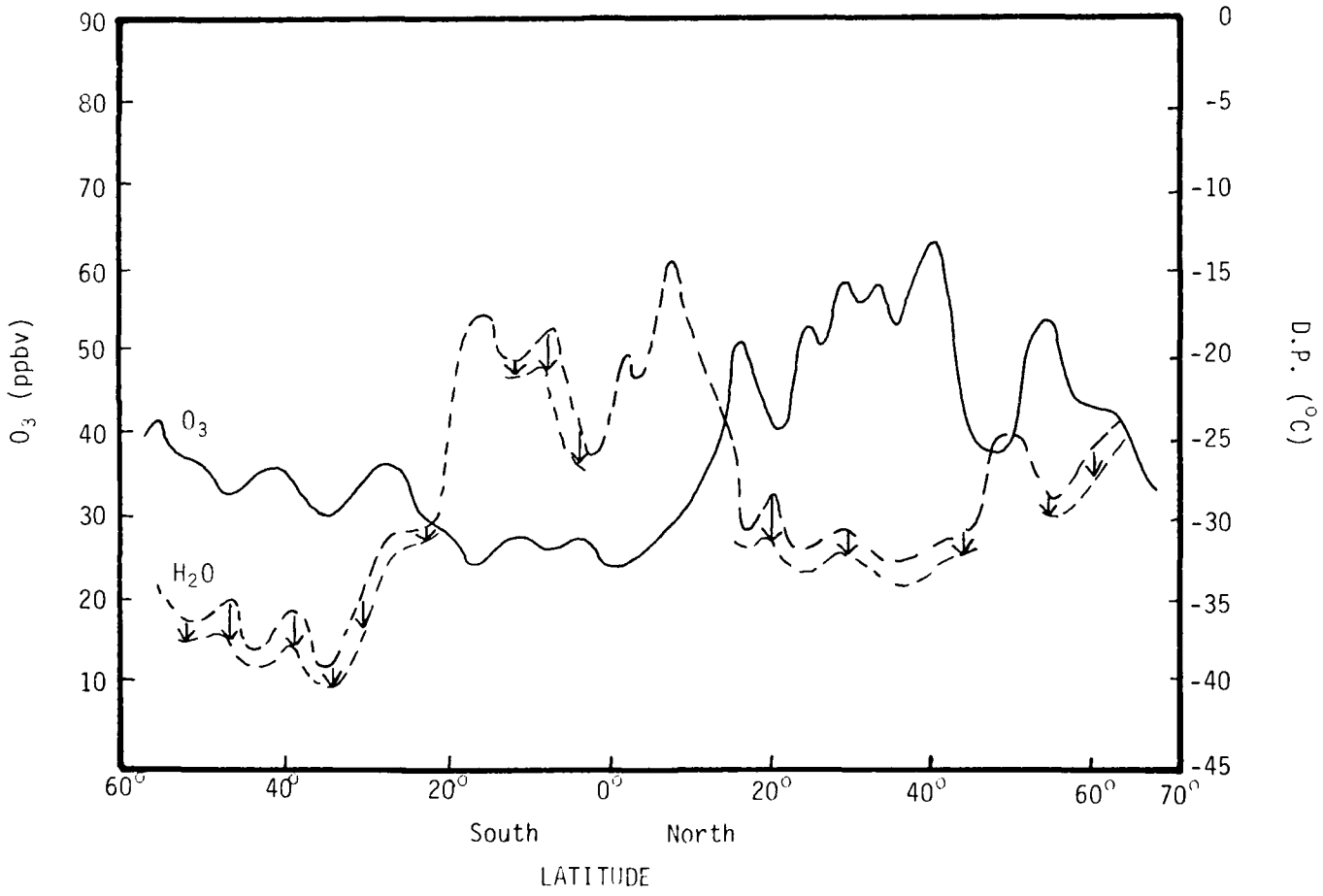

Figure 86. Comparison of 1977-78 GAMETAG Free Tropospheric O_3 and Dewpoint Levels as a Function of Latitude.

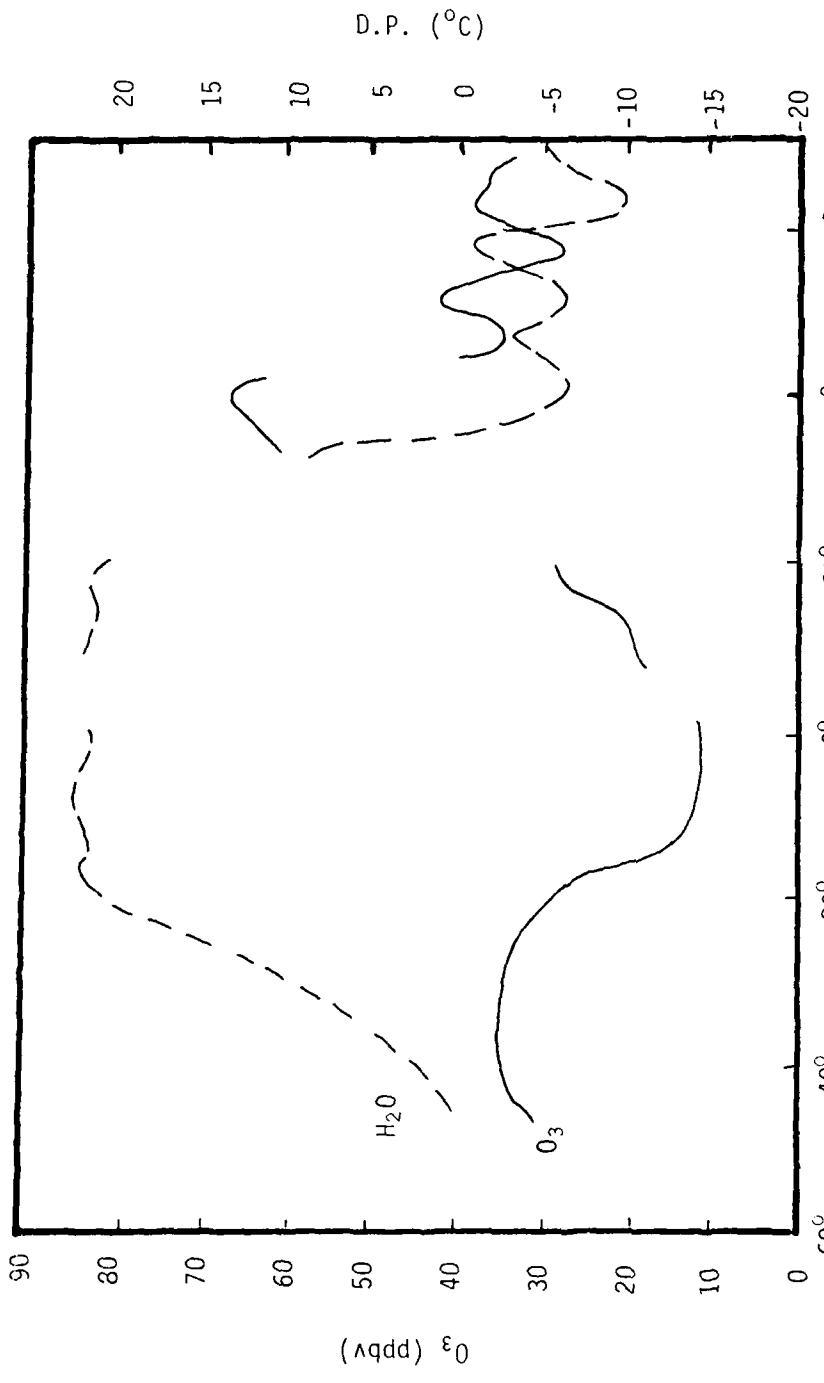

Figure 87. Comparison of 1977/1978 GAMETAG Boundary Layer Ozone and Dewpoint Data as a Function of Latitude.

generally anti-correlated with dewpoint. On the other hand, low ozone levels are not always anti-correlated with dewpoint. There appear to be occurrences of simultaneous low ozone and low dewpoing measurements (i.e., southbound southern leg near 20°N and northbound southern leg leg near 50°N). Figures 81, 82, and 83 show the free tropospheric ozone, dewpoint, and dewpoint depression data from the 1978 GAMETAG flight tracks. They also show consistent anti-correlation between high ozone data and dewpoint.

Figure 84 and 85 indicate the 1977 and 1978 boundary layer ozone, dewpoint, and dewpoint depression data from Project GAMETAG. Although the boundary layer ozone data have less variability than the dewpoint data, the ozone data appear to be anti-correlated with the dewpoint data in that the ozone values increase and the dewpoint values decrease poleward from the equator. There appears to be anomalies in each year's set of boundary layer data near 33°N and 42°N in 1977 and 33°N in 1978. The ozone data peaks near 33°N were collected over the Imperial Valley (California); the ozone data peaks measured near 42°-45°N were collected over Utah, North Dakota, and South Dakota. The data peaks from the Imperial Valley have a high probability of being produced by pollution sources. The data peak from Utah and the Dakota region may also reflect some pollution or, as may be expected from this geographical region's relative remoteness, some eddy transport process that transported mildly diluted

stratospheric air rapidly from the tropopause to the boundary layer. As mentioned earlier in the text, the most significant observation made in the boundary layer was that of the ozone void in the latitude range of 13°S to 2°N during May 1978. The 1977 ozone levels in this latitude region were an order of magnitude higher. The GAMETAG data sets for both years show that in the latitude range 13°S to 2°N the average wind speed was approximately the same (6-7 m/s). Although these wind data can hardly be considered a good statistical average for the area, they do not support any hypothesis suggesting enhanced surface destruction in 1978 as opposed to 1977. Chameides and Davis (1980) have suggested that a chemical mechanism initiated by the photolysis of methyl iodide and followed by a catalytic ozone destruction mechanism may be partially responsible for the 1978 low ozone values. They do not, however, rule out the effect of some unique boundary layer dynamic process or the importance of HO_x photochemistry.

Project GAMETAG free tropospehric and boundary layer ozone and dewpoint data have been combined and plotted as a function of latitude in Figures 86 and 87. The free tropospheric ozone and dewpoint data show a significant negative correlation throughout most of the 58°S to 70°N latitude range; it appears strongest in the northern hemispheric subtropical, middle, and high latitudes. Because of the numerous data gaps, any correlations between the GAMETAG

boundary layer ozone and dewpoint data are difficult to determine from this figure.

c. Pearson (r) Correlation Coefficient Comparison of the GAMETAG O_3 and Dewpoint Data. A second method to illustrate the negative correlation between the GAMETAG ozone and dewpoint data was to calculate a correlation coefficient for these two data bases. The free tropospheric data were divided into ozone and dewpoint data pair sets that were all collected within the same ten degree latitude band. The data sets were then further divided, if possible, as to sampling flight direction through that latitude band. As a result, there were approximately 10,000 raw data pairs for each latitude area band subdivision. According to both Goode (1980) and Walker (1980), a random sampling of 100 data pairs from each 10,000 pairs and the subsequent calculation of the Pearson (r) may be considered as representative. Using the above procedure, the Pearson (r) correlation coefficient was calculated for each year's major flight leg data through each ten degree latitude band. Upper limit dewpoint data were assumed to be the actual dewpoint values.

The Pearson (r) product-moment correlation coefficient varies from +1 (perfect correlation) through 0 (no correlation) to -1 (perfect anti-correlation). According to Downie and Heath (1970), a Pearson (r) of .8 and above is considered a high coefficient, an r around .5 is considered moderate and an r of .3 and below is considered meaningless.

As shown in Table 11, the GAMETAG free tropospheric ozone and dewpoint data correlation ranges from no correlation to strongly negative. In 1977, the latitude bands displaying the strongest negative correlation are north of 30°N and those between 0° and 10°N, and 20° and 26°S. These latitude spans coincide with the regions of maximum observed ozone variability (30°N-70°N and 20°S-26°S) and the ITCZ (0°-10°N). The two latitude bands displaying a slight positive correlation (0°-20°S) coincide with the region of observed minimum ozone. In 1978, the latitude bands between 30°N and 50°N, and 10° and 20°N display the strongest negative correlation. These latitude bands coincide with the regions of peak ozone concentration.

Because the upper limit dewpoint data that corresponds to high ozone data are warmer and therefore probably closer than the actual dewpoint to the dewpoint mean, the use of upper limit data tends to minimize the intensity of the negative correlation. The result then is an underestimation of the strength of the negative correlation for those latitude bands which include some but not all bottomed out dewpoint data. The correlation coefficient for those latitude bands containing only bottomed out dewpoint data appear to be unreliable.

If, as suggested earlier in the text, the ozone layering encountered by GAMETAG is the result of stratospheric-tropospheric exchange processes and subsequent transport,

Table 11. GAMETAG O_3 and Dewpoint Data Correlation Coefficients.

Latitude Band	Pearson (r) Correlation Coefficient	
	1977	
	Southbound	Northbound
70°-60°N	-.848	-.532
70°-50°N	-.494	-.824
50°-40°N	-.709	-.708
40°-30°N	-.837	-.422
30°-20°N	-.403	-.496
20°-10°N	-.347	-.383
10°-0	-.594	-.791
0°-10°S	+.007	-.566
10°-20°S	+.009	-.420
20°-26°S	-.625	-
	1978	
70°-60°N	-.256	-
60°-50°N	-.052	-.396
50°-40°N	-.653	-.576
40°-30°N	-.799	-.803
30°-20°N	-.388	-.056
20°-10°N	-.703	-.699
10°-0°	-.452	-.548
0°-60°S	*	*

*Coefficient values were based on data pairs that almost entirely included bottomed out dewpoint values. These coefficient values were considered unreliable.

the strongest negative correlation should be in those regions where the most significant layering was encountered. In 1977, the regions of maximum layering were between 30° and 40°N (southbound) and 70° and 60°N (southbound); these regions coincide with the most negative correlation coefficient latitude bands. In 1978, significant layering was observed between 30° and 40°N and between 10° and 20°N (north and southbound); as in 1977, these regions of ozone layering coincide with the most negative correlation coefficient latitude bands.

If ozone layering is indicative of stratospheric air intrusion and its mixing with tropospheric air, high ozone levels may be more negatively correlated than low ozone levels which are more representative of tropospheric air. Using 40 ppbv as a dividing line between low and high ozone levels, Pearson (r) coefficients were calculated for the data pairs collected within each ten degree latitude band. These results are contained in Table 12. For both 1977 and 1978, those latitude bands which displayed the highest ozone variability and concentrations also showed significantly more negative coefficients for high ozone data pairs than for low ozone data pairs. This strongly suggests that dry ozone rich stratospheric air at various stages of dilution was responsible for the GAMETAG observed ozone layering, high O_3 variability, and high ozone concentrations.

For the boundary layer, the ozone dewpoint-correlation

Table 12. Comparison of GAMETAG High Ozone-Dewpoint Correlation and Low Ozone-Dewpoint Coefficients.

Latitude Band	Pearson (r) Correlation Coefficient			
	1977			
	Southbound		Northbound	
	$O_3 \geq 40$ ppbv	$O_3 < 40$ ppbv	$O_3 \geq 40$ ppbv	$O_3 < 40$ ppbv
70°-60°N	-.876	-.792	-.562	-.468
60°-50°N	-.494	-[1]	-.722	-.840
50°-40°N	-.367	-	-.712	-
40°-30°N	-.858	-.602	-.477	-
30°-20°N	-.441	-.367	-.527	-.329
20°-10°N	-.347	-.201	-.453	-.201
10°-0°	-	-.599	-	-.791
0°-10°S	-	+.007	-	-.566
10°-20°S	-	+.009	-	-.420
20°-26°S	-.864	-.095		
	1978			
70°-60°N	-.703	-.111	-	-
60°-50°N	+.027	-.226	-.710	-.226
50°-40°N	-.869	-.499	-.612	-.412
40°-30°N	-.803	-	-.803	-
30°-20°N	-.671	-.283	-.089	-
20°-10°N	-.703	-	-.696	-
10°-0°	-	-.452	-	-.548
0°-60°S	-	-	-	-

[1] Dash indicates that either there is no ozone-dewpoint pairs meeting this criteria on the Pearson (r) coefficient cannot be defined because at least one of the standard deviations is zero.

coefficients for clean remote air (central Pacific) were compared with the coefficients for air with a possible anthropogenic input (Imperial Valley). Table 13 shows that remote boundary layer air appears to have no or a negative ozone dewpoint correlation while the air sampled in the Imperial Valley has a positive correlation. This may be particularly significant since the ozone and dewpoint data for the air with a possible photochemical ozone input appear to be far more correlated than previously expected (Chameides and Walker, 1973).

d. Comparison of the GAMETAG Ozone and Dewpoint Data with Mean Circulation Features. A negative correlation between the Project GAMETAG ozone and dewpoint data can be seen across the range of latitudes flown (58°S to 70°N) in both years (1977 and 1978). Although this negative correlation between ozone and dewpoint can be seen in areas away from significant mean vertical motion, it especially stands out in regions of maximum mean vertical motion (ITCZ, subtropical ridge and the polar jet). Tables 14 and 15 contain a summary of the Project GAMETAG ozone and dewpoint data value extremes, their geographic location, and their relationship to mean circulation features.

There appears to be strong evidence that GAMETAG low ozone concentrations, high dewpoint values, and low dewpoint depressions occur near the ITCZ and that high ozone concentrations, low dewpoint values, and high dewpoint depressions

Table 13. Comparison of GAMETAG Boundary Layer Ozone-Dewpoint Correlation Coefficients.

Date	Geographic Location	Pearson (r) Correlation Coefficient
Aug. 26, 1977	3°N-0° (Central Pacific)	+.036
May 2, 1978	15.5°N-17.5°N (South of Hawaii)	-.726
May 6, 1978	28.1°S-31.5°S (Northeast of New Zealand)	-.634
Aug. 22, 1977	32.7°N-33.8°N (Imperial Valley)	+.492
Apr. 27, 1978	33.3°N-33.6°N (Imperial Valley)	+.470

Table 14. Project GAMETAG Free Tropospheric Ozone and Dewpoint Data Extreme Value Comparison.

1977 (August/September)			
O_3 Max	DP Min	DPD Max	Mean Circulation Feature and Location[1]
26°S	26°S	26°S	S.H. Subtropical Ridge ∿30°N
36°N	36°N	30°N	N.H. Subtropical Ridge ∿38°N
60°N	56°N	56°N	N.H. Polar Jet ∿60°N
O_3 Min	DP Min	DPD Max	
19°S	20°-8°S	20°-5°S	
8°S- 5°N	4°-8°N	6°-8°N	ITCZ ∿10°N
46°N	48°N	50°N	
66°N	65°N	65°N	

1978 (Apr/May/Jun)			
O_3 Max	DP Min	DPD Max	Mean Circulation Feature and Location[1]
16°N	16-22°N	17°N	
40°N	40°N	40°N	N.H. Subtropical Ridge ∿36°N
O_3 Min	DP Max	DPD Min	
14°S-10°N	0°-10°N	24°N	ITCZ ∿5°N
22°N	28°N	24°N	
50°N	∿50°N	50°N	

[1] Newton (1972).

AD-A092 518 AIR FORCE INST OF TECH WRIGHT-PATTERSON AFB OH F/G 4/2
LATITUDINAL AND VERTICAL RELATIONSHIP BETWEEN TROPOSPHERIC OZON--ETC(U)
JUN 80 F X ROUTHIER
UNCLASSIFIED AFIT-CI-80-18T NL

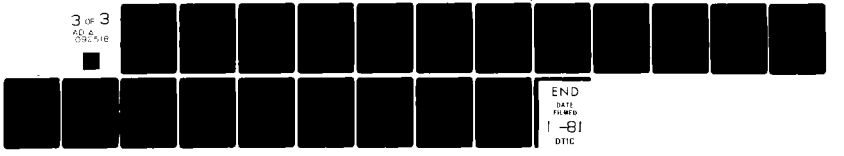

Table 15. Project GAMETAG Boundary Layer Ozone and Dewpoint Data Extreme Value Comparison.

1977 (August/September)			
O_3 Max	DP Min	DPD Max	Mean Circulation Feature and Location[1]
26°S 42°N[2]	26°S 42°N	26°S 42°N	S.H. Subtropical Ridge ∿30°S N.H. Subtropical Ridge ∿36°N
O_3 Min	DP Min	DPD Max	
15°S-10°N	15°S-18°N	5°S-15°N	ITCZ ∿10°N

1978 (Apr/May/Jun)			
O_3 Max	DP Min	DPD Max	Mean Circulation Feature and Location[1]
33°N	-	33°N	N.H. Subtropical Ridge ∿36°N
O_3 Min	DP Min	DPD Max	
12°S 66°N	16°S-18°N 66°N	18°S-18°N 62°N	ITCZ ∿5°N

[1] Newton (1972).

[2] Boundary layer ozone data peaks between 33°N and 44°N may also be due to anthropogenic inputs from the western United States or some eddy type transport mechanism such as tropopause folding.

occur near the subtropical ridge and polar jet.

The lack of variability in the southern hemipsheric 1978 GAMETAG ozone and dewpoint data may be the result of the GAMETAG sampling track location rather than an inherent inter-hemispheric difference. The downward vertical motion associated with the subtropical ridge is not uniform around the earth. Rather, the ridge is constructed of a series of maximum subsidence zones called high pressure cells (see Figure 4). The Pacific Ocean area cells are centered in the Northeast Pacific near 35°N 150°W and the Southeast Pacific near 25°S 95°W. The northern hemispheric cell extends a high pressure ridge from California to China; the southern hemispheric cell extends a high pressure ridge from South America westward to only 150°W. During the southern hemi-spheric winter, a third high pressure cell develops over Australia and extends a ridge eastward to approximately 164°E (Willet and Sanders, 1959). In both years, the Project GAMETAG sampling tracks were flown in close proximity to the North Pacific high pressure cell and in between the two high pressure cells in the South Pacific. The northern hemispheric middle and subtropical latitude GAMETAG data were collected closer to or actually in high pressure regions and therefore closer to areas of strong subsidence.

Concerning the observation of ozone data maximum values (low dewpoint and high dewpoint depressions) in lati-tudes away from mean circulation features, large scale eddy

motion may be responsible. Jet streams, for example, are often observed to transverse wide latitude ranges (Chatfield and Harrison, 1977a). The jet stream motion may cause the injection of stratospheric air into the troposphere. Once in the troposphere, stratospheric air parcels may follow an isentropic trajectory across thousands of kilometers before reaching the surface. As a result, any observed strong negative correlation between high ozone and low dewpoint could have been generated by a very specific stratospheric-tropospheric exchange process that occurred in a location vastly different from the point of observation. Danielsen (1980) has proposed that the large ozone variability and the layers of high ozone concentrations observed by Project GAMETAG investigators on August 23, 1977 between San Francisco and Hawaii were the result of a polar jet related tropopause folding event. Danielsen (1980) has estimated that the stratospheric air encountered by the GAMETAG sampling platform on August 23, 1977 was injected across the tropopause into the troposphere near 65°N 135°E (Western Asia). He also contends that the GAMETAG observed ozone maximum near 60°N in 1977 was caused by tropopause folding.

There appears to be stronger negative correlation between GAMETAG ozone and dewpoint data in those regions which have been suggested as primary zones for stratospheric-tropospheric exchange (Pruchniewicz, 1973; Chatfield and Harrison, 1977b). Additionally, these latitude regions

coincide with the highest levels of ozone variability, layering, and concentration. This coincidence between the general latitudinal position of the mean circulation features, that maximize stratospheric-tropospheric exchange, and the location of the GAMETAG data features, that most strongly reflect stratospheric air within the troposphere, suggest that dynamic processes may have been significantly responsible for controlling the source of ozone in the air that was sampled by GAMETAG.

2. Vertical GAMETAG O_3 and Dewpoint Data

a. High Resolution Analysis of Vertical Data.

According to Reiter (1961), Kroening and Ney (1962), and Danielsen (1980), the appearance of ozone and dewpoint layering in vertical data profiles may be taken as evidence of stratospheric ozone being injected into the tropopause and subsequently transported within it. Of the six vertical ozone and dewpoint data profiles which were selected for microscale analysis (Figures 44-49) four showed indications of significant layering that may be taken as evidence of stratospheric ozone below six kilometers altitude. These four profiles were collected in regions of high free tropospheric ozone variability. The data profile collected on May 2, 1977 near 14°N showed an ozone rich layer between 3000 and 1000 meters altitude. This possible stratospheric or upper tropospheric layer may be construed as having experienced significant mixing during a long middle tropospheric trajectory that may

have started much closer to the subtropical ridge or polar jet. As a result, the obvious negative correlation characteristics have been diluted.

b. Comparison with Other High Resolution Vertical O_3 and Dewpoint Data Set. A comparison of the GAMETAG vertical profiles with other data is difficult. Most published ozonesonde profiles (i.e., Hering and Border, 1964, 1965a,b, 1967) are the product of extensive processing. On an ozonegram which presents stratospheric (>1000 ppbv) as well as tropospheric concentrations, small oscillations on the order of ten or twenty ppbv have been filtered out. However, one report on the vertical distribution of dewpoint and ozone was retrieved from the literature and found to be appropriate for a comparison. Mastenbrook and Purdy (1975) presented vertical water and O_3 profiles over Washington, DC for the time period 1971 to 1973. The water data were derived from standard radiosonde ascents made every day at 1200 Z. The ozonesonde observations were usually completed three to five hours later. One example is illustrated in Figure 88.

Both the dewpoint and ozone profiles indicate layering similar to that observed by Project GAMETAG during ascents and descents. Although the observations were taken four hours apart, there appears to be anti-correlation between ozone and dewpoint, particularly near 380 mb, 480 mb, and 650 mb. The low level increase in ozone (1000-800 mb) reflects possible anthropogenic effects in the Washington, DC area.

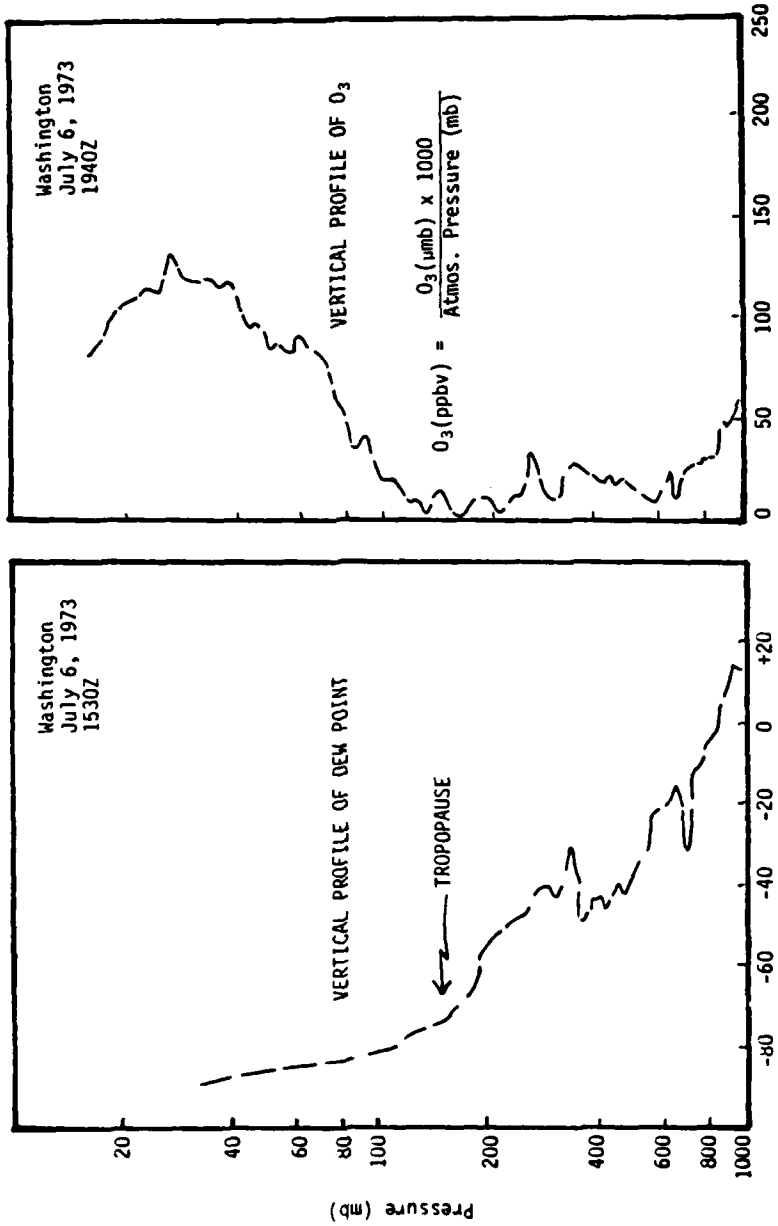

Figure 88. Vertical Ozone and Dewpoint Data Collected on July 6, 1973 Over Washington, DC.

Evidence of ozone layering and ozone-dewpoint anti-correlation exists in other Mastenbrook and Purdy (1975) profiles which were collected four to seven years before Project GAMETAG.

c. Low Resolution Analysis of the Vertical Data. The macroscale analysis (Figures 50-55) of the 1977 GAMETAG ozone and dewpoint data collected during the Electra aircraft ascents and descents show negative correlation in the upper altitude block (>4500 meters). There is an ozone maximum and a dewpoint minimum between 30°N and 40°N; the ozone data has a minimum between 0° and 10°N where a dewpoint maximum may be found. The lower altitude blocks also show negative correlation between the ozone and dewpoint data but the geographic position of the corresponding peaks and valleys is not as well aligned. For the 1978 data analysis (Figures 56-61), the upper altitude block shows the strongest negative correlation of the three blocks. As with 1977, the lowest altitude block provides the least evidence of O_3/H_2O anti-correlation.

The general decrease in ozone with decreasing altitude as well as the negative correlation between ozone and dewpoint vertical data suggests that the main source of the ozone measured by Project GAMETAG was above the aircraft flight level and that the air containing the high ozone levels were layers of stratospheric or upper tropospheric origin.

E. Comparison Between 1978 GAMETAG O_3 and CO Data

As noted in the Introduction (Section I-B-5) carbon monoxide reacts with hydroxyl radicals to initiate a photochemical ozone source mechanism. According to Fishman and Crutzen (1978), carbon monoxide is a major tropospheric ozone precursor. They contend that the apparent higher northern hemispheric O_3 levels are a direct result of the northern hemisphere's higher CO concentrations.

Figure 89 shows O_3, CO, and dewpoint data that were collected during the 1978 GAMETAG flight operations in the free troposphere. From this figure, it can be seen that elevated CO levels in the northern hemisphere do correlate with higher O_3 levels observed in this same hemisphere. But a high resolution comparison of the CO and O_3 data does not show a high degree of correlation in either hemisphere. The possibility exists that the absence of high resolution CO measurements during the GAMETAG flights may explain the absence of a positive correlation with the GAMETAG O_3 data. This suggestion would appear to be corroborated by the high resolution vertical CO and O_3 profiles presented by Fishman, et al. (1980). The latter authors have suggested that an observed positive correlation between simultaneously measured CO and O_3 layers is the result of photochemical processes that involve the HO_2-NO_x-CO cycle. However, Fishman, et al. (1979) have also suggested that the photochemical O_3 producing processes involving CO would have a long time constant and

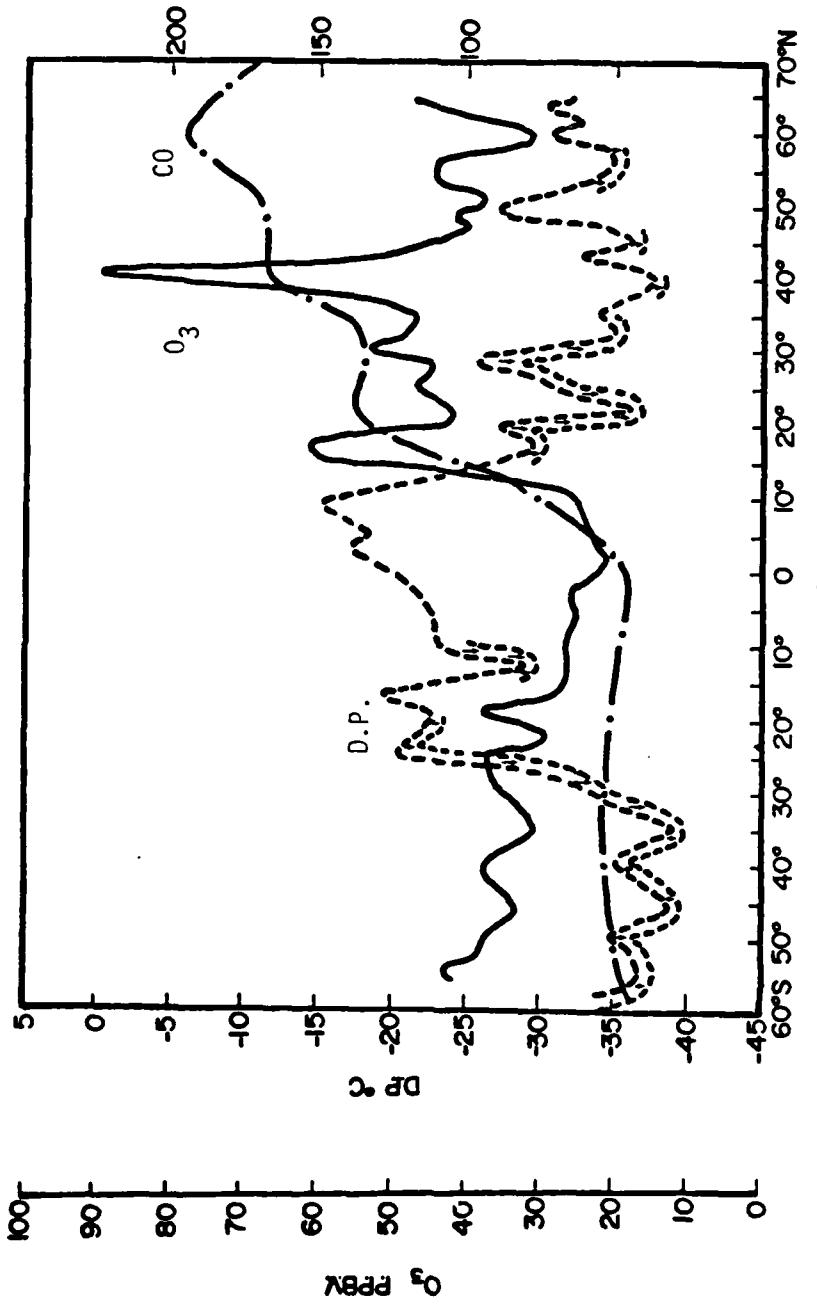

Figure 89. Comparison of 1978 GAMETAG O_3, Dewpoint, CO Data as a Function of Latitude.

therefore would be difficult to identify from short term aircraft sampling. These authors have, in fact, stated that if all the CO oxidized on a global scale resulted in ozone formation, only a one part per billion increase per day at a given free tropospheric point would result. Since the lifetime of a well defined air parcel ($<\sim$2 weeks) is normally much shorter than the time required to convert a significant fraction of that parcel's CO to CO_2 and O_3 (i.e., τ_{CO} = 4-12 weeks), it would appear that the lifetime of the O_3 layers observed by Fishman, et al. (1980) would have had to have been exceptionally long for the necessary O_3 photochemical formation to have occurred.

A further complication in the Fishman, et al. (1980) hypothesis is that the oxidation of each CO molecule can produce only one molecule of O_3($CO + 2O_2 \rightarrow CO_2 + O_3$). Since the O_3 increases observed in the Fishman, et al. (1980) data were always significantly higher than the simultaneously measured CO peaks, there would seem to be a need for an ozone source far greater than that which could be generated from carbon monoxide oxidation.

It thus appears unlikely at this time that the difference in time resolution can provide a simple explanation for the lack of correlation between the GAMETAG CO and O_3 data bases. It now seems more likely that the slowness of the CO oxidation process relative to transport mechanisms is the basis for the poor high resolution CO/O_3 correlation.

CHAPTER V

CONCLUSIONS

The 1977 and 1978 Project GAMETAG field operation recorded free tropospheric and boundary layer ozone, dew point, and temperature data over the latitude range 70°S to 58°N. This data set, which is presented here, is unique in that all the individual measurements were simultaneously recorded on the same instruments over a relatively short time period each year.

A. Observation Summary

Some of the more important findings concerning the GAMETAG O_3 and dewpoint data follow:

1. Significantly greater variability was observed in the northern hemispheric subtropical and mid latitude free tropospheric spring and summer ozone data than in the equatorial or southern hemispheric subtropical and mid latitude fall data.
2. The average northern hemispheric subtropical and mid latitude free tropospheric and boundary layer ozone levels were found to be $\sim$2.0 times higher than the corresponding average equatorial ozone levels and $\sim$1.5 times than the corresponding average southern hemispheric ozone levels.

3. Maximum values in the 1977 free tropospheric ozone data were observed near 60°N and in the latitude bands 22°N-36°N and 26°S-20°S; in 1978, free tropospheric ozone data maxima were seen in the latitude regions 14°N-20°N and 34°N-42°N.
4. Minimum free tropospheric ozone levels were observed in 1977 near the equator (20°S-8°N) and in the latitude band 44°N-52°N; in 1978, free tropospheric ozone minima were also observed near the equator (20°S-12°N) and in the latitude band 46°N-58°N.
5. For most latitude regions, the boundary layer ozone levels were found to be 15-30% lower than the free tropospheric levels; the only boundary layer ozone levels, which were as high as free tropospheric levels (67 ppbv in 1977 and 75 ppbv in 1978) were observed over the United States. In the latter cases, anthropogenic pollution sources were definitely a contributing factor.
6. For both the free tropospheric and boundary layer, the highest dewpoint values occurred in the latitude band 15°S to 15°N and were found to decrease ten to twenty degrees towards the poles.
7. The GAMETAG subtropical free tropospheric dewpoint values for the latitude regions 20°S-40°S and 25°N-40°N were usually found to be lower than the literature values which were based on widely disbursed, mostly continental radiosonde data.

8. Except for the 1977 GAMETAG data collected between the equator and 20°S, the free tropospheric ozone and dewpoint data were generally found to show a moderate to strong negative correlation; except for the GAMETAG boundary layer data collected over the Imperial Valley, the boundary layer ozone and dewpoint data were generally found to show either no correlation or a moderate negative one.
9. Vertical ozone and dewpoint profiles showed that layers of ozone rich, dry air increased in number and intensity with increasing altitude and with increasing closeness to the free tropospheric regions of maximum ozone variability.

B. Conclusions

The observation of ozone layering, coincident with moderate to strong negative ozone-dewpoint correlation suggests that a major source of the free tropospheric ozone, observed during the GAMETAG flights, was that resulting from the generally downward sloping transport of ozone rich upper tropospheric air or, alternatively, ozone rich lower stratospheric air. This implies that dynamic processes which transport ozone of stratospheric origin into and within the troposphere are a major source mechanism of the global tropospheric ozone budget.

One of the most significant segments of boundary layer

O_3 data was recorded in the latitude range of 13°S to 2°N in May 1978. The average O_3 value was 3 ppbv and, could have been as low as 1 or as high as 5 ppbv when the ozone sensor accuracy is considered. No evidence of this phenomenon was observed in 1977. Although meteorological conditions may have played an important role in leading up to this O_3 minimun, it also appears that photochemical destruction of O_3 may have been an equally important factor.

Although GAMETAG sampling operation has expanded the tropospheric ozone and water vapor data base, there are still many questions concerning the tropospheric ozone budget that remain unanswered. One of the major questions concerning ozone layering is that of defining the dynamic mechanism(s) primarily responsible for the transport of ozone rich air into the middle troposphere. The question may also be raised whether or not upper tropospheric photochemical processes contributed, in some degree, to the elevated ozone levels observed in the middle troposphere. These and many other questions concerning atmospheric dynamics, photochemistry, and the three dimensional atmospheric ozone distribution have been approached but have remained unanswered. The development of improved research instrumentation and its application to future global field sampling experiments, such as the proposed GAMETAG II, are essential to understand the global atmospheric budget of this important trace gas.

REFERENCES

Aldaz, L., 1969: Flux measurements of atmospheric ozone over land and water. Journal of Geophysical Research, 74, 6943-6946.

Bates, D. R. and M. Nicolet, 1950: The photochemistry of atmospheric water vapor. Journal of Geophysical Research, 55, 301-327.

Baughner, R. E., 1978: The effect of increased CO_2 on stratospheric ozone. Journal of Geophysical Research, 83, 1326-1331.

Caldwell, M. M. and D. S. Nachtwey, 1975: Impacts of Elevated UV-B radiation intensities on the biosphere. Climatic Impact Assessment Program Monograph 5, Part 1, 1-10-1-29.

Chameides, W. L. and J. C. G. Walker, 1973: A photochemical theory of tropospheric ozone. Journal of Geophysical Research, 78, 8751-8760.

Chameides, W. L. and D. D. Davis, 1980: Iodine: Its possible role in tropospheric photochemistry. Submitted to the Journal of Geophysical Research.

Chapman, S., 1930: A theory of upper atmospheric ozone. Quart. J. Roy. Met. Soc., 3, 103-125.

Chatfield, R. and H. Harrison, 1976: Ozone in the remote troposphere: Mixing versus photochemistry. Journal of Geophysical Research, 81, 421-423.

Chatfield, R. and H. Harrison, 1977a: Tropospheric ozone 1: Evidence for higher background values. Journal of Geophysical Research, 82, 5965-5968.

Chatfield, R. and H. Harrison, 1977b: Tropospheric ozone 2: Variations along a meridional band. Journal of Geophysical Research, 82, 5969-5976.

Chleck, D., 1979: Measurements of upper atmospheric water vapor made in-situ with a new moisture sensor. Geophysical Research Letters, 6, 379-381.

Crutcher, H. L., 1969: Temperature and humidity in the troposphere. World Summary of Climatology, 4, 45-85.

Crutzen, P. J., 1970: The influence of nitrogen oxides on the atmospheric ozone content. Quarterly Journal of the Royal Meteorological Society, 96, 320-334.

Crutzen, P. J., 1971: Ozone production rates in an oxygen hydrogen nitrogen atmosphere. Journal of Geophysical Research, 76, 7311-7327.

Crutzen, P. J., 1973: Gas phase nitrogen and methane chemistry in the atmosphere. In Physics and Chemistry of the Upper Atmosphere, ed., McCormack, Dordrecht, Reidel Company

Crutzen, P. J., 1974: Photochemical reactions initiated by and influencing ozone in the unpolluted tropospheric air. Tellus, 26, 47-56.

Cunnold, D., F. Alyea, N. Phillips, and R. Prinn, 1974: A three dimensional dynamic-chemical model of atmospheric ozone. Journal of Atmospheric Science, 32, 170-194.

Danielsen, E. R., 1968: Stratospheric-tropospheric exchange based on radioactivity, ozone, and potential vorticity. Journal of Atmospheric Science, 25, 502-518.

Danielsen, E. F., 1980: Stratospheric source for unexpectedly large values of ozone measured over the Pacific Ocean during GAMETAG, August 1977. Journal of Geophysical Research, 85, 401-412.

Davis, D. D., 1976: GAMETAG Proposal, submitted to the National Science Foundation. Copies on file with the School of Geophysical Sciences, Georgia Institute of Technology.

Davis, D. D., 1978: Personal communication. Present address: Georgia Institute of Technology.

Dobson, G. M. B., 1973: Atmospheric ozone and the movement of air in the stratosphere. Pure and Applied Geophysics, 106-108, 1520-1530.

Downie, H. M. and R. W. Heath, 1970: Basic statistical methods. New York, Harper and Row, 357 p.

Drake, C. L., J. Imbrie, J. A. Knauss, K. K. Turekian, 1978: Oceanography, New York, Holt Reinhardt and Winston, 444 p.

Dutch, H. U., 1969: Atmospheric ozone and ultra-violet radiation. In World Survey of Climatology, Vol. 4, ed. Rex Elsevier Amsterdam, 383-432.

Dutch, H. U., 1974: The ozone distribution in the atmosphere. Canadian Journal of Chemistry, 52, 1491-1504.

Fabian, P., 1973: A theoretical investigation of tropospheric ozone and stratospheric exchange processes. Pure and Applied Geophysics, 106-108, 1064-1057.

Fabian, P., 1974: Comments on "A Photochemical Theory of Tropospheric Ozone" W. C. Chameides and J. C. G. Walker. Journal of Geophysical Research, 79, 4126-4127.

Fabian, P. and P. G. Pruchniewicz, 1973: Meridional distribution of tropospheric ozone from ground based registrations between Norway and South Africa. Pure and Applied Geophysics, 106-108, 1027-1035.

Fabian, P. and P. G. Pruchniewicz, 1977: Meridional distribution of ozone in the troposphere and its seasonal variation. Journal of Geophysical Research, 82, 2063-2073.

Fishman, J. and P. J. Crutzen, 1978: The origin of ozone in the troposphere. Nature, 274, 835-838.

Fishman, J., S. Solomon, and P. J. Crutzen, 1979: Observational and theoretical evidence in support of a significant in-situ photochemical sources of tropospheric ozone. Tellus, 31, 432-446.

Fishman, J., W. Seiler, and P. Haagenson, 1980: Simultaneous pressure of O_3 and CO Bands in the troposphere. Submitted to Tellus.

Freedman, M., 1980: Personal communication. Mr. Freedman is an engineer with the VIZ Manufacturing Co., 335 Price St., Philadelphia, PA.

Garland, J. A. and S. A. Penkett, 1976: Absorption of peroxyl acetyle nitrate and ozone by natural surfaces. Atmospheric Environment, 10, 1127-1131.

Gaunter, D. J., J. D. Holdeman, D. Briehl, and F. Numeni, 1978: Description and review of global measurements of atmospheric species from the Global Atmospheric Sampling Program (GASP) in Air Quality Meteorology and Atmospheric Ozone, ASTM STP 653, ed. A. Morris and R. Barras. American Society for Testing and Materials, 461-478.

Goode, J., 1980: Personal communication. Present address: Georgia Institute of Technology.

Hanson, J., 1980: Personal communication. Present address: NCAR.

Hazucha, M., F. Silverman, C. Parent, S. Fields, and D. V. Bates, 1973: Ozone toxicology. Archives of Environmental Health, 27, 183-188.

Heidt, L. E., J. P. Krasnec, R. A. Lueb, W. H. Pollack, B. E. Henry, and P. J. Crutzen, 1980: Latitudinal distributions of CO and CH_4 over the Pacific. Submitted to the Journal of Geophysical Research.

Hering, W. S., 1965: Ozone and atmospheric transport. Tellus, 18, 329-335.

Hering, W. S. and T. R. Borden, 1964: Ozonesonde observations over North America, Vol. 1, AFCRL-64-30(I), AFCRL, Bedford, MA.

Hering, W. S. and T. R. Borden, 1965a: Ozonesonde observations over North America, Vol. 2, AFCRL-64-30 (II), AFCRL, Bedford, MA.

Hering, W. S. and T. R. Borden, 1965b: Ozonesonde observations over North America, Vol. 3, AFCRL-65-30 (III), AFCRL, Bedford, MA.

Hering, W. S. and T. R. Borden, 1967: Ozonesonde observations over North America, Vol. 4, AFCRL-65-30 (IV), AFCRL, Bedford, MA.

Holdeman, J. D., 1976: NASA GASP Date Report for Tape VL003, NASA Tech. Note TMX-73506, 12 pp.

Holdeman, J. D. and P. D. Falconer, 1976: Analysis of atmospheric ozone measurements made from a B747 airliner during March, 1975. NASA Tech. Note, TN D8311, 30 pp.

Holton, J. R., 1973: An Introduction to Dynamical Meteorology, New York, NY, Academic Press, 299 pp.

James, M., 1980: Personal communication. Present Address: AWS/LG, Scott AFB, IL.

Johnston, H. S., 1974: An overview of stratospheric ozone chemistry. Climatic Impact Assessment Program, Monograph 1, 5-7-5-33.

Kelley, N. D. and N. Zrubeck, 1973: Instrumentation aboard the Electra. Atmospheric Technology, 1, 18-24.

Kroening, J. L. and E. P. Neg, 1962: Atmospheric Ozone. Journal of Geophysical Research, 67, 1867-1875.

Levy, H., 1973: Photochemistry of the tropospheric. Advances in Photochemistry, 9, 369-524.

London, J., 1963: The distribution of total ozone in the northern hemisphere. Beitr. Phys. Atmos., 36, 254-263.

London, J. and J. Park, 1973: Application of general circulation models to the study of stratosphere ozone. Pure and Applied Geophysics, 106-108, 1611-1617.

London, J. and J. Park, 1974: The interaction of ozone photochemistry and dynamics in the stratosphere: a three dimensional atmospheric model. Canadian Journal of Chemistry, 52, 1599-1609.

Mastenbrook, H. J., 1968: Water vapor distribution in the stratosphere and high troposphere. Journal of Atmospheric Science, 25, 299-311.

Mastenbrook, H. J. and D. R. Purdy, 1975: Vertical distribution of water vapor and ozone over Washington, DC during 1971 through 1973. Naval Research Laboratory Report 7844, 168 pp.

Nastrom, G. D., 1977: Vertical and horizontal fluxes of ozone at the tropopause from the first year of GASP data. Journal of Applied Meteorology, 16, 740-744.

Newell, R. E., 1963: Transfer through the tropopause and within the stratosphere. Quarterly Journal of the Royal Meteorological Society, 89, 167-179.

Newell, R. E., D. G. Vincent and J. W. Kidson, 1969: Interhemispheric mass exchange from meteorological and trace substance observations. Tellus, 21, 641-647.

Newell, R. E., J. W. Kidson, D. G. Vincent, and G. J. Boer, 1973: The General Circulation of the Tropical Atmosphere, Vol. 1, 258 pp.

Newell, R. E., G. J. Boer, and T. G. Dopplick, 1973: Influence of the vertical motion on ozone concentrations in the stratosphere. Pure and Applied Geophysics, 106-108, 1531-1543.

Newton, C. W., 1972: Southern hemisphere general circulation in relation to global energy and momentum balance requirements. Meteor. Monograph, 13, 215-246.

Oort, A. H. and E. M. Rasmussen, 1970: On the annual variation of the monthly mean meridional circulation. Monthly Weather Review, 98, 423-442.

Oort, A. H. and E. M. Rasmussen, 1971: Atmospheric circulation statistics, NOAA Professional Paper 5, 324 pp.

Parent, R. A., 1978: A reivew of ozone toxicology studies in Air Quality and Atmospheric Ozone (ASTM STP 653), ed. A. L. Morris and R. C. Barris, Baltimore, American Society for Testing and Materials, 575-596.

Prabhakara, C., E. B. Rodgers, and V. V. Salmonson, 1971: Global distribution of total ozone derived from Nimbus 3 satellite during April-July 1969 and its implication to upper tropospheric circulation. NASA Tech Note TNX-651-71-463.

Pratt, R. and P. Falconer, 1979: Circumpolar measurements of ozone, particles, and carbon monoxide from a commercial airliner. Journal of Geophysical Research, 84, 7876-7882.

Pruchniewicz, P. G., 1973: The average tropospheric ozone content and its variation with season and latitude as a result of global ozone circulation. Pure and Applied Geophysics, 106-108, 1058-1073.

Rech, G. M., B. D. Briehl, and T. J. Perkins, 1974: Flight testing of a pressure system used to measure minor atmospheric constituents on an aircraft, NAS TN D-7576, NASA.

Regener, V. H., 1964: Measurement of atmospheric ozone with the chemiluminescent method. Journal of Geophysical Research, 69, 3795-3803.

Regener, V. H., 1974: Destruction of atmospheric ozone at the ocean surface. Arch. Met. Geophys. Brok, Ser. A. 23, 131-135.

Reiter, E. R., 1961: Jet Stream Meteorology, Chicago, University of Chicago Press, 515 pp.

Reiter, E. R., 1978: Impact of stratospheric ozone on tropospheric concentrations in Air Quality Meteorology and Atmospheric Ozone (ASTM STP 653) ed. Morris and Barris, Philadelphia, American Society for Testing and Materials, 506-519.

Renzetti, N. A., 1959: Ozone in the Los Angeles atmosphere in Ozone Chemistry and Technology, Washington, DC, American Chemical Society, 230-263.

Reynolds, H. M., 1979: Private communication. Mr. Reynolds was the Electra flight program engineer during Project GAMETAG. Present address: School of Geophysical Sciences, Georgia Institute of Technology.

Ruskin, R. E., 1979: Private communication. Present address: Naval Research Laboratory.

Sellers, W. D., 1965: Physical Climatology, Chicago, University of Chicago Press, 272 pp.

Solomon, S., 1980: Personal communication. Ms. Solomon performed the actual ozone analysis for Fishman and Crutzen (1978). Present address: National Center for Atmospheric Research.

Stallard, R. F., J. M. Edmond, and R. E. Newell, 1975: Surface ozone in the Southeast Atlantic between Dakar and Walvis Bay. Geophysical Res. Lett., 2, 289-292.

Stoker, H. S. and S. L. Seager, 1972: Environmental Chemistry: Air and Water Pollution. Glenview, Il., Scott Soresman and Co., 186 pp.

Stolarski, R. S. and R. J. Cicerone, 1974: Stratospheric chlorine: a possible sink for ozone. Canadian Journal of Chemistry, 52, 1582-1591.

Tiefenau, H., P. G. Pruchniewicz, and P. Fabian, 1972: Meridional distribution of tropospheric ozone from measurements aboard commercial airliners. Z. Geophys., 38, 145-151.

Tiefenau, H., P. Fabian, 1972: The specific ozone destruction at the ocean surface and its dependence on horizontal wind velocity from profile measurements. Arch. Met. Geoph. Biokl, Ser. A, 21, 399-412.

Willet, H. C. and F. Sanders, 1959: Descriptive Meteorology, New York, Academic Press, 355 p.

Vukovich, F. M., 1971: Some observations of ozone concentrations at night in the North Carolina Piedmont boundary layer. Journal of Geophysical Research, 78, 4458-4462.

Walker, J., 1980: Personal communication. Present address: Georgia Institute of Technology.

Wilbrandt, P., 1975: Bestimmung der Spezifisc hen Ozonzerstörungstrate über Buschsteppe und der Ozonflüsses in diese Oberflache mit Hiefe von Ozon und Temperaturprofil-messingen an eindem 120-M Mast in Tsumb Mit Max Planch Inst für Aeron. in Fabian and Pruchniewicz, 1977.


DATE
ILME